32nd DAE - BRNS NATIONAL LASER SYMPOSIUM (NLS - 32)

January 29 - February 01, 2024

BOOK OF ABSTRACTS

Organized by :

Raja Ramanna Centre for Advanced Technology
Indore - 452013, Madhya Pradesh

Sponsored by

Board of Research in Nuclear Sciences, Mumbai

In Collaboration with

Indian Laser Association

National Advisory Committee

Achanta Venugopal	NPL, New Delhi
Bhasin V.	BARC, Mumbai
Bhawalkar D.D.	Indore
Chaturvedi S.	IPR, Gandhinagar
Grover R.B.	BRNS, Mumbai
Gupta P.D.	Indore
Joshi Suhas	IIT Indore
Kakodkar A.	HBNI, Mumbai
Kumar Ajay	IRDE, Dehradun
Kumar G. Ravindra	TIFR, Mumbai
Majumder S. K.	President, ILA
Manna Indranil	BIT, Mesra
Mishra Suman Kumari	CGCRI, Kolkata
Mohanty Ajit Kumar	DAE, Mumbai
Mudali Kamachi, U.	HBNI, Mumbai
Nakhe S. V.	RRCAT, Indore
Nayak Jagannath	CHESS, Hyderabad
Pal Amlan	UGC DAE CSR, Indore
Pathak B. C.	NPCIL, Mumbai
Rao Tata Narsingh	ARCI, Hyderabad
Sharma Archana	BARC, Mumbai
Som Sumit	VECC, Kolkata
Sriram K. V.	LEOS, Bengaluru
Venkatraman B.	IGCAR, Kalpakkam
Vinayak Seema	SSPL, New Delhi

Symposium Organizing Committee

Nakhe S. V.	**RRCAT, Indore: Chairman**
Verma Sunil	RRCAT, Indore: Convener
Saxena Manoj K.	RRCAT, Indore: Member Secretary
Majumder S. K.	RRCAT, Indore & President, ILA
Achanta Venugopal	NPL, New Delhi & Vice-President, ILA
Palani I. A.	IIT, Indore: General Secretary-I, ILA
Paul C. P.	RRCAT, Indore: General Secretary-II, ILA
Benerji N. S.	RRCAT, Indore: Treasurer, ILA
Upadhyay Ajit	RRCAT, Indore: Scientific Secretary
Arya Rajesh	RRCAT, Indore
Babu S. Moorthy	Anna Univ., Chennai
Bhanage V. P.	RRCAT, Indore
Datta Anindya	IIT Mumbai
Deshpande P. P.	RRCAT, Indore
Dixit S. K.	RRCAT, Indore
Ghosh Nirmalya,	IISER, Kolkata
John Renu	IIT Hyderabad
Khare Alika	IIT Guwahati
Krishnamurthy M.	TIFR, Hyderabad
Kundu S.	BARC, Mumbai
Malshe U. D.	BARC, Mumbai
Mascarenhas M. L.	BARC, Mumbai
Mehta D. S.	IIT Delhi
Mishra S. R.	RRCAT, Indore
Moorti A.	RRCAT, Indore
Nagraj A.	BRNS, Mumbai
Om Prakash	RRCAT, Indore
Pant K. K.	RRCAT, Indore
Pradhan Manik	SNBNCBS, Kolkata
Rapol Umakant D.	IISER, Pune
Samuel G. L.	IIT Chennai
Sapra M. K.	BRNS, Mumbai
Saxena Piyush	RRCAT, Indore
Sendhil Raja S.	RRCAT, Indore
Udupa D. V.	BARC, Mumbai

Local Organizing Committee

Majumder S. K.	**RRCAT, Indore: Chairman**
Verma Sunil	RRCAT, Indore: Convener
Saxena Manoj K.	RRCAT, Indore: Member Secretary
Upadhyay Ajit	RRCAT, Indore: Scientific Secretary
Paul C. P.	RRCAT, Indore: General Secretary-II, ILA
Benerji N. S.	RRCAT, Indore: Treasurer, ILA
Talwar Sandeep	RRCAT, Indore: Treasurer, NLS-32
Dave Ishant	RRCAT, Indore: Webmaster, ILA
Narwat Dhruvdeep	RRCAT, Indore: Webmaster, NLS-32
Agnihotri H. P.	BRNS, Mumbai
Agrawal Praveen	RRCAT, Indore
Andrews J. T.	SGSITS, Indore
Bhatnagar Prateek	RRCAT, Indore
Biswal R.,	RRCAT, Indore
Ganesh P.	RRCAT, Indore
Gupta Sharad	IIT, Indore
Khanwalkar Jagriti	RRCAT, Indore
Krishna Hemant	RRCAT, Indore
Kumar Vijay	RRCAT, Indore
Mishra G. K.	RRCAT, Indore
Mishra P. K.	RRCAT, Indore
Misra Pankaj	RRCAT, Indore
Patidar Rajesh	RRCAT, Indore
Rai A. K.	RRCAT, Indore
Rawlani Bharat	RRCAT, Indore
Sahu Khageswar	RRCAT, Indore
Satapathy S.	RRCAT, Indore
Sharma Sanjay	RRCAT, Indore
Shrivastava R.	RRCAT, Indore
Singh C. P.	RRCAT, Indore
Upadhyaya B. N.	RRCAT, Indore
Vanchhani D.	RRCAT, Indore

32nd DAE - BRNS NATIONAL LASER SYMPOSIUM (NLS - 32)

January 29 - February 1, 2024

BOOK OF ABSTRACTS

Sponsored by

Board of Research in Nuclear Sciences Mumbai

In Collaboration with

Indian Laser Association

Organized by :

Raja Ramanna Centre for Advanced Technology
Indore - 452013, Madhya Pradesh

DAE-BRNS National Laser Symposium (NLS-32)
January 29 - February 1, 2024
Book of Abstracts

Designed & Compiled by
Printing and Publication Committee

Printed by
Printing Arts,
A-1/B, Pologround, Industrial Estate, Indore
Tel. 9826604242, email : printingarts1@gmail.com

PREFACE

The 32nd DAE-BRNS National Laser Symposium (NLS-32) is being organized at the Raja Ramanna Centre for Advanced Technology (RRCAT), Indore in collaboration with the Indian Laser Association (ILA) during January 29 to February 01, 2024. The symposium is being held under the aegis of Board of Research in Nuclear Science (BRNS), Department of Atomic Energy (DAE), Government of India. All the major Indian laser laboratories and academic institutions participate in the National Laser Symposium (NLS). The symposium is held every year at a different location so that researchers and students get exposed to the modern science and technological advancements in the fields of lasers and associated technologies. On behalf of the Organizing Committee, it is my pleasure to extend warm welcome to all the delegates of the NLS-32, comprising of postgraduate students, Ph.D. scholars, faculty members, scientists and industry participants.

The National Laser Symposium (NLS) is a well-established pan-Indian annual scientific event wherein four days of intense scientific deliberations bring together scientific and engineering professionals engaged in the expansive realms of laser physics and technology, and their applications. The current symposium marks the 32nd edition in the series which commenced in the year 1992 at IIT Madras. NLS offers an exceptional platform to the delegates for interaction across diverse disciplines involving lasers, which includes Physics and Technology of Lasers; Lasers in Nuclear Science and Technology; Laser Materials, Devices, and Components; Lasers in Chemistry, Biology and Materials Science; and many more. Embracing the transformative influence of Machine Learning and Artificial Intelligence, a new category, Machine Learning and AI in Laser Applications, has been introduced to align with the global trends.

RRCAT, Indore, the host institute of this year's NLS is a premier R & D institute under the Department of Atomic Energy, Government of India. It is dedicated to research and development in the field of lasers and synchrotron radiation sources. Having hosted the symposium seven times in the past, RRCAT promises to be a fertile ground for the exchange of ideas and academic rendezvous for the delegates in the area of optics and laser-based technologies.

This year, we have received overwhelming response from authors in the form of contributory papers and PhD theses. A total of 280 papers have been accepted after the peer review from about 310 papers received. Additionally, 18 PhD theses have been received for presentation by research scholars, which is an important part of the symposium wherein budding scientists will be showcasing the research conducted at different institutes in India in the fields of laser science and technology.

We are privileged and honored to have Shri Bhuwan Chander Pathak, Chairman & Managing Director, Nuclear Power Corporation of India Limited, Mumbai as the Chief Guest of the Symposium. RRCAT and NPCIL, represent two different arms of the Department of Atomic Energy, wherein the former represents the R&D sector whereas the later represents the Public Sector Undertaking. The two institutes have a longstanding collaboration between them, wherein the laser-based technologies developed at RRCAT have been effectively used for

solving certain specific challenging problems of the nuclear reactors operational under NPCIL.

The keynote address will be delivered by Prof. Debabrata Goswami, IIT Kanpur, a distinguished scientist, who will be taking us through the corridors of light-matter interaction during his lecture. There will be a special evening lecture, which will be delivered by Prof. Ajoy K. Ghatak, former Emeritus Professor, IIT Delhi, who is the doyen of optics education in India, having trained multiple generations of optics and laser professionals in our country. We extend sincere appreciation to all the twenty eminent scientists who accepted our request to deliver invited talks on different aspects of lasers science & technology during the symposium. I am sure, all delegates are looking forward to these talks.

To complement the four days of advanced scientific deliberations for the researchers, two short courses are going to be organized by the Indian Laser Association on January 27 and 28, 2024, just preceding the symposium. The topics of the two short courses are: (i) Biophotonics and (ii) Laser-based Manufacturing Technology for Functional Devices and Applications. The course structures are designed to introduce the subject to the participants at a pedagogical level, while at the same time providing them the details of the recent advancements in these two exciting fields. A total of fifty students have registered for the courses. The course coordinators and faculty members of these two courses are highly accomplished researchers in their fields.

In order to have a proper handshake between academia and industry, an industrial exhibition is being organized by the Indian Laser Association during NLS-32. The industrial exhibition will run concurrently with the symposium for the four days of the symposium. Twenty-two industrial partners will be participating in the exhibition along with their foreign principals. The exhibition provides an excellent platform to the industry participants to showcase their products and also present latest global developments in the fields of optics and lasers.

For successful organization of any symposium, dedicated and coherent efforts of several teams are required. NLS-32 is also one such event. The organizing team would like to express deep gratitude to Dr. Shankar V. Nakhe, Director, RRCAT for his unwavering support, encouragement and guidance in every aspect of organization of NLS-32. We are extremely thankful to all those who have been instrumental and contributed in organizing this symposium. We express our gratitude to the members of the "*National Advisory Committee*", "*Symposium Organizing Committee*" and the "*Local Organizing Committee*" for the interest, support and valuable suggestions. We are also indebted to all the referees for the painstaking effort of reviewing the manuscripts to maintain the high technical standards of NLS.

On behalf of the Organizing Committee, we wish all the delegates a scientifically fruitful, enjoyable, and mutually satisfying four days of academic deliberations.

Dr. Shovan K. Majumder: Chairman, Local Organizing Committee, NLS-32

Dr. Sunil Verma: Convener, NLS-32

Dr. Ajit Upadhyay: Scientific Secretary, NLS-32

Dr. Manoj Kumar Saxena: Organizing Secretary, NLS-32

CONTENTS

PROGRAMME SCHEDULE

SCIENTIFIC PROGRAM FOR NLS-32

Venue : RRCAT, Indore

Day 1 : Monday, January 29, 2024

SESSION – 1: INAUGURAL SESSION	
9:30 – 9:45	Welcome of the Chief Guest Lamp Lighting Saraswati Vandana
9:45 – 10:00	Welcome Address by Dr. Sunil Verma, Convener, NLS-32 Opening Remarks by Dr. S.V. Nakhe, Director, RRCAT Address by Dr. S.K. Majumder, President, ILA
10:00 – 10:30	Address by the Chief Guest Shri B. C. Pathak, CMD, NPCIL
10:30 – 11:15	Keynote Lecture Prof. Debabrata Goswami, IIT Kanpur *Controlling Light-Matter Interactions for Applications at Molecular scales*
11:15 – 12:00	Inauguration of Industrial Exhibition followed by High Tea
SESSION - 2	
Invited Talk-1 12:00 – 12:30	Prof. Hirendra Nath Ghosh, NISER Bhubaneswar *Ultrafast Charge Carrier Dynamics at the Interface of p-n Semiconductor Heterojunctions*
Invited Talk-2 12:30 – 13:00	Prof. Nirmalya Ghosh, IISER Kolkata *Quantum Weak measurement meets Spin Orbit Photonics*
LUNCH 13:00 – 14:00	
SESSION – 3	
14:00 – 16:30	POSTER SESSION - 1
TEA BREAK 16:30 – 16:45	
SESSION – 4	
Invited Talk-3 16:45 – 17:15	Prof. Nilesh J. Vasa, IIT Madras *Recent advances in laser-assisted trace gas sensing and their applications*
Invited Talk-4 17:15 – 17:45	Dr. R V L N Sridhar, LEOS -ISRO, Bengaluru *Development of Laser based Sensors and Scientific Instruments at LEOS, ISRO*
Invited Talk-5 17:45 – 18:15	Prof. Dalip Singh Mehta, IIT Delhi *Laser Based Solid State Lighting and Visible Light Communications (VLC) in Free-space and Under Water*
TEA BREAK 18:15 – 18:30	
18:30 – 19:15	ILA General Body Meeting
19:30	Departure for Banquet

Day 2: Tuesday, January 30, 2024

SESSION – 5	
Invited Talk-6 9:30 – 10:00	Prof. Anindya Datta, IIT Mumbai *Single particle dynamics of water-soluble semiconductor nanocrystals*
Invited Talk-7 10:00 – 10:30	Dr. Atasi Pal, CSIR -CGCRI, Kolkata *Impact of optical Components on fiber laser power scaling*
TEA BREAK 10:30 – 10:45	
SESSION – 6	
Invited Talk-8 10:45 – 11:15	Prof. Venugopal Achanta, CSIR-NPL, Delhi *Metamaterials for single molecule detection to single photon emitter*
Invited Talk-9 11:15 – 11:45	Prof. Bodhaditya Santra, IIT Delhi *Quantum simulation and computing using cold atoms with tunable interactions*
SESSION – 7 BRNS AND INDUSTRIAL SESSION	
11:45 – 13:15	BRNS and INDUSTRY PRESENTATIONS
LUNCH 13:15 – 14:15	
SESSION – 8	
14:15 – 16:45	POSTER SESSION - 2
TEA BREAK 16:45 – 17:00	
SESSION – 9	
Invited Talk-10 17:00 – 17:30	Dr. G. K. Sahu, BARC, Mumbai *Design to delivery of laser enriched Lu-176 for production of Lu-177 in India*
Invited Talk-11 17:30 – 18:00	Dr. Aniruddha Kumar, BARC Tarapur *Advances in laser material processing applications with oscillating beam*
TEA BREAK 18:00 – 18:15	
18:15 – 19:15	Special Evening Talk Prof. Ajoy Ghatak, IIT Delhi WHAT IS LIGHT & EVOLUTION OF QUANTUM THEORY
19:15	Dinner

Day 3: Wednesday, January 31, 2024

SESSION – 10	
Invited Talk-12 9:30 – 10:00	Dr. Praveen Kumar Velpula, UGC-DAE CSR, Indore *Post-compression of pulses: An approach to the few-cycle terawatt regime*
Invited Talk-13 10:00 – 10:30	Dr. Sulbha Sharma, SVVV, Indore *Photobiomodulation: Mechanism and Clinical Applications*
TEA BREAK 10:30 – 10:45	
SESSION – 11 PhD Thesis Presentations (Parallel Sessions) 10:45 – 13:15	
LUNCH 13:15 – 14:15	
SESSION – 12	
14:15 – 16:45	POSTER SESSION - 3
TEA BREAK 16:45 – 17:00	
SESSION - 13	
Invited Talk-14 17:00 – 17:30	Dr. Jinto Thomas, IPR, Gandhinagar *Overview of Thomson Scattering Diagnostics Developments for High-Temperature Plasma*
Invited Talk-15 17:30 – 18:00	Prof. Rajeev Paramel Pattathil, STFC Rutherford Appleton Laboratory, UK *Extreme Photonics: Science and Applications*
CULTURAL PROGRAM 18:00 – 20:00	
20:00	Dinner

Day 4: Thursday, February 01, 2024

SESSION – 14	
Invited Talk-16 9:30 – 10:00	Prof. Tushar Kanti Mukherjee, IIT Indore *Doing Reactions within Self-Assembled Molecular Crucibles: From Biocatalysis to Photocatalysis*
Invited Talk-17 10:00 – 10:30	Prof. Sharad Gupta, IIT Indore *Optically Active Nanoparticles for NIR Imaging and Therapy*
Invited Talk-18 10:30 – 11:00	Dr. Tarun Kumar Sharma, RRCAT, Indore *Recent Advancements in Semiconductor Lasers & Detectors*
TEA BREAK 11:00 – 11:15	
SESSION – 15	
Invited Talk-19 11:15 – 11:45	Dr. Ajit Upadhyay, RRCAT, Indore *Electron Acceleration from Laser Produced Plasmas: Simulation Studies*
Invited Talk-20 11:45– 12:15	Dr. Manoj Kumar Saxena, RRCAT, Indore *Raman optical fiber distributed temperature sensor-based Agni-Rakshak system*
SESSION 16: CONCLUDING SESSION	
12:15 – 13:30	Award Presentation and Concluding Ceremony
LUNCH 13:30 – 14:30	

KEYNOTE ADDRESS AND INVITED TALKS

KEYNOTE ADDRESS

Controlling Light-Matter Interactions for Applications at Molecular Scales

Debabrata Goswami
Indian Institute of Technology Kanpur
Kanpur - 208016
Email: dgoswami@iitk.ac.in

One of the most fundamental modes of observation is the detection of light or its associated photons. Spectroscopy uses light-matter interactions to elucidate objects and events at quantum time and length scales. For reporting quantum events as accurately as possible, spectroscopists strive to be ideal passive observers who rarely or minimally perturb the quantum system or process under investigation. In contrast, for steering chemical reactions or for exerting control and manipulating quantum processes, active participation is necessary. Since quantum events are temporally in the ultrafast regime, prevailing only at femtosecond timescales, the manipulations must also occur at ultrafast timescales. To achieve an even higher level of control, "coherent control" becomes necessary. Coherent control involves manipulating the dynamics of a chemical reaction at various stages as it progresses, typically by irradiation with specifically shaped ultrafast laser pulses. This level of control is crucial in fields such as quantum information processing, quantum computing, and the development of molecular interventions for therapeutic purposes. The integration of spatial and temporal control allows a more comprehensive approach to manipulate and control chemical systems. This emerging concept of spatiotemporal control combines spatial and temporal control principles to simultaneously control both the dynamics and position (in time) of observable events. In this presentation, we explore the mechanisms of chemical control using femtosecond pulse shaping, highlighting the need to consider both spatial and temporal domains to maximize control at microscopic scales. In particular, the discussion will also focus on our recent localization studies with femtosecond optical tweezers.

Special Evening Talk

What is Light & Evolution of Quantum Theory

Ajoy Ghatak
Optics & Photonics Centre
Indian Institute of Technology Delhi,
Hauz Khas, New Delhi-110016
Email: ajoykghatak@gmail.com

Abstract: The lecture will briefly discuss various models of light which led to the evolution of quantum theory; this will be followed by the analysis of the double slit interference experiment. If there is time, we will introduce the concept of entanglement and give a simple derivation of Bell's inequality; the 2022 Nobel Prize in Physics was awarded (partly) for experiments with entangled photons, establishing the violation of Bell inequalities.

About the speaker:

Ajoy Ghatak is currently Honorary Professor at the Centre for Optics & Photonics @ IIT Delhi. He was President of The National Academy of Sciences, India (the oldest Science Academy in India) during Jan 2021- Dec 2022. He received his BSc from Agra College, MSc from Delhi University and PhD from Cornell University. After a Research Associateship at Brookhaven National Laboratory, he joined IIT Delhi in 1966. Professor Ghatak has research interests in Fiber Optics & Quantum Mechanics. He has authored several books including his undergraduate text on ***OPTICS*** which has been translated to Chinese and Persian. He is recipient of the 2008 SPIE Educator award in recognition of "*his unparalleled global contributions to the field of fiber optics research, and his tireless dedication to optics education worldwide..*"; the OSA 2003 Esther Hoffman Beller award; International Commission for Optics 1998 Galileo Galilei award and also the CSIR 1979 S.S. Bhatnagar award. He received the OSA 2020 Sang Soo Lee award and the 2021 SASTRA-G N Ramachandran Award for Excellence in Physics .

Invited Talks

IT-01

Ultrafast Charge Carrier Dynamics at the Interface of p-n Semiconductor Heterojunctions

Hirendra N. Ghosh, *National Institute of Science Education and Research (NISER), Bhubaneswar, Odisha 752050, India Email: hnghosh@niser.ac.in, hnghosh2004@gmail.com*

Metal chalcogenides are the potential competitors to traditional crystalline silicon solar cells owing to their unique properties such as high abundance, high absorption coefficients (10^4-$10^5 cm^{-1}$), tunable bandgap, cost-effectiveness, and robust stability. However, their performance is constrained by challenges such as rapid recombination of photogenerated electron-hole pairs and inadequate band edge potentials.To address these limitations, p-n heterojunctions, where a high-bandgap n-type semiconductor is combined with a low-bandgap p-type semiconductor, have emerged as a highly promising approach. This approach facilitates the creation of reliable and efficient photonic devices capable of harnessing a broader spectrum of solar radiation. These junctions serve as the main active sites for efficient charge transfer processes, ensuring rapid separation and migration of photoinduced charge carriers due to the built-in electric field. Furthermore, to gain a comprehensive understanding of the optical and material properties of these heterojunction systems, it is imperative to investigate the ultrafast processes involved such as charge transfer, trapping, and relaxation dynamics of photo generated electrons and holes. To this end, femtosecond transient absorption spectroscopy has been employed as a valuable tool. We have investigated the charge transfer dynamics at the interface of p-type copper, antimony, tin chalcogenides (Cu_2ZnSnX_4, CuX, SnX, Sb_2X_3, $CuInX_2$: X=S, Se,) and n-type cadmium chalcogenides (CdX, X=S, Se) which is widely used in solar cell technology and photocatalysis. By probing into these ultrafast processes, research efforts aim to unlock opportunities for the development of highly efficient photovoltaic and photocatalytic devices, thereby contributing to the mitigation of energy and environmental challenges.

References:

(1) Kaur, A.; Goswami, T.; Babu, K. J.; Ghorai, N.; Kaur, G.;Shukla, A.; Rondiya, S. R.; *J. Phys. Chem. C* **2020**, *124*,19476-19483.
(2) Kaur, A.; Goswami, T.; Rondiya, S. R.; Jadhav, Y. A.; Babu, K.J.; Shukla, A.; Yadav, D. K.; Ghosh, H. N. *J. Phys. Chem. Lett.* **2021**, *12*, 10958-10968.
(3) Ghorai, N.; Sachdeva, M.; Kharbanda, N.; Ghosh, H.N. *ACS Photonics* **2023**, *10*, 733-742.
(4) Kaur, A.; Goswami, T.; Babu, K. J.; Shukla, A.; Bhatt, H.;Ghosh, H. N. *J. Phys. Chem. Lett.* **2022**, *13*, 11354-11362.
(5) Kaur, A.; Goswami, T.; Babu, K. J.; Ghosh, H. N. *J. Phys. Chem. Lett.* **2023**, *14*, 7483-7489.

IT-02

Quantum Weak measurement meets Spin Orbit Photonics

Nirmalya Ghosh, *Centre of Excellence in Space Sciences India (CESSI), Bio-Optics and Nano-photonics (bioNap) Laboratory, IISER – Kolkata, Mohanpur – 741246, India., Email: nghosh@iiserkol.ac.in*

Spin (SAM) and orbital angular momentum (OAM) of photons are usually ascribed to the quantum nature of light. However, classical light beams can also carry both SAM and OAM, which are associated with circular / elliptical polarization and phase vortex, respectively. Thus, the evolution of polarized light beam in curved trajectorymimics the spin orbit interaction (SOI) effects of a massless spin 1particle (photon). In this talk, I shall discuss some of our recently observed intriguing SOI effects of classical light beam, like spin and orbital Hall effect, photonic spin-momentum locking in plasmonic metamaterials etc. In this context, I shall discuss the realization of quantum weak measurements using classical polarized light, which we have employed to amplify the SOI effects. I shall highlight our recent work on extending weak measurements into the domain of plasmonics, and discuss new concepts of weak value amplification (WVA) using standard path interference, using spectral line shape of optical resonance as pointer, natural WVA in Fano resonances and so forth. The potential applications of these in high precision optical metrology will be discussed.

IT-03

Recent advances in laser-assisted trace gas sensing and their applications

Nilesh J. Vasa, *Indian Institute of Technology, Chennai, Tamil Nadu-600036 Email: njvasa@iitm.ac.in*

There is a growing interest in trace gas analysis for widespread applications, such as industrial process monitoring, exhaust sensing, outdoor and indoor air quality analysis, defense, atmospheric sciences and environmental monitoring. Various trace pollutant gases, greenhouse gases and volatile organic compounds emitted from power plants, biogas plants and various industries are essential considering their adverse effect on urban atmospheric pollution, environment and health. Laser-based optical techniques allow non-contact, remote measurements of pollutant gases and emissions with high selectivity and sensitivity. Various optical-based methods will be discussed to monitor and sense trace gases, such as CO_2, CH_4, NH_3, H_2S, water vapor, etc. In the present talk, photonics-based conventional approaches and recent advances in trace gas sensing and monitoring will be outlined. Further, applications of a broadband photoacoustic technique for multiple gas sensing with a wide dynamic measurement range will be described.

Keywords: Trace gas sensing, multiple gas sensing, dual-wavelength absorption, broadband photoacoustic spectroscopy

IT-04

Development of Laser based Sensors and Scientific Instruments at LEOS, ISRO

R.V.L.N. Sridhar, *Laser Systems and Instrumentation Group Laboratory for Electro-Optics Systems (LEOS), Indian Space Research Organization (ISRO), Bengaluru-560058, Email: rvlnsridhar@leos.gov.in*

The LASER has provided amazing solutions to numerous problems since its invention and has become ubiquitous, finding utility in diverse applications in every section of modern society. The last four decades have witnessed a gamut of applications in utilization of these magnificent devices, a noble invention of the 19th century. Both laser technology and space operations have matured substantially in recent decades, offering synergistic possibilities for using lasers from space-based platforms. From the first laser fired on another planet to observatory guide stars and space collision avoidance systems, lasers in space are making news with numerous advances and universal firsts (as far as we know). With the beginning of the lunar laser ranging experiment in the 1960s, the use of lasers in space moved from the realm of science fiction into reality. Our space agency, the ISRO (Indian Space Research Organization) is becoming one of the leading space agencies worldwide in realizing the possibility of low-cost planetary missions, starting the journey with the Chandrayaan-1, followed by the Mangalyaan and the recent historic triumph by landing a craft on the lunar southern high latitude region and roving a 6-wheeled Pragyaan rover. The first use of lasers by the ISRO was in the Chandrayaan-1 mission, which flown an instrument named 'Lunar Laser Ranging Instrument (LLRI)' for the generation of 3-dimensional lunar topography. This payload was developed at Laboratory for Electro-Optics Systems (LEOS), one of the vital branches of the ISRO known for the development of high accuracy electro-optical attitude/navigation sensors, 1-meter class telescope systems, optics and optical assemblies, detectors, and scientific instruments. This invited talk sheds light on the utilization of lasers at LEOS in the development of absolute range and velocity sensors and scientific instruments for space use. A few flown in-house developed laser sensors and instruments are: FOG (Fiber Optics Gyroscope), LASA (Laser Altimeter), LDV (Laser Doppler Velocimeter), LLRI (Lunar Laser Ranging Instrument), LE-LIBS (Low-energy Eye-safe Laser Induced Breakdown Spectroscope) etc. A few of the above have played a crucial role during Chandrayaan-3's Vikram craft landing and the lunar surface chemistry studies. A bunch of promising laser-based technology development programmes, i.e., Range Finder, LiDARs, optical communication terminals, tunable laser spectroscopy, Raman spectroscopy etc., are pipelined for upcoming missions. The purpose of this talk is to amplify the drive in the application of laser technology for the exploration missions. There exists a dire need for the in-house development of space-qualified laser sources to further spread the wings of laser technology to unravel the secrets of the neighbourhood moons, planets and deep space, in unison with you all.

IT-05

Laser Based Solid State Lighting and Visible Light Communications (VLC) in Free-space and Under Water

Dalip Singh Mehta, *Bio-photonics and Green Photonics Laboratory, Department of Physics, Indian institute of Technology Delhi, Hauz-Khas, New Delhi 110016, India, Email: mehtads@physics.iitd.ac.in*

Light emitting diodes are high efficiency solid state lighting devices which are currently being used for various applications, such as, general lighting, automobile lighting, street lighting, display devices, TVs, etc. The LEDs are highly efficient, low power consumption, long lifetime, compact, and environment friendly. But for very high brightness applications LEDs cannot be used, because the maximum brightness that can be obtained using LEDs is 300 Lumen/W. Despite many advantages of phosphor converted-LED source, the efficiency droop in LED under high injection current is limiting factor for high brightness illumination. This is due to the nonradiative carrier loss mechanism either inside or outside the active region's quantum wells (QWs), which is responsible for efficiency droop, and it has a negligible effect at low currents but significant at high currents.

To overcome the efficiency-drop of LEDs laser-driven phosphor-converted (LD-PC) light source is the newly developed solid-state lighting device for high brightness white light applications, such as, streetlights, stadium lights, and automobile high beam lights are possible. The white light generation mechanism in a phosphor-converted laser diode (pc-LD) is similarlike the phosphor-converted LED (pc-LED) source for general illumination purposes. In the development of pc-LD source, the directionality and high scattering property of laser is the main advantage for high brightness illumination. We have developed [1-4] pc-LD based extended white light source with uniform illumination, such as, pc-LD tube-light and pc-LD light sheet. An innovative device for laser-based phosphor-converted tube-light source with uniform illumination developed in which directionality and high brightness is exploited. The transparent tube was coated with Ce doped YAG phosphor. The phosphor absorbs bule photons and generates bright yellow light. In another innovation laser-line-driven phosphor-converted light-sheet with uniform illumination was developed. A high power single laser beam can be converted into a laser line and coupled into a light sheet via total internal reflection and coated glass sheet with Ce:YAG phosphor converts blue light into white light. In another innovation we have designed and developed multilayer-structured extended diffuser system for thermally stable laser-phosphor converted white light source. In the development process, the extended diffuser was used to homogenously distribute the laser power for optimal excitation of the surface coated phosphor layer utilizing the scattering at the diffuser's surface and the total internal reflection (TIR) inside the diffuser [5-7]. We have also developed a prototype of automobile head lamp using laser driven phosphor converted white light source. Experimental results of all the above developed laser based solid state white light devices will be presented. Finally visible light communication (VLC) using LEDs and laser-

driven phosphor converted source will be presented. VLC in free space and under water with be discussed. The current research and development in LD-PC is to generate high-brightness ~2000Lumen per watt and continuous spectrum like Sunlight so that best light source high quality illumination can be realized.

References:

1. A. K. Dubey, M. Gupta, V. Kumar, V. Singh, and D. S. Mehta, "Blue laser diode-pumped Ce: YAG phosphor-coated cylindrical rod-based extended white light source with uniform illumination," Laser Phys. 29, 56203 (2019).
2. A. K. Dubey, M. Gupta, V. Kumar, and D. S. Mehta, "Laser-line-driven phosphor-converted extended white light source with uniform illumination," Appl. Opt. 58, 2402–2407 (2019).
3. A. K. Dubey, V. Kumar, M. Gupta, and D. S. Mehta, "Thermally stable laser-driven phosphor converted white light source using multilayer structured diffuser system," Laser Phys. Lett. 17, 126001 (2020).
4. A. K. Dubey, V. Singh, M. Gupta, V. Kumar and D. S. Mehta, “Monitoring the health laser driven phosphor converted white light source using spectral interference technique” Optics and Laser in Engineering, March 2021.
5. V. Kumar, K. Usmani, V. Singh, A. K. Dubey, M. Gupta, and D. S. Mehta, "Laser speckle reduction using spatially structured and temporally varying beams using double diffractive optical elements," Laser Phys. Lett. 17, 036003 (2020).
6. V. Kumar, M. Gupta, A. K. Dubey, S. Tayal, V. Singh, and D. S. Mehta, "Design and development of laser speckle reduction device using waveguide diffuser and pyramidal cavity for projection imaging," J. Opt. (IOP) 22, (2020).
7. V. Kumar, A. K. Dubey, M. Gupta, V. Singh, A. Bhutola and D. S. Mehta, “Speckle noise reduction strategies in laser-based projection imaging, fluorescence microscopy, and digital holography with uniform illumination, improved image sharpness, and resolution,” accepted in Optics and Laser Technology, March 2021.

IT-06

Single particle dynamics of water-soluble semiconductor nanocrystals

Anindya Datta, *Department of Chemistry, Indian Institute of Technology Bombay, Powai, Mumbai 400 076, India. Email: adutta@iitb.ac.in*

Fluorescence correlation spectroscopy and femtosecond transient absorption spectroscopy have been used to investigate the photoprocesses in two kinds of nanocrystals, namely 3-mercaptopropionic acid (3-MPA) capped Cu(I)-doped CdS (Cu:CdS)[1] and Copper Indium Sulphide (CIS)[2] quantum dots (QDs). Photoactivation of the Cu:CdS QDs via dim/dark to bright particle conversion is observed at higher excitation powers. Dispersive blinking kinetics in undoped QDs reflects the involvement of a broad distribution of trap states. A lesser extent of dispersity is observed for doped QDs, in which the hole-capture by the Cu-defect states predominates. Excitation fluence dependence of blinking rate highlights the role of Auger recombination in undoped QDs, which is suppressed significantly upon doping, due to disruption of electron-hole correlation. On the other hand, for the CIS QDs, an unusual excitation wavelength-dependence of photoactivation / photocorrosion is manifested in the increase in the initial correlation amplitude G(0) for λ_{ex}= 532 nm, but decrease for λ_{ex}= 405 nm. This has been rationalized in terms of different contributions from surface-assisted recombination in the two cases. Blinking times obtained from the Autocorrelation Functions (ACF) of the 100-200 ns lifetime component (core Cu-mediated recombination) are almost unaffected by shelling, but those from the ACF for the 10-30 ns lifetime (surface states) increases significantly. Absence of cross-correlation between the two recombinative states of bare CIS QDs and the emergence of an anticorrelation with the introduction of ZnS shell is observed, indicating the diffusive nature of the two states for CIS-ZnS. The diffusion is inhibited in base CIS QDs due to the preponderance of surface states.

[1] Das S, Rana G, Ali F and Datta A. *Nanoscale*, **2023,** *15, 4469-4476*

[2] Singha P, Kistwal T and Datta A. *J. Phys. Chem. Lett.*, **2023**, *14*, 4289-4296.

IT-07

Impact of optical Components on fiber laser power scaling

Atasi Pal, *Fiber Optics & Photonics Division, CSIR-Central Glass & Ceramic Research Institute, Kolkata, Email: atasi@cgcri.res.in*

Thermal fracture, melting of the core, thermal lens, nonlinear effect, optical damage and finite pump brightness are the conventional constrains to llimit the diffraction-limited power scaling in a fiber laser. Hence, the properties of the gain fiber have strong influence on the laser performance. The talk will discuss about the development of gain giber and other essential component such as brightness conserved pump combiner, grating pair, cladding light stripper and mode filed adaptor. The basic principle, fabrication method, and implementation in fiber laser design will be presented.

IT-08

Metamaterials for single molecule detection to single photon emitter

Venu Gopal Achanta, *CSIR- National Physical Laboratory, Dr. K.S. Krishnan Marg New Delhi – 110012, India, Email: director@nplindia.org*

Metamaterials are designed materials with dielectric constant and magnetic permeability values that do not exist in nature. These are achieved by combining sub-wavelength featured scattering elements of metals and dielectrics. Metamaterials can mimic novel phenomena observed in various branches of science and engineering in the regime of optical to THz frequencies. In addition to the geometrical resonances, coupled plasmon and dielectric modes have led to various interesting demonstrations covering broadband metamaterials, hyperbolic metamaterials, bound state in continuum, reflectionless potentials, among others. These have helped modulate the optical, and magneto-optical properties, emission from quantum emitters including directional emission, study orbital angular momentum states, and impedance matched layers for omnidirectional suppression of reflection. In this talk, I will present some of these metamaterial structures and their applications that include single molecule sensing and single photon emission. For single molecule sensing, ellipsometric measurements offer high sensitivity in combination with perfect absorber metamaterial. Surface enhanced Raman specroscopy (SERS) offers high sensitivity, as well as selectivity but requires SERS substrate that is uniform, stable and offers high local field enhancement. For directional single photon emission, a hyperbolic metamaterial or a bound state in continuum are most suitable.

IT-09

Quantum simulation and computing using cold atoms with tunable interactions

Bodhaditya Santra, *Department of Physics, Indian Institute of Technology, Delhi, New Delhi 110016, India, Email: bsantra@physics.iitd.ac.in*

The rich internal structure of atoms provides unique platform to study various quantum condensed matter phenomena by high precision quantum initial state engineering, manipulation and final state detection. The unprecedented controllability of various quantum states in atomic systems can be achieved by using high precision lasers and magnetic fields. In this talk I will present the progress of our lab towards building Cesium atom based quantum systems such as quantum computer and quantum memories.

Keywords: Quantum computing, Quantum memory, Cold atom

Reference: N. Singh et al. *Collision dynamics of a few atom quantum system with tunable interaction*, Physica Scripta, 98 (2023) 075401

IT-10

Design to Delivery of Laser Enriched Lu-176 for production of Lu-177 in India

G.K. Sahu, ATLAD, *BTDG, Bhabha Atomic Research Centre, Trombay, Mumbai - 400085*
Email: gksahu@barc.gov.in

The isotope of Lutetium (Lu-177) found immense medical application in Targeted Radio Therapy (TRT) for treating cancer patients due to its favourable half-life, radio activity and energy range and its concurrent use for imaging. Lu-177 is synthesised by neutron activation of Lu-176 in a nuclear reactor by (n,**)** reaction (Carrier Added CA route). It can also be synthesised from Yb-176 by (n,) reaction followed by ß-emission (No Carrier Added NCA route). Both have their pros and cons. For achieving required radio-nuclidic purity and specific activity, the precursor isotopes need to be enriched to a requisite high level. ATLA Division of BTDG, BARC has taken up the task of enriching Lu-176 by Laser Isotope Separation method where the targeted isotope is selectively ionised by set of precisely tuned laser beams. The talk will discuss this activity of design to delivery of this enriched Lu-176 isotope which included spectroscopy for identifying suitable wavelength scheme, development of atomic vapor source, tunable laser for selective photo-ionization, efficient ion extraction and product recovery. Lutetium material is kept in a tungsten crucible and an electron bombardment heating is used for generating a collimated atomic beam. The atomic beam interacts with a set of three laser beams of precisely tuned wavelength. Tunable SLM dye laser is used for first two steps for high selectivity whereas a multimode laser is used in third stage for efficient ionization. Multi-pass optics is used for optimum vapor laser overlap. The photo-ions generated are collected onto a plate by a suitable ion extraction electrode setup which allows efficient ion extraction, reducing sputtering loss and minimal neutral atom collection. The entire LIS process is designed indigenously in BARC, and it is able to supply about 4 mg of enriched (> 80% from its natural abundance of 2.59%) Lu-176 per month consistently for neutron activation and dose preparation for its end use in hospitals. This caters to a sizable proportion of present requirement of India. We are planning to enhance the production to meet entire requirement of India in near future by making our country self-reliant.

IT-11

Advances in laser material processing applications with oscillating beam

Aniruddha Kumar, *Fuel Fabrication, Nuclear Recycle Board, Bhabha Atomic Research Centre, Tarapur, Maharashtra, India - 401504, Email: aniruddhak@barc.gov.in*

Commercial introduction of high-power fiber laser with excellent beam quality has enabled rapid development of remote laser scanning (RLS) based applications. In comparison to laser applications with fixed optics technologies, RLS offers increased flexibility, higher operational speed, and reduced cycle time to process a wide range of materials. The major benefit of using high-brightness fiber lasers in remote welding is their ability to increase stand-off distance and scan field, while simultaneously providing a small spot size for higher weld speed and deeper weld penetration. Beam oscillation techniques during laser material interaction offer several possibilities to influence the energy deposition to the substrate. In oscillation laser welding, the laser beam oscillates periodically in a designated path with respect to the beam axis under conventional process conditions. In comparison to conventional laser welding process, additional process variables, e.g. oscillation amplitude, oscillation frequency and oscillation trajectory plays an important role in altering the energy deposition, which in turn modify the morphology and microstructure of the weld. Brilliant laser sources in conjunction with beam oscillation makes the welding process stable against dynamic focal point shift, increases process efficiency, changes the cooling rate and makes it possible to join dissimilar metallic welds which traditionally were non-laser weldable.

In laser cutting, quality of laser fusion cuts has been found to decrease with higher sheet thickness in form of dross formation and striations. These are created by the melt flow along the cutting front, which is induced by the locally absorbed laser power. Very recently it has been found that longitudinal oscillation in the cutting direction increases the cut quality. Laser beam oscillation has also been found to influence laser surface hardening process. High speed laser beam weaving has also found application in laser-based cleaning processes.

The proposed talk will discuss laser oscillation welding process using high brightness fiber lasers. It will also deliberate the major advantages of this process in comparison to conventional laser welding process and the underlying physics behind these advantages. Practical case studies involving oscillation welding of laser cut carbon steel specimens with varying surface roughness, dissimilar welding between pure Copper-Aluminum thin sheets will also be discussed. This talk will also highlight a novel weld heat tint removal process using fiber laser.

IT-12

Post-compression of pulses: An approach to the few-cycle terawatt regime

Praveen Kumar Velpula, *UGC-DAE Consortium for Scientific Research, University Campus, Khandwa Road, Indore, M.P., India, Email: velpulacsr@gmail.com*

The development of compact laser sources with high energy and ultrashort durations has enabled various key applications from laboratory astrophysics to compact particle accelerator sources. One of the most important applications is laser-based particle acceleration which requires a Tera-Watt regime. Most of the laser-based particle accelerators have been currently operating at low-repetition rates (<10 Hz). The particle accelerators at high repetition rates like 1 kHz/10kHz will be greatly benefited. Ytterbium (Yb) -based laser sources are scalable to higher repetition rates and kWs of average power, much beyond widely used Ti:sapphire systems. However, the pulse duration achievable with Yb-based amplifiers can only reach a few hundred femtoseconds (fs) due to the limited gain bandwidth. In this concern, we found a prospective approach of post-compression to produce ultrashort pulses at high repetition rates.

In this talk, I will demonstrate a compact pulse post-compression technique that compresses high-energy pulses from 1.2 picoseconds to 9.6 femtoseconds at 1 kHz repetition rate using gas-filled multi-pass cells (MPCs). Employing dual-stage compression with a second MPC stage supporting a close-to-octave-spanning bandwidth enabled by dispersion-matched dielectric mirrors, a record compression factor of 125 is reached at 70% overall compression efficiency, supporting 6.7 mJ pulses at a peak power of about 0.3 TW. Our results demonstrate the efficient conversion of multi-millijoule picosecond laser systems to high peak-power few-cycle sources, opening up new parameter regimes for laser-plasma physics, high energy physics, biomedicine, and attosecond science.

IT-13

Photobiomodulation: Mechanism and Clinical Applications.

Sulbha Sharma, *Shri Vaishnav Vidyapeeth Vishwavidyalaya, Indore – Ujjain Road, Indore – 453111, Email: sulbhsharma@svvv.edu.in*

Low level light therapy also called photobiomodulation has shown its potential for the treatment of different ailments in the last decade. Lasers have been the most important source of light radiation in this therapy. This interest in photo biomodulation has increased due to unravelling of the underlying mechanism of action on different cells, specially stem cells. A wide range of lasers are available, and their usage is well defined by different parameters, such as: wavelength, energy density, power output, and duration of radiation. Lasers are known to show photobiomodulation effect on the tissues and cells by affecting the behaviour of cells and tissue repair. This photobiomodulatory effectupsurges the cell proliferation, cell viability andstem cell differentiation by stimulating the cellular organelles such as mitochondria, cell membrane, photoreceptors, and ion channels. By affecting these cellular processes lasers are known to reduce inflammation, increase wound healing and help tissue repair and regeneration. Due to these biomodulatory effect lasers have been applied for various diseases and conditions, such as diabetes, brain injury and disorders, spinal cord damage, dermatological conditions, oral irritation, and in different areas of dentistry.

IT-14

Overview of Thomson Scattering Diagnostics Development for High Temperature Plasma

Jinto Thomas, *Institute for Plasma Research, Bhat Village, Near Indira Bridge, Gandhinagar-382428, Gujarat, Email: jinto@ipr.res.in*

Thomson scattering is an important diagnostic tool for diagnosing high-temperature plasma, e.g. in case fusion machines and reactors. However, implementing this method in machines like Tokamaks and other similar devices is rather cumbersome due to low Thomson scattering cross-section of electrons. It requires higher laser energies, good collection optics, efficient transport lines, and excellent background suppression. Pulsed lasers and high-gain detectors are crucial components of this diagnostic technique. In IPR, Thomson scattering diagnostics has been implemented in ADITYA and SST-1 tokamaks to measure plasma temperature and density. The ADITYA Thomson scattering system was a single-point measurement based on a Ruby laser. Currently, this system is being upgraded to a multi-point measurement system. In the case of SST-1, the Thomson scattering system is a multi-point diagnostic with six high-power Nd:YAG lasers. The laser facility for SST-1 is being considered for use in the upgrade of ADITYA. This talk provides an overview of the implementation of Thomson scattering system in these tokamaks and discusses salient features of observed results

IT-15

Extreme Photonics: Science and Applications

Rajeev Paramel Pattathil, *Novel Accelerator Science and Applications, Central Laser Facility,, STFC Rutherford Appleton Laboratory, Harwell Oxford,UK, Email: rajeev.pattathil@stfc.ac.uk*

Lasers with high peak powers combined with high repetition rates have enabled a quantum jump in the field of plasma accelerators in the last decade. As laser-driven plasma accelerators are maturing, facilities based on this technology are currently under design worldwide. With high power laser drivers operating at high repetition rates with kW average power, we are now entering a new era of applications of plasma accelerators in industry, medicine, security, and defence sectors. I will describe the details of the Extreme Photonics Applications Centre (EPAC) – the new £100M plasma accelerator-based facility under construction in the UK – and discuss its anticipated exploitation for cutting-edge science and applications.

IT-16

Doing Reactions within Self-Assembled Molecular Crucibles: From Biocatalysis to Photocatalysis

Tushar Kanti Mukherjee, *Department of Chemistry, IIT Indore, Simrol, Indore 453552, Madhya Pradesh, Email: tusharm@iiti.ac.in*

Enzymes drive various complex tandem metabolic reactions inside the confined, crowded, and heterogeneous cellular environments in a highly regulated and efficient manner. Toemulate Nature, it is essential to understand the under lying mechanistic pathway of enzymatic reactions under confined cellular environments. How the complex and heterogeneous cellular environment spatio-temporally regulates various biochemical reactions with high efficiency and selectivity is a fundamental question in cell physiology that has not been understood yet. Moreover, recent in vitro studies have highlighted the role of crowding on the formation of membraneless biocondensates via soft protein- protein interactions.[1,2]Thesemembraneless cellular condensates are believed to host and accelerate a wide range of complex metabolic processes in a highly regulated and efficient manner. Our recent findings answered few of these fundamental questions. My presentation will mainly focus on our recent efforts to understand and explore the chemical and biochemical reactivity within various self-assembled molecular crucibles. These self-assembled molecular crucibles include biomolecular condensates, synthetic condensates, and micellar assemblies. In the first part, I will discuss about the importance of liquid-liquid phase separation and biomolecular condensation of functional enzymes towards spatio-temporal regulation of enzymatic efficacy and selectivity (Scheme 1A).[1] The second part will focus on the remarkable influence of the charged aqueous interfaces of self-assembled micellar assemblies on the photocatalytic oxidative coupling of arylamines to azoaromatics under ambient air atmosphere (Scheme 1B).[3]

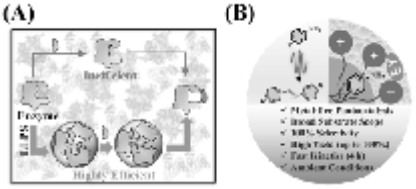

Scheme 1. (A) Spatio-temporal regulation of the efficacy and selectivity of biocataltic transformation via biomolecular condensation. (B) Boosting the photocatalytic efficacy within self-assembled molecular assembly.

References

1. B. Saini, and T. K. Mukherjee,*J. Phys. Chem. B***127**, 180, (2023).
2. C. K. Patel, C. Rani, R. Kumar, and T. K. Mukherjee,*Biomacromolecules***24**,3917, (2023).
3. S. Singh, V. Agarwal, T. K. Sarma, and T. K. Mukherjee,*Green Chem.***25**,9109, (2023).

IT-17

Optically Active Nanoparticles for NIR Imaging and Therapy

Sharad Gupta, *Biosciences and Biomedical Engineering Indian Institute of Technology, Indore, MP, India. Tel: +91-731-6603222, Email: shgupta@iiti.ac.in, sgupta.ucr@gmail.com*

Cancer is a deadly disease. It can be treated well if diagnosed in an early stage. Recent advancements in optical technologies bring new methods for disease diagnosis and treatment. Biological tissue is an optically turbid medium with a dominant scattering and absorption in the visible wavelength range. However, the tissue is relatively transparent, with minimal absorption and scattering in the near-infrared (NIR) wavelength range. This NIR wavelength window could be used for extracting molecular information for diagnostic applications and therapeutics. NIR active nanoparticles could be used as exogenous contrast agents, enabling us to visualize deeply buried inhomogeneities in tissue. We have developed optically active biocompatible nanoparticles for near-infrared fluorescence imaging. Due to significant absorption in NIR wavelength, the nanoparticles could also be used for photothermal therapy applications. Therefore, the tissue transparent NIR wavelength range provides an exciting option for deep tissue visualization and alternate therapeutics.

IT-18

Recent Advancements in Semiconductor Lasers & Detectors

T. K. Sharma[1,2] [1]*Materials Science Section, Raja Ramanna Centre for Advanced Technology, Indore-452013* [2]*Homi Bhabha National Institute, Training School Complex, Anushakti Nagar, Mumbai-400094, Email: tarun@rrcat.gov.in*

Semiconductor quantum structures are the heart of semiconductor lasers and detectors. Understanding the fundamental physics of such quantum structures is critical to optimize the operating characteristics of photonic devices that are made based on them. In our lab, we have been synthesizing quantum structures based on GaAs and GaN semiconductor materials. Advanced photonic devices like high power laser diode arrays and radiation tolerant photodetectors operating over a broad wavelength range are developed by using the grown heterostructures. Prior to the fabrication of devices, an in-depth characterization of the quantum structures is carried out by using optical, electrical and x-ray probes. It provides key parameters of the associated quantum structures which play a pivotal role in fine tuning the operating characteristics of indigenously made photonic devices. During this talk, selected examples on semiconductor lasers and detectors will be presented including their recent status. Special emphasis will be givenon understanding the fundamental physics of semiconductor quantum structures grown by MOVPE and MBE techniques.

IT-19

Electron Acceleration from Laser Produced Plasmas: Simulation Studies

Ajit Upadhyay[1,2] [1]*Homi Bhabha National Institute, Training School Complex, Anushakti Nagar, Mumbai 400 094, India* [2]*Laser Physics Applications Division, Raja Ramanna Centre for Advanced Technology, Indore 452 013, India Email: ajitup@rrcat.gov.in*

Study of dense matter in extreme condition has always been a matter of interest for theoretically study[1]. The invention of high-power pulsed laser paved the way to experimentally study the plasma in extreme condition [1,2]. When such laser pulse is focussed to a size of few μm using suitable focusing optic, it yields an enormous intensity (I) in the range of ~10^{18}-10^{22} W/cm^2, leading to creation of ionized matter under extreme conditions at the laser focus. Further, a number of particles viz. fast electrons, protons, ions and x-rays are accelerated to very high energy (~keV to tens of MeV) from the interaction region. The study of accelerated electrons from gaseous targets and energetic fast electrons generated in dense solids is a subject of research investigation for various potential applications including laser Wakefield acceleration[4], laser driven fast ignition[5], proton and ion acceleration[6], creation of ultrashort x-ray sources[7] and creation of warm dense matter.

The coupling of laser energy to electrons is fundamental to almost all topics in intenselaser–plasma interactions, including laser-driven particle and radiation generation, relativistic optics, inertial confinement fusion and laboratory astrophysics. In the case of laser irradiation of bulk solid targets, laser absorption takes place through electrons gaining energy (sub-MeV to tens of MeV) via various mechanisms governed by laser and plasma parameters. In addition to the well understood and studied mechanism of resonance absorption, there are mechanisms specific to the ultra-short laser pulse regime, viz., vacuum heating, JxB heating, etc. Energetic electrons, also termed as fast or hot electrons, dump energy in the over-dense plasma and solid density cold target, and even can escape from the target. Angular distribution of fast electrons is a direct manifestation of the applicable acceleration/absorption mechanisms and, therefore, has been widely investigated during last the two decades.

In this talk, I will discuss some results on Wakefield acceleration as well as some results on fast electron generation through JxB heating, both verified byparticle-in-cell (PIC) simulations and their experimental manifestation in ultra-short intense laser plasma interactions.

1. P. McKenna, D. Neely, R. Bingham, and D. Jaroszynski, editors,*Laser-Plasma Interactions and Applications* (Springer International Publishing, 2013).
2. P. Gibbon, *Short Pulse Laser Interactions with Matter* (Imperial college press, London, 2005).
3. D. Strickland and G. Mourou, *Opt. Commun.***56**, 219 (1985).
4. Gonsalves, A. J. et al. Petawatt laser guiding and electron beam acceleration to 8 GeV in a laser-heated capillary discharge waveguide. *Phys. Rev. Lett.* 122, 084801 (2019).
5. M. Tabak et al, *Phys. Plasmas***1**, 1626 (1994).
6. A. Macchi, M. Borghesi, and M. Passoni, *Rev. Mod. Phys*. **85**, 751 (2013).
7. H. Schwoerer et al, *Phys. Rev. Lett*.**86**, 2317 (2001).

IT-20

Raman optical fiber distributed temperature sensor system & 'Agni-Rakshak'

Manoj Kumar Saxena, *Fiber Sensors & Optical Spectroscopy Section, RRCAT, Indore & Homi Bhabha National Institute, Mumbai. Email: manojsaxena@rrcat.gov.in*

The advent of optical fiber sensors has significantly transformed the landscape of sensing technologies. Among these innovations, the Raman optical fiber distributed temperature sensor (ROFDTS) stands out as a remarkable class, offering the unique capability to not only measure the magnitude of temperature elevation but also discern its spatial distribution continuously along the entire length of the optical fiber. In the ROFDTS system, every bit of the optical fiber serves a dual purpose as both a sensing element and a data transmission medium, effectively functioning as an array of distributed sensors.

This presentation will delve into the groundbreaking applications of ROFDTS, particularly its potential to replace conventional point sensors such as thermocouples and RTDs, along with the associated wiring complexities. The inherent advantages of ROFDTS become particularly evident in diverse scenarios, including temperature monitoring and fire detection in nuclear and harsh environment. Noteworthy applications span various critical areas such as fire detection in power supply cables, extensive gas pipelines, oil wells, the sodium coolant loop of fast breeder test reactors, conveyor belts in cement and coal industry etc.

The Raja Ramanna Centre for Advanced Technology (RRCAT) has successfully developed and optimized the ROFDTS system, aptly named 'Agni-Rakshak,' with a primary focus on fire detection application. This talk will comprehensively cover the journey of 'Agni-Rakshak,' encompassing its design, development, practical applications, real-life deployments, and the subsequent technology transfer to Indian industries.

Throughout the presentation, the speaker will address the challenges encountered during the development of the 'Agni-Rakshak' system and discuss innovative solutions implemented using non-stationary digital signal processing models. The talk aims to provide insights into the advancements, practical implications, and the broader impact of ROFDTS technology, showcasing its evolving potential in ensuring safety across diverse industrial applications.

References

1. B. Culshaw, A Kersey, 'Fiber-Optic Sensing: A Historical Perspective,' Journal of Lightwave Technology, 26, 1064 (2008).
2. M. K. Saxena, O. Prakash et. al., 'Studies on thermal profile measurement and fire detection in a power supply cable of a synchrotron radiation source by Raman optical fiber distributed temperature sensor system,' Optical Fiber Technology, 73, 103020 (2022).
3. M. K. Saxena et. al., 'Empirical mode decomposition-based detection of bend-induced error and its correction in a Raman optical fiber distributed temperature sensor,' IEEE Sensors Journal, 16(5), 1243 (2016).
4. M. K. Saxena et. al., 'Raman optical fiber distributed temperature sensor using wavelet transform based simplified signal processing of Raman backscattered signals,' Optics & Laser Technology, 65, 14 (2015).

CONTRIBUTORY PAPERS

Category - 1
Physics and Technology of Lasers

CP-01-01

Development of high repetition-rate second harmonic mid-ultraviolet radiations from a sealed-off copper bromide laser

*R. Biswal[*1,2], G. N. Tiwari[1], R. K. Mishra[3], O. Prakash[1,2], S. V. Nakhe[4] [1]Fiber Sensors and Optical Spectroscopy Section, RRCAT, Indore-452013 [2]Homi Bhabha National Institute, Anushaktinagar, Mumbai-400094 [3]Laser Power Supplies Division, RRCAT, Indore-452013 [4]RRCAT, Indore-452013 [*]Email: rbiswal@rrcat.gov.in*

This paper presents development of high pulse repetition-rate, watt-level average power, nanosecond pulsed, coherent mid-ultraviolet (UV) radiations by second harmonic generations (SHGs) from both the green and yellow radiation components of an in-house developed sealed-off copper bromide laser. At 19 kHz repetition-rate of the high beam quality pump laser and with type-I, critically phase matched β-BBO nonlinear crystals, average UV output powers of about 1.26 W at λ = 255.3 nm and 0.9 W at λ = 289.1 nm were generated corresponding to optical conversion efficiencies of about 9.2% and 12.5% respectively.

CP-01-02

Frequency Noise characterisation of in-house developed Non-Planar Ring Oscillator (NPRO) laser at 1064 nm and measuring the Linear Spectral Density (LSD) of the Frequency Noise

George J., Khursheed M., Reddy T. S. and Raja S.S, AEOSS, RRCAT, Indore-452013. Email: jogy@rrcat.gov.in

We developed and calibrated a frequency noise LSD measurement setup, bench-marking it against commercially available LSD data for an NPRO laser at 1064 nm. Minor deviations were observed in the measured LSD in the 100 Hz to 1 kHz Fourier frequency range, attributed to acoustic disturbances in the laboratory. The calibrated LSD setup successfully measured the frequency noise LSD of the in-house developed E-NPRO Laser at 1064 nm, with a noise floor of ~30 Hz/$\sqrt{}$Hz and has the capability to measure up to 5 kHz Fourier frequency.

CP-01-03

Four pass end pumped amplifier stage for the Ultra-narrow line width oscillator at 1064 nm

George J., Khursheed M., Reddy T. S., Pant B. C. and Raja S.S, AEOSS, RRCAT, Indore-452013, Email: jogy@rrcat.gov.in

A compact diode end-pumped four-pass MOPA amplifier was developed in-house capable of amplifying of an ultra-narrow line-width seed NPRO CW oscillator with a sub-100 Hz line-width at 1064 nm. The system achieved over 10 W output at 1064 nm with a pump power of 27.5 W per stage and a seed input power of 320 mW at 1064 nm..

CP-01-04

Line Tunable Operation of a Cryo-Cooled CO laser operating with CO_2 Laser Gas Mixture

Tatsat Dwivedi[1, 2], M B Sai Prasad[1], R C Das[1,2] , J Padma Nilaya[1, 2,] [1]Laser and Plasma Technology Division, BARC, Mumbai 400085, India [2]Homi Bhabha National Institute, Anushaktinagar, Mumbai 400094, India [*]Email: jpnilaya@barc.gov.in*

Cryo-cooled CW-CO laser utilising CO_2 laser gas mixture has been operated in dispersive cavity mode and lasing on more than fifteen CO transitions has been recorded. The wavelength and corresponding power obtained were measured and the corresponding CO transitions identified. A method to introduce the grating into the free running cavity was devised for its easy alignment. These CO transitions are not generally reported in conventional CO laser operation. The difference in the composition of the gain medium of this laser compared to a conventional system is responsible for this observation.

CP-01-05

Generation of 103 W of average power and 3.4 mJ of pulse energy from all-fiber Yb-doped Q-switched fiber laser using MOPA configuration

Ravindra Singh[*], Avdhesh Kumar, Usha Chakravarty, B. N. Upadhyaya, R. Arya, Laser Technology Division, Raja Ramanna Centre for Advanced Technology, Indore-452013 [*]Email: ravindrasingh@rrcat.gov.in

Generation of 103 W of average output power and 3.4 mJ of pulse energy from an all-fiberYb-doped Q-switched fiber laser at 1064 nm has been carried out using master oscillator power amplifier (MOPA) configuration.From all-fiber Q-switched Yb-doped fiber laser oscillator, an average output power of 1 W with a pulse duration of 175 ns at 30 kHz of repetition rate was achieved, which was further amplified using thepre-amplifier stage to generate an average output power of 16 W at the same pulse duration and repetition rate.The output signal power was further amplified using themain-amplifier stage to generate an average output power of 103 W with a pulse duration is 175 ns at 30 kHz of repetition rate. Laser output pulse characteristics have also been studied as a function of modulation frequency in the range of 30 kHz to 100 kHz. This nanosecond fiber laser has potential applications in micromachining.

CP-01-06

All DPSS Green Laser Pumped High Repetition Rate, High Power Dye Laser Oscillator-Amplifier Chain

Paramjit Rana, A. K. Tiwari, S. P. Sahoo, Anchal Gupta, S.K. Mishra, V.S. Rawat, Advanced Tunable Laser Applications Division, Bhabha Atomic Research Centre, Trombay, Mumbai 400085 Email: paramjit@barc.gov.in

High power dye laser plays an important role in various applications like selective photo ionization of targeted isotope, spectroscopy, lidar, photodynamic therapy etc. Copper vapor lasers (CVL) and frequency doubled diode pumped solid state green lasers (DPSSGL) are the possible pump lasers for generating the high average power, high p.r.f. dye laser beams in visible region (green-orange). We have demonstrated an optical fiber delivered, all DPSSGL pumped dye MOPA (Master Oscillator Power Amplifier) chain operating at 9 kHz pulse repetition frequency and compared the characteristics to that of a CVL pumped system. It was observed that operational efficiency of 8.5% was obtained with DPSSGL pump Rh 6G dye oscillator, which was similar to that with CVL pump beam.Amplification efficiency of 16.4 % and 30 % was obtained in a DPSS pumped pre-amplifier and main amplifier modules of the dye MOPA chain, while obtaining a total average output power of 28W. Pulse width of DPSS green laser pumped dye oscillator, pre-amplifier and main amplifier were measured to be 33 ns, 40 ns and 40 ns respectively where as the pulse width of DPSSL pump was measured to be around 40 ns. The performance efficiency and the temporal characteristics of CVL and DPSSGL pumped dye laser MOPA chain were found to be similar. Therefore, we concluded that DPSS green laser is an efficient and compact alternative to the CVL systems for pumping dye lasers to generate high PRF, high average power beams for various applications like selective photoionization of the isotopes.

CP-01-07

Development of 2 W narrow linewidth (<5 MHz) green laser at 532 nm.

Bhuvnesh,[1] C.P. Singh,[1,2] P.K. Gupta,[1,2] A. Nigam,[1,2] P. Hedaoo,[1] B. Prasad,[1] P. K. Mukhopadhyay,[1,2] R. Arya,[1] and S. K. Dixit.[1,2] [1]Solid State Laser Section, Laser Technology Division, RRCAT, Indore-452013. [2]Homi Bhabha National Institute, Training School Complex, Anushakti Nagar, Mumbai-400094 E mail: bhuvneshk@rrcat.gov.in.

We demonstrate 2 W green laser at 532 nm using Second Harmonic Generation (SHG) from the output of a lab made all-fiber master oscillator power amplifier continuous wave laser system delivering 25 W power at 1064 nm with linewidth <5 MHz. The seed is a fiber coupled single frequency laser at 1064 nm (linewidth < 5 MHz, 10 mW power). Amplification is carried out in multi-stage all-fiber amplifier system which allows power scaling of seed source from 10 mW to ~25 W without any signifiant contribution from pump, amplified spontaneous emmision and stimulated Brillouin scattering. A periodically poled lithium niobate crystal is used for SHG at 532 nm. The setup generate a

higly stable 2 W green laser at 532 nm. The immediate applications of the laser system can be a laser source for the light detection and ranging (LIDAR) and pumping source for developmet of other lasers.

CP-01-08

Development of cavity ring-down based ultra-high reflectivity measurement setup

V.V.V. Subrahmanyam[1], Talwar S[3], Rajiv. K[1],C. Mukherjee[1,2] and N.S. Benerji[1] [1]Optical Coatings laboratory, High EnergyLasers and Optics Section, RRCAT, Indore-452013. [2]Homi Bhabha National Institute, Training School Complex, Anushakti Nagar, Mumbai, 400094. [3]Software development laboratory, Laser controls & Instrumentation division,RRCAT,Indore-452013 Email: vsub@rrcat.gov.in

In this paper, the development of a cavity ring-down-based reflectance measurement setup for measuring the ultra-high reflectance of an optical mirror is presented using a simple diode laser. Filtered optical feedback re-injection concept adopted to enhance the better coupling between laser and external ring-down cavity. To avoid weakly coupled decay events, camera imaging and threshold timer circuit were incorporated. With this setup, the measured reflectance of the given ultra-high-reflecting mirror is determined to be 99.9960% with 0.0015% reproducibility.

CP-01-09

Development of 1.145 kW CW laser output power using signal combination of two fiber lasers

Avdhesh Kumar, [*]Pushkar Misra, Rajpal Singh, B. N. Upadhyaya, R. Arya, Laser Technology Division, Raja Ramanna Centre for Advanced Technology, Indore-452013, India [*]Email: avdhesh@rrcat.gov.in

In this paper, the work on development of 1.145 kW CW laser output power from fiber laser using signal combination of two single transverse mode all-fiber Yb-doped fiber lasers using fiber optic signal beam combiner (SBC)is reported. The signal beam combination comes under incoherent beam combination technique. Module-I & Module-II are identical to each other in terms of output spatial beam profile i.e., with M^2 ~1.24 and output spectrum peaks at 1080.2 nm & 1079.5 nm. The optical-to-optical slope efficiencies of Modules-I & II are 51% and 56%, respectively. The SBC technique of signal combination is very useful in power scaling of fiber lasers to multi-kilowatt level for material processing applications.

CP-01-10

Generation of 14 W average output power from all-fiber acousto-optic Q-switched Thulium-doped fiber laser at 1940 nm

Usha Chakravarty[*], A. Kuruvilla, Unniyarcha Somraj[#], Rajpal Singh, B. Ekka, B.N. Upadhyaya and R.Arya, Laser Technology Division, Raja Ramanna Centre for Advanced Technology, Indore-452013 [#]Department of Optoelectronics, University of Kerala [*]Email: ushac@ rrcat.gov.in

In this work, we report on the generation of 14 W average output power from the single stage Thulium-doped fiber laser in master oscillator power amplifier (MOPA) configuration. Pulse characteristics of an acousto-optic Q-switched Thulium doped fiber oscillator was studied by varying the modulation frequency in the range from 40 kHz to 80 kHz. The output pulse width from an oscillator can be tuned from 100's of ns to 1µs range by the variation of modulation frequency and pump power of the oscillator. Pulses with an average power of 640 mW and pulse energy of 8 µJ at 80 kHz was amplified in the Thulium doped fiber amplifier to obtain maximum pulse energy of 175 µJ with an average power of 14 W. The slope efficiency of the amplifier is 53%, and optical to optical conversion efficiency is 48 %.The output spectrum is centered at 1940 nm with the FWHM line-width of 1 nm. There is no sign of any nonlinear effects in the output. This laser is suitable for the material processing of polymers and transparent plastics.

CP-01-11

Development of a long cavity regenerative amplifier for amplification of long duration pulses;

R. K. Patidar[*], D. Daiya[#], N. K. Varshnay, S. Jain, A. Singh, Srikanth Gurram & N. S. Benerji; High Energy Laser & Optics Section, Raja Ramanna Centre for Advanced Technology, Indore 452 013, M.P; # also affiliated to Homi Bhabha National Institute, Mumbai, 4000064 [*]Email : rkpatidar@rrcat.gov.in

In conclusion, the development and characterization of a long diode pumped Nd: YLF regenerative amplifier for high energy laser is reported. The amplifier cavity length is ~ 6.3 m corresponding to roundtrip time of 42 ns. The amplifier amplifies laser pulses of estimated pulse energy of ~ 150 pJ to ~ 40 mJ, at a pulse repetition rate of 10 Hz and with an overall gain of ~ 2.7 x 10^8 in 14 roundtrips. The amplifier has been characterized for various parameters viz. pulse buildup, amplified energy, spatial beam profile etc.

CP-01-12

Multi-Beam All-Fiber Optic Front End System for High Energy Nd: Glass laser

Srikanth Gurram, N.K. Varshnay, O.B.Dongre, D.Daiya, A.Singh, J.Sharma, R.K.Patidar, N.S. Benerji, High Energy Laesr & Optics Section, Raja Ramanna Centre for Advanced Technology, Indore-452013, Email: srikanth@rrcat.gov.in

The develpment of an eight arm Fiber Optic Front End System (FOFES) with central a wavelength of 1053 nm has been reported here. The FOFES is a seed laser system for future multi-beam kJ class Nd:Glass lasers to be developed at RRCAT. The FOFES is based on a modular all-fiber architecture for ease of customization, upgrade, and alignment-free-ruggedness. The system delivers laser pulses with a pulse width of ~3ns and pulse energy of 10 nJ per beam at 100 kHz, with an average power variation of about 5% among the eight arms. The FOFES incorporates an Arbitrary Waveform Generator (AWG) for temporal shaping of laser pulses. The manuscript describes developement and preliminary results of an eight arm FOFES.

CP-01-13

Development of diode end pumped AO Q-switched Nd:YVO4 laser with short pulse duration suitable for LIBS applications

S. Sahu, A J Singh, , S. Ahlawat, P. K. Mukhopadhyay, R. Arya and S. K. Dixit, Solid State Laser Section, Laser Technology Division, RRCAT, Indore 452013. Email: ajsingh@rrcat.gov.in

In a compact linear cavity, diode end pumped AO Q-switched Nd:YVO_4 laser at high repetition rate with short pulse duration was developed. Laser generate 4 mJ of pulse energy at 2 kHz pulse repetition rate whereas at relatively high repetition rate ~80 kHz output pulse energy of ~80 µJ was obtained. The FWHM pulse duration was measured to be ~ 13ns. At the maximum output, beam quality parameter of laser was found to be ~1.3. The laser was successfully used in Laser induced breakdown spectroscopy (LIBS) setup and spectra for different elements were recorded.

CP-01-14

Diffraction phase profilometry of large size optics using aperture stitching

S. Chakraborty[1], P. Sharma[1], Y. Verma[1, 2], S. Raja S.[1] [1]Advanced Electro-Optics Systems Section, RRCAT, Indore, Madhya Pradesh 452013, India [2] Homi Bhabha National Institute, Anushaktinagar, Mumbai, Maharashtra 400094, India Email: subhamoy@rrcat.gov.in

We propose a white light diffraction phase interferometer that can perform surface profiling of reflective samples with a field of view (FOV) of ~ (1.2x1.8 mm^2). Our experimental setup is based on the diffraction phase imaging technique, which can provide full field whit light imaging without any mechanical movement. We validated the performance of our system by measuring the surface profile of a high-reflective plane sample. The measured surface peak to valley value of the plane sample is observed to be ~(20 ± 14) nm with a temporal sensitivity of 2.9 nm. For larger optics having aperture size around a few hundreds of mm, multiple interferogram images with partial overlap were acquired at different lateral positions. These partially overlapped adjacent phase images are aligned and stitched together using cross-correlation and fringe matching techniques to obtain the global surface topography of the larger optics.

CP-01-15

Novel method for identifying topological charge of discrete optical vortices

Vasu Dev, and Vishwa Pal, Department of Physics, IIT Ropar, Rupnagar, Punjab 140001, India. Email: vishwa.pal@iitrpr.ac.in

A discrete optical vortex (DOV), formed through a one-dimensional (1D) ring array of lasers, exhibits higher output power in comparison to a traditional continuous vortex, hence DOVs have attracted significant attention due to their potential high-power applications across diverse fields. In this study, we introduce a methodology for identifying both the magnitude and sign of the topological charge (l) of an unknown DOV. This is achieved through the analysis of the interference pattern generated by a 1D ring array of lasers. The interference pattern of an unknown DOV with $l \neq 0$ is averaged with the interference pattern corresponding to $l = 0$, resulting in a variation in fringe visibility as a function of the laser number (j) within the 1D ring array. The number of observed dips in the fringe-visibility curve is directly proportional to the magnitude of the topological charge of the DOV. Following the identification of magnitude, the sign of l is identified by averaging its interference pattern with that of $l = 1$. This results in a reduction of 1 dip for positive l values and an increase of 1 dip for negative l values in the fringe-visibility curve. Furthermore, we investigated the robustness of our method against phase disorder, demonstrating that phase disorder does not compromise the accurate identification of the topological charge of a DOV. The working principle, along with numerical and experimental results, is presented for DOVs spanning topological charges from small to large values. Our method can be exploited for applications involving DOVs, particularly in situations where continuous optical vortices face power limitations.

CP-01-16

Evolution and Kinetics of Gain-switched Ti:sapphire Laser

*Siba Prasad Sahoo[*1,2], V. S. Rawat[1,2], [1]Homi Bhabha National Institute, Anushaktinagar, Mumbai 400094 [2]Advanced Tunable Laser Applications Division, Bhabha Atomic Research Centre, Trombay, Mumbai 400085 Email: sibaps@barc.gov.in*

Temporal evolution and kinetics of a gain-switched Ti:sapphire laser are presented in this work. A four-level rate-equation-based theoretical model is developed and its numeral solutions are reported. The evolution of the upper laser level (ULL) population and laser pulse is evaluated by solving the rate-equations of photon density inside the cavity and the population density of different levels in which the spiking behaviour was observed. The effect of the pump pulse parameters and output coupler transmission on the output laser pulse was studied in detail. It was observed that the laser spiking effect increases with a decrease in the pump pulse energy, an increase in the pump pulse width, and an increase in the output coupler transmission.

CP-01-17

Fiber Optic-based DPSSL Pumped Single Longitudinal Mode High Repetition Rate Pulsed Dye Laser

Siba Prasad Sahoo[1, 2],P. Rana[1], A. K. Tiwari[1], S.K. Mishra[1], A. Gupta[1], V.S. Rawat[1,2] [1]Advanced Tunable Laser Applications Division, Bhabha Atomic Research Centre, Trombay, Mumbai 400085 [2]Homi Bhabha National Institute, Mumbai 400094 Email: sibaps@barc.gov.in

Development and characterization of a fiber optic-based diode pumped solid-state laser (DPPSL) pumped single longitudinal mode (SLM) high pulse repetition rate dye laser oscillator is presented in this paper. The green beam of the 9 kHz DPPSL was delivered to dye cell through bare optical fiber of 600-micron diameter and 0.22 numerical aperture with coupling efficiency of ~ 85%.A line image of 16 mm x 0.5 mm was generated at the centre of the dye cell using a designed fiber collimator and a cylindrical lens. A Littrow grating-based single longitudinal mode (SLM) laser oscillator with a solid etalon was developed and characterized using this fiber-optic pumped DPSSL beam. SLM operation was achieved in which time average bandwidth of nearly 250 MHz was attained. A tuning range of 562 nm to 611 nm was achieved using Rhodamine 6G ethanolic solution having peak wavelength of 572 nm and peak efficiency of 5.8 %.The SLM dye laser pulse shape mimics the pump laser pulse with reduced pulse duration as well as rise time. The green beam of DPSSL can be used to generate high average power, high repetition rate SLM dye laser by utilizing in MOPA configuration.

CP-01-18

Design and Development of Mechanical System for Refurbishment of Glass Tube sealed-off CO_2 laser

L B Rana, Rajiv Kumar Yadav, AvantikaGautam, Manoj Kumar and R Kaul. Laser Materials Processing Division, MSATG, RRCAT, Indore *Email:lbrana@rrcat.gov.in*

In this paper, we report design and development of mechanical system for Refurbishment of Glass Tube sealed-off CO_2 laser. AutoCAD and Solid Edge software were used to design and generating manufacturing drawings. Vacuum cavity which operates at pressure $1.01325x10^5$ Pa leads to the compressive forces acting inside the vacuum cavity. Mechanical design and manufacturing of vacuum cavity were carried out. Minimum achievable leak rates were estimated for the O-ring grooves with best achieved surface finish. The mechanical system has been manufactured and tested for its vacuum integrity. The system was used to refurbish the aged (Scrap from the market) 80W glass tube sealed-off CO_2 laser and we have achieved desired result in terms of output power and sealing.

CP-01-19

Unraveling frequency and temperature dependent dielectric behaviorof a-Mn_2O_3@SiO_2core shell nanocomposites

S. Divya[1], M. Jose[1] [1]Department of Physics, Sacred Heart College (Autonomous), Tirupattur-635601, India. [*]Corresponding author Email: jose@shctpt.edu; mjosh1231@gmail.com*

This article investigates the dielectric response of α-Mn_2O_3@SiO_2 core shell nanocomposites in the frequency range 1Hz-1MHz at various temperatures (323K-673K). The powder XRD analysis, TEM analyses were employed to confirm the structure, morphology and crystallinity respectively. The SAED patterns strongly support the XRD findings and reveal the formation of α-Mn_2O_3@SiO_2 core shell nanocomposites. The value of $e_t$and tand increases with increasing temperatures at lower frequencies though they decrease at high frequencies. The cole-cole plots reveal non-Debye type of relaxation and positive temperature coefficient of resistance type behavior.

CP-01-20

Development and power scaling of a diode pumped multi-pass CW Yb:YAG thin-disk laser

J. K. Soni[*], P. S. Hedaoo, K. S. Deohare, K. Rangnathan, B. N. Upadhyaya, R. Arya, *Laser Technology Division, Raja Ramanna Centre for Advanced technology, Indore-452013 [*]Email:* jksoni@rrcat.gov.in

This paper presents development and power scaling of diode pumped multi-pass continuous wave Yb:YAGthin disk laser at 1030 nm by pumping with laser diode at 940 nm. We have designed and developed a 16 pass pump head, pump beam, disk and folding mirror alignment technique and successfully demonstrated Yb:YAG thin disk laser for the first time in India. A maximum CW output power 142 W with an optical-to-optical conversion efficiency of 35.5% has been achieved.

CP-01-21

Development and characterization of Mamyshev Oscillator

Anshuman Nigam[1,2,3], P.K. Gupta[1,2], C.P. Singh[1,2], Bhuvnesh[1], P.K. Mukhopadhyay[1,2], R. Arya[1] and S.K. Dixit[1,2] [1]Laser Technology Division, Raja Ramanna Centre for Advanced Technology, Indore-452013. [2]Homi Bhabha National Institute, Training School Complex, Anushakti Nagar, Mumbai-400094, India [3]Email: anshumannigam@rrcat.gov.in

We present the development and characterization of Mamyshev oscillator (MO) in our lab. The MO consists of alternate self-phase modulation induced spectral broadening and offset spectral filtering of the pulse propagating inside the cavity. The saturable absorber effect in the MO is provided by the offset spectral filters. A seed source generating pulses at ~ 40 MHz repetition rate has been developed to initiate the pulse operation in the MO.

Stable pulse operation at ~9.6 MHzrepetition rate is observed in MO by momentarily injecting the seed in MO. A detailed characterization of the pulse operation in MO is performed by observing pulse train, spectra at different locations, radio frequency spectra, and autocorrelation traces. The MO generates ~ 9.5 ps duration pulses which are compressed to ~215 fs by agrating pair basedpulse compressor.This work provides a platform to study the pulse dynamics in fiber oscillator and in addition, provides a suitable seed for high energy amplifier due to its stability towards environmental perturbation.

CP-01-22

Studies of Pt/CeO_2 and Pt/SnO_2 Catalyst for CO oxidation towards Development of Sealed-off CO_2 Laser

Avantika Gautam[*]*, Manoj Kumar, B T Rao, Rajiv Kumar Yadav, L B Rana, Shweta Verma, and R. Kaul, Laser Materials Processing Division, MSATG, RRCAT, Indore* [*]*Email: avantika@rrcat.gov.in*

This study aimed to investigate the CO oxidation efficiency of Pt supported on reducible oxides ($CeO_2$and SnO_2) at room temperature and higher temperature (150°C).Catalytic Characterization and testing results of Pt/CeO_2 and Pt/SnO_2 series has been presented and discussed in this paper. Post-reduction treatment at higher temperature is found to be important step for CO_2 conversion activity test carried at high temperature as compared to room temperature. Higher temperature of catalyst results in increased reaction rate and hence higher catalytic activity.

CP-01-23

Effect of auxiliary discharge pulse on performance of 6.25 kHz high voltage pulse power supply for copper vapor laser

Hitesh Choudhary[1,2]*, R.K. Mishra*[1]*, P.K. Agrawal*[1,2]*, and M.S. Ansari*[1,2] [1] *Laser Power Supplies Division, Raja Ramanna Centre for Advanced Technology, Indore* [2] *Homi Bhabha National Institute, Anushakti Nagar, Mumbai - 400094, India, Email:* hitesh@rrcat.gov.in

A high voltage pulse power supply generates voltage pulse of 20 kV at rise time 80 ns for copper vapor laser having application the field of medical isotopes, FBG etc at 6.25 kHz repetition rate. The timer control unit of command charging unit generates charge, auxiliary discharge and discharge pulses to provide controlled charging & discharging of voltage pulses. Initially the storage capacitor is charged to low voltage (~ 750 V) and then discharged, step up, compressed to generate fast rise time high voltage pulse for copper vapor laser. The auxiliary discharge pulse is used to remove the residual voltage from storage capacitor before the start of next charging pulse. The paper presents the effect of auxiliary discharge pulse on performance parameters like stage voltages, timing jitter and laser output power.

CP-01-24

Investigating the optical and luminescent characteristics of Cobalt ferrite nanoparticles

T. Jose Antony, K. Jagannathan Department of Physics, SRM Institute of Science and Technology, Vadapalani Campus, No.1, Jawaharlal Nehru Road, Vadapalani, TN, India. Email: kjagan81@gmail.com*

The Cobalt ferrite ($CoFe_2O_4$) nanoparticles were synthesised using the solvothermal method. The synthesised sample was characterised for studying its properties. The XRD analysis was used to analyse the structural property. The UV spectroscopy was used in analysing the optical nature of the material. Further, the Tauc plot was utilised to find the material's bandgap (E_g). The functional group studies were carried out with the aid of FTIR spectroscopy. The Photoluminescence property of the sample was studied using the PL spectroscopy. The optoelectronic applications of $CoFe_2O_4$ nanoparticles have been studied in this work.

CP-01-25

Optimization of Pump Source in a 725 W Ytterbium Doped Monolithic Fiber Laser Oscillator for Uniform Heat Load Distribution

Sajib Chowdhury, Shubranil Maity, Abdul Malek Mallick, Atasi Pal, Debashri Ghosh, CSIR-Central Glass & Ceramic Research Institute, Kolkata, India, Academy of Scientific& Innovative Research (AcSIR), India, Email: chowdhurysajib17@gmail.com

In this paper, a monolithic Ytterbium doped fiber laser was developed by using pump diodes at 915 nm and 976 nm respectively with peak emission wavelength at 1080 nm in both cases. The thermal heat load and lasing performance were studied and compared for both types of diodes. It was observed that the pump diodes at 915 nm provided uniform and more efficient pump absorption than the pump diodes with emission wavelength at 976 nm. This eventually led to lower temperature of the active fiber and better heat load distribution in the laser cavity when pump diodes at 915 nm were used. The laser power was further scaled to 725 W using 915 nm pump diodes with 70% efficiency.

CP-01-26

Investigation of abrupt autofocusing and self-healing of obstructed circular Airy derivative beams

Anita Kumari, and Vishwa Pal, Indian Institute of Technology Ropar, Rupnagar 140001, Punjab, India, Email: anita.21phz0014@iitrpr.ac.in

We present a numerical and experimental study of the exotic propagation properties such as abrupt autofocusing and self-healing abilities in the free space of circular Airy derivative beams (CADBs). The CADB consists of multiple concentric rings and during propagation exhibits abrupt autofocusing property where maximum intensity increases abruptly by several orders of magnitude just before the focal point due to their lateral self-acceleration.

The autofocusing distance can be controlled by beam parameters. The CADBs also possess good self-healing abilities under various types of obstructions which are quantified by overlap integral and are found to be maximum at the autofocusing point, indicating the maximum self-healing of CADBs. Further, the abrupt autofocusing is quantified by analyzing the maximum k-value and how fast it changes around the autofocusing point. Particularly, obstructed CADBs show reduced k-value and depend on the type of obstruction. We have found a good agreement between the numerical simulations and experimental results.

CP-01-27

Design and implementation of 3 kW high efficiency dc-dc stage of Laser Diode Driver

*A. Sharma, Dipen M. Vachhani, K. K. Pant, Sajith Kumar T R, Prince Pandey, Ravi Porwal, P. Saxena, R. Arya, Laser Technology Division, RRCAT, Indore. *Email: ashu@rrcat.gov.in*

Fiber lasers come in the category of most efficient laser systems, have zero moving parts, are free from misalignment and are rugged systems. The paper presents design and implementation of phase-shifted PWM controlled dc-dc full-bridge converter based current source that drives a low ripple and regulated current of 1A to 11A through multiple high power Laser Diodes in series,at 270V maximum. The topology employs auxiliary inductors to achieve zero voltage switching (ZVS) of power MOSFETs at no load or light loads and employs much lower value of commutating inductor Lc to extend ZVS range to full load. This leads to threefold advantages when compared to competing PSPWM techniques viz. (*a) much reduced duty cycle loss (b) low ringing and overshoot of secondary diodes further alleviated by SiC schottky clamp diodes and (c) full load range ZVS.*Selection of major power elements of the 3170W high efficiency dc-dc converter and description of the control scheme is presented along with the experimental results.

CP-01-28

Design and implementation of 3.3kW high power factor ac-dc stage of Laser Diode

*A. Sharma, Dipen M. Vachhani, P. Pandey, R. Porwal, R. Varma, K. K. Pant, Sajith Kumar T R, P. Saxena, R. Arya, Laser Technology Division, RRCAT, Indore. *Email: ashu@rrcat.gov.in*

The paper presents design and implementation of a 3300W switch mode power factor corrected (PFC) pre-regulator based on two interleaved boost converter cells and controlled by two loop average mode control. It generates a semi-regulated 414V+/-10Vdc link to power the downstream dc-dc stage while drawing near sine current from 1ø ac utility mains and enabling the Laser Diode Driver to comply to the IEC61000-3-2 regulations. Design and selection of key power elements and controller scheme is discussed and experimental results are presented. Design of input EMI filter is also given. High efficiency of 97% is achieved due to interleaved switching of switch mode converter cells, use of resonant turn-off snubber across power MOSFET and use of SiC Schottky as the boost diode.

CP-01-29

Experimental analysis of copper vapor laser power with varying repetition rates

*Rajasree Vijayan[2], Dheeraj Kumar Singh[*1,2], Vinod Singh Rawat [1,2] [1]Homi Bhabha National Institute, Anushaktinagar, Mumbai, India [2] Advanced Tunable Laser Division, Bhabha Atomic Research Centre, Mumbai, India [*]Email: dheeraj@barc.gov.in*

This paper explores the optical output power of copper vapor laser (CVL) at varying repetition rate operation of IGBT and magnetic pulse compression-based power supply. The pulse power supply (PPS) designed for a 9 kHz repetition rate is tested at the repetition rate of 7 kHz, 8 kHz, 9 kHz, 10 kHz, and 10.5 kHz. The purpose of this study is to experimentally find the optimum repetition rate of the PPS for CVL. Additionally, this study tests the feasibility of utilizing the IGBT and MPC-based PPS for various applications requiring different repetition rates.

CP-01-30

Investigation of the Electric Double Layer in Microcapillaries and Its Effect on Laser-Induced Liquid Microjets

Rakshith Kamath[1] , Kailash C. Jena[1,2,] [1]Department of Physics, Indian Institute of Technology Ropar, Rupnagar, Punjab-140001, India [2]Department of Biomedical Engineering, Indian Institute of Technology Ropar, Rupnagar, Punjab-140001, India [*]Email: kcjena@iitrpr.ac.in*

The electric double layer has a significant impact on the processes of electrostatic interactions, ion diffusion, and charge transfer at the interface of liquid and solid. Understanding and manipulating these phenomena can result in better control over microjet production and its velocity, which has implications in various fields including microfabrication, material processing, and biomedical research. Our research focused on the impact of the electric double layer on the inner surface of the microcapillary on jet velocity. We studied the effect of electrostatic interactions and ion diffusion on jet velocity, which is affected by the screening effect in the electrical double layer (EDL). We used NaCl of different concentrations in our experiments. Our findings show that the presence of EDL has a minor impact on jet velocity since the thickness of EDL is less compared to the microcapillary diameter. We found that physical properties such as surface tension, viscosity, and density have a significant impact on jet velocity over EDL.

CP-01-31

Effect of Dielectric Interface Tight Focusing Properties of Azimuthally Polarized Hollow Gaussian Beam

M. Udhayakumar[1], K.B. Rajesh[2], P. Indira[1] [1]Department of Physics, Gnanamani College Of Technology, Namakkal, Tamilnadu, India [2]Department of Physics, Chikkanna Government Arts College, Tiruppur, Tamilnadu, India. Corresponding author Email id:udhayaphy1985@gmail.com*

The tight focusing properties of azimuthally polarized Hollow Gaussian Beam (HGB) with on-axis spiral optical vortex focused through a dielectric interface is investigated theoretically by vector diffraction theory. It is observed that the presence of dielectric interface generates focal shift due to the mismatch of refractive indices in the focal volume due to the presence of thin dielectric interface. However, it is noted that by properly tuning the phase parameter leads to focal shift along optical axis towards the aperture and makes the focal segment exactly coincides at the geometrical focus. In addition, focal shift direction can also be adjusted by changing the direction of phase parameter.

CP-01-32

Establishment of repeatable operation of the IR-FEL at RRCAT

Tushar Dave[1,], Sona Chandran[1,2], Bhaskar Biswas, R. S. Saini[1], Shankar Lal[1,2], Arvind Kumar[1], R. K. Pandit[1], Pravin Nerpagar[1], U. Kale[1], S. K. Gupta[1] and K. K. Pant[1] [1]FEL and Utilization Section, Raja Ramanna Center for Advanced Technology [2]Homi Bhabha National Institute, Training School Complex, Anushakti Nagar [*]Email: tushard@rrcat.gov.in*

The Infra Red Free Electron Laser (IR-FEL) at Raja Ramanna Center for Advanced Technology (RRCAT) is designed to operate in an oscillator configuration to emit radiation in the wavelength range of 12.5-50 μm. The facility achieved its first saturated lasing at a wavelength of 28 μm in 2020 with a Continuous Wave (CW) average power of ~7.3 mW. Subsequently, with the tuning of the injector and transport line parameters, a maximum out-coupled power up to 30 mW could be achieved. Repeatable operation of the IR-FEL is essential for its utilization for user experiments. This has been established with ~ 15 mW of out-coupled CW average IR power obtained regularly at a wavelength of 21.8 μm over several months of operation, out of which ~ 5 mW has been successfully transported to the laser diagnostic room. This paper discusses the improvements in the repeatability of operation of the IR-FEL, and the methodology employed to achieve this. The present status and future plans for the facility are also discussed.

CP-01-33

Experimental analysis and modification in trigger circuit of flash lamp driver for Nd: glass laser

Deepak naphade[*], Abrat Verma, Bhupinder Singh, Anand Pagare, M.S. Ansari, Laser Power Supplies Division, Raja Ramanna Centre for Advanced Technology, Indore - 452013 [*]Email: naphaded@rrcat.gov.in

Experimental analysis of voltage stresses (reverse voltage, dV/dt) on SCR switch of series trigger circuit of 10kV, 250mA flash lamp power supply have been carried out. This flash lamp power supply is used to create discharge in 900mm flash lamp load to optically excite Nd: glass laser. Voltage stresses on triggering switch (SCR) reduces life of switch and lead to frequent maintenance of flash lamp power supply. Modification in trigger circuit and snubber circuit have been carried out and tested to reduce voltage stresses to minimum level. Optimization of modified trigger circuit components have also been carried out.

CP-01-34

Performance optimization of the IR-FEL optical transport line

Sona Chandran[1,2,] and Bhaskar Biswas[11]FEL and Utilization Section, RRCAT, Indore [2]Homi Bhabha National Institute, Training School Complex, Anushakti Nagar, Mumbai[*] Email : sona@rrcat.gov.in*

The Infra-Red Free Electron Laser (IR-FEL) developed at Raja Ramanna Centre for Advanced Technology (RRCAT) has an output wavelength that is continuously tunable in the wavelength range 12.5–50 μm, with a Continuous Wave (CW) average out-coupled power ~ 30 mW at 10 Hz pulse repetition rate (PRR). The IR-FEL has achieved repeatable and stable saturated lasing at a wavelength of 21.8 μm, with an average power up to 30 mW at 2 Hz PRR. With the original optical beam transport line design, only <1% of the laser power at theout-coupling mirror could be transported up to user area. The optical transport line has been redesigned with additional beam matching sections, one at the start of the transport line, and the another one in the diagnostic room; and additionally and larger aperture mirrors. This has improved the power transmission up to the user station to > 42% at a wavelength of 21.8 μm. This paper discusses the re-design of IR-FEL optical transport line.

CP-01-35

Studies on Spatial Resolution Enhancement Techniques for Raman Optical Fiber Distributed Temperature Sensor System

A. K. Sahoo[1,2], M. K. Saxena[1,2,3], R. K. Sharma[1], J. Kishore[1], S. Kumar[1], C. K. Suman[1], O. Prakash[1,2] [1]Fiber Sensors & Optical Spectroscopy Section, Raja Ramanna Centre for Advanced Technology, Indore, [2]Homi Bhabha National Institute, Mumbai [3]Email: manojsaxena@rrcat.gov.in

In this paper, the results of a study carried out on spatial resolution enhancement for a Raman optical fiber distributed temperature sensor (ROFDTS) is presented. The spatial resolution of a ROFDTS system is mainly limited by the pulse width of the laser source. Using theoretical modelling, it has been shown that the power of the Raman back-scattered stokes (St) and anti-stokes (AS) signals is equal to the convolution of laser pulse power and a function of temperature profile along the optical fiber. This function can be estimated using deconvolution algorithms. In this paper, we investigate three deconvolution algorithms that can be used to improve the spatial resolution without reducing the pulse width of the laser source. Simulation results have shown an improvement in spatial resolution from 2 m to 1 m in a ROFDTS system with a 20 ns laser pulse width.

CP-01-36

XANES and EXAFS Studies of copper(II) Complexes

Deepti Nagar[1], A. Mishra[2] [1]SGSITS, Indore, School of physics, DAVV Email: A.Mihra1976@gmail.com, mailtodeepti_2008@rediffmail.com

In the present chapter, we have carried out study of X-ray K-absorption spectra of copper(II) complexes with ligands 3-((4-bromophenyl)diazenyl)-2-hydroxybenzaldehyde and 2-hydroxy-3-((2-nitrophenyl)diazenyl) benzaldehyde. XANES spectra have been recorded at the K-edge of Cu using the dispersive beam line at 2.5GeV Indus-2 synchrotron radiation source RRCAT (Raja Ramanna Center for Advance Technology), Indore, and India. X-ray absorption parameters like chemical shift, edge-width and shift of the principal absorption maximum have been calculated in the present study. These parameters have been utilized to explain the structure of the complexes. XANES data have been analyzed using the computer software Origin 6.0 professional and Athena.

Category - 2
Lasers in Nuclear Science & Technology

CP-02-01

In-situ laser cutting of 30 mm thick SS316L recirculation piping loop in TAPS-1 reactor

M. K. Bairwa[1], B. K. Saini[1], Ranveer Singh Meena[1], Vijay Bhawsar[1], Sudheer Kushwaha[1], Dhruvdeep Narwat[1], Pawan Kumar[1], Vinayak V. Rasankar[1], K. S. Deohare[1], S. K. Sharma[1], Jagriti Khanwalkar[1], Vinay Thattey[2], B. N. Upadhyaya[1], R. Arya[1] [1]Laser Technology Division, Raja Ramanna Centre for Advanced Technology, Indore-452013, India [2]Tarapur Atomic Power Station-1&2, NPCIL [*]Email: mkbairwa@rrcat.gov.in*

There was a specific requirement for removal of segments of 684 mm diameter and 30 mm thick SS316L recirculation piping loop in Tarapur Atomic Power Station (TAPS-1&2) for replacement purpose due to intergranular stress corrosion cracking (IGSCC). This report provides details of single pass in-situ laser cutting of two number of joints of 30 mm thick SS316L pipe of recirculation piping loop-A of TAPS-1 reactor using 1 kW average power fiber coupled pulsed Nd:YAG laser. A compact laser cutting tool and laser cutting nozzle has been specially developed and laser cutting process parameters have been optimized for cutting of 30 mm thick SS316L piping. This remotely operable single pass laser cutting technology has been successfully deployed for cutting of 30 mm thick SS316L recirculation piping loop in TAPS-1 reactor with minimum radiation dose consumption and time as compared to conventional mechanical methods.

CP-02-02

Studies on underwater laser cutting process of zircaloy-4 plate with fiber coupled pulsed Nd:YAG laser

Sunil Kumar Sharma, M. K. Bairwa, Rajpal Singh, Ranveer Singh Meena, Vijay Bhawsar, Jagriti Khanwalkar, B. N. Upadhyaya, R. Arya, Laser Technology Division, Raja Ramanna Centre for Advanced Technology, Indore-452013, India, Email: sksharma@rrcat.gov.in

In this paper, experimental investigation on underwater laser cutting process of 1.6 mm thick zircaloy-4 plate to have minimum impression on back plate kept at a gap of 2 mm is reported. Laser cutting parameters have been optimized for underwater laser cutting of zircaloy-4 plate using remotely operable fiber coupled pulsed Nd:YAG laser of 250 W average power and 5 kW peak power. It was found that minimum impression on back plate can be achieved by a combination of laser process parameters and reducing depth of focus of cutting nozzle.

CP-02-03

Laser based technique for internal diameter measurementof cylindrical tubes

Sanjiv Kumar Tiwari[1], Sarvendra Singh[1], Y. Pavan Kumar[1], Deepak Daiya[1,3], G. Muralidharan[1], Ashutosh Pratap Singh[2], Saranjeet Singh[2], Abhay Kumar[2], N. S. Benerji[1], [1]High Energy Lasers and Optics Section, Raja Ramanna Centre for Advanced Technology, Indore, [2]Technology and Product Development Section, Raja Ramanna Centre for Advanced Technology, Indore,[3]Homi Bhabha National Institute, Training School Complex, Anushakti Nagar, Mumbai, [*]Email: sanjiv@rrcat.gov.in*

A laser based technique for measurement of the internal diameter of cylindrical tubes using an axicon generated diverging hollow beam is presented. The cylindrical tube is kept on a motorized translation stage and the tube axis is aligned with the propagation axis of the hollow beam. The hollow beam, whose diameter increases linearly with the propagation distance, intersects the internal surface of the cylindrical tube in a form of circle, which is imaged using a CCD camera and the internal diameter of the tube is measured at that location. Scanning of the tube along the beam axis enables probing the whole internal surface so that local surface imperfections can be visualized and the internal diameter can be measured at any desired location of the tube.

CP-02-04

Design, Development & Deployment of a Programmable Power Supply for 1kW Pulsed Nd:YAG Laser based Thick Metal Cutting Applications

Vijay Bhawsar, Sudheer Kushwaha, A A Raju, M.K. Bairwa, Jagriti Khanwalkar, B.N. Upadhyaya, P. Saxena, R. Arya, Laser Electronics Division, RRCAT, Indore, Email: vijay@rrcat.gov.in

High average power and high peak power pulsed Nd:YAG lasers with initial high peak are useful in large depth cutting and welding of metals and alloys with minimum heat affected zone, shrinkage and distortion. The main advantage of Nd:YAG lasers is their capability for beam delivery through rugged and flexible, fiber optics that allow remote placement of the laser system in controlled environment. In this paper the work on design and development of a microcontroller based modular power source for a quad flash lamp pumped 1 kW quasi-CW Nd:YAG laser and its deployment at TAPS 1&2 nuclear reactor site at Tarapur, Maharashtra, for laser cutting of 30 mm thick SS pipe used in reactor recirculation loop, is presented. The power source can be programmed to provide current pulses with high initial peak required for thick metal cutting applications, with adjustable pulse parameters for required laser pulse energy and average power for different cutting thickness and speed. A microcontroller based power supply controller has been developed to provide simultaneous control and drive for four pulsed power sources to deliver a maximum average electrical power of 20 kW to four electrically non-linear flash lamp

loads and peak electrical power of 100 kW to each of the flash lamps that pump optical energy to a dual-Nd:YAG rod configuration.

CP-02-05

Effect of Laser Beam Homogenizer in LA-ICP-MS - towards Spatial Profiling of Irradiated Nuclear Fuel

U. K. Maity[*] Materials Chemistry & Metal Fuel Cycle Group, Homi Bhaba National Institute, Indira Gandhi Centre for Atomic Research, Kalpakkam, TN-603102, India.
[*]Email : ukm@igcar.gov.in/ujjwalm4@gmail.com

Laser ablation coupled to inductively coupled plasma mass spectrometry (LA-ICP-MS) is employed in spatial profiling mode to determine isotopic ratios and burn-up of simulated nuclear fuel containing fissile atom (U) and burn-up monitor (Nd). Different laser spots on the sample pellets are sampled across diametric directions to study spatial profiling. As LA-ICP-MS demands optimized laser parameters, present study is a quantitative estimation of laser beam homogenizer (LBH) influence on spatial profiling by measuring isotopic ratios of selected elements of interest. Data obtained from LA-ICP-MSwith LBH appears to be more promising (~ 6 times better in terms of relative standard deviation (RSD)& accuracy) for surface profiling compared to LA without a LBH. The possible reason for the above observation is discussed based on crater morphology and ablation characteristics. Outcomes from LA-ICP-MS with LBH are validated by comparing with results obtained from liquid sampling ICP-MS.

CP-02-06

Utilization of Drawback for ns-Laser Ionization Source to Resolve Isobaric Interference in LIMS

U. K. Maity[*] Materials Chemistry & Metal Fuel Cycle Group, Homi Bhaba National Institute, Indira Gandhi Centre by Atomic Research, Kalpakkam, TN-603102, India.
[*]Email : ukm@igcar.gov.in/ujjwalm4@gmail.com

The determination of ^{148}Nd, ^{90}Sr and ^{137}Cs isotopes is important in nuclear industry. The isobaric interference in conventional mass spectrometry (MS) techniques limits their ability to estimate these isotopes. The present study demonstrates the potential application of Laser Ionisation Mass Spectrometry (LIMS) technique to resolve isobaric interference at ^{148}Nd, ^{90}Sr and ^{137}Cs without prior chemical separation and abundance correction. LIMS with optimised laser parameters eliminates the isobaric interference *in-situ* and shortcomings of conventional mass spectrometry techniques. This study discuss the findings of the species formed at different laser fluence, the optimised laser fluence to eliminate isobaric interference and most probable reason behind the result.

CP-02-07

Development of Laser-Based BARCIS Alignment System for PHWR's coolant channels

Sarvendra Singh[1], Sanjiv Kumar Tiwari[1], Y. Pavan Kumar[1], Surjya Jena[2], Vishal Jadhav[2], Sudhir Jaiswal[2], Irfan Ahamed[3], D. S. Sakaria[3], A. K. Mishra[4], Abhishek Varshney[4], A. K. Tripathi[3], Devendra Kumar Jain[2], Vineet Kumar Thakur[4], M. P. Kamath[1], N. S. Benerji[1], Ashok Bhatia[4], Deependra Nath Sanyal[2] and D. S. Rao[4] [1]High Energy Lasers and Optics Section, Raja Ramanna Centre for Advanced Technology, Indore [2]Nuclear Power Corporation of India, Mumbai, [3]Kakrapar Atomic Power Station 1&2, Kakrapar, [4]Rajasthan Atomic Power Station 3&4, Rawatbhata. [*]Email: sarvendra@rrcat.gov.in*

Development of laser-based BARCIS (BARC Channel Inspection System) alignment system is reported. BARCIS is used for the movement of different types of probes through the coolant channels of Pressurized Heavy Water Reactors (PHWRs) for the periodic inspection and monitoring of the coolant channels during In-Service Inspection (ISI) activity. Misalignment of the BARCIS rotary shaft axis and the drive mechanism axis with the axis of the corresponding coolant channel hampers the free movement of the probe through the channel which may lead to damage the channel and/or probe. Therefore, prior to the inspection of a coolant channel, alignment of BARCIS is extremely necessary. A laser-based alignment system is developed to align the axis of the BARCIS drive mechanism and its rotary shaft with the axis of the coolant channels of PHWRs. The system was initially tested at RRCAT and then the mock-up test trials were successfully conducted at the reactor sites KAPS-1&2 and RAPS-3&4.The ergonomically designed, light weight laser-based BARCIS alignment system has been found to facilitate fast and efficient alignment of the BARCIS drive mechanism with the respective coolant channel of a PHWR. Deployment of laser-based BARCIS alignment system is expected to result in significant reduction in the shut down time of the reactor and the radiation exposure to the inspection personnel as well.

Category - 3
Laser Materials, Devices and Components

CP-03-01

Growth of 5.5 kg flat-top KDP crystal using indigenously developed crystal growth workstation for electro-optic switching of high power Nd:Glass laser,

S. K. Sharma[1], Yashpal Singh[1], Indranil Bhaumik[1], B. K. Sajith[1], Rajeev Bhatt[1], C. Mukherjee[2] and Rakesh Kaul[1], [1]Laser and Functional Materials Division, [2]Optical Coating Lab., High Energy Lasers & Optics Section, Raja Ramanna Centre for Advanced Technology, Indore, (M.P.) 452013, [*]Email:* sks@rrcat.gov.in.

We report the growth of a flat-top KDP single crystal of dimensions 165×155×120 mm^3 (5.5 kg) using an indigenously developed crystal growth workstation. This is the largest size KDP crystal grown so far in our country. The grown crystal was sliced using a wire saw and prepared Z-cut elements of maximum dimensions 150×150×18 mm^3 for electro-optical switching application in high power Nd:Glass laser. Orientational accuracy of the prepared plates was confirmed by optical conoscopy technique. Optical transmission homogeneity measured at different locations of a 3.5 mm thick plate at 1064 nm wavelength is 89.7 ±0.3 %. Laser induced surface damage threshold was determined for the plate using a pulsed Nd:YAG laser at 15 different points showing crystal to be safe up to 1.4 GW/cm^2 confirming its suitability for our high power laser program.

CP-03-02

Luminescence and radiation shielding properties of Nd^{3+}-doped bismuth borate and phosphate glasses

Ch. Basavapoornima[1], R. Rajaramakrishna[2], C.R. Kesavulu[1], Shobha Rani Depuru[1], C.K.Jayasankar[3,] [1]Institute of Aeronautical Engineering, Hyderabad, India. [2]Siberian Federal University, 79, Pr, Svobodny, Krasnoyarsk, 660041, Russia. [3]Department of Physics, Sri Venkateswara University, Tirupati, India. [*]Email: ckjaya@yahoo.com*

The luminescence and radiation shielding properties of two different glass compositions (in mol %) of $49.5H_3BO_3$+$49.5Bi_2O_3$+$1.0Nd_2O_3$(B50Bi$Nd_{1.0}$) and $47.5P_2O_5$+47.5BaO+4.0 La_2O_3+$1.0Nd_2O_3$(PBaLa$Nd_{1.0}$) have been studied. The spectroscopic quality factor for $^4F_{3/2} \rightarrow {}^4I_{11/2}$ of B50Bi$Nd_{1.0}$ and PBaLa$Nd_{1.0}$ glasses is found to be 0.82 and 0.70, respectively. Similarly, the quantum efficiency for $^4F_{3/2}$is found to be 50 and 94 for B50Bi$Nd_{1.0}$ and PBaLa$Nd_{1.0}$, respectively. Theoretical mass attenuation co-efficient (MAC) of various glasses doped with neodymium content has been analyzed. X-ray 'K' and 'L_{III}' edge of bismuth element in B50Bi$Nd_{1.0}$ glass was observed. X-ray 'K' and 'L_{III}' edge of barium,

lanthanum, and neodymium were observed in the $PBaLaNd_{1.0}$ glass. It is observed that bismuth borate glass shows higher MAC than barium lanthanum phosphate glasses beyond 0.1MeV.

CP-03-03

Establishment of polishing technique for polishing of large size Potassium Di-hydrogen Phosphate crystal

Y. Pavan Kumar [1], Sanjiv K. Tiwari[1], G. Ragoubady[1], S. S. Thangavel[1], Deepak Daiya[1], Rishipal[1], G. Muralidharan[1], Sarvendra Singh[1], Sarthak Gupta[2], A. K. Biswas[1], N. S. Benerji[1]. [1]High Energy Lasers and Optics Section, [2]Laser Controls and Instrumentation Division, Raja Ramanna Centre for Advanced Technology, Indore 452013. Email: ypk@rrcat.gov.in.*

Potassium dihydrogen phosphate (KDP, KH2PO4) is a nonlinear photoelectric crystal which has excellent optical and electro-optical properties. Due to these properties, KDP crystals finds application in laser systems, various frequency convertors, electro-optic switches and in fusion energy. The technical requirements of KDP crystal are low surface roughness and surface waviness and high precision surface shape quality. As the crystal is soft, hygroscopic and thermally sensitive in nature, it is difficult to polish using conventional polishing techniques and extreme care needs to be taken while grinding, polishing and cleaning of the crystal. In this paper we report establishment of polishing technique for polishing of large size, 150 mm x 150 mm, home grown KDP crystal using soft polishing pad, anhydrous polishing slurry and cleaning agent.

CP-03-04

Design and development of pyramidal mirror fabrication for magneto optical trap application.

Y. Pavan Kumar [1], Sanjiv K. Tiwari[1], G. Ragoubady[1], G. Muralidharan[1], Sarvendra Singh[1], Rishipal[1], A. K. Biswas[1], R. Kamparath[2], C. Mukherjee[2,3], N. S. Benerji[1, 2], [1]Optical Design and Development Lab, [2]Optical Coatings Lab, High Energy Lasers & Optics Section, Raja Ramanna Centre for Advanced Technology, Indore 452013. [3]Homi Bhabha National Institute, Training School Complex, Anushakti Nagar, Mumbai, 400094. Email: ypk@rrcat.gov.in.*

A pyramidal mirror is a combination of four prisms, of which, two prisms are standard 45^0-90^0-45^0 prisms and the remaining two are modified 45^0-90^0-45^0 prisms. These prisms are arranged such that the adjacent faces make an angle of 120^0 and the opposite faces makes an angle of 90^0, with respect to each other. A single wide laser beam incident upon the pyramidal mirror will result in three sets of counter propagating reflected beams. Such a beam configuration is required for magneto optical trap (MOT) of cold atoms. Pyramidal mirror is commercially not available. In this paper we describe the design and fabrication of the pyramidal mirror with a hole at its apex.

CP-03-05

Synthesis and characterization of NIR emitting Cr^{3+} doped zinc gallogermanate ($Zn_3Ga_2Ge_2O_{10}:Cr^{3+}$) long phosphor nanoparticles for bioimaging applications

*C. Debnath[1], Rachel S. Johnson[1], A. Pal[1,2], S. Kar[1,2], Raj Mohan S.[3], R. Shrivastava[1,2], Sunil Verma[1,2], S.K. Majumder[1,2] [1]Laser Biomedical Applications Division, Raja Ramanna Centre for Advanced Technology, Indore – 452013 [2]Homi Bhabha National Institute, BARC Training School Complex, Anushakti Nagar, Mumbai – 400094 [3]Laser Materials Processing Division, Raja Ramanna Centre for Advanced Technology, Indore – 452013 *Email: cdebnath@rrcat.gov.in,*

A type of long persistence luminesce nanoparticles, chromium doped zincgallogermanate ($Zn_3Ga_2Ge_2O_{10}$:1%Cr^{3+}; ZGGO) nanoparticles, were synthesized using citrate gel method. The phase of the prepared material was confirmed using X-ray diffraction by comparing the JCPDS data files available in literature. The size of the nanoparticles was obtained using dynamic light scattering experiments. The photoluminescence and its decaying properties were characterized under UV (320 nm) excitation. Finally, NIR (698 nm) fluorescent bioimaging experiments under in situ UV excitation of 254 nm wavelength have been performed on HaCat cells.

CP-03-06

Novel methodology for growth of trans-stilbene organic crystal and investigation of the scintillation properties by photoluminescence, x-ray luminescence and neutron-gamma pulse shape discrimination studies

Anjan Pal[1,2], Sujan Kar[1,2,], C. Debnath[1,2], Raj Mohan S. [1,2], Sonu[3], Mohit Tyagi[3], Sunil Verma[1,2], Shovan K. Majumder[1,2] [1]Homi Bhabha National Institute, BARC Training School Complex, Anushakti Nagar, Trombay 400094, MH [2]Laser Biomedical Applications Division, Raja Ramanna Centre for Advanced Technology, Indore 452013, MP [3]Technical Physics Division, Bhabha Atomic Research Centre, Trombay, 400094, MH *Email: sujan@rrcat.gov.in.*

A novel modified Bridgman technique has been presented for growth of organic crystals, and it has been successfully implemented for growth of trans-stilbene crystal. A special furnace has been designed and fabricated for the growth experiments. The phase and optical quality of the grown crystal was assessed using x-ray diffraction and UV-Vis-NIR spectrophotometry and optical interferometry. Since the end-application of the grown crystal is in radiation detection, therefore the detector properties have been assessed through photoluminescence, radio-luminescence, and n-? pulse shape discrimination studies.

CP-03-07

Suppression of defect luminescence in GaN epitaxial layers grown by Molecular Beam Epitaxy technique

Krishnapada Maity[1,], Abhishek Chatterjee[1], V. Agnihotri[1], R. Kumar[1,2], P. Taya[1], S. Porwal[1], Salahuddin Khan[1,2], V. K. Dixit[1,2] and T. K. Sharma[1,2] [1]Materials Science Section, Raja Ramanna Centre for Advanced Technology, Indore, 452013. [2]Homi Bhabha National Institute, Training School Complex, Anushakti Nagar, Mumbai, India - 400085. *Corresponding Author Email: krishnapadam@rrcat.gov.in*

Gallium nitride and its alloys with Aluminium and Indium are important due to their numerous applications in light emitters and detectors. Compared to Silicon and GaAs-based devices, GaN-based devices are more radiation tolerant owing to their wider bandgap. It makes GaN-based materials an attractive candidate for applications in high radiation environments like nuclear reactors, particle accelerators, and spacecrafts. In this work, growth of GaN epilayer is carried out by nitride molecular beam epitaxy (MBE) technique by varying layer thickness. GaN layer is grown under slightly Ga-rich condition, which demonstrates an optimal crystalline quality with a streaky reflection high energy electron diffraction pattern. The full width at half maximum of high-resolution x-ray diffraction pattern reduces from 0.16^{o} to 0.09^{o} with increasing layer thickness, indicating an improvement in the crystalline quality and reduction in dislocation density at large thicknesses. In photoluminescence, the intensity of defect related yellow luminescence band is reduced and an improved surface morphology is observed with one order reduction in surface roughness for the sample with larger thickness, which demonstrates a good quality growth of GaN on Sapphire substrates by the nitride MBE system.

CP-03-08

Powder Morphology Effect on Transmission Property of Cr-doped Alumina Ceramic

S. K. Pathak[1,], Purvi Bilthare[2], Aarti[3], S. Karmakar[1], and S. M. Gupta[1,4] [1]Laser and Functional Materials Division, Raja Ramanna Centre for Advanced Technology, Indore-452013, [2]Department of Physics and Electronics, Institute for Excellence in Higher Education, Bhopal-462016, [3]Department of Physics, Guru Jambheshwar University of Science and Technology, Hisar, Haryana-125001, [4]Homi Bhabha National Institute (HBNI), Training School Complex, Anushaktinagar, Mumbai-400094 *Email: pathak@rrcat.gov.in*

Nano-powder of chromium doped aluminum oxide ($Cr:Al_2O_3$) is synthesized using co-precipitation route while maintaining pH or not maintain pH during precipitation followed by vacuum sintering at 1800 ^{o}C for 4 hours to investigate the powder morphology effect on the transmission properties for its possible use as laser host. Phase analysis has shown slowing down of q to a Al_2O_3 phase transformation, when pH is maintained during

precipitation. Microstructural investigation has revealed different extent of agglomeration in the precursor and calcined powder depending upon the pH, which has resulted in large variation in the transmission properties of sintered ceramic. A transmission of ~ 45% at 1000 nm for 0.34 mm thickness is observed in the ceramic prepared in which the pH is not maintained during precipitation and allowed to increase up to ~ 8 during aging of the precipitates.

CP-03-09

CW Lasing with High Slope Efficiency using in-house Grown Nd:$GdVO_4$ Single Crystal

*M. Soharab[*1], R. Bhatt[1,3], B.K. Sajith[1], K. Rajiv[2] and Indranil Bhaumik[1,3] [1]Crystal Growth and Instrumentation Section, Laser and Functional Materials Division, [2]Optical Coating lab., High Energy Lasers & Optics Section, Raja Ramanna Centre for Advanced Technology, Indore-452 013, India [3]Homi Bhabha National Institute, Training School Complex, Anushakti Nagar, Mumbai-400 094, India Corresponding authors: [*]Email: sohrab@rrcat.gov.in*

Nd (0.5 at%) doped $GdVO_4$ single crystals of length ~20-25 mm and diameter 6 mm were grown by optical floating zone technique. The presence of strong absorption band (absorption coefficient: 10.5 cm^{-1}) at 808 nm of Nd:$GdVO_4$ crystalsis used for efficient pumping of the Nd doped $GdVO_4$ laser gain medium using diode laser. The emission intensity at 1064 nm is the highest for excitation at 808 nm. The lasing was tested in [100]-oriented laser element using plane-plane resonator cavity. The absorption of pump beam was found to be around 87%. The continuous wave laser emission at 1064 nm with output power of 12.23 W was achieved for power pump of 23.5 W. The slope efficiency is 59%, which is higher than the commercially available Nd:$GdVO_4$laser crystals (50%).

CP-03-10

Development of high damage threshold AR coating on large size Nd:glass laser rods for high energy laser

C. Mukherjee[1,2], Rajiv. K[1], V.V.V. Subrahmanyam[1] and N.S. Benerji[1], [1]Optical Coatings laboratory, High energy Laser & Optics Section, Raja Ramanna Centre for Advanced Technology, Indore-452013. [2]Homi Bhabha National Institute, Training School Complex, Anushakti Nagar, Mumbai, 400094. Email: cmukh@rrcat.gov.in

Large size (300 mm long & 50 mm dia.) Nd:glass laser rods are polished and AR coated indigenously at RRCAT. Two, three and four layer AR coatings have been designed and optimized for achieving very low reflection loss over a large wavelength range. Electric field intensity profile along the depth of the multilayers are also calculated. This profile provides insight into the laser damage phenomena. AR coatings were deposited by dual ion-beam sputtering. Transmission of more than 99.5% at 1054 nm is achieved. High LIDT

of > 21 J/cm^2 @ 5.2 nsec is achieved in 3 layer AR coating after annealing at 450^{0}C for 4 hours. This is associated with 60% improvement in absorption coefficient. The large size AR coated Nd:glass laser rod delivered 15 J output at 1.5 ns.

CP-03-11

Development of large size super-smooth anti-reflection coated optics with 13 J/cm^2 damage threshold for high energy laser

C. Mukherjee[1,2], Abhik Biswas[3], Rajiv. K[1], D. Raghunathan[3], V.V.V. Subrahmanyam[1], Sushmita Bhartiya[4], and N.S. Benerji[1], [1]Optical Coatings laboratory, [3]Optical Design and Development laboratory, High Energy Laser & Optics Section, [4]Nano-Functional Materials Lab, Laser & Functional Materials Division, Raja Ramanna Centre for Advanced Technology, Indore-452013. [2]Homi Bhabha National Institute, Training School Complex, Anushakti Nagar, Mumbai, 400094. Email: cmukh@rrcat.gov.in

Nd:glass disk amplifier and spatial filters of the high energy laser chain require large size (150 x 150 mm & 150 mm dia.) anti-reflection coated windows with high transmission and high damage threshold. Bowl-feed Chemical Mechanical Polishing (CMP), polishing has been employed to achieve low r.m.s. roughness (2.7 Å), high flatness (/10) and low scratch/dig (40/20) on large size (150 mm) substrates. Three layer anti-reflection coatings have been designed and optimized for achieving very low reflection loss for high energy Nd:glass laser. Measurements show 99.4% transmission and LIDT 13 J/cm^2 for AR coated optics. Super smooth substrate with low scratch/dig and half-wave layer adjacent to the substrate, lead to such improvement in LIDT. Such coated optical components are deployed in high energy Nd:glass laser being developed at HEL&OS, RRCAT.

CP-03-12

Effect of Nitrogen Partial Pressure on the Optical Bandgap of Magnetron Sputtered AlN Thin Films

Neha Sharma[1], Rajiv K.[1], Suparna Pal[1,2], C. Mukherjee[1,2], N.S. Benerji[1]; [1]OpticalCoatings Laboratory, High Energy Lasers and Optics Section, Raja Ramanna Centre for Advanced Technology, Indore, MP-452013, India; [2]Homi Bhabha National Institute, Training School Complex, Anushakti Nagar, Mumbai, 400094.,Email: nehas@rrcat.gov.in*

AlN thin films were grown on fused silica substrates by reactive pulsed-dc magnetron sputtering using a mixture of ultra high pure argon (Ar) and nitrogen (N_2) gases with different N_2-partial pressures. X-ray diffraction investigations revealed that polycrystalline AlN thin films were obtained at 5% N_2-partial pressure. Crystalline order was found to reduce with increase in N_2 to 15% and 20%. UV-VIS spectrophotometry has been employed to delineate the effect of different N_2-partial pressure on the optical bandgap (E_g) of grown AlN thin films in transmittance mode. At 5% N_2, $E_g$was found to be ~5.9±0.2 eV, which was found to decrease to ~5.8±0.15 eV and ~5.83±0.1 eV with increase

in N_2 to 15% and 20%, respectively. This may be attributed to the incorporation of excess sub-surface defects created by the reactive ion flux at higher partial pressures ofN_2during deposition of AlN thin films, generating disorder in film microstructure. Refractive index (n) and extinction coefficient (k) for AlN thin films, grown at 5% N_2- partial pressure, were also calculated.

CP-03-13

TiO_2 –PMMA composite thin film fabricated by sol-gel method for high LIDT optical coating

*Suparna Pal[1,2], Rajiv Kamparath[1], V. V. V. Subramaniyam[1], Neha sharma[1], C. Mukherji[1,2], N.S. Benerji[1] [1]Optical Coatings Laboratory, High Energy Laser & Optics Section, RRCAT, Indore 452013, M.P., India [2]Homi Bhabha National Institute, Training School Complex, Anushakti Nagar, Mumbai, 400094. *Email:suparna@rrcat.gov.in*

High-quality TiO_2 thin films with large-area coverage prepared by sol-gel process are reported for application in optical coating. Addition of polymethyl methacrylate (PMMA) to the sol exhibits significant improvement in the optical quality as well as morphology of the TiO_2 films. Refractive index and bandgap of TiO_2 are tailored by controlling TiO_2 sol:PMMA volume ratio. The refractive index are varied in the range of 2.4 to 2.0 at 550 nm by changing the TiO_2:PMMA composition. The absorption of the TiO_2 film is found to be 1000 ppm measured by photothermal abosorption. The absorption value reduced to 20 ppm for TiO_2:PMMA composite film (1:1). Consequently, laser induced damage threshold (LIDT) value also exhibits a four-fold enhancement for the TiO_2-PMMA composite film compared to that of TiO_2 film. An LIDT value of 9.4 J/cm^2@ 6 ns is obtained at 1064 nm for the TiO_2–PMMA composite film. A reflectivity of 87% is obtained for a 13 layer TiO_2-SiO_2 HLH multilayered films.

CP-03-14

Establishment of super polishing technique for the fabrication of ultra-low roughness cylindrical mirror substrates for laser plasma x- ray application,

*Rishipal Singh[*1], Anil Kumar[1] , Y. Pavan Kumar[1] A.K. Biswas[1], Sarvendra Singh[1], D. Raghunathan[1], Dinesh Kumar[2], Sanjay Sharma[2] , Nageswararao Pothana[3] , Rahul Shukla[3] and N. S. Benerji[1], [1]High Energy Lasers & Optics Section,[2] Engineering design and manufacturing section, [3] X-Ray Diffraction & metrology Section, Raja Ramanna Centre for Advanced Technology, Indore. Email: rps@rrcat.gov.in*

Cylindrical mirrors are required for laser plasma, synchrotron X-ray applications and optical experimental setups. The extremely smooth surface of the mirror improves the intensity of the image at the focus point. Super polishing technology is presented to polish the cylindrical surface of the work piece by using a special fixture and rectangular pan

slurry system. The cylindrical polishing machine was also modified, a special fixture and rectangular pan slurry system for surface super finishing was designed and manufactured. In this technique, the roughness of a mirror of size 115 mm x 38 mm x 10 mm was obtained on the order of 4.54 A° and generated a cylindrical radius of 152.6 mm within 1.7% error with respect to a radius of 150 mm.

CP-03-15

Establishment of polishing technique for polishing large size Neodymium doped glass laser rods for high energy laser

*Rishipal Singh[*1], Anil Kumar[1], Y. Pavan Kumar[1], Sarvendra Singh[1], D. Raghunathan[1], S.S. Thangavel[1], A.K. Biswas[1], C.P. Paul[2] and N. S. Benerji[1] ,[1]High Energy Lasers & Optics Section, [2] Engineering Design and Manufacturing Section, Raja Ramanna Centre for Advanced Technology, Indore, Email: rps@rrcat.gov.in*

Higher energy laser systems require larger size neodymium glass laser rods. A chemical mechanical polishing process for polishing large-sized neodymium glass rods is presented. Special jigs and fixtures were designed and developed for the grinding and polishing process. Matching glass was fitted to the end surface of the jig. Sodium fringe system is used to check flatness and autocollimator is used to check parallelism of the rod. Ovens are used to control the temperature to avoid cracks in the rod while fixing the rod in the jig. Flatness of both surfaces of the rod was achieved better than ? /8 at 5893 Aº wavelength over 100 mm diameter. Parallelism was controlled on the order of 5 arc seconds.

CP-03-16

Growth and Characterization Study of Organic Benzimidazole L-tartrate Single Crystal for NLO Applications

Hiral Shah[1,2], Vijayalakshmi Iyer[1], Vidit Patel[1], Bharatkumar Parekh[1] [1]Pandit Deendayal Petroleum University, Gandhinagar 382007, India [2]L.D. Engineering College, Ahmedabad 3800015, India *Email: dr.bharatparekh@gmail.com*

Optically transparent high-quality, non-hygroscopic, crystals of imidazole derivative, benzimidazole L-tartrate (BILT) were successfully grown using a controlled slow evaporation technique. Analysis of the powder X-ray diffraction pattern, conclusively established the monoclinic structure. The intra molecular bonding, charge distribution and transport mechanism were systematically studied. Verification of the available distinct functional groups was studied through FTIR–ATR response. Using UV-VIS spectra, crystalline quality was further analysis. Unveiling a lower cut-off of 288 nm wavelength. Optical parameters, such as variation in the refractive index with wavelength, the band gap, extinction coefficient values, and lower cut-off of 288 nm wavelength supported the material's potential use for optoelectronic devices. The material's reactivity analysed by HOMO –LUMO studywith a wide band gap of 4.2 eV. Thermal stability, as confirmed by

TGA and DTA analyses, and observed that decomposition occurred as a single phase within the temperature range between 180 °C to 250°C. The material's suitability for nonlinear optical (NLO) devices was substantiated by a lower dielectric constant and less dielectric loss. The Kurtz and Perry powder technique, remarkably, the second harmonic generation (SHG)efficiency of the material was calculated to be 2.69 times higher than that of potassium dihydrogen phosphate (KDP). This underscores the material's potential for advanced optical applications.

CP-03-17

Development of narrow band interference filters for LASER altimeter

Girish M. Gouda, Sivaramsudhan S., S. Ajith Kumar, R. Venkateswaran, K.V. Sriram Laboratory for Electro-Optics Systems (LEOS), ISRO, Bengaluru-560 058 Corresponding author: girish@leos.gov.in, *Email: girishmg.g@gmail.com*

Optical interference filter with narrow band pass is required for the refractive optics of Laser Altimeter. A single component narrow band width filter was designed, developed and space qualified indigenously. The narrow band pass interference is an important component of the receiver optics which need to designed to transmit only LASER band and avoid the detector saturation. The paper describes the development of the narrow band filter for LASER Altimeter (LASA) applications.

CP-03-18

Geometric phase induced tunable optimum output coupling in optical parametric oscillators

Chahat Kaushik,[1,2] AadhiA, [3]Anirban Ghosh,[1], R.P. Singh[1], S. Dutta Gupta[4,5], M.Ebrahim-Zadeh[6,7] and G.K. Samanta[11]Physical Research Laboratory, Ahmedabad, Gujarat 380009, India [2]Indian Institute of Technology- Gandhinagar Ahmedabad, Gujarat 382424, India, [3]Photonics Devices and System Group, Singapore University of Technology and Design, Singapore, 487372, Singapore [4]Tata Institute of Fundamental Research, Hyderabad, Telangana 500046, India [5]Department of Physical Sciences, IISER Kolkata, Mohanpur 741246, India [6]School of Physics, Hyderabad Central University, Serilingampally, Telangana 500046, India [7]ICFO Institutde Ciencies Fotoniques, The Barcelona Institute of Science and Technology, 08860 Ca telldefels (Barcelona), Spain [8]Institucio Catalanade Recercai Estudis Avancats (ICREA), Passeig Lluis Companys23, Barcelona 08010, Spain, Email: kaushikchahat96@gmail.com*

We present a Geometric phase (GP)-based Sagnac anti-resonant ring (ARR) interferometer mirror (GP-mirror) forachieving tunable optimum output coupling in continuous wave (CW) doubly resonant optical parametric oscillators (DRO). The DRO is designed using an online arcrystal MgO:PPsLT of 30mm length and grating period of 7.97 μm with GP mirror in one arm of the standing wave cavity. The GP mirror is constructed

using quarterwave-plate (?/4), half wave plate (?/2), quarter wave-plate(?/4) at +45?, ? , -45?with respect to vertical polarization, respectively. The DRO output transmission can be varied continuously from 0.6% to 50%, attaining optimum output coupling of 1.4% for maximum power extraction of 2.45W when pumped with an incident power of 5 Wat 47? Ccrystaltemperatureatsignalandidlerwavelengthof1054nmand1074nm,respectively.The maximumpumpdepletionof89%isobtainedwithaconversionefficiencyof49%.Thetransmis sionthrougha≥GP-based mirror delivers the tunable optimum output power across the tuning wavelength range90 nm. This demonstrated GP-mirror concept offers a promising approach for advancing the capabilities and control of coherent sources tunable across different spectral regions and in all time-scales from continuous-wave to ultrafast femto second domain.

CP-03-19

Cr:Al_2O_3 Nanoparticles for lasing applications: a method for a-Al_2O_3 Phase in Minutes

Prinston Melroy Lewis, K.S. Choudhari, Suresh D. Kulkarni Department of Atomic and Molecular Physics, Manipal Academy of Higher Education, Manipal, India *Email: suresh.dk@manipal.edu*

Swift and facile synthesis of optical materials for lasers, at modest temperature and cost is an ever-ending demand among the phosphor research community. Achieving high-quality phosphors for various applications in an economically feasible way is a challenge. Here, we propose a swift, simple, one-step, rapid pyrolysis-assisted combustion (RPAC) method to obtain a-Al_2O_3 and Cr^{3+}-doped a-Al_2O_3 nanoparticles ($Al_{2-x}Cr_xO_3$, $0 \leq x \leq 0.02$) with judicious tuning and optimization of various experimental parameters. a-alumina phase is achieved in Cr^{3+}:Al_2O_3 nanoparticles within minutes at 450 °C with crystallite sizes up to 61 nm, as evidenced by the XRD patterns. Diffuse reflectance spectra showed broad bands at 402 and 557 nm corresponding to the Cr^{3+} transitions, which became prominent with increase in Cr^{3+} concentration. Photoluminescence studies showed the sharp red emission at 694 nm (ruby line) for all samples, the maximum intensity for x = 0.01. The phosphorescence lifetimes decreased from 5 to 2.4 ms with the increase in Cr^{3+} concentration. A Dq/B value of *ca.* 2.6 for each sample confirmed the presence of Cr^{3+} ions in the octahedral crystal field. Chromaticity diagrams displayed the maximum red appearance for the sample with x=0.01. The samples $Cr_{0.01}$:α-$Al_{1.99}O_3$ and $Cr_{0.015}$:α-$Al_{1.985}O_3$ exhibited internal and external quantum efficiencies of 15 and 43% and 16.7 and 38.8%, respectively, at 402 nm excitation. The color coordinates showed a color purity of up to 76%, referenced to NTSC 1953 red standard at 402 nm excitation and up to 94% for UHD: ITU BT.2020 red standard at 557 nm excitation. Further, the post-synthesis processing of $Cr_{0.01}$:α-$Al_{1.99}O_3$ nanoparticles by cyclic RP at 800 °C (35 min) induced greater crystal growth than the 2-hour furnace anneal at 1200 °C. The improvement of the quantum

efficiency from 15 to 18% further established the superiority of the cyclic RP, compared to the 1200 °C annealing. These highly crystalline Cr^{3+}:Al_2O_3 nanoparticles with near monochromatic emission can be used as active medium in lasers along with various other applications, including plant growth LEDs, display phosphors, anticounterfeit, and bioimaging applications.

CP-03-20

Design of an all-fiber Q-switched laser by using a bismuth-erbium-vanadium co-doped optical fiber as saturable absorber at 1550 nm

A. Ghosh[1,2], U. K. Samanta[1,2], S. Das[1], M. C. Paul[1],[1]CSIR-Central Glass and Ceramic Research Institute, [2]Jadavpur University, Email : arunaghosh9@gmail.com

The performance of a passively Q-switched pulsed laser has been presented in this report by using a segment of bismuth-erbium-vanadium co-doped optical fiber as a physical saturable absorber (BEV-FSA) in an all-fiber laser cavity configuration. Exploiting a double-clad erbium-ytterbium co-doped fiber (DC-EYDF) as the gain medium, the output characteristics of the laser has been studied by varying the pump power. The output spectrum of the laser centered at 1550.86 nm and delivered stable Q-switched pulses with repetition rate 47.5 kHz. A minimum pulse width of 1.8 μs with maximum output power 17.6mW at maximum pump power 2.31W has been observed.

CP-03-21

Comparative Study of Laser Texturing of FEP and Aluminum on Triboelectric Nanogenerator for Vibration Sensing

Diksha Jaurker[1], Suhas S. Joshi[1], I. A. Palani[1] [1]Department of Mechanical Engineering, Indian Institute of Technology Indore, India * Email: palaniia@iiti.ac.in*

Triboelectric nanogenerators (TENGs) have advanced as versatile and efficient devices with applications expanding beyond harvesting electricity. TENGs provide electrical signal outputs corresponding to the amplitude and frequency of delivered vibrations or mechanical disturbances. In literature, different surface modification techniques have been deployed to improve the performance of TENGs. Among all, Laser texturing is an advanced surface modification technique to enhance triboelectrification due to no requirement of mask or toxic chemicals, also it has less processing time and greater dimensional precision.. This work aims to perform a comparative study on the influence of laser texturing of Fluorinated Ethylene Propylene (FEP) sheet and aluminum (Al), with pulsed Nd^{+3} :YAG laser at 532nm wavelength at different spot overlap, on TENG's performance in contact separation mode. The electrical performance is observed to be improved by the laser texturing, due to the increase in the surface roughness effective area of contact, and surface charge density increased, but after a certain value of spot overlap the output decreased. This is due to the increased aspect ratio leading to charge

entrapment within the crater and recast formed by laser processing. The laser-textured TENG was able to detect the working state of air compressor by generating voltage signals corresponding to the vibration, which shows its ability to be used as a vibration sensor in different machine tools.

CP-03-22

2D Photonic Crystal L3 Cavities based Biosensor

Puja Sharma[a], Nilaksha Ghosh[a], Sarang Medhekar[a] Department of Physics, Central University of Jharkhand, Ranchi 835222, Jharkhand, India Email : sarang.medhekar@cuj.ac.in.*

A2D photonic crystal biosensor is proposed here using two L3 cavities anda defect waveguide. Its performance is analyzed using Plane Wave Expansion Method and 2D Finite Difference Time Domain Method. It exhibits high-quality factor (Q-factor) of 25x87 with a spectral width of 0.6 nm at the resonant wavelength of 1552 nm. Further, it shows a high figure of merit 666 RIU^{-1}) a low detection limit ($1.49x10^{-4}$ RIU) and a maximum sensitivity of 400nm/RIU. The proposed biosensor might have potential applications in detection of many blood related disease.

CP-03-23

Ultra-low roughness flat fused silica substrates fabricated using bowl-feed chemical-mechanical-polishing technique

A K Biswas[1], D Raghunathan[1], Sumit[2], Rishipal[1], Y Pavan Kumar[1], R Shukla[2,3], Nageswar Rao[3], M KSwami[3], S K Rai[3], Tapas Ganguli[2,3] and N. S. Benerji[1,4] [1]Optical Design and Development Laboratory, [2] Homi Bhabha National Institute, Anushaktinagar, Mumbai, [3]Accelerator Physics & Synchrotron Utilization Division, [4] High Energy Laser & Optics Section, Raja Ramanna Centre for Advanced Technology, Indore 452013 *Email: abhik@rrcat.gov.in*

The work presented here is an attempt to fabricate large, flat fused silica (FS) glass substrates with ultra-low surface roughness ~ 1-3 Å and a high form accuracy better than /10 using bowl-feed chemical-mechanical polishing (Bowl-feed CMP). The methodology of super-smooth polishing of FS glass with bowl-feed CMP and detailed surface roughness characterization with AFM and x-ray reflectivity (XRR) are presented. We demonstrate that large size, flat, ultra-low roughness FS substrates could be fabricated using bowl-feed CMP technique. High-spatial frequency r.m.s roughness of ~ 1 Å has been measured using AFM and that estimated from XRR measurements is about 4 Å, making them suitable for indigenous development of high LIDT laser optics and synchrotron x-ray mirrors.

CP-03-24

Novel Optical Waveguide Michelson Interferometer using Photonic Crystal Structure

Ashish Singh Bais and Joseph Thomas Andrews Applied Photonics Laboratory, Department of Applied Physics and Optoelectronics, Shri G. S. Institute of Technology and Science, 23 Park Road Indore, MP 452003 India. Email: jtandrews@sgsits.ac.in*

We designed a novel loop mirror-based Michelson interferometer using photonic crystal structures. We used semiconductors such as GaAs as well as the standard polymer photoresists such as SU8, S1813 as waveguide structures. The Novel mirror loop uses clockwise and anti-clockwise motion of waves, such that the phase and coherent properties remian same in both the paths. The fabrication of similar device would help to miniaturise optical devices using Michelson interferrometer. The designed and simulated structures exhibits the interference phenomena and promises as a suitable candidates for the realization of proposed devices for use in biomedical instrumentation.

CP-03-25

Gold-assisted mechanical exfoliation for preparinglarge area flakes of monolayer MoS_2

Rajkumar Balan[1,#], Salahuddin Khan[1,2,], Saleem Khan[1,2], Asha Singh[1], Rahul Aggarwal[3], Geetanjali[1,2]and T. K. Sharma[1,21]Materials Science Section, Raja Ramanna Centre for Advanced Technology, Indore, 452013.[2]Homi Bhabha National Institute, Training School Complex, Anushakti Nagar, Mumbai, India - 400085.[3]Laser Physics Applications Division, Raja Ramanna Centre for Advanced Technology, Indore, 452013[#]Shri R. Balan was a M.Sc. project student from PSG College of Arts & Science, Coimbatore.*Corresponding author: skhan@rrcat.gov.in*

Monolayers of two-dimensional semiconductors are potential candidates for optoelectronic and flexible devices. Two-dimensional (2D) semiconductor materials such as molybdenum disulfide (MoS_2) are van der Waals materials that are strongly bonded in two dimensions. These are stacked layers that are weakly bound in the third dimension. Due to this weak bonding in the third dimension, it is possible to prepare monolayers and a few layers of these materials. It actually transforms from indirect to direct bandgap when it is reduced to single layer. Such direct bandgap monolayer 2D materials have high carrier mobility, broadband optical absorption, and a large surface area, resulting in strong light-matter interaction. These materials make an attractive system for fundamental physics studies and optoelectronic applications.In this work,atomically thin monolayer MoS_2films are formed using an inhouse developed mechanical exfoliation technique. PDMS gel-assisted exfoliation with stamping approach is used to make high-quality, residue-free monolayer MoS_2. Gold-assisted exfoliation approachis also used which yields in the formation of in

few hundred microns size of monolayer MoS_2. The prepared monolayers of $MoS_2$are characterized using an in-house developed optical microscope, AFM and Raman measurement techniques which confirms the formation of monolayerMoS_2.

CP-03-26

Effect of Carbon Crucible on Multi-Crystalline Silicon Ingot During Directional Solidification Process: Numerical Simulation

P. Periyannan, M. Bharathwaj, P. Karuppasamy, and P. Ramasamy, Department of Physics, SSN Research Centre (SSN RC), Sri Sivasubramaniya Nadar (SSN) College of Engineering, Kalavakam-603110, Tamil Nadu, India Email: karupppasamyp@ssn.edu.in*

Multi-crystalline silicon (mc-Si) ingot is grown by a directional solidification process. To investigate the growth process by using a 2D axis-symmetric global transient model. Numerical simulation was practiced for simulating the Directional solidification process (DS). In this work, we have exchanged the carbon crucible instead of quartz in the DS system. The growth process has been simulated using CG-Sim Software and their results have been analyzed. The Impurities such as oxygen, and carbon arise from the parts of the furnace and are segregated in the multi-crystalline silicon ingot based on the crystal solubility. Similarly, von-Mises stress, maximum shear stress, average growth rate, and power consumption were analyzed for both conventional and modified systems. Solar cell performance depends directly on the quality of the mc-Si ingot. The modified grown ingot is more favourable for PV applications.

CP-03-27

Impact of fast cooling process on mc-silicon ingots grown by developed copper plate DS system: Optical Studies.

Muthukumar R, Aravinth K, Ramasamy P, Department of Physics, Sri Sivasubramaniya Nadar College of Engineering, Chennai - 603110, India. *Email: aravinthk@ssn.edu.in*

Multi-crystalline silicon ingots are mainly created by a widely recognized directional solidification process.The directional solidification techniqueestablished on copper plates was used for producing the boron-doped multi-crystalline silicon (mc-Si) ingots. In order to generate multicrystalline silicon, a novel design of copper plate created directed solidification furnace is suggested based on numerical simulation. In an experiment, grown ingots were used to make bricks, followed by wafers. The wafers are subjected to surface morphology, UV analysis and minority carrierlife time measurement.The result demonstrates that the copper plate created DS system may yield greater crystal quality.

CP-03-28

Heat removal using aluminium nitride and boron arsenide heat spreaders in high-power laser diode arrays: A comparative study

*Ravi Kumar[1,2], Venus[1,2], Deepesh Nimje[1,2], Geetanjali Vashisht[1,2], Abhishek Chatterjee[1,2], Vishal Agnihotri[1], Sunil Kumar Sharma[3], Alexander Khakha[1], S. Porwal[1], B.N. Upadhyaya[2,3], V. K. Dixit[1,2] and T. K. Sharma[1,2] [1]MaterialsSemiconductor Materials Lab., Raja Ramanna Centre for Advanced Technology, Indore, 452013 [2]Homi Bhabha National Institute, Training School Complex, Anushakti Nagar, Mumbai, India, 400085 [3]Industrial Lasers and Applications Section,Raja Ramanna Centre for Advanced Technology, Indore, 452013 *Corresponding Author Email: ravi@rrcat.gov.in*

The process of heat removal from the laser diode arrays is addressed via computational fluid dynamic numerical simulations on laser diode modules with two types of heat spreader materials. In this work, heat dissipation from laser diode arrays is analysed by choosing aluminium nitride and boron arsenide as the heat spreader materials. Numerical simulations are used to understand the experimental results of the solid-state laser's output power (>50W) that is powered by inhouse bonded and packaged laser diode arrays. The arrays are operated at two different temperatures (15.5 and 19.5 °C) with an optimized fluid flow of 4 slpm. It is found that while AlN-based heat spreader material removes sufficient heat from the module at an optimized flow of 4 slpm at 15.5°C, the overall pumping efficiency is reduced. On the other hand, the usage of boron arsenide as heat spreader materials can overcome such limitations to enable the laser diode arrays to operate at very high output power. Boron arsenide is found to be a better heat spreader material for potential application in high power laser diode arrays.

CP-03-29

Vertical Bridgman Growth of 2-Methoxy Benzoic Acid Single Crystal: A Promising Approach for Nonlinear Optical Applications

Jithin Kuriakose, P. Karuppasamy, M. Senthilpandian, P. Ramasamy, SSN Research Centre, Department of Physics, Sri Sivasubramaniya Nadar College of Engineering, Kalavakkam-603110, Email: jithink@ssn.edu.in

Organic optical single crystals play a crucial role in the field of nonlinear optical (NLO) applications. Therefore, increasing fascination with investigating organic compounds as NLO in recent years, owing to their distinctive characteristics. This research paper focuses on the exploration of 2-methoxy Benzoic Acid (2MBA) as a potential sparkling substance. We explore the vertical Bridgman techniques used forthe growth of a 2MBA single crystal, its structural, optical, Z-scan and thermal properties have been investigated. We emphasize its possible uses in the NLO application.

The use of the vertical Bridgman method of crystal development is inspired by its power to

produce massive, single crystals with greater structural perfection and optical homogeneity. This approach enables for regulated solidification along a vertical axis, minimizing flaws and ensuring the consistency of crystal quality. In the context of 2MBA, the application of the vertical Bridgman approach attempts to leverage these benefits for the precise customization of crystal characteristics tuned for optimal nonlinear optical performance. This work provides a complete examination of the growth process, crystallographic characterization, and optical properties of 2MBA single crystals generated by the vertical Bridgman approach.

CP-03-30

Ab-initio simulations for calculating optical properties of glasses: case study on iron-phosphate glass

Shakti Singh[a,b,c,] and Sharat Chandra[b,c] [a]Laser Biomedical Applications Division, Raja Ramanna Centre for Advanced Technology, Indore, MP,India 452013 [b]Materials Science Group, Indira Gandhi Centre for Atomic Research,Kalpakkam, TN, India 603102 [c]Homi Bhabha National Institute, Anushaktinagar, Mumbai, Maharashtra, India 400094 Email: shaktisinghstephen@gmail.com, shaktis@rrcat.gov.in*

The application of glass as laser host material and in optical fibers is well known. In this study, we present a methodology to simulate optical properties of glasses and for a case study iron phosphate glass is chosen. Random-network model is developed using potential-free Monte-Carlo (MC) method, which is then optimized using DFT. The optimized model is used for obtaining the optical properties of IPG. Functional dependence of the electronic density of states (EDOS), optical properties such as absorption coefficient, reflectivity, refractive index and extinction coefficients are presented. Calculated band-gap and Urbach energy values are compared with experimental values and found to be in good agreement.

Category - 4
Nonlinear, Quantum and Atom Optics

CP-04-01

Laser cooling and radio-frequency evaporative cooling of ^{87}Rb atoms in same ultra-high vacuum chamber

Sourabh Sarkar[a,b], S. P. Ram[a], Kavish Bhardwaj[a], Gunjan Verma[a], V. B. Tiwari[a,b], S. R. Mishra[a,b] [a]Laser Physics Applications Division, Raja Ramanna Centre for Advanced Technology, Indore-452013, [b]Homi Bhabha National Institute, Training School Complex, Anushakti Nagar, Mumbai -400094 [*]Email: sourabhs@rrcat.gov.in*

We have demonstrated the magneto optical trap (MOT) loading, magnetic trapping and radio-frequency (rf) evaporative cooling of ^{87}Rb atoms in the same ultra-high vacuum (UHV) chamber. Initial experimental work on trapping of Rb atoms in radio-frequency (rf) dressed potential has also been carried out and trapping of atoms in double-well potential is demonstrated. The work is in progress to demonstrate trapping of evaporatively cooled atoms in rf-dressed potentials of different types.

CP-04-02

Synthesis and Nonlinear Optical Response of the Schiff Bases Derivative for Optoelectronic Devices

Sultan[1,], Mohd Mehkoom[1,$], S. M. Afzal[1], and Salman A. Khan[2], [1]Department of Physics, Aligarh Muslim University, Aligarh -202002, India [2]School of Sciences, Maulana Azad National Urdu University, Hyderabad-500032, India, Email: *shahidsultan100@gmail.com,[$]mehkoom@outlook.com*

The current research on titled compound (2-hydroxy-4-methoxyphenyl) (phenyl) methylene) amino) 4,5,6,7-tetrahydrobenzo[b] thiophene-3-carbonitrile (HPTC) has been done to explore the third-order nonlinear response for optoelectronic devices. HPTC compound was synthesized using the condensation method and nonlinear optical characterization was done by Z-scan approach with continuous wave (CW) diode laser. We have measured third-order nonlinear refractive index (n_2), absorption (ß), and susceptibility (?$^{(3)}$) at variable solution concentrations(0.75, 1.25, 2.50, 3.75, and 5.0 mM) at fixed laser input power of 60 mW (with 4.02 kW/cm^2 peak irradiance at focus) and laser power (in mW) and at a laser power of (40, 50, 60, 70, and 80 mW) for a fixed concentration of 3.75 mM.The values of n_2, β, and $\chi^{(3)}$ are found in the order of 10^{-8} cm^2/W,10^{-4} cm/W, and 10^{-6}esu respectively, and vary linearly with concentration and power. We have also looked at HPTC's optical limiting behavior for laser safety devices.

CP-04-03

Blue photon in non-linear alkali medium

Vinay Shukla[1,2] , Ayan Ray[1] [1]Variable Energy Cyclotron Centre, Kolkata 700064, West Bengal India. [2]Homi Bhabha National Institute, Training school complex, Anushaktinagar, Mumbai 400094, India ,Email : vinayshukla2018@gmail.com.

In this work we present the two photon coherence[1] in a non-linear medium consisting of hot Rubidium(^{87}Rb) atom. Here we follow two photon transitions under ladder type excitations, $5S_{1/2}(F) \rightarrow 5P_{3/2}(F') \rightarrow 5D(F'')$ and we focus simultaneously on Electromagnetic Induced Transparency (EIT)[2] and Electromagnetic Induced Absorption[3] by observing the blue photon emanating from decay channel $5D \rightarrow 6P_{3/2} \rightarrow 5S_{1/2}$. Here, the $5S \rightarrow 5P$ excitation arm is modified by adding another excitation arm, which is slightly detuned to the former. Therefore, we have degenerate two level system[4] and V-type system[5] at the same time depending on detuning condition and this leads to variation of Amplified Spontaneous Emission (ASE)[6]. This work tries to bridge between velocity selective and velocity non-selective transitions, which is novel in itself. Coherent blue photons find their applications in many technological advancements and thus this paper provide an insight between correlated and non-correlated blue photons [7].

CP-04-04

Measurement of earth's gravitational acceleration (g) using cold atom gravimeter

*S. Singh[*1], S. P. Ram[1], Kavish Bhardwaj[1], Vijay Kumar[1,2], B. Jain[1], V. B. Tiwari[1,2], S. R. Mishra[1,2] [1]Laser Physics Applications Division, Raja Ramanna Centre for Advanced Technology, Indore - 452013, India. [2]Homi Bhabha National Institute, Training School Complex, Anushakti Nagar, Mumbai - 400094, India. [*]Email: surendra@rrcat.gov.in*

Precision measurement of earth's gravitational acceleration (g) has applications in geophysics, gravity surveys, fundamental research, natural resource explorations, monitoring seismic activities, and space science and technology. The cold atoms based Raman pulse atom interferometer setup for measurement of g, called “cold atom gravimeter” (CAG), has been developed and made operational at RRCAT, Indore. The local value of 'g', estimated using this gravimeter, has been found to be 9.78617±0.00003 m/s^2 with an accuracy of milli-Gal level. Further work is in progress to improve the accuracy of our gravimeter.

CP-04-05

Interacting four-level tripod configuration in Zeeman sublevels of ^{87}Rb leads to power-broadening immune electromagnetically induced transparency

P. Seth[1,2], D. Bhattacharyya[3], N.S. Mallick[1,2] and S. De[1,2] [1] Saha Institute of Nuclear Physics,

1/AF, Bidhannagar, Kolkata – 700064, India. [2] Homi Bhabha National Institute, Training School Complex, Anushaktinagar, Mumbai – 400094, India. [3] Santipur College, Santipur, Nadia, West Bengal, PIN – 741404, India. Email: sethpriyabrata@gmail.com.

We experimentally demonstrate double EIT resonances in a four-level tripod system,formed within the Zeeman sublevels of F=2 - F' = 1 transition of 87Rb with co-propagating, phase coherent pump and probe beams. We observe two EIT peaks with unequal peak heights in the probe transmission signal. The larger EIT peak shows linear power broadening with the variation of pump power and longitudinal magnetic field. However, the linewidth of the smaller EIT peak which appears because of the earth's non-zero transverse magnetic field present in our setup, does not change with the pump power and shows a mixed behaviour with longitudinal magnetic field variation. To simulate these EIT signals theoretically, density matrix equations are derived from Liouville's equation for a tripod system interacting with three fields. We have solved these equations under steady-state conditions and calculated the analytical expression of Doppler averaged probe susceptibility. We observed that at certain domains of the higher fields, the interactive stronger Ù system starts dominating over the weaker one, thus affecting its normal behaviour. This is further confirmed through our theory that the imaginary part of susceptibility of the weaker Ù system gives a complex structured equation allowing its linewidth to remain immune to the power broadening. Our theoretical simulations match well with the experimental observations. This study has important applications in atom-based magnetometry and precision measurement.

CP-04-06

Studies on Rabi oscillations in two photon Raman transition in a cold Rb atomic fountain

Vijay Kumar[1,2], S. Singh[1], Kavish Bhardwaj[1], S. P. Ram[1], B. Jain[1], V. B. Tiwari[1,2], S. R. Mishra[1,2]*
[1]Laser Physics Applications Division, Raja Ramanna Centre for Advanced Technology, Indore - 452013, India. [2]Homi Bhabha National Institute, Training School Complex, Anushakti Nagar, Mumbai - 400094, India. [*]Email: vijaykr@rrcat.gov.in

Rabi oscillations in populations in two ground hyperfine states ($5\,^2S_{1/2}$, F = 1 and F = 2) of ^{87}Rb atoms have been studied in an atomic fountain under two-photon Raman transition between states. We observed Raman p-pulse duration (τ_π) as ~12 μs for total power of ~13 mW in Raman beams at a red detuning of ~480 MHz from the excited state $5\,^2P_{3/2}$ (F' = 1). These results will be useful to generate appropriate Raman p- and p/2-pulses for atom interferometry measurements in the atomic fountain.

CP-04-07

Exploring Classical Bell's State through Wavefront Shearing Interferometry: A Comprehensive Investigation

Shouvik Sadhukhan, Applied and Adaptive Optics Laboratory, Department of Physics,

Indian Institute of Space Science and Technology(IIST), P.O: Valiamala, Trivandrum - 695547, State: Kerala; India. Email: shouvikphysics1996gmail.com

In our quest to explore quantum entanglement, we've used a clever device called a wavefront shearing folded Mach-Zehnder Interferometer. This tool allows us to create a special kind of entanglement called spatial-polarization entanglement.We achieved this by tilting one beam's path using mirrors after it passed through a special splitter called a polarizing beam splitter (PBS). Our experiment had four setups, each designed to create a different kind of entanglement. Here's the interesting part: we played with tilted Gaussian beams and special plates called Quarter-wave and Half-wave plates. These plates acted like choreographers, making the entanglement dance diverse with horizontal and diagonal moves. Surprisingly, whether the light beams spread out or stayed focused, the entanglement results were similar. We didn't stop at creating entanglement; we also studied how it changed over time. By turning a special plate, we could see the dance evolve. What amazed us most was that even with different beams, the entanglement outcomes were always in sync. This means our method is flexible and can work in various situations. Looking at the numbers behind entanglement, we found that its features stayed consistent across our four setups. This discovery opens up new possibilities for understanding and using quantum entanglement.

CP-04-08

Determination of third order nonlinearity(n_2&ß) of semi-organic single crystal (NaAP) usinga CW laser(?=532 nm) source at different intensities.

T. Mondal[1)], S. Das[1)] and N.Vijayan[2)],1) Department of Physics, University of Burdwan, Golapbag, Burdwan, India 713104 ,e-mail: [1)] iamtapasmondal.95@gmail.com & buphysd@gmail.com*; 2) Indian Reference Materials Division, National Physical Laboratory, New Delhi-110012, Email: vjnphy@gmail.com*

Sodium acid phthalate (NaAP) is a favorable nonlinearoptical material in the field of nonlinear optical applications. The third order nonlinear optical properties such as nonlinear refraction and nonlinear absorption was investigated under the excitation of Continuous Wave (CW) laser source (?=532 nm). And the value of nonlinear refraction (n_2) and nonlinear absorption coefficient (ß) was evaluated for six different optical intensities of the laser source(?=532 nm) using the familiar Z-scan method.

CP-04-09

Compact magneto-optical trap with hollow pyramidal mirror

S. Supakar [1,], Vivek Singh [1,3], Y. Pavan Kumar [2], S. K. Tiwari [2], C. Mukherjee [2,3], M. P. Kamath [2], V. B. Tiwari [1,3] and S. R. Mishra [1,3] [1]Laser Physics Applications Division, Raja Ramanna Centre for Advanced Technology, Indore 452013, India [2]High Energy Lasers and Optics Section, Raja Ramanna Centre for Advanced Technology, Indore 452013, India [3]Homi Bhabha National Institute, Training School Complex, Anushakti Nagar, Mumbai*

*400094, India *Email: subhajits@rrcat.gov.in*

Here, we report the development and working of a compact rubidium (Rb) atom magneto-optical trap (MOT) operated with a hollow pyramidal mirror and a single laser beam. This type of compact MOT is suitable for developing portable atom-optic devices, as it works with less number of optical hardware as compared to a conventional MOT setup.

CP-04-10

Third Harmonic Generation from Frequency Selective Surface Using Split Ring Resonator at THz Frequencies

M. Sahu[1], P. Roy Chaudhuri[1], [1]Department of Physics, Indian Institute of Technology Kharagpur, Kharagpur 721302, India, Email: roycp@phy.iitkgp.ac.in*

we report here new designs for metamaterials using a patterned split-ring resonator (SRR) arrangement to achieve third harmonic generation (THG) at Terahertz (THz) frequencies. The effectiveness of THG is achieved by aligning the fundamental (?) and third harmonic (3?) frequencies with the resonance of our suggested metasurface structure. This results in leading to energy confinement during both the excitation at ? (3.7 THz) and the radiation at 3? (11.1 THz), with an input intensity of 0.5 MW/cm$^{\wedge 2}$. We choose SRRs for the structure due to their strong sensitivity to electromagnetic waves.

CP-04-11

Study of spatial evolution of laser beam in NIM with Kerr nonlinearity using NLSE

Dimishree Neog, Abhijeet Das, Subrata Hazarika, Department of Physics, Assam University, Diphu Campus, Diphu, Karbi Anglong, Assam-782462, *Email: abhijeet_das@yahoo.com*

Spatial evolution of an elliptical Gaussian beam is investigated in a representative non-linear negative index medium using the non-linear Schrodinger equation(NLSE), solved numerically with the split-step Fourier method(SSFM). As negative index of refraction 'adds new twist to virtually all EM phenomenon', unconventional and interesting results are observed in IDRI of negative index medium, particularly in self-focusing and formation of filaments. Analysis shows that basically these results are outcome of the reversal of wave vectors in negative index medium.

CP-04-12

Nonlinear Optical Characteristics of natural pigments extracted from *coleus amboinicus*

P. Praveen Kumar, E.R. Rashis Varma, S. Jeyaram, S. Madhu, Department of Physics,

Takshashila University, Ongur (PO), Tindivanam (TK), Villupuram-604305, Tamilnadu Email : praveenkumartuphy@gmail.com, rashisvarmaphysics@gmail.com

The present work reports the study of nonlinear optical (NLO) features of natural green pigment *chlorophyll* extracted from the medicinal plant *coleus amboinicus* for the first time to the best of authors knowledge. The functional groups in the green pigments are identified by FT-IR spectrometer. The NLO features such as nonlinear refractive index and nonlinear absorption coefficient are measured by facile Z-scan method using closed and open aperture technique, respectively. The calculated values of nonlinear refractive index (n_2), nonlinear absorption coefficient (ß), real part of third-order NLO susceptibility (Re (? ^{3})) and imaginary part of third-order NLO susceptibility (Im (? ^{3})) are respectively found to be – 1.96 X 10^{-7} cm^2/W, 6.06 X 10^{-3} cm/W, 6.65 X 10^{-7}esu, 1.06 X 10^{-7}esu. Third-order NLO susceptibility of *chlorophyll* extracted from *coleus amboinicus* is measured to be 6.75 X 10^{-7}esu.

CP-04-13

Trapping of optical pulse in Kerr induced ENZ regime of negative index material

Dimishree Neog, Abhijeet Das, Subrata Hazarika, Department of Physics, Assam University, Diphu Campus, Diphu, Karbi Anglong, Assam-782462, *Email:* abhijeet_das@yahoo.com

We investigate the mechanism of trapping of an optical pulse at intensity I_{th}, I_{th} being the threshold intensity for a negative index material (NIM) where Kerr induced non-linearity leads to a vanishing effective permittivity ϵ_{eff} 0) resulting in the characteristics of an epsilon-near-zero (ENZ) material. The present analysis shows that Kerr induced slowing down of group velocity of an optical pulse can be an alternative means to trap light by controlling the intensity of the light pulse resulting in the phenomena of slow light, stopped light or stationary light which are conventionally achieved through EIT based methods.

CP-04-14

Microwave assisted generation of non-degenerate four-wave mixing pulse

Nawaz Sarif Mallick[1,2],Priyabrata Seth[1,2] and Sankar De[1,2] [1]Saha Institute of Nuclear Physics, 1/AF, Bidhannagar, Kolkata 700064, West Bengal, India. [2]Homi Bhabha National Institute, Training School Complex, Anushaktinagar, Mumbai, 400094, India. Email : nawazsarif.mallick@saha.ac.in

Atomic coherence induced by laser-atom interaction leads us to uncover many spectacular optical nonlinear effects. Among the most well-known effects is Four wave mixing (FWM)[1,2] in which three electromagnetic fields of frequencies ? $_1$, ω_2 , ω_3 nonlinearly interact with the atoms and generate FWM signal which has a new frequency ? $_g = \pm\omega_1 \pm \omega_2 \pm \omega_3$. Most of the initial studies on FWM in atomic systems are carried out with continuous

wave (CW) lasers. In this article, we investigate a N-type 87 Rb atomic system for efficient generation and control of a non-degenerate four wave mixing (FWM) signal in pulsed regime. We demonstrate how the FWM conversion efficiency can be enhanced three times using a MW field. The MW field is generated using a microwave cavity which has a resonant frequency of 6.834 GHz. We observe 15.55% conversion efficiency in presence of a MW field of intensity of 90 $\mu W/cm^2$. Along with the improvement of FWM conversion efficiency, the shape of the generated FWM signal at medium output becomes equally important. Here, the FWM signal obtains the exact shape of the probe pulse and travels without changing the shape. A well shaped FWM signal has important applications in diverse fields such as signal processing, optical communication and information science.

CP-04-15

Bouncing Dynamics of a 2D Bose -Einstein Condensate under gravity: Application to optical field mapping

Gunjan Verma[a], V. B. Tiwari[a,b], S. R. Mishra[a,b] [a]Laser Physics Applications Division, Raja Ramanna Centre for Advanced Technology, Indore-452013 [b]Homi Bhabha National Institute, Training School Complex, Anushakti Nagar, Mumbai - 400094 [*]Email: gverma@rrcat.gov.in*

Reflection dynamics of a 2D Bose-Einsteincondensate of ^{87}Rb atoms bouncing off a potentialbarrier formed by a far detuned light sheet has been studied theoretically, considering gravitational potential as responsible for fall of condensate on the barrier sheet.The Gross – Pitaevskii equation has been solved numerically to calculate reflected condensate wave-function as a function of time. We investigate the effects of short range atom-atom interactions, strength of barrier and position of the barrier relative to the condensate on the reflection dynamics. The increase in short range interactions not only found to increase the rate of collapse of condensate wave function, but also increases the time require to complete subsequent bounces. The height of the barrier potential is found to control the fraction of condensate reflected and transmitted off the barrier. We take a case study where we infer about the optical field distribution of the barrier from the reflected density of the condensate.

CP-04-16

Kerr beam self-cleaning in a graded-index multimode fiber under different conditions with anomalous dispersion

Love Kumar Sharma, Dr. Vishwa Pal, Indian Institute of Technology Ropar, Rupnagar, Punjab, India Email: love.21phz0018@iitrpr.ac.in

In this work, we investigated the phenomenon of Kerr beam self-cleaning (KBSC) under different sets of input energy conditions in the anomalous dispersion region of a graded index multimode fiber (GRIN MMF) by solving the multimode generalized nonlinear Schrodinger equation. Our results clearly indicate that the phenomenon of spatial beam

self-cleaning is critically dependent on the initial launching conditions among the guided modes and the power threshold required for beam self-cleanup is different for different sets of input energy conditions considered. We also found that not every set of initial launching conditions leads to the phenomenon of KBSC and the phenomenon of spatial beam self-cleaning is accompanied by the onset of spatiotemporal instabilities in the system.

CP-04-17

Investigation on the structural, optical and third order nonlinear optical properties of a new centrosymmetric single crystal: 2-cyanopyridinium salicylate

Kintali Manohor Prasad[a], P. Srinivasan[a], Subrat Kumar Barik[a], B. Sahaya Infant Lasalle[b], MS Pandian[b], P. Ramasamy[b] [a]Department of Physics, National Institute of Technology Silchar, Silchar 788010, Assam, India [b]Department of Physics, SSN Research Centre, Sri Sivasubramaniya Nadar College of Engineering, Chennai 603110, Tamilnadu, India, Email: manoharprasad522@gmail.com

A new 2-cyanopyridinium salicylate (2-CPSC) single crystals were grown for the first time by using the slow evaporation of solvent technique. The single crystal X-ray diffraction studies were used to ascertain the grown crystal's cell parameters. The lower cutoff wavelength of the 2-CPSC crystal was found out from the UV–Vis–NIR studies for deliberating the optical transmittance window. A 632.8 nm He-Ne laser was used in the Z-scan technique to study the nonlinear optical properties, such as nonlinear refractive index (n_2), absorption coefficient (β), and susceptibility (χ^3).

CP-04-18

Benjamin-Feir instability in *pt*-symmetric Bragg grating with quintic saturable nonlinearity.

Satyabrata Sahu[1], P Mohanraj[2], R. Sivakumar[1] [1]Department of Physics, Pondicherry University, Puducherry-605014 [2]Department of Physics, Vel Tech Rangarajan Dr.Sagunthala R & D Institute of Science & Tech, Chennai-62 Email: satyabrata1307@pondiuni.ac.in

In a system of Fibre Bragg grating (FBG) with coupled effects of quintic and saturable nonlinearity, we look at the nontrivial characteristics of modulational instability (MI).Then, in order to examine the MI dynamics of the continuous waves perturbed by an infinitesimal perturbation, we use a standard linear stability analysis.Due to the quintic, saturable nonlinearity, loss/gain, and perturbed system, a range of instability spectra, such as the typical side bands, monotonically growing gain, the development of a single spectrum in either of the Stokes wave number regions, etc., are produced.

CP-04-19

Investigation of the Optical Properties of 2-Ethylimidazolium D-Tartrate Single Crystal in (001) direction for Optical limiting Applications

Mohamad Asikali Abdul Hakkim[1], Rajesh Paulraj[1], Ramasamy Perumalsamy[1], Rajeev Bhatt[2,3], Indranil Baumik[2,3], Mohammed Soharab[2,3] [1]Department of Physics, Sri Sivasubramaniya Nadar College of Engineering, Kalavakkam, Chennai, Tamilnadu – 603 110, India. [2]Crystal Growth and Instrumentation Section, Laser and Functional Materials Division, Raja Ramanna Centre for Advanced Technology, Indore, 452 013, India. [3]Homi Bhabha National Institute, Training School Complex, Anushakti Nagar, Mumbai-400 094, India. *Email:rajeshp@ssn.edu.in*

A potential organic single crystal of 2-Ethylimidazolium D-Tartrate was grown in the (001) direction using Sankaranarayanan-Ramasamy (SR) method. The transmission of the harvested SR crystal is more than 80% in the range of 400 to 800 nm. The in-plane refractive index was measured by prism coupling technique. It is observed that as the wavelength increased, the refractive index decreased. Third order NLO properties were scrutinized using Z-scan method. The calculated third order susceptibility value is 1.7×10^{-9} esu.

CP-04-20

Influence of Raman Scattering on two-soliton interaction in Highly Nonlinear Materials

Abhisek Roy and Partha Roy Chaudhuri Department of Physics, Indian Institute of Technology Kharagpur, Email:aroy95@kgpian.iitkgp.ac.in.*

Solitons are self-reinforcing wave packets that can maintain their shape and amplitude over long distances. The interaction of solitons can be harnessed to encode and transmit information reliably without distortion. We report our studies on two-solitondynamics along highly nonlinear chalcogenide fiber. The investigation is focussed on two temporally separated solitons propagating in a single-mode fiber, revealing significant modification of Kerr-induced interaction by interpulse Raman scattering.We have observed that that in highly nonlinear materials, the solitons propagate shorter distances without any Raman scattering-induced interaction.

CP-04-21

Computational Analysis of P-SHG Cartilage Image Features

Kausalya Neelavara Makkithaya[1], Guan-Yu Zhuo[2], Nirmal Mazumder[1] 1Department of Biophysics, Manipal School of Life Sciences, Manipal Academy of Higher Education, Manipal – 576104 2[2]Institute of Translational Medicine and New Drug Development, China Medical University, Taichung 404333, Taiwan *Email: nirmal.mazumder@manipal.edu*

The investigation introduces a pioneering approach for discerning between healthy and

degenerating cartilage tissues by scrutinizing collagen fibril degradation patterns through polarization resolved second harmonic generation microscopy (P-SHG). In addition, the study employs textural analysis to extract quantitative information, advancing our comprehension of tissue characteristics during disease progression.Cartilage samples from normal, osteoarthritis (OA), and rheumatoid arthritis (RA) tissues underwent preparation and analysis utilizing P-SHG imaging and quantitative image texture analysis. The resulting enhanced molecular contrast is anticipated to facilitate the differentiation between healthy and diseased cartilage tissues.P-SHG imaging analysis unveiled distinctive parameters in cartilage samples, reflecting variations in collagen fibril arrangement and organization across different pathological states. The planar orientation distribution of collagen fibrils revealed a more directional orientation in OA samples, linked to heightened type I collagen, while RA samples exhibited a heterogeneous molecular orientation. In conclusion, this study establishes the potential of the proposed imaging technique and quantitative analysis as a diagnostic reference for cartilage-related diseases, providing insights into collagen fibril degradation and contributing to a comprehensive understanding of tissue pathology.

CP-04-22

Elliptical Core Chalcogenide Fiber for Ultra-Broad Supercontinuum Generation

P. Roy[1] and P. Roy Chaudhuri.[1], [1]Department of Physics, Indian Institute of Technology Kharagpur, Kharagpur 721302, Email: roycp@phy.iitkgp.ac.in

In this article, we present our findings on Supercontinuum Generation (SCG) using an exceptionally wide wavelength range of 1410 nm. The results indicate that by modifying the shape of the fiber core and employing a highly nonlinear chalcogenide material, we can expand the range of flat wavelengths. By optimizing the structural parameters, we successfully achieve improved dispersion characteristics, leading to a significant SCG up to 1410 nm using a chalcogenide fiber with an elliptical core ($As_{40}S_{60}$ and $As_{42}S_{58}$ as core and cladding materials) that is 5 cm long. Furthermore, we demonstrate that by increasing the concentration of Arsenic in the Arsenic (As)-Sulphide (S) material combination (As-S), it is possible to generate an extremely broad SCG.

CP-04-23

Photon up-conversion in pure and doped carbon quantum dots synthesized from gelatine

Dr. Vijeesh P [a], Muhammed Rashid P S [a], and Flagon Xavier [a] [a] Department of Physics, The Cochin College, Kochi, Kerala, India, Email: namastheviji@gmail.com

Photon up-conversion is the process of absorbing lower-frequency radiation and emitting higher-frequency radiation, in contrast to the case of fluorescence. Pure and doped carbon quantum dots (CQD) have been synthesized from gelatin using the hydrothermal method.

The synthesized CQDs and doped CQDs were characterized using UV-Vis absorption, PL-life time, and fluorescent excitation studies Along with the fluorescent nature the pure and doped samples showed photon up-conversion and are being investigated. It is the process of absorbing low-energy visible light and emitting high-energy ultraviolet light. The pure and 2 doped samples show up-conversion. Further investigations were done to study the variation in up-conversion frequency with variation in excitation frequency. The up-conversion frequencies vary with dopants but showed a stable emission for various excitations. Biocompatibility studies of the grown samples also conducted to check the activity of the samples and the up-conversion UV light on the biological specimens.

CP-04-24

Biosynthesis of Silver Nanoparticles Using Moringa Oleifera aqueous leaf extract for nonlinear applications

Bini P Pathrose [1,a], A Mujeeb [1,b] [1]International school of Photonics, Cochin University of Science and Technology, Email: [a]binivibin@gmail.com, [b]mujeeb@cusat.ac.in

Recent advancement in the field of nanotechnology and their increased applications led to the development of novel synthesis techniques of nanostructures. The nanomaterials were used widely in several areas like photonics, microelectronics and catalysis. Commonly nanoparticles were prepared by physical and chemical methods. But the disadvantage of this method i.e., the inclusion of chemicals and the toxic by-products are unavoidable. Synthesis using biological methods which is an environment friendly approach will be the best solution. Moringa oleifera leaf extract is successfully used as the reducing agent for the synthesis of silver nanoparticles. The nanoparticles are spherical in size with good stability and with an average size of 70 nm. The synthesized nanoparticles are found to be promising candidates for nonlinear applications.

CP-04-25

Study of Optical nonlinearities in CuNiO thin films

R. Chouhan[1], A. Agrawal[2], P. Sen[3] [1]Department of Applied Physics & Optoelectronics, S.G.S.I.T.S.,Indore (M.P.) India [2]Department of Physics, Shri Neelkantheshwar Government PG College, Khandwa (M.P.) India [3]School of Physics, Devi Ahilya University Khandwa, Road, Indore (M. P.), India Email: romitachouhan15@gmail.com

We report the nonlinear optical properties of pure and Cu doped NiO thin films prepared by ion beam sputtering technique. The structural, linear and nonlinear optical properties are studied by XRD, UV–Vis and Z-scan, respectively. Increased in grain size is observed in doped film whereas the band gap value decreases upon addition of Cu ion on Ni site. The nonlinear optical properties such as nonlinear refraction coefficient (n_2) and third order nonlinear susceptibility are investigated. The calculations have been made by performing Z- scan experiment using CW He-Ne laser source in off resonant regime. The improved nonlinearity in doped film suggests that this material can be considered as a promising candidate for future optical device applications.

Category - 5
Ultrafast Lasers and Applications

CP-05-01

Generation of 1 µJ, 500 fs compressed pulses from Yb-doped fiber oscillator-amplifier

C.P. Singh[1,2], Bhuvnesh[1], Anshuman Nigam[1,2], P.K. Gupta[1,2], B. Prasad[1], P. Hedaoo[1], P.K. Mukhopadhyay[1,2], R. Arya[1] and S.K. Dixit[1,2] [1]Laser Technology Division, Raja Ramanna Centre for Advanced Technology, Indore-452013. [2]Homi Bhabha National Institute, Training School Complex, Anushakti Nagar, Mumbai-400094, India Email: cpsingh@rrcat.gov.in

We present development of ytterbium (Yb) doped all-fiber multi-stage amplifier in chirped pulse amplification (CPA) scheme using Yb-doped lab made mode-locked oscillator as a seed source. The oscillator generates chirped pulses of 5 ps duration at 1060 nm which have been stretched to ~250 ps duration by propagating them through a spool of passive fiber. Pulse picking arrangement is implemented in the amplifier to reduce the repetition rate from 40 MHz to 250 kHz. After the amplifier, transmission grating pair based pulse compressor generates ~500 fs duration pulses with 260 mW average output power which corresponds to 1 µJ energy per pulse.

CP-05-02

Analytical studies of nano-particle formation using ultrashort laser pulse ablation in vacuum

U. Chakravarty[1,2], Y.B.S.R. Prasad[1] [1] High Energy Laser Physic Section, Laser Plasma Division, Raja Ramanna Centre for Advanced Technology, Indore 452 013 [2]Homi Bhabha National Institute, Training School Complex, Anushaktinagar, Mumbai 400094, Email: uday@rrcat.gov.in

Ultrashort Pulsed Laser Ablation (UPLA) stands as a versatile technique for producing nanoparticles. A simple analytical model for predicting the size distribution and time scales of nanoparticle production is much needed for precise understanding of the physical processes involved in UPLA. In this work we employ an analytical model based on fragmentation and thermodynamics to elucidate the process of particle formation during heated matter expansion. It highlights that higher irradiation intensities lead to the creation of smaller particle fragments and emphasizes that specific laser focusing conditions and target parameters are crucial for efficiently generating nanoparticles with a narrow size distribution. Furthermore, the investigation identifies distinct time scales for particle

formation, indicating that smaller particles form earlier on a sub-picosecond scale compared to larger particles. The theoretical model substantiates the experimental observations of aluminum nanoparticle formation post-laser ablation in the fluence range of 0.1–1J/cm^2 having sizes typically in the range between 10–50nm.

CP-05-03

Development of a TR-MOKE Setup for Investigating Ultrafast Magnetization Dynamics in Magnetic Thin Films

*Chitra Dolai[*1], Debkanta Ghosh [*1], Shailab Singh Bodra [*1] and Prasanta Kumar Datta[1] [1] Department of Physics, Ultra-fast Science Lab, Indian Institute of Technology Kharagpur, Kharagpur 721302, India [*] Email: chitradolai721246@kgpian.iitkgp.ac.in*

Ultrafast magnetization dynamics study in nano-scale is nowadays an important field because of the increasing interest in magnetic storage systems, fast magnetic switching, and more over magnonic devices and spintronic devices. For this purpose, the study of spin wave dynamics along with ultrafast demagnetization is crucial. Time Resolved Magneto Optic Kerr (TRMOKE) effect is a very efficient and no destructive experimental procedure to follow the study. Here in our work, we have established the microscopic TRMOKE setup in our lab with a dual-color pump-probe mechanism. We have experimental evidence of its success in producing magnetic Kerr signal with delay time. We used Ni thin film as a ferromagnetic sample prepared in the EBV process.

CP-05-04

Ultrafast Carrier Dynamics of few layer MnTe using Femtosecond Transient Absorption Spectroscopy

A. Karmakar[(1)], S. Prodhan[(1)]*, C. Gowda[(2)], CS. Tiwary[(2)], PK. Datta[(1)] [1]Department of Physics, Indian Institute of Technology (IIT) Kharagpur, Kharagpur 721302, India [2]Department of Metallurgical and Materials Engineering, Indian Institute of Technology Kharagpur, Kharagpur 721302, India *These authors contributed equally Email : ayon95karmakar.iitkgp.ac.in.*

Manganese telluride (MnTe), member of transition metal based binary compounds, is well-known for it's magnetic, optical, and transport properties. To investigate ultrafast charge carrier dynamics, we have performed Femtosecond Transient Absorption Spectroscopy(FTAS) on few layer MnTe. Here we shows a broadband exited state carrier dynamics(ESA) dominated by free carrier absorption(FCA) in the visible region. We also shows the carrier recombination process is dominated by trap state assisted recombination. We has observed increase in carrier lifetime with pump fluence which is due to saturation of defect states in high pump fluence regime.We also calculate a high two-photon absorption (TPA) cross section of 2D MnTe from Pump wavelength dependent TA spectroscopy. Optimized carrier lifetime in one photon absorption regime and presence of

TPA absorption unravels the possibility of 2D MnTe to be used as above and below band gap photo-detector material.

CP-05-05

Leveraging Dual Saturation in Ag-550 Nanocrystals for Enhanced Ultrafast Optical Manipulation and Wavelength-Dependent Optical Limiting

Amit Kumar Pradhan[1], Suman Kumar[2], Amiya Priyam[2], Prasanta Kumar Datta[1] [1]Department of Physics, Indian Institute of Technology Kharagpur, Kharagpur-721302, India [2]Department of Chemistry, School of Physical and Chemical Sciences, Central University of South Bihar, Gaya-824236, India Email: amitkumar95@iitkgp.ac.in, pkdatta@phy.iitkgp.ac.in**

In order to determine the suitability for optoelectronic applications, anisotropic silver nanocrystals having surface plasmon resonance (SPR) at 550 nm (Ag-550) are examined for nonlinear optical characteristics at both resonant and off-resonant wavelengths using femtosecond pulse laser. The nonlinear absorption (NLA) in Ag-550 is caused by the competition between two contradicting phenomena: saturable absorption (SA) and reverse saturable absorption (RSA). SA is contributed by both one-photon absorption (1PA) and two-photon absorption (2PA) saturation. The RSA effect is enhanced with increasing wavelength. The outcomes, i.e., optical transparency and SA- RSA switching, will open ways for a variety of diverse applications such as optical switching, limiting, and bio-imaging.

CP-05-06

Understanding the Influence of Capping Layer on Spin Wave Modes: An In-Depth Investigation with a Custom Time-Resolved Magneto-Optical Kerr Effect (TR-MOKE) Setup

*Debkanta Ghosh[*1],Chitra Dolai[*1], Shailab Singh Bodra[*1], Biswajeet Nayak[2], Prasana Kumar Sahoo [2], and Prasanta Kumar Datta[1] [1] Department of Physics, Ultra-fast Science Lab, Indian Institute of Technology Kharagpur, Kharagpur 721302, India [2]Materials Science Centre, Quantum Materials and Device Research Laboratory, Indian Institute of Technology Kharagpur, Kharagpur, 721302, West Bengal, India [*]These authors contributed equally, Email: debkantaghosh99@kgpian.iitkgp.ac.in*

Here we investigated ultrafast magnetization dynamics of Ni thin film (10nm thickness) employing the time-resolved magneto-optical Kerr effect (TR-MOKE) with a two-color pump-probe setup in polar geometry. Systematically examining films with and without HfO_2 capping layer of 4nm thickness, we observe the influence of external magnetic fields on magnetic precessional modes. Additionally, our study sheds light on the impact of capping layers on the Gilbert damping parameter (a) in relation to spin wave frequency.

The outcomes provide insights into the recovery and potential improvement of spin mobility in Ni films.

CP-05-07

Development of two photon fluorescence lifetime imaging system to assess metabolic dynamics of brain in hypoxia

Gagan Raju[1], Gireesh Gangadharan[2], Krishna Kishore Mahato[1] and Nirmal Mazumder[1] [1]Department of Biophysics, Manipal School of Life Sciences, Manipal Academy of Higher Education, Manipal, Karnataka, India-576104 [2]Department of Ageing Research, Manipal School of Life Sciences, Manipal Academy of Higher Education, Manipal, Karnataka, India-576104, Email: nirmal.mazumder@manipal.edu*

Understanding the intricate metabolic dynamics of the brain in hypoxic conditions is essential for deciphering the complexities of neurological responses to reduced oxygen levels. This study introduces an innovative approach employing femtosecond laser technology to establish an advanced Two-Photon Fluorescence Lifetime Imaging (TP-FLIM) system for *in vivo* metabolic imaging. Integrated with a time-correlated single photon counter (TCSPC), TP-FLIM quantifies the lifetime of NADH, a crucial coenzyme in cellular metabolism. NADH autofluorescence serves as a metabolic sensor in FLIM, enabling real-time quantification and assessment of metabolic shifts in hypoxic conditions. The goal of the system is to offer unprecedented insights into the real-time monitoring of metabolic activities within the deep-seated regions of the brain experiencing hypoxic stress, providing a unique perspective on cellular responses to oxygen deprivation.

CP-05-08

Characterization of Conical Emission in femtosecond laser generated spectral super broadening

Akhil Varghese, AnuAvarachan, Akhil Krishnan S, Riju C Issac Intense Laser-matter Interactions(ILAI) Group, Cochin University of Science and Technology *Email : akhilvarghese@cusat.ac.in*

Spectral and spatial properties of conical emission associated with the supercontinuum generation are investigated in detail. Among various models that describe the angular distribution of the wavelength in the conical emission, the Cerenkov model is found to be more consistent with the experimental data. The pattern of the emission is in contrary to the phenomena of diffraction that as we go from the center to the periphery of the conical rings, wavelength distribution is from red region to blue region. The conical emission does not contain any frequencies lower than the pump frequency, but most of the input energy is found to be redshifted from the pump frequency. This indicates that the entire stokes spectrum during supercontinuum generation is trapped inside the Kerr-lensed region while the anti-stokes lines escape out to form rings around the propagation axis. Thus, conical

emission can be regarded as a counter mechanism to self-focusing to avoid complete ionization of the medium.

CP-05-09

Two photon polymerized structures as scaffolds for tissue regeneration

Meenu M S, Lakshmy T A, Riju C Issac Intense Laser – matter Interaction (ILAI) Group, Cochin University of Science And Technology, Cochin – 22, Kerala E.mail: riju@cusat.ac.in

In tissue engineering, the role of scaffolds is inevitable. The scaffolds give mechanical support to the growing tissues and allow the cells to proliferate as it is inside the body. Direct laser writing via two photon polymerization (TPP) can be applied for the 3D printing of these scaffolds. A Ti: Sapphire femtosecond laser of peak wavelength 800 nm is used as the energy source of TPP. The photosensitive resin contains poly(ethylene glycol)diacrylate (PEGDA) as a monomer and Michler's ketone as the photoinitiator. PEGDA is a biocompatible hydrogel oligomer widely used for biological applications. Michler's ketone is a non cytotoxic photoinitiator. Since these scaffolds have to be used for tissue regeneration, they should have good mechanical strength and be biodegradable and show swelling nature. These requirements are verified in this study.

CP-05-10

Development of novel Laue X-ray diffraction setup using fs laser plasma X-ray source

R. Rathore[1,2], H. Singhal[1,2], D. Bansal[3], R. Kulkarni[4], A. Thamizhavel[4], and J. A. Chakera[1,2]*
*[1]Homi Bhabha National Institute, Training school Complex, Anushaktinagar, Mumbai, MH 400094, India [2]Laser Plasma Division, Raja Ramanna Centre for Advanced Technology, Indore, MP 452013, India [3]Department of Mechanical Engineering, Indian Institute of Technology Bombay, Mumbai, MH 400076, India [4]Department of Condensed Matter Physics & Materials Science, Tata Institute of Fundamental Research, Mumbai, MH 400005, India *Email: ranjana@rrcat.gov.in*

Laue X-ray diffraction has been used for over 100 years to determine the crystal orientation and symmetry, and assess the crystal quality. In the Laue diffraction method, when a white (polychromatic) X-ray beam falls on a single crystal at a fixed angle, each set of planes diffracts a particular wavelength that satisfies Bragg's law for the value of d and ? involved. Here, we have developed a Laue diffraction setup using a fs laser plasma X-ray source for the first time. The laser plasma X-ray source is generated by focusing the 50 fs Ti:sapphire laser pulse on the moving Cu wire target. To record the Laue diffraction pattern, the spectral range of the source is increased by optimizing the laser intensity and the target parameters. The Laue diffraction pattern is recorded from the novel $EuTe_4$ sample (~10 µm thick) in transmission geometry. The advantage of developing a Laue

diffraction setup from a fs laser plasma X-ray source is that it will allow us to perform time-resolved Laue diffraction in the future and provide more detailed information on sample evolution after laser excitation.

CP-05-11

Femtosecond Laser Texturing of Borosilicate Glass: The role of scan speed in the generation of nanoscale ripple structures

Rajeev Rajendran[1], Theja Raj E[1], K. K. Anoop[1] Department of Physics, Cochin University of Science and Technology, Kochi-22 *Email: anoopkk@cusat.ac.in*

We investigated the role of scanning speed on the generation of nanoscale ripple structures in the femtosecond laser texturing of Borosilicate glass at atmospheric conditions. Ultrashort laser pulses (35 fs, 800 nm, 1 kHz) from a Ti:Sa laser was used for nanoscale texturing process. Prior to the large-area texturing, we measured the ablation threshold ($F_{th(1)}$ = 4.39±0.35 J/cm^2) and the incubation coefficient (S = 0.74±0.02) of Borosilicate glass. Laser processing was carried for four different scan speeds, and we found that it has significant role in the generation of ripple structures on the glass surface. The more precise and clear ripples, which are categorised as high spatial frequency LIPSS (HSFL) and having an orientation parallel to the laser beam polarization, were observed at higher scan speeds. As the scan speed decreases the ripple structures loses its fine structure and also the orientation is changed.

CP-05-12

Noise-like pulse generation at 2 μm from a NALM-based Thulium-doped fiber laser

S. Maity[1,2], U.K. Samanta[1,2], D. Pal [1], A. Pal [1,3], [1]CSIR-Central Glass and Ceramic Research Institute, [2]Jadavpur University, [3]Academy of Scientific and Innovative Research, Email: 2013shubhranil@gmail.com

Noise-like pulse train in an anomalous dispersion domain is observed in a nonlinear amplifying loop mirror (NALM) based thulium mode-locked laser (TMLL) at 2000 nm having a 3 dB spectral width of 15 nm.The repetition rate of the TMLL is 4.54 MHz matches with the cavity length of 44 m. The pulse width of the TMLL is increased from 844 ps to 3 ns with the pump power. TMLL delivers an average output power of 253 mW with a pulse energy of 56 nJ. Intensity noise of the designed TMLL is also characterized and integrated relative intensity noise (IRIN) is about 0.04% in the 100 Hz-1 MHz offset frequency range.

CP-05-13

Experimental observation of optical Hilbert's Hotelin Polarization

*Anirban Ghosh,[1] * SubithKumar,[1,2] ChahatKaushik,[1,2] Arash Shiri,[3] Greg Gbur,[3] Sudhir Sharma,[4] and G.K.Samanta[1] 1. Physical Research Laboratory, Ahmedabad, Gujarat 380009, India 2. Indian Institute of Technology-Gandhinagar Ahmedabad, Gujarat 382424, India 3. Department of Physics and Optical Science, University of North Carolina Charlotte, Charlotte, North Carolina 28223, 4. Dynotech Instruments Pvt Ltd, Delhi 110058, India *Email: anirbang@prl.res.in*

We report on the simple experimental implementation of Hilbert's hotel using a fractional vector vortex beam generated by illuminating the spiral phase-plate of integer topological charge for a designed wavelength by supercontinuum laser of tunable wavelength.

CP-05-14

Ultrafast dynamics of excitons in monolayer MoS_2 using a white light probe beam

Asha Singh[1], Saleem Khan[1,2], Salahuddin Khan[1,2], and T. K. Sharma[1,2,] [1]Nano Science Laboratory, Materials Science Section, Raja Ramanna Centre for Advanced Technology, Indore, 452013.[2]Homi Bhabha National Institute, Training School Complex, Anushakti Nagar, Mumbai, India - 400085. *Email: skhan@rrcat.gov.in*

Monolayers of two-dimensional semiconductors are potential candidates for optoelectronic and flexible devices, where MoS_2 is known to be a promising material.Ultrafast carrier dynamics studies in $MoS_2$are of pivotal importance for understanding and optimization of the associated devices. Interesting features related to the photogenerated quasiparticles known as A/B excitons, trions and biexcitonsare already reported for MoS_2 in literature. Such particles are formed due to strong Coulomb interactions caused by reduced dimensionality and weak dielectric screening in the monolayers of MoS_2. Biexcitons and trions in monolayer MoS_2 have substantially large binding energy, typically in the range of 50-70 meV, which makes them stable even at room temperature. Ultrafast carrier dynamics studies down to femtosecond time scale are of paramount importance for the realization of MoS_2based optoelectronic devices. In this work, ultrafast dynamics of A-exciton, B-exciton, and biexcitons of B-exciton is studied in monolayer MoS_2using pump probe technique with a femtosecond white light probebeam. Features associated with A-exciton, B-exciton, and biexcitons of B-exciton are clearly observed. It is seen that the formation of excitons occurs on a timescale of tens of fs whereas the formation of biexcitons is bit slower.

CP-05-15

Ultrafast exciton dynamics in WSe_2 Monolayer

Saleem Khan[1,2], Asha Singh[1], Yogesh Kumar Yogi[1#], Sanjay Porwal[1], Salahuddin Khan[1,2], and T. K. Sharma[1,] [1]Materials Science section, Raja Ramanna Centre for Advanced Technology, Indore, 452013.[2]Homi Bhabha National Institute, Training School Complex, Anushakti Nagar, Mumbai, 400085.[#]M.Tech Project Student from Center for Converging Technologies , University of Rajasthan, Jaipur*Email: skhan@rrcat.gov.in*

Monolayers of varioustwo-dimensional (2D) semiconductors like MoS_2, $MoSe_2$, WS_2 and $WSe_2$are attractive because of their optical and electrical properties and especially from a flexible device point of view. WSe_2 is an important material for potential applications in spintronics, valleytronics and quantum technology. In the present paper, chemical vapor deposition (CVD) grown WSe_2 monolayer on SiO_2/Si substrate is studied using photoluminescence measurement technique. Ultrafast carrier dynamics studies are carried out using dual color transient pump probe spectroscopy setup where a clear role of defect statesis revealed. All the measurements are performed at room temperature. The probe beam is kept in resonance with the A-exciton of WSe_2 monolayer. Presence of A-exciton is first confirmed by the PL measurements. It is seen that the formation of A-exciton occurs within 280 fs of excitation. Subsequently, exciton decay via Auger and defect states is observed to occur over 130 fs and 28 ps respectively. Finally, the radiative recombine occurs over 100s of ps timescale leading to the generation of PL signal. Ultrafast measurements thus provide useful insight on the carrier dynamics in WSe_2 monolayer.

Category - 6
Lasers in Materials Science

CP-06-01

Structural, optical and dielectric properties of pulsed laser grown MgO/ZnOmultilayernanolaminates

*P. S. Padhi[1,2]and P. Misra[1,2,*1]Laser Materials Processing Division, Raja Ramanna Centre for Advanced Technology, Indore 452013, India [2]Homi Bhabha National Institute, Training School Complex, Anushakti Nagar, Mumbai 400094, India *Email: pmisra@rrcat.gov.in*

Binary metal oxide nanolaminates (NLs) have recently demonstrated certain promising dielectric properties, arising from the tailorable Maxwell-Wagner (M-W) relaxation mechanism. In this work, ~60 nm thick MgO/ZnO NLs with sublayer thickness (t_s) varying between 4 to 1 nm are deposited using an optimized pulsed laser deposition system. Owing to enhanced M-W interfacial polarization effectin these NLs, with t_s reducing from 4 to 2 nm, the low frequency dielectric constant and loss values are improved from ~ 35 to 90 and from ~ 0.35 to 0.06, respectively. However, the trend reversed with further reduction in t_s down to 1 nm, plausibly owing to enhanced interface interdiffusion. The observed blue shift of band gap energy in these NLs with reduction int_s was explained by quantum confinement effect and its correlation with the observed dielectric properties is established. These findings provide insight to understand the interplay between M-W relaxation and quantum confinement effect in MgO/ZnO NLs,which is required for energy storage applications.

CP-06-02

Synthesis, Growth, Laser damage threshold Investigation of organic Piperazinium bis (P-aminobenzoate) dihydrate single crystal for Nonlinear Optical Applications

B. Sahaya Infant Lasalle, Muthu Senthil Pandian P. Karuppasamy, and P. Ramasamy [1]Department of Physics, Research Centre, SSN College of Engineering, Chennai, Tamil Nadu, India. [a)] Email: senthilpandianm@ssn.edu.in*

The organic single crystal Piperazinium bis (4-aminobenzoate) dihydrate (PPABD) was successfully grown through the slow evaporation solution growth method. Several characterizations were done in the PPABD crystal such as structural and NLO properties. The structural information was investigated by Single crystal x-ray diffraction (SXRD), SXRD results demonstrate that PPABD material belongs to the monoclinic system with non-centrosymmetric space group P21/n. The LDT analysis was investigated by ND: YAG

laser and the wavelength of laser is 1064 nm. The open aperture z-scan technique was used to investigate the NLO absorption of the sample at 632.8 nm

CP-06-03

Parametric Optimization of Laser-Induced Graphene Using a Conventional CW CO_2 Laser

Tatsat Dwivedi[1,2], Hrithik Gupta[3], Sunita Kedia[1,2], R. C. Das[1,2] and J. Padma Nilaya[1,2] [1]Laser & Plasma Technology Division, BARC, Mumbai [2]HBNI, Anushakti Nagar, Mumbai [3]Somaiya College, Mumbai University *Email: jpnilaya@barc.gov.in*

Laser-induced graphenisation of a biodegradable substrate, specifically coconut shell, has been successfully carried out and the results are presented here. The experimental setup includes a carbon dioxide (CO_2) laser, mechanical chopper, translation stage, and a system for detecting and measuring the laser output power. This work identified unique optimal laser fluence parameters and scan speeds, distinct from those reported in existing literature, to achieve efficient graphene formation. The quality of the generated graphene was confirmed through Raman spectroscopy, while scanning electron microscope images revealed diverse LIG structures, including porous foam and fibrous bundles, depending on the laser power used. XRD and sheet resistance measurements helped assess the quality of generated Laser-Induced Graphene (LIG).

CP-06-04

Contactless measurement of thickness of $LiNbO_3$/PMMA nanocomposite films using optical coherence tomography (OCT)

*Alka[1], Chiranjit Debnath[1], Sujan Kar[1,2], Suman Bagchi[1,2], Sunil Verma[1,2] and Shovan K. Majumder[1,2] [1] Laser Biomedical Applications Division, Raja Ramanna Centre for Advanced Technology, Indore-452013 [2]Homi Bhabha National Institute (HBNI), Training School Complex, Anushakti Nagar, Mumbai-400094 *Email: alkak@rrcat.gov.in*

A preliminary study on use of optical coherence tomography (OCT) technique to characterize the thickness of $LiNbO_3$/PMMA nanocomposite films has been reported. The thickness of different films was calculated by obtaining optical coherence tomographic images and compared with vernier caliper readings. The percentage variation in thickness was less than 7%. The OCT technique was also used to qualitatively differentiate $LiNbO_3$/PMMA samples of fixed thickness with varying concentration of $LiNbO_3$ in PMMA matrix (0.01 wt.% $LiNbO_3$/PMMA to 0.20 wt.% $LiNbO_3$/PMMA).

CP-06-05

Thermoplasmonic Biometamaterial of Al, Cu and Ag fabricated using Pulsed Laser Deposition for Solar evaporation of water

U. Chakravarty[1,5], C. Mukherjee[2,5], Rashmi Singh[3], Sunita Ahlawat[4], Y.B.S.R. Prasad[1] [1]High

Energy Laser Physic Section, Laser Plasma Division, [2]High Energy Lasers and Optics Section, [3]Nano-Functional Materials Lab, Laser and Functional Materials Division, [4]Solid State Laser Section, Laser Technology Division, Raja Ramanna Centre for Advanced Technology, Indore 452 013 [5]Homi Bhabha National Institute, Training School Complex, Anushaktinagar, Mumbai 400094, Email: uday@rrcat.gov.in

We have employed pulsed laser deposition to create Bio-metamaterial of Al, Cu and Ag on the surfaces of Hydrophobic Palash leaves, aiming to develop a highly efficient, broad-spectrum absorber thermoplasmonic material for solar-to-thermal conversion applications. The goal was to compare the best material for enhanced optothermal conversion implying a high Temperature rise on exposure to Sunlight. Another aim was to find the best material among Al, Cu and Ag that should be chosen for coating on hydrophobic leaf (Palash) for enhanced Solar evaporation of water. Ag coating in particular was best for absorption which is accompanied by an exceptional broad-spectrum absorption efficiency, reaching approximately 95 % across the UV, visible, and infrared regions. The maximum temperature increase on the different metal coated leaf surface, upon exposure to solar radiation, was directly correlated with the strength of absorption in the fabricated thermoplasmonic material. Water drop evaporation on solar exposure of the fabricated plasmonic material was also studied and apart from absorption contact angle was also found to be very crucial for influencing the evaporation rate. This study provides valuable insights for selecting suitable plasmonic metals that excel in the absorption of broadband solar radiation and temperature enhancement as well as the water evaporation when the fabricated thermoplamonic substrate is kept under the Sun.

CP-06-06

Effect of Femto-second Laser Annealing on Pulsed Laser Deposited Yttria Stabilized Zirconia (YSZ) Thin Film

*Jai Khare[1], P. Gupta[2], and S. K Rai[2,3] [1]Photonics Nanomaterial Lab, Laser Materials Processing Division, [2]X-ray Diffraction & Metrology Section, Accelerator Physics and Synchrotrons Utilization Division Raja Ramanna Centre for Advanced Technology, Indore 452 013 [3]Homi Bhabha National Institute, Training School Complex, Anushaktinagar, Mumbai 400094 *Email: jkkhare@rrcat.gov.in*

Femtosecond laser annealing is a powerful technique used in thin films to engineer atomic-scale changes. In this study, we explored the impact of femtosecond laser annealing on oxygen vacancy association in yttria-stabilized zirconia (YSZ). By employing ultra-short laser pulses, controlled perturbations in the material's oxygen vacancies were induced. Our findings reveal that femtosecond laser annealing could reduce the concentration of highly mobile oxygen vacancy in YSZ and changed the crystal structure of thin film. Thin films of YSZ on quartz glass and n-type silicon substrates substrate were grown by ablating pellet of YSZ using pulsed laser deposition technique. The X-ray diffraction analysis of films before and after femtosecond laser annealing revealed that films were in amorphous phase and cubic phase respectively.

CP-06-07

Use of Spectral Domain Common Path Low Coherence Interferometry for Simultaneous Measurement of Thermal Expansion Coefficient and Thermo-refractive Coefficient

K. K. Malakar[1, 2], S. Chakraborty[1], Y. Verma[1, 2], S. Raja S.[1] [1]Advanced Electro-Optics Systems Section, RRCAT, Indore, Madhya Pradesh 452013, India [2]Homi Bhabha National Institute, Anushaktinagar, Mumbai, Maharashtra 400094, India Email: yogesh@rrcat.gov.in

Simultaneous measurement of coefficient of thermal expansion and thermo-refractive coefficient are important to maintain optimal performance of the optical systems under varying thermal conditions. In this paper, we present the use of spectral domain common pathlow coherence interferometric system for simultaneous measurement of Thermal Expansion Coefficient and Thermo-refractive Coefficient of transparent glass sample. The scheme has been validated by measurement of a sapphire sample. The measured values of a , ß and a_{eff} of the sapphire sample are $7.750x10^{-6/o}C$, $1.240x10^{-5/o}C$, and $1.423x10^{-5/o}C$ respectively. These measured values reasonably match with the values reported in the literature.

CP-06-08

A Novel Approach to Dye-Doped Random Lasing from Disordered Anisotropic Structures

Nideesh Padiyakkuth [a], Rodolphe Antoine [b], Nandakumar Kalarikkal [a,c,d,] [a] School of Pure and Applied Physics, Mahatma Gandhi University, Kottayam, 686 560, Kerala, India [b]Institut Lumi'ere Mati'ere UMR 5306, Univ Lyon, Universit'e Claude Bernard Lyon 1, CNRS, F-69100, Villeurbanne, France [c] International and Inter University Centre for Nanoscience and Nanotechnology, Mahatma Gandhi University, Kottayam, 686560, Kerala, India [d] Unversity Centre for Ultrafast Studies,, Mahatma Gandhi University, Kottayam, 686 560, Kerala, India Email : pknideesh@mgu.ac.in, nkkalarikkal@mgu.ac.in*

In this study, we explore the use of polymer nanofibers for novel photonic devices, with a focus on their application in random lasers (RLs). Specifically, we employ electrospun Polyvinylidene fluoride (PVDF) polymer as a scattering medium, combined with Rhodamine 6G (R6G) as the gain medium. By increasing the gain concentration from 1 mM to 3 mM, we observe a transition from amplified spontaneous emission to coherent lasing, characterized by the emergence of sharp laser peaks with a narrow peak width of ≈ 0.2 nm, superimposed on a broader emission band. These findings underline the potential of R6G-doped electrospun PVDF materials as an effective platform for controlled light emission, offering promise in optical sensing and versatile microlaser applications.

CP-06-09

Angle Dependence on the Sensitivity and Transmittance of One-Dimensional Organic Liquid Sensor

Agape Mary Mammen and Alok Sharan Department of Physics, Pondicherry University, Kalapet, Puducherry, India-605014, Email: agapemary6@gmail.com, aloksharan@gmail.com

A numerical study has been done to study the angle of incidence dependence on the transmittance and the sensor characteristics of a one-dimensional photonic crystal organic liquid sensor. A comparative study has been done between $(CdS/SiO_2)^5$/ water/$(SiO_2/CdS)^5$/glass and $(SiO_2/CdS)^5$/ water/ (CdS/ SiO_2)/glass with defect layer thickness as 441.42nm and 882.84nm. Transfer matrix method has been used to study the transmission spectrum. It is seen that $(SiO_2/CdS)^5$/ water/ (CdS/ SiO_2)/glass exhibits better sensitivity and transmittance compared to $(CdS/SiO_2)^5$/ water/$(SiO_2/CdS)^5$/glass for both the defect layer thicknesses. Therefore $(SiO_2/CdS)^5$/ water/ (CdS/ SiO_2)/glass has been taken as the final structure for sensor studies. The parameters of the final structure for sensor have been taken as N=5, d_D=882.84nm and ? =0°. This structure exhibits maximum sensitivity of 350nm/RIU, FoM of 217.48 RIU^{-1} and LoD of $2.70*10^{-4}$ RIU. The shift in the central peak position can be used to determine the organic compound in the cavity. Thus, we demonstrate how PBG structures can also be used as liquid sensors.

CP-06-10

Laser Speckle Technique for the assessment of dye-sensitized TiO^2 thin film Texture, Waviness and Roughness

R. Balamurugan, R.Prakasam , S. Inbakumar , R.G.Sethuraman, Department of Physics, Kumaraguru College of Technology, Coimbatore, Tamilnadu, India. Email: balamurugan.r.sci@kct.ac.in

This paper determines the dye-sensitized TiO2 thin film roughness by the process of laser images. Self-interference of scattered laser from the optically rough exterior of the dye-sensitized TiO2 thin film produces the tiny granular appearance of dark and bright parts called speckles. The speckle pattern is generated by scattering the coherent source of light with various incident angles recorded. The intensities of speckle shapes are a little bit dissimilar with one another and the specimen sheet roughness by the correlation method. The correlation is related to the roughness of the sample. Moreover, angular speckle-correlation as a novelty fractal counting box method is also presented.

CP-06-11

Development of SS304L and Ti Transition joint with Ni/Mo Interlayer using Laser Directed Energy Deposition

Ch. Prem Singh[1], A. K. Rai[1,3], G. K. Mishra[1], C. P. Paul[1,3],and S. K. Dixit[1,3] [1]Raja Ramanna*

*Centre for Advanced Technology, Indore452013, INDIA [2]Homi Bhabha National Institute, Mumbai- 400094, India *Email: cpremsingh@rrcat.gov.in*

A study on development of transition joint between pure Ti and SS 304 L steel using laser directed energy deposition process is reported in this paper. To avoid unwanted intermetallic phase formation between Ti and steel, dual interlayer of Ni and Mo is used in view of better metallurgical compatibility. To develop crack and porosity interlayer joint between SS 304 L steel and Ti different process parameters are optimized. At optimized laser power of 1000 W with scan speed of 600 mm/min and powder feed rate of 8 g/min, transition joint between SS 304 L steel and Ti is successfully developed. Further the developed joint is characterized using optical and scanning electron microscopy attached with energy dispersive spectroscopy (EDS) mapping to assess the build quality and interface. In addition, hardness measurement is also carried out along different interface for mechanical integrity assessment.

CP-06-12

Novel metal-organic framework and crystal engineering of Bismorpholinium mercury (II) tribromo chloride (BMMC) for optoelectronic applications

Thiyagarajan Maadhu[a] and Vinitha Gandhiraj[a] [a]Division of Physics, School of Advanced Sciences, Vellore Institute of Technology, Chennai-600127, India, Email : vinitha.g@vit.ac.in*

Optically transparent novel metal-organic non-linear optical single crystals of Bismorpholinium mercury (II) tribromo chloride (BMMC) have been grown by slow evaporation solution growth technique (SEST). The formation of the new crystalline structure and the morphology of the grown crystal were determined using single-crystal X-ray diffraction (SXRD) analysis. The BMMC material crystallizes in a monoclinic crystal system with space group, $P2_1/c$. The unit cell has four molecules accumulated in it (the unit cell parameters are a = 6.8056(6) Å, b = 14.0027(10) Å, c = 17.2152(14) Å, β = 93.148 (3)°and Z=4). The grown crystal's crystalline phase and crystalline quality has been analysed by powder X-ray diffraction (PXRD) study. The formation of new molecular structure and multifarious functional groups were unveiled using ^{1}H and ^{13}C Nuclear Magnetic Resonance (NMR) spectroscopy and Fourier transform infrared (FT-IR) spectroscopy analyses respectively. The BMMC single crystal with a thickness of 2 mm shows a good optical transmittance of about 75% in the visible and NIR regions with a cut-off wavelength of 328 nm. The crucial thermal parameters such as thermal stability, decomposition point and the melting point of the BMMC crystal have been determined using Thermogravimetric (TG) and Differential thermal analysis (DTA) under nitrogen atmosphere. The laser damage threshold of the grown crystal was found to be 2.242 GW/cm^2 with the irradiation of nanosecond, 1064 nm Nd: YAG laser. Third-order non-linearity of the BMMC crystal has been evaluated by open and closed aperture Z-scan

measurements using Nd:YAG laser at 532 nm. The optical limiting property of the grown crystal is found to have its amplitude at 530 mW and threshold at 28 mW respectively.

CP-06-13

Effect of Antimony on Supercontinuum Generation in Lithium Zinc Borate Glasses.

Alan. B. Samuel[1], V.V Ravi Kanth Kumar[1], S.Sree Harsha[2], Samuel Anurag Nalam[2], P. Prem Kiran[2] [1] Pondicherry University, Kalapet, Puducherry, India,605014,[2]ACHREM, University of Hyderabad, Gachibowli, Hyderabad,500046, Email: ravi.phy@pondiuni.edu.in

Glasses composed oflithium zinc borate with the addition of antimony at different concentrations were synthesized through the conventional melt quenching method. Supercontinuum(SC) generation from the glasses was recorded using a femtosecond laser pulse at various pump powers. The optical band gap values of the glass samples were determined from the UV-Vis absorption spectra. It is observed that the SC broadening for the glass sample having the lowest bandgap saturates at lower laser pump power itself, and there is no appreciable increase in the broadening with further higher pump powers. The structural properties of the glasses were investigated through Raman Spectroscopy. The formation of different borate structural units in the glass network with the improved addition of antimony leading to the creation of Non-Bridging Oxygens(NBOs) in the glass network and their impact on the SC broadening were further discussed in the article.

CP-06-14

Effect of rare earth doped perovskite on the structural, linear/nonlinear optical properties of the fabricated pva/cmc polymeric blends for optical limiting applications.

Vinola Johnson and Vinitha Gandhiraj Division of Physics, School of Advanced Sciences, Vellore Institute of Technology, Chennai-600127, India. *Email: vinitha.g@vit.ac.in*

Poly (vinyl alcohol) and carboxy methyl cellulose, PVA/CMC doped with (1, 5,8) Wt% of Lanthanum Dysprosium aluminate ($LaDyAlO_3$) nanoparticles were prepared via traditional solution casting method. The influence of the concentration of $LaDyAlO_3$ nanoparticles on optical and spectroscopic properties was investigated. The molecular and the crystalline structure of PVA/CMC/$LaDyAlO_3$ polymer nanocomposites were obtained through the Fourier transform infrared (FTIR) spectroscopy and X-ray diffraction (XRD). The optical characteristics were investigated via UV-Visible spectrophotometer. For all samples, the absorption coefficient was determined. The direct and indirect allowed transitions have a multi graded bandgap structure. The thermal stability was investigated and the activation energy was determined which is found to be dependent on the concentration of $LaDyAlO_3$ nanoparticles. Furthermore, the PVA/CMC/$LaDyAlO_3$ (8wt%) demonstrated excellent optical limiting threshold properties at low transmission

value which is a favorable result for optoelectronic devices like optical limiters, long-lasting optical filters and photonic devices like organic/Polymer LEDs, Optical switches and perovskite solar cells.

CP-06-15

Plattnerite (-PbO_2) exhibits enhanced performance via doping Bi^{3+} on -PbO_2: A Novel Approach for Positive Electrode Optimization in Energy Storage Systems.

H. Mohammed Iliyaskhan[a], M. Ajith Kumar[a], M. Kirubanidhi [a], Misbahul Batool [a], A. Mohamed Ibrahim [a], J. Joel Abraham [b], J. Prince Joshua [a,] [a] Department of Physics, The New College, Chennai-600014, India. [b] Department of Mechanical Engineering, Jeppiaar Engineering College, 600119, India. Email: jprincejoshua@thenewcollege.edu.in*

The objective of this work is to showcase the enhanced efficacy of lead dioxide, comprising two distinct polymorphs, namely Scrutinyite (a -PbO_2) and Plattnerite (ß-PbO_2). The tetragonal crystal structure of Plattnerite contributes to its enhanced electrochemical potential compared to Scrutinyite, resulting in a more accessible and responsive arrangement. The stability of plattnerite contributes to the extended lifespan of lead-acid batteries. The present study aimed to explore the cyclic voltammetric behavior of a lead dioxide working electrode in a 30% sulfuric acid solution, employing different scan speeds ranging from 5 to 100 mV/s. Scanning within the range of -1.40 to -0.60 V (against the standard hydrogen electrode) potentially took place. The formation of $PbSO_4$ from the Pb electrode is correlated with the observed oxidation peak at around -0.95 V (against the standard hydrogen electrode). In the field of energy storage, the optimization of battery efficiency is of utmost importance. The aforementioned demand has served as a driving force for our concentrated research in this particular field. The substance Bi^{3+} was selected for this purpose. Bi^{3+} ions are incorporated into the lead dioxide lattice at the desired concentration. Subsequently, the Bi^{3+} doped ß -PbO_2 specimens were subjected to analysis employing X-ray diffraction, UV-Vis Spectroscopy, and Cyclic Voltammetry (CV) techniques in order to ascertain the physical and chemical characteristics of the material.

CP-06-16

A comparative analysis of MgO and Co doped MgO, along with an evaluation of the impact of cobalt doping on magnesium oxide in the domain of spintronics and magnetic property

M. Ajith Kumar[a], H. Mohammed Iliyaskhan[a], M. Kirubanidhi [a], Misbahul Batool[a], A. Mohamed Ibrahim[a] J. Joel Abraham[b], J. Prince Joshua[a,] [a] Department of Physics, The New College, Chennai-600014, India. [b] Department of Mechanical Engineering, Jeppiaar Engineering College, 600119, India. Email: jprincejoshua@thenewcollege.edu.in*

The present investigation involved the synthesis of pure and Cobalt-doped MgO nanoparticles through the utilization of the sol-gel technique. The analysis of the nanoparticles involved the utilization of Powder X-ray diffraction (P-XRD), UV-Vis spectroscopy, and Photoluminescence spectroscopy (PL). The X-ray diffraction pattern revealed the presence of a cubic spinel structure, whereas the diffraction peaks of Co-doped MgO provided evidence for the production of a nanostructure with a rock salt MgO phase. The UV-visible absorption properties of magnesium oxide nanoparticles were examined at a specific wavelength of 203 nm. Additionally, the absorption spectra of magnesium oxide doped with increasing concentrations of cobalt (Co) were observed within the range of 255-270 nm.The excellent quality photoluminescent activity of undoped MgO was confirmed by the emission peaks observed at 315.2 and 343.8nm. Additionally, the luminescent behavior of Co doped MgO was verified by the emission band observed at 314.6 and 340.7nm.The results of the study indicate that the compounds under investigation have potential utility in the fields of spintronics and magnetic characteristics.

CP-06-17

Investigation of microstructure modification in zirconium under laser-shock loading

P. Leshma, K. K. Pandey, K.C. Gupta, A. Mohan, A. B. Garg, T. Sakuntala, High Pressure & Synchrotron Radiation Physics Division, Bhabha Atomic Research Centre (BARC), Mumbai. Email: leshma@barc.gov.in

Post laser-shock microstructure modifications in polycrystalline zirconium under a variety of laser-shock loading conditions are investigated using X-ray diffraction (XRD) technique. The variation in relative intensities of XRD peaks and their broadening presents the information about texture, grain size and microstrain present in shocked zirconium. It is observed that the grain size variation and texture of shocked samples have strong dependence on the laser pulse duration. Strong texturing effects are observed when zirconium is shocked with longer duration laser pulses.

CP-06-18

Fabrication of Gold Nanoparticles Embedded Laser-Induced Graphene (LIG) Electrode for Hydrogen Evolution Reaction

Deepak Deepak[1], Vennela Vuruputuri[1], Gourav Bhattacharya,[2] and Susanta Sinha Roy[1] [1]Department of Physics, School of Natural Sciences, Shiv Nadar Institution of Eminence, GautamBudh Nagar 201314, Uttar Pradesh, India [2] Nanotechnology and Integrated Bioengineering Centre, School of Engineering, Ulster University, Newtownabbey, Belfast BT37 0QB, Northern Ireland, United Kingdom *Email: susanta.roy@snu.edu.in*

The advancement of renewable energy technologies like water electrolysis and hydrogen fuel cells relies on the fabrication of effective and reliable catalysts for the hydrogen

evolution process (HER). In this regard, we report gold nanoparticles embedded laser induced graphene electrode for regulation of overpotential and electrocatalytic performance of hydrogen evolution reaction. Gold nanoparticles were deposited onto the LIG surface using electrode deposition via cyclic voltammetry (CV) at different cycle lengths. The catalyst fabrication technique enables the manipulation of many electrochemical parameters, such as overpotential value, charge transfer resistance, electrochemical active surface area, and tafel slope, through the adjustment of cyclic voltammetry (CV) cycles. The LIG-AU@50 sample demonstrates remarkable electrocatalytic characteristics, as evidenced by its low overpotential of 141 mV at a current density of 10 mA/cm^2 and reduced tafel slope of 131 mV/decade in an acidic environment. Furthermore, the presence of an augmented electrochemical active surface area, a mass activity of 8.80 A/g, and a high turnover frequency of 0.0091 s^{-1} suggest elevated and significant accessibility to plentiful active sites.

CP-06-19

Fabrication of Copper and Copper Oxide Nanocolloids by Pulsed Laser Ablation in Deionized Water: A green synthesis Approach

J. Patra, P. Das, S. Nanda, M. Dandapat, U. Tripathy, A. Adak†, Department of Physics, Indian Institute of Technology (Indian School of Mines) Dhanbad, India, Email: 21dr0069@phy.iitism.ac.in, amitavaadak@iitism.ac.in*

In this work, we employed nanosecond pulsed laser ablation of copper in deionized water to produce chemical free copper oxide nanocolloids. The experiment was performed with Nd:YAG nanosecond laser source of fundamental wavelength with 7 ns of pulse width. The ablation process was carried with the pulse energy of 20 mJ and for 25 minutes. Particle size and morphology was studied from Transmission Electron Microsopy. Spherical nanoparticles having particle size of 8-9 nm was observed. Optical properties were investigated using UV-Vis and Photoluminiscence spectroscopy. The band gap value from Tauc plot was found to be 3.77 eV. The photoluminiscence emission was observed in the range 344(3.6 eV)-354(3.5 eV) nm.

CP-06-20

Laser-Induced Breakdown Spectroscopy coupled with Statistical Methods for the Purity Analysis of Precious Alloys

K.S. Choudhari, Rajesh Nayak, and V.K. Unnikrishnan, Department of Atomic and Molecular Physics, Manipal Academy of Higher Education, Manipal 576104, Karnataka, India *Email: choudhari.ks@manipal.edu*

Laser-Induced Breakdown Spectroscopy (LIBS) was utilized to acquire spectra from precious metal alloys, namely, gold samples of various purity categories. The primary objective was to classify the samples into six distinct karatage classes: Au14, Au16, Au18,

Au20, Au22, and Au24. For this, Principal Component Analysis (PCA) was employed to analyze the LIBS spectra, revealing clear and distinct clustering for each karatage class. Further, to validate the robustness of the clustering and classification process, advanced statistical approaches, including Mahalanobis distance and Spectral residual calculations, were implemented. These analyses provided additional support for the accuracy and reliability of the identified gold purity categories. Furthermore, Receiver Operating Characteristic (ROC) analysis and Youden's index were performed to determine diagnostic thresholds essential for the effective classification of diverse gold purity samples. Sensitivity, specificity, and discriminative accuracy were calculated based on the established optimum thresholds. These statistical results emphasize the potential of LIBS coupled with advanced statistical procedures for practical field applications in the identification and sorting of precious metal alloys. Thus, the integration of LIBS and statistical analyses offers a promising approach for routine use in the field of mining, jewellery and electronics, demonstrating its efficacy in the accurate classification and sorting of various gold purity samples. This study contributes to the advancement of analytical techniques for precious metal analysis and has implications for such industries requiring reliable quality assessment methods for the sorting of precious metal alloys.

CP-06-21

Unravelling the utilization of laser Micro-3D printing towards micron level ceramic printing using novel laser decal transfer technique

Arpit Kumar Singh[1], Anshu Sahu[1], I.A.Palani[1] [1] Mechatronics and Instrumentation Lab, Indian Institute of technology, Indore, Email : Palaniia@iiti.ac.in.

3D printing or Additive manufacturing has gained its popularity due to its high design freedom, material freedom, and high degree of complexity. Most of the 3D printing process used wire or powder as raw materials which restrict the further usage of this technology from end applications. With advancement in technologies, a thin film based laser micro 3D printing is used for the printing of thin film. Laser decal transfer can be deployed for transfer of thin film over substrates are possible making it substrate independent. This work focusses on detailed investigation on micron level printing of ZnO ceramic over a thin film of ITO coated over glass using Laser decal transfer technique. A CO_2 laser (? =10.6 μ m) is utilized in the proposed work where detailed investigation in performed on laser processing parameters for effective control over ZnO transfer and its further selective positioning which includes influence of laser pulse overlap andlaser fluence is analyzed. Laser pulse overlap has greater effect on formation of heat affected zone and effective material transfer and is analyzed in detail as well.Finally, based on optimized parameters, the capability of selectively controlling and transferring ceramic over metal and sandwiching multiple materials over each other is analyzed. The proposed technology of laser micro-3D printing using novel principle of laser decal transfer would pose greater advantages in complex sensors fabrications with controlled gradient based properties.

CP-06-22

Exploring the efficacy of 1064 nm Pulsed Nd:YAG and 433 nm diode laser towards annealing of Zinc Oxide for functional analysis

Shruti Pankaj Sharma[1],ShubhiTiwari[1],Arpit Kumar Singh[1], I.A.Palani[1] [1]Mechatronics and Instrumentation Lab, Indian Institute of Technology, Indore, Email : mt2302103022@iiti.ac.in, mt2302103023@iiti.ac.in

Crystallinity of ZnO in order to improve its functional properties is essentially required for its improvement in intended applications such as sensor fabrications or photovoltaic applications.The present work focuses on utilization of lasers to improve the crystallinity of thin film RF sputtered ZnO. The thin films were deposited on c-Si substrate using sputtering at room temperature and then annealed using a pulsed Nd-YAG laser and Diode laser. Annealing was performed at a wavelength of 1064 nm using Nd: YAG solid state laser and at 433 nm using Diode Laser. The characteristics of films were systematically analyzed using scanning electron microscopy (SEM), Raman spectroscopy, UV-vis spectroscopy, electrical resistance measurement using precision multimeter and Hall measurement at room temperature. The findings of this work suggested that crystallinity can be improved and device performance can be enhanced using laser annealing of the samples.

CP-06-23

Improving the laser-based actuation of NiTi Shape-Memory Alloy bimorph-based actuator by laser annealing of Kapton polyimide

Kaushal Gangwar,I.APalani* Mechatronics and Instrumentation Lab, Department of Mechanical Engineering, Indian Institute of Technology Indore, Madhya Pradesh, India*
Email: mtphd2106103001@iiti.ac.in,palaniia@iiti.ac.in

The Nickel titanium-based bimorph presents better actuation and improved substrate-to-film adhesion on laser annealing. Laser interaction improves the performance of bimorphs by altering the surface crystallinity and wettability of the polyimide substrate. This work explores the annealing process with a 355 nm Nd: YAG laser for its fluence to achieve improved polyimide surface properties. The laser fluence value of 1.83J/cm² has increased polyimide's surface roughness from 0.075 µm to 0.588 µm.It also reduced the contact angle from 82° for plain polyimide to 62.9±0.5° for laser fluence of 1.63 J/cm². Finally, the actuation life of the smart actuator was improved by 71.4 % for the bimorph fabricated over laser laser-annealed polyimide surface at a fluence of 1.63J/cm² compared to the pristine sample.

CP-06-24

NIR Study of fluoroapatitestructure $Ba_3Ca_2(PO_4)_3F$: Nd^{3+} phosphor.

Shruti Dhale[(a)], Nilesh Ugemuge[(a)], Vartika S. Singh[(b)],S.V.Moharil[(c)] [a]Anand Niketan College, Anandwan, Warora, Dist-Chandrapur, 442914, India. [b]Advanced Carbon

*Products and Metrology, CSIR-NPL, New Delhi-110012, India. [c]Department of Physics, RTM Nagpur University, Nagpur, 440033. India.*Email: shrutidhale98@gmail.com / nileshugemuge@gmail.com*

FluoroapatitestructureBa$_3$Ca$_2$(PO$_4$)$_3$F phosphor has been synthesized by high-temperature solid-state reaction. The X-ray diffraction analysis confirms the formation of the Ba$_3$Ca$_2$(PO$_4$)$_3$F compound. The Rietveld refinement analysis shows that the crystal structure is a Hexagonal Crystal structure system with space group P 63/m. Detailed results on photoluminescence emission and excitation spectra, concentration dependence of emission intensity, scanning electron microscope (SEM) are presented respectively. Characteristic luminescence of Nd^{3+} was observed. Among lanthanide ions Nd^{3+} is the most successful in inducing lasing in both the crystalline and glass hosts [,]. For Nd^{3+} which exhibits f-f excitation, luminescence got quenched at 2.0 mol % concentration. Luminescence characteristics are explained using the known energy level diagrams for the lanthanide activators.Ba$_3$Ca$_2$(PO$_4$)$_3$F:Nd^{3+} phosphor shows emission peak at 1067 nm under excitation of 589 nm.The Ba$_3$Ca$_2$(PO$_4$)$_3$F doped with Nd^{3+} phosphor is excited at the wavelength of 589nm of NIR spectrum. The excitation spectrum is expanded over from the visible to the NIR region. ThePL emission is obtained in the NIR region with a emission line at 1067 nm.Different applications have diverse requirements on the luminescence performance of the phosphors.NIR emission can be important for various applications such as in vivo and in vitro imaging, food inspection, surveillance camera, horticulture and solar photovoltaics.

CP-06-25

Investigation of Laser process parameters on Laser Surface Hardening using nanosecond pulsed Nd:YAG laser

Himanshu Sharma, Naveen Kumar, Rushikesh A. Mali, I.A. Palani, Applied Optics and Laser Technology, Indian Institute of Technology, Indore, Email:palaniia@iiti.ac.in

Surface operations play a significant role in increasing the life of components and controlling the degradation of sensitive alloys. The laser transformation hardening process is an appropriate method that has higher accuracy and speed than traditional processes such as flame hardening[1] In this study, Laser surface hardening of AISI 431 stainless steel was performed using nanosecond Nd:YAG pulsed laser. After laser surface processing the structure consists of three regions (hardened zone, heat affected zone, and base metal). The effect of the laser process parameters were investigated on the geometrical dimensions of the hardened zone, by micro hardness distribution, and microstructure characterisation of AISI 431 stainless steel.

CP-06-26

Investigating LASER surface strategy to develop hydrophobic Aluminum surface using microsecond Yb doped fibre laser.

Vivek Ranjan Singh, Abneesh Prajapati, Nikhil Pandey, I.A. Palani, Applied optics and

laser Technology, Indian Institute of Technology, Indore, Email: mt23020103024@iiti.ac.in, ms2304103007@iiti.ac.in, palaniia@iiti.ac.in

Laser texturing is an emerging technique to functionalize materials with high precision and flexibility without any chemical treatment. However, when it is necessary to treat large area surfaces laser-based methods are still too slow to be exploited in industrial productions. In this work, we show that by improving the laser texture strategy it is possible to reduce the laser processing time to produce hydrophobic Aluminium alloy surfaces. While similar strategy has been demonstrated using femtosecond [1] laser, we are using a microsecond Yb-doped fibre laser, as these types of lasers are more readily available in industries and can be utilised to scale production. which integrate to creating a strategy for large scale application and production. We involve systematic experimentation with varying microsecond fibre laser parameters such as power, pulse width, and pulse duration and different surface texture geometries were micromachined; namely, square, circular, triangular, and hexagonal lattice grooves.

CP-06-27

Laser cleaning for rust removal on mild steel sample using nanosecond Nd;YAG pulse laser

Davinder Singh, Prabhat Kumar Dhurve, I A Palani, Applied Optics and Laser Technology, Indian Institute of Technology Indore, Email: mt2302103017@iiti.ac.in, mt2302103019@iiti.ac.in, palaniia@iiti.ac.in

The current study involves systematic experimentation with varying laser parameters such as power, pulse width, and pulse duration. Laser cleaning is employed to create controlled surface cleaning on the rusted mild steel plate. The surface roughness, hardness and microstructure aimed at investigating experimentally the effect of fluence of laser on properties of surface after laser processing. This work contributes to the evolving field of surface engineering by providing insights into the intricate interplay of laser parameters and surface cleaning. The anticipated outcomes hold promise for applications in de-rusting.

CP-06-28

Structural and Optical Properties on Ca Doped $BaTiO_3$

M. Soni[1)], A. Mishra[2)] School of Physics, Vigyan Bhawan, Devi Ahilya University, Khandwa, Road Campus, Indore 452001, India, Email: madhurisoni22@gmail.com.

Hereby, the synthesis of $Ba_{1-x}Ca_xTiO_3$ [x = 0, 0.33] perovskite has been reported. The samples were prepared conveniently by ceramic route i.e. solid state reaction method. The phase and structure of the synthesized samples were confirmed using x-ray diffraction technique. The room temperature XRD data recorded in the angular range of 2? (200 < 2? < 800) was analyzed and the analysis revealed that the prepared samples have acquired the tetragonal structure exhibiting space group (P4mm). The samples were highly crystalline and possessing larger average particle size > 40 nm. Further, the sample formation was confirmed via Fourier Transformation Infra-red spectroscopic characterization. The

optical bandgap was calculated using UV-Vis technique and the values found were 3.1eV and 3.03 eV for pristine and Ca Doped $BaTiO_3$. Keyword: Perovskites, Structure, Optical bandgap, opto-electronics.

CP-06-29

Growth of Multilayer Graphene Thin Films by UsingAerosol Assisted CVD Technique

KrutikaNatu,Applied Science, Symbiosis Institute of Technology (SIT), Near Lupin Research Park, Lavale, Pune,412115, India VipinK. Kaushik,Department of Applied Physics & Optoelectronics, Shri G. S. Institute of Technology and Science, 23, Sir M. Visvesvaraya Mark, Vallabh Nagar, Indore, 452003, Madhya Pradesh, India Meena Laad, Applied Science, Symbiosis Institute of Technology (SIT), Near Lupin Research Park, Lavale, Pune,412115, India Email: Krutikanatu@gmail.com

This study investigates multi-layer graphene films produced via aerosol-assisted chemical vapor deposition, utilizing benzene as the carbon source. Films were deposited onto copper foil maintained at temperatures of 100, 150, and 200 °C. Graphene growth progression was tracked by transferring it from Cu to a sapphire substrate. UV-VIS spectroscopy revealed average optical transmittance values of approximately 80%, 72%, and 75% for films deposited at 100, 150, and 200 °C, respectively. Raman analysis showcased distinctive peaks (D, G, and 2D), confirming graphene growth by highlighting carbon bond disorder. X-ray diffraction exhibited bumps at 2? ˜ 17 and 26 degrees, corresponding to the 002 peak of graphene oxide for 100 and 150 °C growth, while the absence of peaks at 200 °C supported the deposition of multilayer graphene. Field emission scanning electron microscopy images indicated an increase in nano-flake surface area with rising growth temperature during graphene synthesis.

CP-06-30

Sintering temperature induced Raman studies of $BiFeO_3$ nanostructures

R. R. Awasthi[1], B. Das[2] [1]Faculty of engineering and technology, Khwaja Moinuddin Chisti Language University Lucknow, 226013, U.P., India [2]Department of Physics Lucknow University 226007 U.P. India, Email: rrawasthi1947@gmail.com

In the present paper single phase bismuth ferrite $BiFeO_3$ (BFO) nanoparticles were prepared by co-precipitation method. Nanostructures have now a day become the centre of great attentions because of their distinctive size and shape-dependent properties as well as their relevant applications for nanoscale device fabrication. The Raman studies of nanomaterials sintered at various temperatures 400 ^{0}C, 500 ^{0}C, 600 ^{0}C and 700 ^{0}C reveal the rhombohedral crystal structure.

CP-06-31

Reduced Band Gap Black TiO_2 Nanoparticles Grown by Femtosecond Laser Based Ablation

Amita Chaturvedi[a], V. Srihari[b], and Sharad Karwal[c,] [a]Photonics Nanomaterials Lab,*

*Laser Material Processing Division, Raja Ramanna Center for Advanced Technology, [b]High Pressure & Synchrotron Radiation Physics Division, Bhabha Atomic Research Centre , [c]AIPES Beamline, UGC-DAE Consortium for Scientific Research, Indore (M.P.)-452013 *Email: amita-chaturvedi@rrcat.gov.in*

Femtosecond laser based ablation was utilized to growreduced band gapblackTiO_2 nanoparticles. TiO_2 is a widely used material for photocatalysis and photoelectrochemical applications such as pollutant degradation and water splitting respectively [1,2]. Major drawback with TiO_2 is its wide band gap in UV range which makes it sensitive to UV light [3] and therefore limits its solar induced applications. Various methods are being utilized in order to reduce band gap of TiO_2. One of the idea is to introduce defect states in TiO_2which mayresult in bandgap reduction by forming mid gap states. We have utilized femtosecond laser based ablation to grow defect rich black TiO_2 nanoparticles. These defect rich black TiO_2 nanoparticles were also found to be of reduced band gap with a shift in onset of absorption from UV range (~350nm) to visible range (~600 nm).

CP-06-32

Process Parameter Optimization for Development of SS 316 LN steel using Laser Directed Energy Deposition.

G. K. Mishra[1,4], A. K. Rai[1,4], A. K. Agrawal[3], V. Karthik[2,4], C. P. Paul[1,4], and S. K. Dixit[1,4] Raja Ramanna Centre for Advanced Technology, Indore-452013 [2]Indira Gandhi Centre for Atomic Research, Kalpakkam-603102 [3] Bhabha Atomic Research Centre Mumbai, 400 078 [4] Homi Bhabha National Institute, Anushakti Nagar, Mumbai-400 078 [*]Email: gkmishra@rrcat.gov.in

In the present study, austenitic grade SS 316 LN steel is developed using laser directed energy deposition (LDED) process. During the deposition of SS 316 LN using LDED, the laser power is varied between 950 to 1250 W with keeping powder feed rate of 7.5 g/min and scan speed 900 mm/min constant. Microscopic and synchrotron-based X-ray micro-computed tomography (SR-CT) examination reveals that the LDED built structure at laser power of 1100 W have no porosity and defect formation compared to same built at lower and higher laser powers of 950 and 1250 W. Further, the microstructural characterization confirmed the transition from cellular to equiaxed dendrites formation across the melt pool and in overlapped region due to significant change in temperature gradient and interface velocity upon solidification.

CP-06-33

Development of Inconel 625-SS 304L Bimetallic Structures using LDED Process with Functionally Graded Interface

Upendra Kumar[1,], A. K. Rai[1,3], C. P. Paul[1,3], D. Samantaray[2,3]and S. K. Dixit[1,3] [1]Raja Ramanna Centre for Advanced Technology, Indore-452013, [2]India Indira Gandhi Centre for Atomic Research, Kalpakkam-603102 [3]Homi Bhabha National Institute, Mumbai-400094 *Email: upendra@rrcat.gov.in*

In the present study, bimetallic performs of Inconel 625-SS 304L are fabricated using laser directed energy deposition (LDED) at optimized process parameters with graded interface. Microstructural and phase field analysis across the interface is carried out to assess the microstructure evolution and formation of different phases using optical and electron microscopy. Further to assess the of metallurgical bonding strength, microhardness measurement and compression testing at room and high temperatures are carried out. The as built bimetallic performs does not show any crack and delamination along the interface up to compression strain of 55% at room and high temperatures.

CP-06-34

Development of Cu-Ni Tubular Structure using Laser Directed Energy Deposition

*Suresh Kumar[1], [*]Neeraj Saini, A. K. Rai[1,2], Upendra Kumar[1], G. K. Mishra[1], C. P. Paul[1,3], and S. K. Dixit[1,3] [1]Raja Ramanna Centre for Advanced Technology, Indore 452013, INDIA [2]Homi Bhabha National Institute, Mumbai- 400094, India *Email: ksuresh@rrcat.gov.in*

In present study, laser directed energy deposition (LDED) based process is deployed for the development of bimetallic tubular structure of Cu and Ni with50 mm height having 2.5 mm wall thickness and15 mm OD. Tubular structure hasalternate layer of Cu and Ni with thickness around 0.5 mm.To deposit defect free tubular structure using LDED process, different process parameters such as laser power, powder feed rate and scan speedwere optimized. The optimized process parameters for Ni deposition are found to be 700 W (laser power), 8 g/min (powder feed rate)and 1000 mm/min (scan speed)and for Cu the laser power is found to be 900 W and other parameters remains same. To assess the quality of as built tubular structure, structural, microstructural characterization is carried out using optical, hardness tester and electron microscopy.

CP-06-35

Effect of inert gas on Laser Powder Bed Fusion Process

Sunil Kumar[1], S. K. Mishra[1], Sabir Ali[1], A. K. Rai[1], C. P. Paul[1,2], and S. K. Dixit[1,2] [1]Laser Group, Raja Ramanna Centre for Advanced Technology, Indore-452013, , Raja Ramanna Centre for Advanced Technology, Indore-452013, [2]Homi Bhabha National Institute, Mumbai- 400094 *Email: sunilkumar@rrcat.gov.in*

In the present sutdy effect of inert and open atmosphere on built quality of laser powder bed fusion (LPBF) printed Incoenl 625 and SS 316 LN is studied. During priting of the above mentioned matrerials, laser power (250 W), scan speed and layer thickness are kept constant and only the atmosphere is changed., scan speed:, hatch spacing: 0.250mm and powder layer thickness of 75micron. It is observed that when SS 316 LN and Inconel 625 are printed in open atmosphere, un-melted layer, porosity, crakcformation are observed. However, when the same materials printed in the inert gas flowing environment of Ar gas then except crack formation nothing else is observed. Further, it is noticed that in the case of Inconel 625, the formation of unmelted layer, cracks and porosity is significantly lesser

than that of SS 316 LN. This is attributed to higher oxidation resistance of Inconel 625 than SS 316 LN.

CP-06-36

Optical and vibrational properties of Boron Nitride layers grown by indigenously developed nitride MOVPE

Abhishek Chatterjee[1], Payal Taya[1], Vishal Agnihotri[1], Geetanjali Vashisht,[1,2] Rahul Agrawal[3] V. K. Dixit[1,2], and T. K. Sharma[1,2\1]1Semiconductor Materials Lab., Raja Ramanna Centre for Advanced Technology Indore, 452013 [2]Homi Bhabha National Institute, Training School Complex, Anushakti Nagar, Mumbai, 400094 [3]Laser Physics Applications Division, Raja Ramanna Centre for Advanced Technology, Indore, 452013 *Email: cabhishek@rrcat.gov.in*

Boron Nitride epitaxial layers are grown on (0001) sapphire substrates by an indigenously developed nitride MOVPE system using triethyl boron (TEB) and ammonia (NH_3) as the precursors for B and N, respectively. The layer growth is performed through a two-step process where the buffer layer is first grown at 550 ^{o}C prior to the growth of main layer at 1200 ^{o}C. Optical and vibrational properties of Boron Nitride layers are studies by Transmission, Fourier transform infrared (FTIR) and Raman spectroscopy techniques. While characterizing the samples using FTIR, the absorption bands at 745 and 1352 cm^{-1} are observed, which are related to in-plane stretching mode and an out of plane bending mode of sp^2-bonded BN phase referred as A_{2u} (IR), 783cm^{-1} and E_{1u} (IR), 1367cm^{-1} active modes of hBN. Raman spectra also revealed the presence of the characteristic E_{2g} mode of sp^2 bonded BN at 1362 cm^{-1}. The FTIR and Raman data indicates the presence of strain as well as inhomogeneity in the grown layer. From UV-Visible absorption spectra, the optical band gap is determined to be 5.8 eV which is similar to the values reported in literature confirming growth of strained hexagonal Boron Nitride epilayer.

CP-06-36

Development of borosilicate glass-metal sealed discharge tube for Sealed-off CO_2 laser

Ajay Kak[1], M. Murugan[1], S.Sitole[1],S.Sowrirajan[1], Manoj kumar[2,3], C.P.Paul[1,3 1]EDMS, Raja Rammana Centre for Advanced Technology,Indore-452013,[2]LMPD, Raja Rammana Centre for Advanced Technology, Indore-452013,[3]Homi Bhabha National Institute, Anushakti Nagar, Mumbai [1]Email: kakajay@rrcat.gov.in

We report development & fabrication of a sealed off discharge tube cavity for making a sealed off CO_2 laser.The discharge cavity consists of a water-cooled tube (outer tube), a gas storage tube (outermost) and a tube (inner) for gas circulation. The discharge tube is the key component in the CO_2 laser, which basically determines the characteristics of the laser output, and the length of the discharge tube and output power are just proportional.

Category - 7
Laser Plasma Interaction

CP-07-01

Self-compression of femtosecond laser pulses from the self-guided filament in long cells

A. Ansari[a,b], M. Kumar[b], H. Singhal[a,b] and J.A. Chakera[a,b], [a]Homi Bhabha National Institute, Anushaktinagar, Mumbai, [b]Raja Ramanna Centre for Advanced Technology, Indore, Email: ajmal@rrcat.gov.in

An experiment has been carried out to investigate the self-compression of ultrashort laser pulses in the self-guided filament in long gas cell. Laser pulses from Ti:sapphire laser system with an energy of ~ 6 mJ at a repetition rate of 1 kHz and a pulse duration of 55 fs is used in the investigation. Self-compressed laser pulses with a pulse duration of 26 fs and energy of ~ 2 mJ have been generated without external compensation. These pulses are characterized using a single-shot second harmonic auto-correlator. The self-compression of laser pulses depends critically depend upon the laser parameters, gas pressure and gas type.

CP-07-02

High Resolution Phase Contrast Imaging of Biological Samples using Betatron X-rays generated from Laser-Plasma Electron Accelerator

Shikha Mishra[1,2], B. S. Rao[1,2], A. Moorti[1,2] and J. A. Chakera[1,2], [1]Raja Ramanna Centre for Advanced Technology, Indore, [2]Homi Bhabha National Institute, Mumbai, Email: shikham@rrcat.gov.in

We demonstrate high-resolution phase contrast imaging of biological samples (leaf, mosquito, and spider) employing betatron x-rays generated by a laser-plasma electron accelerator. The x-ray imaging was performed in both single pulse and multiple pulse exposure mode in different x-ray energy ranges of 7-30 keV at a peak x-ray flux of ~1.5-2.5×10^{20} photons/sr/s in 0.1% BW and a resolution of ~6 micron was achieved. Betatron x-rays in different energy ranges were generated by interaction of Ti: Sapphire laser (150 TW, 25fs) with 4 mm long Helium/Nitrogen gas targets at a laser intensity of ~3×10^{19} W/cm^2.

CP-07-03

Stable high-harmonic generation from a semi-infinite gas cell,

M. Kumar[1], A. Ansari[1,2], H. Singhal[1,2] and J. A. Chakera[1,2], [1]Raja Ramanna Centre for*

*Advanced Technology, Indore 452 013, India; [2]Homi Bhabha National Institute, Anushakti Nagar, Mumbai-85; *Email: mukund @ rrcat.gov.in*

An experimental study has been performed to achieve high stable high harmonic source generated from an argon filled semi-infinite gas cell. Harmonic orders from 23rd to 39th are generated in the harmonic spectrum. The experimental parameters like gas cell pressure and focal position inside the gas cell are carefully optimized to achieve a stable harmonic intensity with a rms deviation of < 1%. The study will be useful for applications of the harmonic source where the high stability of the source is desirable viz. study of ultrafast thermal transport in materials, study of ultrafast demagnetization etc.

CP-07-04

Experimental study on estimation of plasma density scale-length using optical shadowgraphy

S. Bidoliya[1,2], [#]S. Bagchi[2], M. Tayyab[2], A. Moorti[1,2] and J. A. Chakera[1,2]; [1]Homi Bhabha National Institute, Anushakti Nagar, Mumbai – 400 094, [2]LPD, RRCAT, Indore – 452 013, Email: shivangib@rrcat.gov.in

In the present work, the characterization of the pre-plasma using optical shadowgraphy technique has been performed. A pump-probe based geometry was setup to characterize the pre-plasma density scale length. A separate low intensity pre-pulse has been used to form pre-plasma before the arrival of the main intense fs laser. Second harmonic of the fundamental laser pulse has been used as a probe. The technique of shadowgraphy enables a quantitative evaluation of scale lengths within probed plasma. The density scale-length of the plasma plume has been estimated at different probing time intervals, which grows progressively as the plume expands freely into the vacuum. Also, the corresponding expansion velocity has been calculated.

CP-07-05

Study of thermal and non-thermal K shell x-ray line emission from the aluminium plasma heated by ultra-short high intensity laser pulse

P.Singh[2,3], R. Roy[1,2], T. Mandal[2], V. Arora[2,], A. Moorti[1,2], and J. A Chakera[1,2], [1]Homi Bhabha National Institute, Training School Complex, Anushaktinagar, Mumbai 400 094, [2]Laser Plasma Division, Raja Ramanna Centre for Advanced Technology, Indore 452 013, [3] School of Physics, Devi Ahilya Vishwavidyalya, Indore 452 001, *Email: arora@rrcat.gov.in*

We report a study of the thermal and non-thermal K shell x-ray line emission from the aluminium plasma generated by the 150 TW, 25 fs laser pulses. X-ray spectra as a function of the laser focus position and pulse duration is analysed. Thermal x-ray line intensity maximizes at best focus position and shows non-symmetrical behaviour on either side of

the best focus position. The thermal x-ray intensity increases with laser pulse duration also suggesting at least few ps time is required for ionization equilibrium. Maximization of non-thermal line occurs away from best focus indicating role of optimal laser intensity.

CP-07-06

Laser Third Harmonic Generation in Arrays of Vertically Aligned Carbon Nanotube

Ashish Varma[1], S P Mishra[1], Arvind Kumar[2] and Asheel Kumar[2], [1]Laser Plasma and Material Research Group, Department of Physics, K. N. Govt. P. G. College, Gyanpur, Bhadohi-221304, India [2]Plasma Physics Research Group, Department of Physics, University of Allahabad, Prayagraj, India-211002 *Email: varmaashish331@gmail.com*

In this present study, we have theoretically investigated the enhanced cosh-Gaussian laser beam third harmonic generation via the nonlinear interaction with vertically aligned arrays of carbon nanotube. As a high power cosh-Gaussian laser interacts with this nano dimension medium, the atoms of this medium are quickly ionized formed the performed plasma and by this electron cylinder having lighter mass might be displaced with respect to ion cylinder. The nonlinearity is raised due to electrostatic restoration force on electrons. This laser beam has enough potential to imparts the oscillatory velocity to the conducting electrons of nano tube and efficiently absorbed at surface plasmon resonance frequency. Analytic expression of nonlinear third harmonic current density and laser third harmonic field is derived. The plotted graphical profiles promise the efficient and tunable generation of laser third harmonic field via the variation of beam decentered parameter, laser beam width, nanotube radii, inter carbon nanotube separation initial electric field amplitude of laser beam and electron-ion collisional frequency. Resonant field amplitude of laser third harmonic is observed at the laser beam frequency become the ½ times the electron plasma frequency. As the laser beam transverse propagation distance become near the 0.95 times the initial beam width, enhanced third harmonic might be generated. The laser beam decentered parameter plays an effective role for field enhancement of third harmonic with without change of laser beam frequency.

CP-07-07

Study the effect of dc-bias onTerahertz radiation generation by non-linear mixing of lasers in n-InSb slab

Narender Kumar[1], Kartik Joshi[1] [1]Department of Physics, Sri Venkateswara College, University of Delhi, New Delhi-110021, India. *Email: narenderk@svc.ac.in*

InSb has emerged as a very promising material in recent studies of the nonlinear interaction of high-intensity electromagnetic waves with semiconductors because it exhibits nonlinear effects at relatively low fields due to its high mobility and non-parabolic energy

bands. At optical frequencies, the III-V compound's free-carrier contribution to nonlinear phenomena is crucial. We use the nonlinear mixing of two p-polarized lasers with frequencies of ω_1 and ? $_2$and corresponding wave numbers of k_1 and k_2 to investigate the impact of dc bias on the generation of terahertz radiation over a rippled surface of an n-type semiconductor (n-InSb). The electron mass and collision frequency can be expanded in terms of the light intensity for moderately strong fields, where the variations in the carriers parameters can be viewed as perturbations. The nonlinear current that drives resonant THz radiation at beat frequency with a suitable wave number $k=k_1- k_2+q$ is brought about by the nonlinearity. The effect of dc biased electric field affects the yield of THz radiation.

CP-07-08

Characterization of LiF windows for 1550 nm laserunder shock compression

Swati Gandhi[1,], D.Mukherjee[1], A.S Rav[1] and K.D. Joshi[1, 2] [1]Applied Physics Division,Bhabha Atomic Research Centre, Mumbai, India 400085 [2]Homi Bhabha National Institute, Mumbai, India 400094 *Email: gandhis@barc.gov.in*

Laser interferometry based instruments *e.g.*VISAR, ORVIS, Fabry-Perot interferometer, HetV etc. play an important role as diagnostic tool for probing target materials under dynamic loading. Commonly measured parameter using these instruments is free surface velocity. When this free surface velocity measured through a transparent backing window in shock experiment employing laser interferometry gives information about particle velocity of the target-window interface. It is well known that, the apparent velocity of target-window interface measured through a transparent backing window is different than the actual particle velocity. To compensate for this difference, it is important to characterize the window material in terms of its equation state and pressure dependent refractive index at working wavelength prior to use in experiments. We have spanned such studies for wavelength 1550 nm at pressures <5GPa in Lithium fluoride (LiF) which is widely used as window in shock loading experiments. For this, five plate-impact experiments were conducted employing interferometer with 1550 nm laser source. In each experiment, the true value of Al2014/LiFinterfacial velocity wasderived from measured free surface velocity and found to be matching within ~1% with thatderived from the reported relations. The change in refractive index of the window at different shock compressed densities, in present experiments, were determined and plotted along with the available literature data. Our data, spanning the lower pressure regime, also agree well with the proposedrelation ofRigg *et al.*[3] for 1550 nm. Additionally, usingmeasured shock and free surface velocity the applicability of the reported Hugoniot parameters, *i.e.* C_0 and *s,* for LiF was examined in this low-pressure regime.

CP-07-09

Time-resolved imaging of underwater plasma generated by laser in the presence of an external electric field

Kavil Mehta[1], Swetapuspa Soumyashree[2], Prashant Kumar[2], Rajesh K. Kushawaha[2], Prahlad K. Baruah[1] [1]Department of Physics, Pandit Deendayal Energy University, Gandhinagar-382426, Gujarat, India [2]Physical Research Laboratory, Ahmedabad-380009, Gujarat, India, Email: prahlad.baruah@sot.pdpu.ac.in*

Laser-produced plasma from a silver target in liquid ambient was studied using fast imaging technique in presence of electric field (EF). Laser ablation in liquid (LAL) is a versatile technique to synthesize nanoparticles (NPs) It is atop-down method as the bulk target breaks down to plasma, followed by the nucleation of the vaporizedmass to form NPs. The properties of NPs are strongly dependent on the dynamics occurring due to the interaction of laserat the solid liquid interface. The images of plasma were taken at different time delay with respect to the laser pulse, and its evolution was studied. Parameters such as plasma size and intensity were estimated from the images. It was found that the size of plasma increases by 1.15 times whereas the intensity of plasma increases by 3 times, in presence of EF. Further results of the experiments will be presented in detailduring the conference.

CP-07-10

Particle acceleration using two color laser pulses in homogenous plasma

D. Mishra, B. Kumar, Department of Physics, University of Lucknow, Lucknow, Uttar Pradesh India - 226007, Email : dinkarmishra.edu@gmail.com

3-D PIC simulation results shows that, two color laser pulses may generate greater acceleration gradients than single color laser pulse. From figure 1, it is seen that, when the direction of polarization for the two laser pulse is same, acceleration gradient is approximately 10 GeV/m whereas when they are in opposite direction of polarization, acceleration gradient is approximately 80 GeV/m. It may also be noted that, acceleration gradient is continously increasing due to increase in arbitrary angle between the direction of polarization of the two laser pulse. This interaction can be well used for generating higher field gradients up to the order of TeV/m by using more intense and powerful lasers.

CP-07-11

Simulation study of wakefield generation by interaction of laser pulses and inhomogeneous plasma

S. Singh and B. Kumar, University of Lucknow, Lucknow, 226007, India, Email: saumyasingh.phy@gmail.com

Study of interaction of intense laser pulses with preformed plasma results to generation of wakefield which is of great importance due to its wide range of applications. These generated wakefields oscillate at the plasma frequency. A parabolic density variation

(plasma channel) is applied to the plasma embedded with a constant magnetic field to increase the interaction time of electrons and laser pulse. PIC simulation has been done to analyse the transverse and longitudinal wakefields for inhomogeneous plasma. An enhancement of electric and magnetic wakefield by ~77% in the inhomogeneous plasma as compared to homogeneous case has been reported.

CP-07-12

Self-compression and Self-focusing of Laguerre-Gaussian Laser in an Under-dense, Cold Collisionless Plasma

Subhajit Bhaskar[(a)], Hitendra K. Malik, PWAPA Laboratory, Department of Physics, IIT Delhi, New Delhi-110016, India [(a)]Email: sbhaskar.iitd@gmail.com

In the present work, we have considered the spatiotemporal profile of a circularly chirped Laguerre-Gaussian (LGpl) laser and investigated its propagation inside an under dense, cold, and collisionless plasma, where ponderomotive force and relativistic factor cause optical nonlinearities in the medium. As a mathematical approach, we have adopted the WKB method under paraxial approximation and obtained a differential equation for the beam width parameter in the reduced form of the nonlinear wave equation. The effects of the plasma density and the pulse duration on the self-focusing and self-compression phenomena are studied for laser with topological charge i=1 The laser with smaller pulse duration is observed to show convergence and compression earlier. Whereas plasma with higher density causes earlier self-focusing and compression of the laser. This study can be used for the particle trapping and particle acceleration phenomena.

CP-07-13

Investigation on Fundamental Plasma Parameters of Molybdenum Oxide using Laser-Induced Breakdown Spectroscopic Technique

A. Ajith and S. Sankararaman, Department of Optoelectronics, University of Kerala, Trivandrum, India. Email: aajith.opto@gmail.com

Laser-Induced Breakdown Spectroscopy (LIBS) is a powerful atomic emission spectroscopic technique utilizing energetic laser pulses to create plasma from various material surfaces. The study explores the fundamental plasma parameters- electron temperature and density - of Molybdenum Oxide (MoO_3) using a Q-switched Nd: YAG laser and the investigation is carried out under local thermodynamic equilibrium (LTE). Results indicate the influence of laser fluence on plasma parameters. The Boltzmann plot reveals a correlation between electron temperature and laser power, which increases from 14193.48 K to 24079.73 K with laser power. Stark-broadened profile analysis confirms LTE compliance, with electron density increasing proportionally to laser power. The study contributes valuable insights into plasma characteristics, advancing the understanding of LIBS for practical applications, particularly in laser material processing and thin film deposition.

CP-07-14

Time-Resolved Wollaston Interferometry for Laser-produced Plasma Characterization

Anu Avarachan[1], Akhil Varghese [1], Sreelakshmi V [2], Adhithyan C.S [1], Riju. C Issac[1] [1]Cochin University of Science and Technology, Kochi, Kerala, India, [2]St. Thomas College, Thrissur, Kerala, India, Email: anu_avarachan@cusat.ac.in

A stable, long-lasting plasma channel can be used as an optical waveguide for applications likelaser Wakefield acceleration, and X-ray lasers. In this experiment, we have created a hot plasma columnby focusing intense laserpulses with 35 fs pulse duration, in air at atmospheric pressure, which grows into an on-axis low-density profile suitable for intense laser beampropagation. Polarization-based interferometer setups using a Wollaston prism were used to analyze the plasma density profiles. Dimensions of the observed plasma channel were about 100μm diameter and 1mm in length. Time and space-resolved measurements on the evolution and decay of the electron density oscillations were also done after 2.4 ps from the initiation of the plasma.

CP-07-15

Tunable Nonlinear Current Density Generation by Beating of Two Hermite-cosh-Gaussian Laser Beams in Plasma Embedded with Nanocluster

S. Kumar[1], K. Ali[1], A. Kumar[1], A. Kumar[1], S. P. Mishra[2] and A. Varma[2],[1]Department of Physics,University of Allahabad, [2]Department of Physics, K. N. Govt. P. G. College, Gyanpur *Email: asheel2002@gmail.com*

In this paper, we study the generation of nonlinear current density by the interaction of two copropagating high power Hermite-cosh-Gaussian (HChG) laser beams in nanoclustered plasma medium. It is assured that nanocluster become ionize owing to the interaction of intense electromagnetic radiation of laser field with it and hereafter clusters are converted into the plasma plume balls. As the interaction process takes place each electromagnetic radiation of laser beam conveys the oscillatory velocity to the both medium electrons. The two copropagating HChG laser beams might be undergoes to the beat process of wave with beat wave number k=k1-k2 and frequency w=w1-w2 and surely a nonlinear force acts on electron associated with nanoclustered plasma which is generally termed as ponderomotive force. The effective surface plasmons oscillation is become resonant as the beat wave frequency becomes the 3 times the electron plasma frequency causes the much more generation of current density in clustered plasma. The nonlinear current density is tuned and controlled by cluster radius, cluster density, beam decentred parameter, electron-neutral collisional frequency and laser mode index m. This enhanced and tunable nonlinear current density might have possible applications in terahertz radiation generation, anomalous resistivity, harmonic generation, and many more.

CP-07-16

Nonlinear Absorption of High Power Laser Beam in Carbon Nanotubes

K. Ali[1], S. Kumar[1], A. Kumar[1], S. P. Mishra[2] and A. Varma[2],[1]Department of Physics, University of Allahabad, [2]Department of Physics, K. N. Govt. P. G. College, Gyanpur *Email: asheel2002@gmail.com*

In this present study, we investigate the nonlinear absorption of high power cosh-Gaussian laser beam in array of carbon nanotubes. The laser beam propagates normally to the parallel aligned carbon nanotubes. The electric field profile of laser beam produces the electrostatic restoration force due to displaced electron and ion cylinder. This net restoration force with respect to ion cylinder and electron cylinder causes the nonlinearity. An analytic expression of high-power laser beam absorption coefficient is derived. The resonant absorption is achieved as the laser beam frequency approaches near the effective surface plasmons frequency $w \sim w_{pe}//2$ The laser beam absorption process is tuned by varying the laser beam decentered parameter, carbon nanotube length, radius, density, and collisional frequency. This enhanced and tunable absorption of laser beam in carbon nanotubes might have application in heating process.

CP-07-17

Study of ultrafast phase transition dynamics of ultra-high contrast high-intensity femtosecond laser irradiated fused silica by time resolved reflectometry

P. Das[1], A. Dulat[2], S. Dam[2], S. Rakeeb[2], A. Lad[2], Y. M. Ved[2], J. Patra[1], S. Nanda[1], G. R. Kumar[2], A. Adak[1], [1]Dept. of Physics, IIT(ISM) Dhanbad, Dhanbad, [2]Dept. of Nuclear and Atomic Physics, TIFR, Mumbai. Email: 22dr0163@iitism.ac.in

Study of the ultrafast phase transition dynamics of matter induced by intense ultrashort laser pulses have great importance in fundamental plasma physics, astrophysics, fusion reaction and in novel material synthesis processes. We investigated this early time ultrafast phase transition dynamics of fused silica by time resolved probe reflectometry technique. The target is excited by highly intense (10^{13} W/cm^2-10^{14} W/cm^2) 800 nm, 25 fs pump pulse and probed by a low intensity beam with highest temporal resolution of 25 fs. The results show a sudden rise in the probe reflectivity at the initial stage of the interaction, which confirms the formation of an overdense plasma state of silica for high and moderate intensity of the pump beam irradiation. At lower intensity irradiation, two prominent peaks in the probe reflectivity are observed, which could be related to an ultrafast phase transition between two metallic phases through a non-metallic intermediate state. Thus, with the variation of pump intensity we could achieve distinct phases of plasma.

CP-07-18

Unravelling the influence of plasma temperature in the evolution of molecular signatures in laser induced plasma

Anandhu Mohan[a], Anannya Banerjee[b] and Arnab Sarkar[ab] [a]HomiBhabha National Institute, Anushakti Nagar, Mumbai 400 094, India [b]Fuel Chemistry Division, Bhabha Atomic Research Centre, Mumbai 400 085, India, Email:arnab@barc.gov.in*

This study covers the exploration of plasma temperature's influence on molecular signatures in Laser-Induced Plasma (LIP), emphasizing the significance of plasma temperature in the formation and evolution of molecular bands. A thorough analysis, correlating the decay times of plasma temperature and molecular intensity,confirmed the direct relationship between plasma temperature and molecular band formation. Signal-to-envelope ratio (SER) diagrams provided insights into optimal conditions for molecular emission, revealing a consistent temperature range for maximum molecular signature formation. The study identified the temperature range of 10,000-11,000K for BO and 8,000-9,000K for BO_2 as optimal conditions for molecular emission, regardless of laser wavelength and atmospheric conditions. These findings highlight the crucial role of plasma temperature in the formation and evolution of molecular signatures in LIP.

CP-07-19

Spatio-temporal analysis of transient boron species inlaser induced plasma

Anandhu Mohan[a], Anannya Banerjee[b], and Arnab Sarkar[ab] [a]Homi Bhabha National Institute, Anushaktinagar, Mumbai 400 094, India [b]Fuel Chemistry Division, Bhabha Atomic Research Centre, Mumbai 400 085, India [c]Lawrence Berkeley National Laboratory, Berkeley, CA 94720, USA, Email:arnab@barc.gov.in, asarkar@ymail.com*

This study explores the spatial and temporal dynamics of transient molecular species, particularly focusing on the (0-2) and (100-000) ro-vibrational bands of BO:B-X and BO2:A-X transitions ofboron, within laser-induced plasma (LIP). The spatial evolution of BO:B-X emission increased from the sample surface to the plasma core, peaking in the middle where high temperatures favored excited BO species. Conversely, polyatomic species like BO2 showed a distinct trend, with maximum spectral information observed at the plasma exterior due to lower temperatures favoring their formation. Spatial distribution analysis suggested recombination of atoms as the predominant mechanism for both BO and BO2, ruling out direct ejection from the sample surface. The spatio-temporal evolution analysis also illustrated the expansion and contraction of the plasma, indicating the fading of the LIP with increasedacquisition delay time. This investigation enhances the understanding of boron molecular species in LIP, offering valuable insights for analytical applications and advancing scientific knowledge in diverse fields where boron is pivotal.

CP-07-20

Study of the spatial evolution of laser induced Copper plasma

Anannya Banerjee[a] , Abhinandan Majumder[b], Anandhu Mohan[c], Anil K. Pulhani[b]and Arnab Sarkar[a,c,a]Fuel Chemistry Division, Bhabha Atomic Research Centre, Mumbai 400 085, India [b] Laser and Plasma Technology Division, Bhabha Atomic Research Centre, Mumbai 400 085, India [c]Homi Bhabha National Institute, Anushaktinagar, Mumbai 400 094, India, Email: arnab@barc.gov.in,* asarkar@ymail.com

This study presents a comprehensive overview of the research conducted on Laser-Induced Breakdown Spectroscopy (LIBS) and the temporal evolution of plasma properties, using an Oxygen-Free-High-Conductivity (OFHC) copper sample. The study emphasizes the significance of understanding plasma properties to fully grasp the LIBS technique for both qualitative and quantitative analytical purposes. Experimental details are outlined, elucidating the setup using a Q-switched Nd:YAG laser, a plano-convex lens for laser beam focusing, a Czerny-Turner spectrometer, an iICCD detector, an oscilloscope for timing coordination, and instruments for laser energy measurement and analytical calculations .The study diverges from typical LIBS investigations by employing initial acquisition delays in the nanosecond range, moving gradually to the microsecond region. Methods for correlating iCCD detector pixels to plasma height, utilizing an Hg-Ar lamp image, and calculating plasma heights are detailed. Plasma images captured reveal notable changes in shape and size over various time scales, with the plasma exhibiting expansion, shape alterations, and a dying nature after reaching maximum height. The study underscores the implications of observed plasma size and shape alterations at different time intervals, suggesting a crucial link between temporal plasma evolution and associated physics. Establishing this connection is vital in comprehending both plasma physics and the LIBS methodology, providing a foundational understanding for future comprehensive investigations. This fundamental study lays the groundwork for a more in-depth comprehension of these processes in the future.

CP-07-21

Electron Bernstein Wave Aided Laser Beam Absorption in Magnetized Plasma

S P Mishra[1a], Arvind Kumar[2], Asheel Kumar[2], Ashish Varma[1, 1]Laser Plasma and Material Research Group, Department of Physics, K. N. Govt. P. G. College, Gyanpur, Bhadohi-221304, India, [2]Plasma Physics Research Group, Department of Physics, University of Allahabad, Prayagraj, India-211002 [a]Email: drspmishra2001@gmail.com

In this present paper, we have theoretically studied the electrostatic electron Bernstein wave assisted Hermite cosh-Gaussian laser (HChG) beam absorption in plasma embedded with static magnetic field. The electron Bernstein wave assists the strong nonlinear coupling. This HChG laser beam couples the pre-existed electron Bernstein wave in

plasma at couple wave number k1=k + k0 and couple wave frequency .... where .... k and k0 are the electron Bernstein wave and laser beam wave number respectively and and are the electron Bernstein wave and laser beams frequency respectively. Linear and nonlinear current densities are generated by the combined effect of electron Bernstein wave aided HChG laser beam. An analytic formalism of absorption coefficient has been developed. When the electron Bernstein wave assisted HChG laser beam coupled mode is in phase with nonlinear current density, it gives rise the resonant absorption. The graphical profile assurances that the nonlinear absorption coefficient is strongly depends on static magnetic field (electron cyclotron frequency), Hermite polynomial m, laser beam width parameter, laser beam frequency, beam decentered parameter d, electron thermal velocity and parameter b. The laser Absorption process is increased very large with very small fraction aided of electron Bernstein wave. Laser beam decentered parameter associated with cosine term is a very sensitive parameter and plays a significant role in absorption coefficient. This enhance and tunable electron Bernstein wave assisted HChG laser absorption process might be applicable in second, third harmonic generation and plasma electron heating.

CP-07-22

A study on fast electrons transport and K-shell x-ray emission from Cu foil target irradiated by high intensity ultrashort Ti:Sapphire laser pulse.

*R. Roy[1,2], T. Mandal[2], P.Singh[2,3], V. Arora[2], A. Moorti[1,2] and J. A. Chakera[1,2],[1]Homi Bhabha National Institute, Training School Complex, Anushaktinagar, Mumbai 400 094, [2]Raja Ramanna Centre for Advanced Technology, Indore 452013, [3]School of Physics, Devi Ahilya Vishwavidyalya, Indore 452 001. *Email: riyaroy@rrcat.gov.in*

K-shell x-ray emission is studied in the interaction of ultrashort (25 fs), intense (? 4×10^{19} W /cm^2) laser with thin Cu foil. Flux of Cu K shell line is studied by varying foil thickness, laser energy and focal spot size to investigate the fast electron transport, in particular role of sheath field and refluxing. It is found that with increasing foil thickness (7 µm to 50 µm) the x-ray flux reduces~1.4X indicating effect of refluxing. X-ray conversion efficiency is found to be nearly constant with the laser energy variation. X-ray line intensity as a function of laser focal spot size indicate importance of optimal laser intensity.

CP-07-23

Proton Acceleration and alpha particle generation by Intense Laser Plasma Interaction

Arun kumar R M[+], Santhosh Krishnamurthy, Bhuvanesh Ramakrishna Department of Physics, Indian Institute of Technology Email: *bhuvan.phy@gmail.com, [+]ph20resch11012@iith.ac.in*

The interaction of high intense laser with matter opened up the new frontiers in physics for exploring the hot dense matter, production of high-energetic particles and radiation, and

also generation of energy using fusion reactions. The proton boron reaction ($p^{11}B$) is considered as the holy grail of advanced fusion fuels, where the primary reaction produces three energetic alpha (a) particles. The energy gain from the fusion reactions is very hard to achieve in thermal fusion conditions due to high nuclear binding energy and bremsstrahlung energy losses. With the advance of high intense Laser systems, Proton-boron fusion reaction is of greater interest owing to aneutronic reaction and also generation of alpha particles which is promising for its various multi-disciplinary applications especially in medicine. Recent experiments with high-intensity laser have shown record production of α particles by irradiating boron-hydrogen targets using the pitcher-catcher target geometry. The numerical simulations used are EPOCH PIC for the interaction between the main pulse and the plasma to generate protons and Monte-Carlo code FLUKA for the propagation of the ion beams in the secondary target. Alpha particle energies observed in the simulation are around 15 MeV and 10 MeV in front end rear end respectively through energy transfer from 20 MeV of protons. Flux of the alpha particles is also measured using the incoming protons.

CP-07-24

Effect of controlled pre-plasma on the ultra-short laser driven proton acceleration

S. Bidoliya[1,2], M. Tayyab[2], #S. Bagchi[2], A. Moorti[1,2] and J. A. Chakera[1,2];[1]Homi Bhabha National Institute, Anushakti Nagar, Mumbai – 400 094,[2]LPD, RRCAT, Indore – 452 013, Email: shivangib@rrcat.gov.in

In the present work, the effect of controlled pre-plasma on proton acceleration from a 12.5 μm thick Copper foil has been investigated. A separate low intensity pre-pulse has been used to form pre-plasma before the arrival of the main intense fs laser pulseresponsible for proton acceleration. The relative timing between the pre-pulse and the main pulse was varied and its effect on proton cut-off energy and flux has been studied. An enhancement in the TNSA accelerated proton energy have been demonstrated by using controlled pre-plasma present at the target front surface. The proton cut-off energy was observed to be initially increasing before gradually declining. The most substantial enhancement (~ 30%) in proton energy was observed at an optimal delay between the pre-pulse and the primary fs laser pulse. The observations are explained through increased laser energy absorption into the plasma and subsequent rise in the hot electron temperatures.

CP-07-25

Ion acceleration from aluminum foil embedded with gold nanoparticles layer irradiated by ultrashort laser pulses

D. Balusu[1,2], S. Krishnamurthy[1], M. Murakami[2] and B. Ramakrishna[1] [1]Department of*

*physics, Indian Institute Technology Hyderabad, Sangareddy, Telanganna 502285, India [2]Institute of Laser Engineering, Osaka University, Osaka, 565-0871, Japan, Email: ph20resch01002@iith.ac.in *bhuvan@phy.iith.ac.in*

Enhancement of proton energy has always been a key aspect addressed via laser-driven proton acceleration. As the Target Normal Sheath Acceleration (TNSA) protons are driven by the electric field produced at the target rear surface, the presence of a nanoparticle layer on the surface of the target foil will enhance the energy of acceleratedion beams. In our study, we used a 30 fs laser pulse with a wavelength of 800 nm and a peak intensity of 3 x 10^{20} W/cm^2. The targets were 2µm thick aluminum foils coated with a gold (Au) nanoparticle. It was observed that the dynamics of proton acceleration from the foil target is a function of the position of the nano particles layer (front or rear surface). 2D particle-in-cell simulation was also performed in support of the observed experimental results.

CP-07-26

Relativistic Attosecond Electron Sheets from Laser Wakefield Acceleration

R. S. Anandu, Bhuvanesh Ramakrishna[†] Department of Physics, Indian Institute of Technology, Hyderabad, Telangana, India, Email :*ph20resch11023@iith.ac.in, [†]bhuvan@phy.iith.ac.in.*

This research paper presents the observation of ultra-relativistic attosecond electron sheets generated through Laser Wakefield Acceleration (LWFA) in a plasma medium by making use of the miss matched bubble regime in LWFA. By employing an intense laser pulse, electrons were accelerated to energies of more than 300 MeV over a short distance within the plasma. The interaction between the laser pulse and the plasma density variation created a Wakefield, resulting in the formation of attosecond electron sheets. These electron sheets exhibited ultra-short durations in the attosecond regime, offering unprecedented insights into electron dynamics and interactions. The observed ultra-relativistic attosecond electron sheets hold promise for advancing fields such as ultrafast physics, attosecond science, and plasma-based particle acceleration, with implications for high-energy physics, materials science, and ultrafast spectroscopy.

CP-07-27

Distortion of the laser pulse shape in Inhomogeneous Plasma

Ram Gopal Singh, Faculty of Physical Sciences, Shri Ramswaroop Memorial University, Barabanki, U.P, India, Email: dr.rgsingh@gmail.com

In the course of intense laser pulse propagation through a plasma medium, the group velocity of the laser pulse undergoes modification owing to changes in the refractive index associated with nonlinear variations in plasma density. As a consequence, the leading edge of the pulse experiences sharpening, while the trailing portion undergoes broadening, resulting from disparities in group velocity across different segments of the laser pulse.

This leads to an anticipated distortion in the overall shape of the laser pulse. In the present study the propagation and distortion of short laser pulse in axially inhomogeneous plasma is studied.

CP-07-28

Simulation Study of Terahertz Radiation Generation by Propagation of Laser Pulses in Plasma

Nirmal Kumar Verma and Ram Gopal Singh, Faculty of Physical Sciences, Sri Ramswroop Memorial University, Lucknow, Email: nirmalkumarverma.physical@srmu.ac.in

A simulation study of terahertz radiation generation by two co-propagating laser pulses in an unerdense magnetized plasma has been presented. A transverse electric and magnetic fields oscillating at plasma frequency is generated due to the presence of the external static magnetic field. Simulation results show that the larger amplitude radiation can be generated by two co-propagating laser pulses as compared to the single laser pulse propagating in plasma.

CP-07-29

Generation of second harmonic radiation by the interaction of laser beam with obliquely magnetized plasma

Pooja Sharma and Pallavi Jha (*Retired Professor), Department of Physics, University of Lucknow, Lucknow-2260007, Email : shubhpooja.77@gmail.com*

An analytical study of second harmonic generation by the propagation of a circularly polarized laser beam in obliquely magnetized plasma has been presented. Considering a mildly relativistic regime of laser plasma interaction, a perturbative technique is used to evaluate the amplitude of second harmonic frequency. Its variation with obliqueness of the applied magnetic field is graphically depicted. The generated second harmonic radiation is seen to be circularly polarized.

Category - 8
Lasers in Industry and Defence

CP-08-01

Development of Laser cladding of Inconel-625 on P91 steel using Laser Directed Energy Deposition

Ambar Choubey[1], Sunil Yadav[2], C. H. Prem Singh[1], A. K. Rai[1,2], C. P. Paul[1,2] and S. K. Dixit[1,2]
[1]Raja Ramanna Centre for Advanced Technology, Indore-452013. [2]Homi Bhabha National Institute, Anushakti Nagar, Mumbai-400 078. [*]Email: ambarchoubey@rrcat.gov.in

In this work, a study on development of clad layer of Incone-625 on P91 steel using laser directed energy deposition is carried out. To develop defect and crack free clad layer with uniform thickness different process parameters are optimized. At optimized laser power of 1200 W with scan speed of 400 mm/min and powder feed rate of 8 gm/min, defect free and uniform clad layer of Inconel 625 with thickness ~ 871 µm is achieved. Optical microscopic characterization affirms no porosity and defect formation. The average micro hardness of the Inconel-625 clad layer is found to be ~269 $HV^{0.5}$ which is significantly higher than that of the 9Cr–1Mo base (~131 $HV^{0.5}$).

CP-08-02

Pulsed fiber laser texturing on SiC for the improvement of self-cleaning performance

*Ambar Choubey[*1,2], C.S. Mandloi[1], A.K. Rai[1], C.P. Paul[1, 2], and S.K. Dixit[1, 2 1]Raja Ramanna Centre for Advanced Technology, Indore-452013 [2]Homi Bhabha National Institute, Mumbai-400078 [*]Email: ambarchoubey@rrcat.gov.in*

In the present work, the laser texturing on SiC surface was carried out to improve its hydrophobicity at different laser process parameters using a pulsed fiber laser-based autogenous surface modification system. Effect of different process parameters on improving super hydrophobicity and self-cleaning behavior is investigated in detail. At optimized process parameters well defined surface texture having the square pillar of size 110 µm and depth 8 µm is generated with a hatch spacing of 170 µm. The textured samples were characterized using water contact angle goniometer and optical microscopy and 3D profilometer. A super hydrophobic surface with a maximum self-cleaning efficiency of 98% was achieved on SiC surface by laser texturing process.

CP-08-03

Laser drilling of micro-holes in copper using pulsed Nd:YAG laser for cryo-cooler application

Vijay Shukla[1], Pawan Kumar[1], Vinayak V. Rasankar[1], Ranveer Singh Meena[1], Rajvir Singh Doohan[2], Rajpal Singh[1], M. K. Bairwa[1], B. K. Saini[1], B. Ekka[1], B. N. Upadhyaya[1] and Rajesh Arya[1] [1]Laser Technology Division, Raja Ramanna Centre for Advanced Technology, Indore-452013, INDIA [2]SCRF Cavity Characterization and Cryogenics Section, Raja Ramanna Centre for Advanced Technology, Indore-452013, INDIA *Email: shuklavs@rrcat.gov.in*

In this paper, we report on laser drilling of ~ 100 µm to 350 µm diameter micro-holes in 500 µm thick copper disks of 12 mm diameter using direct beam of millisecond pulse duration Nd:YAG laser. Laser process parameters such as pulse energy and pulse duration were optimized and characterization of cut edges were performed using optical microscope. These laser drilled copper disk orifices are being successfully used in ultra-pure helium compressor developed for indigenous cryo-coolers in RRCAT.

CP-08-04

Laser Directed Energy Deposition Based Additive Manufacturing of Copper-Stainless Steel Multi-Material Injection Mould for Improved Performance

S Yadav[a,b], Suresh K[b], A K Rai[a,b], C P Paul[a,b], and S K Dixit[b,a] Homi Bhabha National Institute, Anushaktinagar, Mumbai - 400094, Maharashtra, India. [b]Raja Ramanna Centre for Advanced Technology, Indore - 452013, Madhya Pradesh, India, Email: sunilcem@gmail.com

Growing demands for sustainable manufacturing, shorter lead time, and improved efficiency in the tooling industry (including injection moulding) can be met by selective deposition of Copper (Cu) and Stainless steel (SS) as per the mould design. As multi-materials are a potential solution, Laser Directed Energy Deposition based additive manufacturing (LDED) is investigated in the present study with the objective to build Cu-SS multi-material injection mould. The present investigation deploys an indigenously developed 2 kW fibre laser-based LDED system for fabricating Cu-SS multi-material structures by varying process parameters (scanning speed, laser power and powder feed rate) and powder composition. Process parameters and deposition strategy are identified for depositing tracks and bulk structures using Cu and different Cu-SS compositions (CuxSS100-x, X varies as 20, 40, 50, 60, 80). Deposited bulk structures of individual blended compositions reveal that lower Cu concertation yields cracks and porosity, whereas bulk structures built using higher Cu concentration yield defect-free deposition. Further, a multi-material injection mould of Cu-SS is built at identified parameters yielding defect-free depositions. In addition, numerical investigation reveals a significant

reduction in cooling cycle time (~17-23%) by deploying Cu-SS multi-material moulds over conventionally fabricated SS mould during injection moulding. Reduced tooling cost, near net shaped manufacturing and multi-material fabrication with minimal material wastage establish LDED as one of the green manufacturing routes for building multi-material injection moulds fostering its improved performance.

CP-08-05

Indigenous Development of Hybrid Laser-Gas Metal Arc Welding System

Harish Kumar[1,] and C P Paul[1,2], [1]Raja Ramanna Centre for Advanced Technology, Indore 452013, INDIA [2]Homi Bhabha National Institute, Mumbai- 400094, India, *Email: harishk@rrcat.gov.in*

Hybrid laser- gas metal arc welding(HL-GMAW) combines laser and conventional gas metal arc welding process to overcome the limitations posed by both processes individually. Laser welding attributes less distortion, low heat affected zone, deep penetration, and high welding speed, but has poor gap bridging. On the other hand, gas metal arc welding provides good gap bridging but excessive distortion resulted due to high heat input. Recognizing the advantages and importance for thick plate welding for departmental applications, initiatives are taken to indigenously develop the HL-GMAW system. This paper reports the development work carried out in this direction.

CP-08-06

Design, Development and Deployment of a Control System for CO_2 Laser assisted rocket fuel testing facility at VSSC-ISRO, Trivandrum

Rajiv Kr. Yadav, Manoj Kumar, Shubjayan K P[1], L B Rana, Avantika Gautam and R Kaul [1], Vikram Sarabhai Space Centre-ISRO, Trivandrum Laser Materials Processing Division, MSATG, RRCAT, Indore *Email: rajivyadav@rrcat.gov.in*

Laser Surface and material treatment lab (LSMTL), RRCAT has been rigorously working towards design and development of industrial grade CO_2 lasers, cutting edge technology to refurbish aged lasers and deploy CO_2 laser applied control system at different strategic installations of the nation i.e., BRIT, Mumbai [1]. Recently, the RRCAT has refurbished an imported RF excited 150 W metal tube aged laser and returned to VSSC-ISRO on their urgent need. In parallel, RRCAT also supplied an indigenously developed 80W CO_2 laser tube along with an application specific control system (ASCS) to VSSC Trivandrum to enable them to use it to test and characterize varieties of rocket fuel samples. The touch HMI based supplied control system has been developed and tested to control the refined operation of the system. The control system uses source-based hardware and software components only in its development. ASCS features interlocked based operation and control of the system components to ensure personnel and system safety. This open platform-based system is certainly capable of including more features in future on their mark.

CP-08-07

Thickness quantification of the hidden phase object using lens less Fourier transform digital holography

Subhash Utadiya,[1] Vismay Trivedi,[2] Atul Srivastava,[3] Humberto Cabrera,[4] Gyanendra Sheoran,[2] Arun Anand[5], [1]Applied Physics Department, Faculty of Technology and Engineering, The Maharaja Sayajirao University of Baroda, Vadodara 390001, India, [2]Department of Applied Sciences, National Institute of Technology Delhi, India, [3]Department of Mechanical Engineering, IIT Bombay, Mumbai, 400076, India, [4]MLAB, STI Unit, The Abdus Salam International Centre for Theoretical Physics, Trieste,34151, Italy, [5]Optics Laboratory, Department of Physics, Sardar Patel University, Vallabh Vidyanagar, Anand 388120, India, Email: subhashutadiya@gmail.com*

Thickness measurements is a prime parameter for inspection and characterization of the phase objects. In many situations, it is challenging to measure the thickness of the sample directly when samples are inaccessible or hidden by other objects. the alternative way to determining the thickness of such object relies on the indirect measurements, specifically by quantifying a property of the sample that is directly influenced by its thickness. Opto-thermal properties of the sample was chosen for this purpose and quantifying the spatio-temporal refractive index changes induced by thermal loading. Refractive index changes of the sample generate spatial phase change of the probe wavefront passing through it. Digital holography easily maps these spatial phase change over time. Lens less Fourier transform holography facilitated phase change mapping in real time by simplifying the reconstruction process to a single Fourier transform of recorded hologram. The presented techniques utilizes lens-less Fourier transform holography and thermal loading for thickness measurements of the occluded phase objects.

CP-08-08

Development of a 200 W Thulium Fiber Laser at 1940 nm

V A Gomes[1,2], A Pal[1], [1]CSIR-Central Glass & Ceramic Research Institute, Jadavpur, Kolkata, India 2 Academy of Scientific & Innovative Research (AcSIR), Ghaziabad, Uttar Pradesh, India *Email: gomesvincent12@gmail.com*

Development of a high-power thulium fiber laser (TFL) is presented. A total laser output power of 207 W is achieved with an optical-to-optical slope efficiency of 52% for a total pump power of 400 W at 793 nm. Also, a high wall plug efficiency of 20% is achieved. The thulium doped fiber (TDF) length optimisation method is discussed. It is experimentally shown that the optimum length of the TDF is in the range of 4.1-4.8 m for the designed TFL. The co-relation of the heatsink water temperature with the optical-to-optical slope efficiency and the lasing threshold of the TFL is also discussed.

CP-08-09

Laser-Formed Die-less Manufacturing: Investigating Multiple Bending of Mild Steel Plates

Mohd Washique Ahemad[1], I.A Palani[1], Suhas S. Joshi[1] [1]Mechatronics and Instrumentation Lab, Department of Mechanical Engineering, Indian Institute of Technology Indore, Indore - 453532, India, Email: washique05@gmail.com, palaniia@iiti.ac.in

Laser forming is a promising technology in manufacturing such as in shipbuilding, automobile, microelectronics, and aerospace. Laser forming is a complex thermo-mechanical process in which its mechanisms are determined by the temperature profile across the sheet thickness which is influenced by laser power, scan speed, no of passes, laser beam diameter, and workpiece geometry. Material deforms because of compressive stress generated in the underneath region due to the thermal expansion of the irradiated region. In this study, we focused on the multiple bending and effect of different process parameters on laser bending of the sheet. Experiments were performed on 4 mm sheet thickness using a 2 KW fiber laser with various influencing parameters such as power, number of passes, scan speed, and laser spot diameter. Hardness and grain size measurements of laser-formed surfaces at different combinations of influencing parameters were performed. Also, we did analysis of features formed due to laser irradiation.

CP-08-10

High-aspect-ratio micro-hole generation in metals using quasi-continuous-wave (QCW) fiber laser drilling

A.K. Gupta, R. K. Singh, and D. Marla Department of Mechanical Engineering, Indian Institute of Technology Bombay, Mumbai-400076. *Email: dmarla@ iitb.ac.in.*

The quasi-continuous-wave fiber laser drilling process widely employed in industries such as aerospace, bio-medical, automobiles, and micro-electronics generates high-aspect-ratio micro-holes with remarkable productivity. This paper details an experimental investigation into the performance of single-pulse drilling on stainless steel using a quasi-continuous wave (QCW) fiber laser having high pulse energies and long pulse durations (milliseconds). The experimental design encompasses a 2-factor factorial analysis, considering power and pulse duration as process parameters. Single-pulse ablated samples underwent characterization via an optical microscope, facilitating the measurement of hole diameters, depth, taper angle, hump, burr, and heat-affected zone (HAZ). The study reveals that the hole diameter consistently surpasses the laser spot diameter, with a minimum of 300 μm noted at the lowest pulse duration and power settings. Hole depths ranged from 359

to 3000 µm with an aspect ratio of 10. The resulting holes exhibited a minimum taper angle of 0.38 minimum hump height of 25, minimum burr height of 39, and a minimum HAZ of 14 µm. The findings suggest that a QCW laser is well-suited for generating high-aspect-ratio holes with commendable quality.

CP-08-11

Development of Laser Powder Bed Fusion based Additive Manufacturing System

S. K. Mishra[1], C. P. Paul[1,3], C. S. Mandloi[1], M. O. Ittoop[2], B. S. Rawat[2] and S. K. Dixit[1,3] [1]Laser Group, Raja Ramanna Centre for Advanced Technology, Indore-452013, [2]Materials Science and Advanced Technology Group, Raja Ramanna Centre for Advanced Technology, Indore-452013, [3]Homi Bhabha National Institute, Mumbai- 400094 *Email: smishra@rrcat.gov.in*

Additive manufacturing (AM) processes make a three-dimensional (3D) product by gradually adding thin layers of materials controlled by a digital model, which is opposed to conventional manufacturing processes. Due to the additive build-up principle of AM, complex three-dimensional parts can be directly made from CAD data by eliminating the intermediate tooling steps. This leads to the shortening of production time and reducing associated costs. Its geometric freedom enables the designer to realise lightweight, complex hollow structures, overhangs, and lattice structures, which are being used particularly in the aerospace, automobile, nuclear industry, etc. This paper describes the development of a laser powder bed fusion-based additive manufacturing system with controlled environment and the demonstration of its capability by the fabrication of some complex 3D geometry of some engineering material such as SS 316 LN, Incoenl 625 and Ti alloy.

CP-08-12

Development of 10kW Fibre Laser based Directed Energy Deposition System for Metal Additive manufacturing

G. K. Mishra[1,4], C H Premsingh[1], C. P. Paul[1,4], and S. K. Dixit[1,4], [1]Raja Ramanna Centre for Advanced Technology, Indore-452013, [4] Homi Bhabha National Institute, Anushakti Nagar, Mumbai-400 078 [*]Email: gkmishra@rrcat.gov.in

Laser Additive Manufacturing (LAM) is one of the novel technique for manufacturing engineering parts directly from 3D CAD model by using layer by layer material build-up approach. LAM can be broadly classified into two major groups based on the material feeding technique - Powder Bed Fusion (PBF) and Directed Energy Deposition (DED). Laser based Directed Energy Deposition System is one of the promising additive manufacturing technologies for the fabrication of functionally graded solid and porous structures having complex geometry. A 10 kW LAM-DED system has been developed at

RRCAT and being used for fabricating the metal part as well as welding of thick (~ 20 mm) metal plates. This paper describes the development of 10 kW fibre laser based LAM-DED system for fabrication of metallic components and welding of thick metal plates.

CP-08-13

Macro Laser Polishing of LAM-PBF Built Inconel-625 for Surface Quality Improvement

Sabir Ali[1], S. K. Mishra[1], A. K. Choubey[1], Sunil Kumar[1], C. P. Paul[1,2] and S. K. Dixit[1,3]
*[1]EDMS, Raja Ramanna Centre for Advanced Technology, Indore-452013 [2]Homi Bhabha National Institute, Anushakti Nagar, Mumbai-400 078 *Email: sabirali@rrcat.gov.in*

Additive manufacturing, specifically metal 3D printing, has revolutionized the manufacturing industry by providing efficient and versatile methods for producing complex components. However, the inherent layer-by-layer nature of metal 3D printing can result in surface roughness and porosity, which can compromise the mechanical properties and performance of the printed components. So, the components made from laser-based powder bed fusion (LPBF) system cannot be used in as built condition and require post processing. This paper explores the application of laser surface smoothening as a post-processing technique for enhancing the surface finish of Inconel 625 built using LPBF process. Post to laser surface polishing, the average surface roughness (Ra = 0.1µm) is reduced significantly reduced as compared to as built sample (Ra = 0.96µm). Similarly, the peak to valley amplitude (Rz) is also reduced to 0.3 µm (polished surface) as compared to as built (3.35 µm).

Category - 9
Laser Spectroscopy and Applications

CP-09-01

Studying of Kerr effect in Graphene oxide liquid crystals using Stokes Mueller Polarimetry

Athira A, Alok Sharan, Department of Physics, Pondicherry University, Puducherry, India, Email: athira7rythm@gmail.com, aloksharan@gmail.com

We explored graphene oxide liquid crystal (GOLC) for its Kerr electro-optic performance by Stokes Mueller Polarimetry. We studied the switching response of GOLC dispersions under a crossed polarizer setup using 633 nm. Due to the preferential orientation of dipoles as a function of electric field strength, we have observed a maximum birefringence (Δn) having a magnitude of around $5x10^{-6}$ at 12 V for the optimized GO concentration in water. We have obtained different Δn for different polarization combinations, indicating the anisotropic behavior of GOLC. In the process, we could also estimateother optical properties like depolarisation, diattenuation, and retardance (both linear and circular) in GOLC. We noted thelinear and circular retardancein GOLC, thereby validating the optical anisotropy as well as the birefringence property of the material.

CP-09-02

Steel Sample Classification using DPSS Laser-Induced Breakdown Spectroscopy

S. Ahlawat, A. Singh, S. Sahu, P. K. Mukhopadhyay, R. Arya, S. K. Dixit, Laser Technology Division, Raja Ramanna Centre Advanced Technology, Indore, M.P. 452013, India, *Email: rsunita@rrcat.gov.in*

A laser induced breakdown spectroscopy (LIBS) setup has been developed using a home-built DPSS Nd:YVO_4 laser at a repetition rate of 2 kHz and pulse energy of 2 mJ. The low energy and high repetition rate of the laser necessitated acquiring the spectra by integrating data from a large number of laser pulses and continuously scanning the samples. The experimental parameters such as pulse energy and sample scanning rate were investigated for their influence on the intensity and fluctuations of the LIBS spectra. Under the conditions that yielded both strong signal intensity and the lowest relative standard deviation between signals, LIBS spectra from various steel samples were recorded. For classification of samples using LIBS spectra, a machine learning model was developed and an accuracy of ~ 100% was achieved for majority of the tested samples.

CP-09-03

Observation of a $^2S^+$ excited electronic state in LuO

Sheo Mukund[1], Soumen Bhattacharyya[1,2],[1]Atomic & Molecular Physics Division, Bhabha Atomic Research Centre, Mumbai, India.[2]Homi Bhabha National Institute, Bhabha Atomic Research Centre, Mumbai, India. [*]Email: sheo@barc.gov.in

We report the observation of a $^2S^+$ excited electronic state with T_v = 22842.06(1) cm^{-1} of $^{175}Lu^{16}O$. This state was characterized by analyzing the laser-induced fluorescence spectrum of jet-cooled LuO molecules. The LuOmolecules were produced in a pulsed supersonic molecular beam setup by the reaction of laser-ablated lutetium metal plasma with 2% molecular oxygen seeded in helium gas. Perturbations have been observed in the *e*-parity rotational levels for J 19.5 and in the *f*-parity levels for J 12.5. The molecular constants of the excited state were determined by fitting the rotational lines, which were free from perturbations, to the $^{2+}$molecular Hamiltonian. The deperturbed molecular constants could not be determined, as the perturbing electronic state was not detected in the current investigation. The observed $^{2+}$ excited electronic state could be a vibrational progression in the vibration v=6 of an earlier reported uncharacterized *A* state.

CP-09-04

Determination of the fundamental parameters of charge carriers in modulation doped InGaAs/GaAs quantum well by using magneto-photoluminescence spectroscopy

Geetanjali Vashisht,[1,2]S. Porwal,[1]T. K. Sharma[1,2]and V. K. Dixit[1,2], [1]Semiconductor Materials Laboratory, Materials Science Section, RRCAT, Indore- 452013, [2]Homi Bhabha National Institute, Training School Complex, Anushakti Nagar, Mumbai-400094, [*]Email:geetanjali@rrcat.gov.in*

The fundamental properties of the charge carriers in modulation doped InGaAs/GaAs quantum well (QW)are investigated by using magneto-photoluminescence spectroscopy. The diamagnetic-Landau shift of the ground state transition with magnetic field yields the effective mass(~ 0.055 ± 0.005 m_0) of the excitons associated with the InGaAs/GaAs QW. The sequential sweeping of the Landau levels during magnetic field scanat various probe energies, is used to estimate Fermi energy (~18 ± 0.9 meV) and carrier concentration (~ $4\times10^{11}cm^{-2}$) accumulated with-in the Landau states of the QW. It is concluded that the magneto-photoluminescence spectroscopyisa better alternative to the contact-based magneto-resistance method for probing the fundamental properties of semiconductor quantum structures particularly when contact formation is extremely difficult.

CP-09-05

Potential of the laser-induced fluorescence spectroscopy for the non-destructive early stage detection of photosynthetic pigments of the pea plants (*Pisum sativum L.)* exposed to the titanium dioxide nanoparticles (NPs)

Chhavi Baran[1] and K N Uttam[2] Centre for Environmental Science, IIDS, University of Allahabad, Prayagraj [2]Saha's Spectroscopy Lab, Department of Physics, University of Allahabad, Prayagraj, Email: chhavi.charvi16@gmail.com

The use of nanoparticles (NPs) is increasing in different fields such as agriculture, food science, medicine, and environmental remediation due to their unique physico-chemical properties which leads to the inevitable release of nanoparticles into the environment and their subsequent interactions with living organisms presenting a complex and challenging problem. Fluorescence spectroscopy is a widely used high-sensitivity technique for the analysis of plant state by analysing its chlorophyll fluorescence. Therefore, the current study provides the feasibility of the use of laser-induced fluorescence spectroscopy as a robust, rapid, label-free, non-destructive, non-invasive, and environmentally friendly probe for evaluating the impact of the nanoparticles on pea plants. For this, pea plants have been cultivated within laboratory conditions, and exposed to thoroughly controlled parameters including light intensity, temperature, and humidity levels. Later, when the secondary leaf appeared, plants were treated with different concentrations of titanium dioxide nanoparticles (viz. 0.2, 0.4, 0.6, and 0.8 mM) of the size ~ 7 nm. The laser-induced fluorescence spectra of the adaxial surface of leaves of control and titanium dioxide nanoparticles treated pea plants have been recorded in the spectral region 400-800 nm. The analysis of the recorded fluorescence spectrum shows the chlorophyll bands at 686 and 734 nm. The curve fitted areal intensity of the chlorophyll bands has been evaluated and used for the semi-quantitative changes of the chlorophyll pigment. The increase in the fluorescence intensity and intensity ratio of the chlorophyll bands due to the treatment of titanium dioxide nanoparticles indicates a decrease in the photosynthetic activity and chlorophyll content in the leaves of pea seedlings. The findings of the present study propose the use of fluorescence spectroscopy technique for the monitoring of crop health and determining the impact of photosynthetic activity in pea plants exposed to varying concentrations of titanium dioxide nanoparticles without any pre-processing, non-destructively, rapid and sensitive manner.

CP-09-06

Nondestructive, Extraction Free and Prompt Evaluation of Alteration of Biochemical Profile of the Leaves of Maize Seedlings Due to the Impact of Iron Oxide NPs by Confocal Micro Raman Spectroscopy

Aradhana Tripathi and K.N. Uttam, Saha's Spectroscopy Lab, Department of Physics, University of Allahabad, Prayagraj, Email: aradhnagate@gmail.com

This study was undertaken to explore the potential of non-destructive, sensitive and advance confocal micro-Raman spectroscopy to analyze the effect of iron oxide nanoparticles on physiological and biochemical response of maize seedlings. For this, the maize seedlings were developed in the laboratory under controlled conditions of the light flux, temperature and humidity in sand matrix. When the secondary leaf appeared in the seedlings then the nanotoxicity of different concentration of the spherical shape 30 nm iron oxide nanoparticles were introduced through the roots for five alternate days. The analysis of the acquired Raman spectra of the adaxial surface of the leaf of the control and iron oxide treated maize seedlings shows that iron oxide nanoparticles affect the biochemical profile, growth and development of maize seedlings. In fact, the treatment of iron oxide nanoparticles increases the level of biochemical like carotenoid, cellulose, carbohydrates, lignin, protein, pectin and aliphatic compounds present in the leaves of maize seedlings as compared to control in dose-dependent manner which indicates iron oxide is favorable for the cell wall component, carotenoid and other biochemical present in the maize leaves.

CP-09-07

Investigation of Bow-Tie Photoconductive Antennas for Terahertz Imaging Applications

*E. Nisha Flora Boby[1], Sachin Kumar[1], Shyamal Mondal[2*1]Department of Electronics and Communications Engineering, SRM Institute of Science and Technology, Kattankulathur 603203, Tamil Nadu, India [2]Department of Applied Physics, Defence Institute of Advanced Technology, Pune 411025, India, Email: shyamalkgec@gmail.com*

Terahertz (THz) generation and detection can be made efficiently using photoconductive antenna (PCA), which can be used in the fields of imaging, spectroscopy, and deep space studies. In this paper, the proposed PCA, which consists of semi-insulating-gallium arsenide substrate (SI-GaAs), over which the thin layer of low temperature grown-gallium arsenide (LTg-GaAs) has been grown and the silver electrodes are patterned on the substrate, is investigated by varying the geometry of the electrodes. The disadvantages of terahertz sources, such as low THz output power and optical to THz conversion efficiency, can be overcome by the proposed interdigitated and tip-to-tip bow-tie PCA. The interdigitated bow-tie PCA outperforms the conventional dipole PCA with improved gap conductance of 0.0078 ? , THz radiated output power of 3.9892 μW, and optical-to- THz conversion efficiency of 0.195%.

CP-09-08

Machine Learning Algorithms Based Confocal Micro Raman Spectroscopy Detection of Alteration of the Biochemical of the Leaf of Mung Seedlings Caused by the Exposure of Iron Oxide Nanoparticles

Aishwary Awasthi and K.N. Uttam, Saha's Spectroscopy Lab, Department of Physics, University of Allahabad, Prayagraj, Email: aish91298@gmail.com

This study demonstrates the potential of the confocal micro Raman spectroscopy technique coupled with machine learning algorithms for the detection, classification and alteration in biochemical of the mung plant due to the exposure of different concentrations of iron nanoparticles without any sample pre-treatment, non-destructively, rapidly, label-free and robust manner. For this, the mung seedlings were developed inside the laboratory under controlled conditions of light flux, temperature and humidity and treated with the different concentrations (0.2, 0.6, 1.0 and 1.4 mM) of the 30 nm iron oxide nanoparticles (Fe_2O_3 NPs). The analysis of the acquired Raman spectral data shows that the level of biochemical profiles like carotenoids, pectin, lignin, protein, cellulose, carbohydrates and aliphatics of the leaf of the mung seedlings is increased due to the treatment of different concentrations of the Fe_2O_3 NPs. For the rapid categorising and precise prediction, machine learning algorithms viz. principal component analysis (PCA), linear discriminant analysis (LDA) and principal component analysis-linear discriminant analysis (PCA-LDA) have been applied to the acquired Raman scattering spectral data, of the control and Fe_2O_3 NPs treated mung leaves. The results show that PCA-LDA provides the best predicting and clustering realization with an accuracy of 70 %, higher recall, precision, and f1 score and area under ROC curves compared to LDA for the different concentrations of Fe_2O_3 NPs. The findings of the study shows that Raman spectroscopy coupled with machine learning algorithms has a great potential for confirmatory, non-destructive and label-free assessment of various stresses and their impact on the plants.

CP-09-09

Spatiotemporal Evolution Of Nanosecond Laser-Produced Plasma From Unstructured And Structured Metal Targets: A Comparative Study

*Nikhil Varghese [a, *], Jijil J J. Nivas [b], S. Amuruso[b], Reji Philip [c], Smijesh N [a, *] [a]Ultrafast Optics Group, School of Pure and Applied Physics, Mahatma Gandhi University, PD Hills (P.O.), Kottayam - 686 560, Kerala, India. [b] Dipartimento di Fisica "Ettore Pancini", Università degli Studi di Napoli Federico II, Complesso Universitario Monte S. Angelo, Via Cinthia, I-80126 Napoli, Italy. [c] Ultrafast and Nonlinear Optics Lab, Light and Matter Physics, Raman Research Institute, Bangalore -560080, Karnataka, India. *Email: varghesenikhil@mgu.ac.in, smijeshn@mgu.ac.in*

Emission characteristics of nanosecond laser produced plasma (LPP) depend on laser parameters as well as the nature and pressure of the ambient gas into which it expands. Here, the spatio-temporal evolution of plasmas generated using 7 ns, 532 nm, 30 mJ laser pulses from unstructured and structured Cu targets are investigated for the enhancement in emission properties of the plume. The emission from neutrals and ions generated from a structured target are ≈1.5 times more than that of the emission from an unstructured target at 10 Torr ambient pressure of air. Measurements at different time delays (*td*) and integration times (*ti*) for both targets reveal the spatio-temporal evolution of the emission intensities of neutrals and ions. Emissions from ions persist longer in LPP from structured

targets than that from unstructured targets. Temperature (*Te*) and number density (*Ne*) of LPPs are calculated and compared for both targets.

CP-09-10

Surface Enhanced Raman Scattering Detection of Iron Ions in Aqueous Solution by Synthesized Silver Nanoparticles

Aparna Tiwari[1], Sweta Sharma[2], and K.N. Uttam[1], [1]Saha's Spectroscopy Lab, Department of Physics, University of Allahabad, Prayagraj, [2]Department of Environmental Science, Dr. Hari Singh Gour University, Sagar, Email: aparnatiwari945@gmail.com; kailash.uttam@rediffmail.com

This study has been conducted to examine the potential of surface enhanced Raman scattering of the violet plum fruit extract used synthesized silver nanoparticles for the detection of metal ions Fe (II) in aqueous solution. For this, extract of the pulp of violet plum fruit has been prepared by boiling the mixture of pulp and double distilled water for 30 minutes. Then the water extract of the violet plum mixed with aqueous solution of silver nitrate of different concentration is kept into the microwave for 5 seconds of 600 W. The analysis of the recorded ultraviolet-visible spectra shows the surface Plasmon transition at 411 nm depicting average size of 15 nm. The synthesized silver nanoparticles have been used for the detection of Fe (II) ions in aqueous solution in the concentration range upto 650 µM. The limit of detection and limit of quantification has been determined as 59 µM and 181 µM, respectively.

CP-09-11

Examination of Spectral Signatures of the Carbohydrate in the Millets Flour by Confocal micro–Raman Spectroscopy

Shristi Sharma, Aparna Tiwari, Aradhana Tripathi, and K.N. Uttam, Saha's Spectroscopy Lab, Department of Physics, University of Allahabad, Prayagraj, Email : shristi0109@gmail.com; kailash.uttam@rediffmail.com

Utilizing a 785 nm SLM laser as an excitation source, confocal micro-Raman spectroscopy has been utilized to examine the spectral signatures and carbohydrate content of millets such as buckwheat, ragi, and maize flour. To do this, the spectral region <2000 cm^{-1} of the Raman spectra of the flour made from buckwheat, ragi, and maize has been obtained. Upon analyzing the obtained spectrum, multiple spectral bands pertaining to carbohydrates are revealed. Based on the obtained spectral signature's peak intensity, a comparison of the amount of carbohydrate has been carried out. The study suggests that the confocal micro-Raman spectroscopy is a potent tool for quality monitoring of the various types of millets and for the selective detection of carbohydrates present in the millets without the need for sample preparation.

CP-09-12

Pigment determination of the Raspberry by Laser Induced Fluorescence Spectroscopy

Chhavi Baran, Aradhana Tripathi, Aparna Tiwari and K N Uttam, Saha's Spectroscopy Laboratory, Department of Physics, University of Allahabad, Prayagraj, Email:kailash.uttam@rediffmail.com

Raspberry (*Physalis peruviana*) fruits are an important source of minerals, vitamins, fibre, antioxidants that results in reducing the risk of major health problems such as diabetes, blood pressure, heart disease, cancer, inflammation and also promotes optimal health. Therefore, it is essential to investigate biochemical especially the presence and amount of photosynthetic pigments by using non-destructive, non-invasive, robust, rapid, extraction free and cost effective technique such as laser induced fluorescence spectroscopy. The laser excited fluorescence spectra of the exocarp, mesocarp and seed part of the ripen of cape gooseberry fruits were recorded by using steady state laser induced fluorescence spectroscopy by exciting 405 nm laser in the spectral region of 400-800 nm. The acquired fluorescence spectrum reveals many spectral bands like spectral signatures of the photosynthetic pigments present in the fruits. The well developed bands at 681-684, and 725-733 nm in the exocarp and mesocarp parts of the fruit denote the presence of chlorophyll. The exocarp and mesocarp part of pre-matured Raspberry depicts a definite increase in the fluorescence signal of both the chlorophyll bands as compared to post-matured Cape gooseberry. The observed band located at 515-518 nm in the exocarp and mesocarp part belongs to the caretonoid while the weak band seen at 616 nm arises due to anthocyanin. The simultaneous presence of chlorophyll, carotenoid, and anthocyanin photosynthetic pigments in the Raspberry makes this fruit very useful for reducing the risk of major health problems. The study demonstrates that laser induced fluorescence is a powerful, non-destructive, extraction free evaluation technique for determining the change in photosynthetic pigments like chlorophyll, carotenoid, anthocyanin content in the different parts of the fruits like Raspberry.

CP-09-13

Study of Odd Parity Autoionisation Levels of Lutetium by Resonance Ionisation Mass Spectroscopy

Diptimayee Biswal[1,2], Laxmi p Meher[2], Vipul Kumar[1], D R Rathod[1], Asawari D Rath[1,2], [1] Advanced Tunable Laser Applications Division, BTDG, BARC, Mumbai-400085, [2]Homi Bhabha National Institute, Mumbai-400094, *Email: asawarim@barc.gov.in*

Lutetium-177 (Lu-177), crucial in targeted radionuclide therapy, is being produced by neutron irradiation of enriched Lu-176 (> 80%) in a nuclear reactor. The laser based enrichment method relies on an efficient multi-step multi colour photo-ionisation scheme to produce enriched Lu-176 with high single stage selectivity and high throughput. The information on the discrete autoionisation (AI) levels of Lu is inevitable to design an

efficient photo ionisation pathways. We have measured 14 AI resonances using 560 nm transition, earlier predicted by us connecting from 17427.28 cm^{-1} to 35274.5 cm^{-1} as second step transition by employing three-step three-colour resonance ionization mass spectroscopy in a linear time of flight mass spectrometer and identified 5 new AI levels in the range 50590 cm^{-1}-51200 cm^{-1} from an intermediate excited level at 35274.46 cm^{-1} (J = 5/2). Using angular momentum selection rule, possible J values of the AI levels have been assigned. For this study we have used 573 nm transition as first step excitation. The three step three colour PI scheme is 0 cm^{-1} →17427.28 cm^{-1}→35274.5 cm^{-1}→AI Levels.

CP-09-14

Spectroscopic Analysis of Gallbladder Stones using Partial Least Square Discriminative Analysis

V. Bali[1], Y. Khajuria[1], N. Sharma[1], S. Kumar[2], Y. Lee[2],P. K. Rai[3], V. K. Singh [1,4,] [1]School of Physics, Shri Mata Vaishno Devi University, Katra 182320, Jammu and Kashmir, India, [2]Department of Chemistry, Mokpo National University, Muan-gun, Korea, [3]Department of Nephrology, Opal Hospital, Kakarmatta, Varanasi 221005, Uttar Pradesh, India, [4]Department of Physics, University of Lucknow, Lucknow 226007, Uttar Pradesh, India, Email: vivekksingh2005@gmail.com (Vivek K. Singh)*

Gallstone formation is a serious health concern and it is crucial to investigate their compositions to create preventive measures. We have carried out elemental studies of different parts (surface and core) of gallstones to identify the possible role of minerals and toxic elements in their pathogenesis. The stone samples were analyzed using laser-induced breakdown spectroscopy (LIBS) and energy-dispersive X-ray spectroscopy (EDS). Samples were classified using Fourier transform infrared (FTIR) spectroscopy. The findings of LIBS and EDS studies revealed that the content of essential and non-essential elements was higher in the core than inthe surface part. Elements such as strontium, mercury, and nickel were present only in the core indicating their possible role during the initial phase of gallstone formation. Other toxic elements observed in different portions of gallstones include arsenic, cadmium, lead, mercury, etc. Partial least square discriminative analysis (PLS-DA) was successfully applied to the LIBS data to discriminate the stone samples.

CP-09-15

Ligh-directed reversible plasmonic assembly of gold nanoparticles and in-situ nanogap tuning for optimum SERS

Cheviri Ghanashyam[1], Rajeev K. Sinha[2] and Aseefhali Bankapur[1],[1]Department of Atomic and Molecular Physics, Manipal Academy of Higher Education, Manipal, 576104, India, [2]Department of Physics, Birla Institute of Technology, Mesra, Ranchi, 835215, India Email: asif.bankapur@manipal.edu*

A dynamic reversible assembly of gold nanoparticles (AuNPs) in an aqueous environment addresses the need for SERS substrate with an in-situ nanogap tuning. Here, we demonstrate surface plasmon polariton (SPP)-assisted dynamic assembly of AuNPs at laser power density as low as 100 nW/μm^2. The major advantage of our method is that the interparticle nanogap is tunable to achieve analyte and AuNP-specific optimum SERS enhancement. The assembly experiments revealed the influence of AuNP surface charge and the resulting polarizability on the SPP forces. The developed system and method could detect SR101 dye molecules at concentrations as low as 10^{-10} M.

CP-09-16

Photoionization and density functional theory investigations of small yttrium monoxide clusters

Varun Vinayak Deshpande[1,2,], Vaibhav Chauhan[1], Soumen Bhattacharyya[1,2]*, [1]Atomic & Molecular Physics Division, Physics Group, Bhabha Atomic Research Centre, Mumbai - 400085, INDIA, [2]Homi Bhabha National Institute, Anushaktinagar, Mumbai - 400094, INDIA, Email : varund@barc.gov.in, sbhatt@barc.gov.in*

The photoionization (PI) spectra of yttrium monoxide clusters, in the size range of metal-containing 3 to 5 atoms, have been recorded. The structures of these species have been investigated systematically by density functional theory, and the lowest-energy structures (LES) have been identified. The theoretical PI spectrum has been calculated for a species by simulating the vibrational transitions between the neutral and its ion. The ground state geometric structures and spin states have been assigned based on a favourable agreement between the experimental and simulated PI spectra. The Y_nO is 3-dimensional from n = 4 with the Y_3O a planar distorted rhombus in its ground state. A trigonal pyramid and a trigonal bipyramid with an O atom capping a face are the ground state structures of Y_4O and Y_5O, respectively. The geometric structures of Y_nO clusters are similar to the La_nO clusters.

CP-09-17

Unveiling Breast Tissue Architectural Properties by Photoacoustic Spectroscopy *ex vivo*

Shimul Biswas[1], Bhavya K P[2], Satyapriyanka[2], Jackson Rodrigues[1], Darshan Chikkanayakanahalli Mukunda[1], Subhash Chandra[1], Shaik Basha[1], Ameera K[1], Stanley Mathew[2], Krishna Kishore Mahato[1] [1]Department of Biophysics, Manipal School of Life Sciences, Manipal Academy of Higher Education, Karnataka, Manipal-576104, India [2]Department of General Surgery, Kasturba Medical College, Manipal Academy of Higher Education, Karnataka, Manipal- 576104, India, *Email: mahato.kk@manipal.edu*

Photoacoustic spectroscopy (PAS) is a powerful tool for biomedical research by enabling noninvasive and real-time detection of bio-macromolecules in tissues. In this pilot study, we have differentiated normal and cancer tissues by photoacoustic (PA) spectroscopy using collagen as a biomarker. The tissue samples were excited at 325 nm pulsed laser light

and the corresponding recorded PA spectra were preprocessed, wavelet transformed, and subjected to principal component analysis. Principle Component Analysis (PCA) suggested2 principal components (PCs) covering 98.9 % of the variances (PC1: 89.650065 and PC2: 9.306943613).The current work successfully illustrated the unique properties of collagen by means of photoacoustic spectroscopy and spectral data analysis. This approach demonstrates the great potential of photoacoustic spectroscopy in clinical a setting and emphasizes how much it can help with diagnostic efforts.

CP-09-18

Investigating the impacts of glycation on protein using Fluorescence Spectroscopy

*Ameera K[1], Darshan Chikkanayakanahalli Mukunda[1], Shaik Basha[1], Subhash Chandra[1], Jackson Rodrigues[1], Shimul Biswas[1], Vijendra Prabhu[2], M Mukhyaprana Prabhu[3], Krishna Kishore Mahato[1 * 1]Department of Biophysics, Manipal School of Life Sciences, Manipal Academy of Higher Education, Manipal – 576104, Karnataka, India. [2]Department of Biotechnology, Manipal Institute of Technology, Manipal Academy of Higher Education, Manipal – 576104, Karnataka, India. [3]Department of Medicine, Kasturba Medical college, Manipal Academy of Higher Education, Manipal – 576104, Karnataka, India. [*]Email: mahato.kk@manipal.edu, kkmahato@gmail.com*

Glycation causes structural modifications and functional decline in proteins and the formation and accumulation of advanced glycation end products (AGEs). Fluorescence spectroscopy is a commonly employed method for measuring glycation. The present study utilizes deep UV LED (285 nm) as an excitation source. In this work, the impact of fructose-induced glycation on fibrinogen was evaluated using LED-induced autofluorescence (LED-IAF).

CP-09-19

Minor additive (UF_4, ThF_4) determination in Indian MSR fuel - an approach through Laser Induced Breakdown Spectroscopy (LIBS)

Anannya Banerjee[a], Anandhu Mohan[b], Sumanta Mukherjee[c], S.C Parida[a,c] and Arnab Sarkar[a,b], [a]Fuel Chemistry Division, Bhabha Atomic Research Centre, Mumbai 400 085, India [b]Homi Bhabha National Institute, Anushaktinagar, Mumbai 400 094, India, [c]Product Development Division, Bhabha Atomic Research Centre, Mumbai 400 085, India, Email: arnab@barc.gov.in, asarkar@ymail.com*

MSR is an ambitious addition in the list of India's clean energy drive through the approach of nuclear energy. The inherent safety features and the use of mixed fluoride salts (U,Th,Li) as molten-liquid fuel make this reactor a unique one. This paper explores the application of Laser Induced Breakdown Spectroscopy (LIBS) to ensure the chemical composition of the fuel. The study focuses on quantifying UF4 (uranium tetrafluoride) and ThF4 (thorium tetrafluoride) through univariate calibration. Various normalization techniques are applied

to the raw spectral data, and the results are compared based on a statistical parameter Standard Error of Prediction (SEP). Comparative analysis of different methods reveals that the most accurate and precise quantification falls within the range of 1.57% to 3.93% for UF_4 and 0.36% to 0.45% for ThF_4 respectively.

CP-09-20

In-situ Time-Resolved Spectroscopic Investigation of Laser-shocked s-Triazine

Ashutosh Mohan[1,2,], T. Sakuntala[1,2], [1]HP&SRPD, BARC, Mumbai - 400085, [2]HBNI, Mumbai - 400094, Email: ashutoshm@barc.gov.in*

We have examined the behaviour of heterocyclic aromatic compound 1,3,5-triazine ($C_3H_3N_3$) under laser-driven shock compression using time-resolved Raman spectroscopy. The sample undergoes a reversible phase transition from phase-I (R-3c) to phase-II (C2/c) at 600 mJ pump energy (~1.7 GPa). The study confirms the possibility of studying reversible phase transitions in opaque samples under laser driven shock by utilizing the reflected shock method.

CP-09-21

Dislocation-induced thermal diffusivity control in ZnO-diesel soot hybrid nanofluid: A mode mismatched thermal lens study

V. Gokul[1], M.S. Swapna[2] and S. Sankararaman[1], [1]Department of Optoelectronics, University of Kerala, Trivandrum, 695581, India, [2]Laboratory for Environmental and Life Science, University of Nova Gorica, Vipavska 13, Nova Gorica, SI-5000, Slovenia. *Email: gokul.opto@gmail.com*

The work enfolds the development of an energy-efficient hybrid nanofluid (HNF) comprising zinc oxide (ZnO)-diesel soot (DS) to address heat transfer limitations in thermal systems. The study employs a highly sensitive mode-mismatched dual beam thermal lens technique to analyze the concentration-dependent thermal diffusivity variations of the HNF. The hybrid composite is synthesized by solid-state mixing and annealing of ZnO and DS.The structure characteristics of the hybrid composites are understood from X-ray diffraction (XRD) analyses. The structure dislocations present in the prepared composites are revealed through the detailed analysis of the XRD patterns. A two-step synthesis process involving 1 h of ultrasonication is chosen for the preparation of ZD nanofluid (NF) in ethylene glycol as the base fluid. The thermal lens study is conducted in the NFs, revealing the impact of crystallite dislocations on the thermal behavior of the synthesized hybrid composites. Thus, the study suggests the possibility of dislocation-induced thermal diffusivity tuning in ZnO-diesel soot hybrid nanofluid.

CP-09-22

Thermal lens-based trace iron detection in drinking water

P Anju Abrahama, M S Swapnab, and S Sankararamana, [a]Department of Optoelectronics, University of Kerala, Trivandrum 695581, India, [b]Laboratory for Environmental and Life Sciences, University of Nova Gorica, Vipavska 13, Nova Gorica, SI-5000, Slovenia, *Email: sranju.opto@gmail.com*

The study addresses the crucial issue of iron contamination in well water in the Kazhakoottam region, Kerala, using a highly sensitive mode-mismatched thermal lens setup as an innovative detection method. Traditional techniques for iron quantification can be expensive and require specialized training. The research involves the systematic collection of water samples, synthesis of iron oxide for calibration, and characterization of both particulate matter in water and synthesized iron oxide using X-ray diffraction and UV-visible spectroscopy. The thermal lens technique, known for its exceptional sensitivity, is employed for ultra-sensitive detection, showing a linear calibration curve with a low limit of detection (0.1 ppm). The method is applied to estimate iron oxide concentrations in water samples over different settling durations. This study proposes a cost-effective and reliable approach to detect and quantify iron content in water, especially in regions facing challenges related to iron contamination.

CP-09-23

A new dimension in single-cell Raman spectroscopy with the help of light sheet optical tweezers

Panchanil Sarmah, Smrithi Jayaraj, Cheviri Ghanashyam and Aseefhali Bankapur, Department of Atomic and Molecular Physics, Manipal Academy of Higher Education, Manipal, India – 576104, Email: asif.bankapur@manipal.edu*

Studying physiochemical properties at cellular level is of utmost importance as it is the fundamental unit of life. Optical trapping at microscopic level, combined with Raman spectroscopy can serve a good way of understanding the cell. This has invariantly led to the development of Laser tweezers Raman spectroscopy (LTRS) (i.e., combining Micro-Raman spectroscopy with optical trapping). This techique is label free, robust and ability to study cells in native environment. In this study we have used light sheet having a line focus spot instead of the generally employed cylindrical beams having point focus. This has led to a better probing of the whole cell and efficient signal collection leading to improved spectral features even at lower power density.

CP-09-24

Development of Hadamard Transformation Based Single Pixel Spectrometer

V. Shrivastava[1], P. Sharma[2], T. S. Reddy[2], S. Kumar[2], Y. Verma[2,3] and S. Raja S.[2], [1]Institute of Excellence in Higher Education (IEHE), Barkatullah University, Bhopal, [2]Advanced

Electro-Optics Systems Section, RRCAT, Indore, [3]Homi Bhabha National Institute, Anushaktinagar, Mumbai. Email: yogesh@rrcat.gov.in

Measurement of the spectrum of light provides us with valuableinformation about the material with which it has interacted.Conventional spectrometers have limited resolution and are optimized for limited wavelength range. They are often bulky and time-consuming in nature. The key advantage of a single-pixel Hadamard spectrometer is its ability to simultaneously acquire all spectral components using a single detector element or pixel. This makes it suitable for scenarios where traditional spectrometers with multiple detectors are impractical or expensive. In this paper we describe the development of a Hadamard transformation based single pixel spectrometer that was used for reconstruction of a test spectrum.

CP-09-25

Three-color photoionization spectroscopy of atomic gadolinium

P K Mandal[1], A C Sahoo[1], Jaya Mukherjee[2], A D Rath[1], M L Shah[1], [1]Advanced Tunable Laser Applications Division, Bhabha Atomic Research Centre, Mumbai 400085, India, [2]Technology Deployment Division, Department of Atomic Energy, Mumbai-400 001,India, Email: pkmandal@barc.gov.in

Even-parity autoionizing levels and their total angular momenta of atomic gadolinium have been studied near the ionization potential using three-color three-step photoionization spectroscopy. These studies were performed in an atomic beam using three tunable dye lasers. We have observed 40 new autoionizing levels. Using angular momenta selection rules, total angular momenta of 10 levels have been determined uniquely and possible total angular momenta for remaining autoionizing levels have been assigned.

CP-09-26

Mass Spectrometry and Photoionization Spectroscopy of Y_nO_m (n=1-9; m=1-4) nanoclusters

Vaibhav Chauhan[1], Varun Vinayak Deshpande[1,2], Soumen Bhattacharyya[1,2#] [1]Atomic and Molecular Physics Division, Physics Group, Bhabha Atomic Research Center, Mumbai 400 085, India, [2]Homi Bhabha National Institute, Mumbai 400 094, India Email: [*]vibhu9494@gmail.com; [#]sbhatt@barc.gov.in*

Yttrium oxide clusters, Y_nO_m (n = 1 – 9, m = 14), were produced in a laser vaporization supersonic metal cluster beam setup and were investigated by time-of-flight mass spectrometry. The vertical ionization energy (VIE) and threshold ionization energy (IE_{th}) of yttrium monooxides, Y_nO (n = 1 – 9), and higher oxides, Y_nO_m (n = 4– 6; m = 2–4) were determined from their respective photoionization efficiency spectra. We report the ionization energies of Y_nO_m (m =46, m = 24) and Y_2O clusters for the first time in literature while our values for the monoxides are in excellent agreement with a previous report.The

VIE and IE_{th} of the yttrium monooxides decreased rapidly and nonmonotonically upto n = 6 atoms. Also, for higher oxides of Y_nO_m (n = 4–6; m = 2–4), no such monotonous pattern was observed in the VIE and IE_{th}. The absence of magic numbers or odd–even alternations, with respect to the number of metal atoms, is taken as evidence that threshold photoionization occurs from 4*d* orbitals of metals rather than a delocalized band derived from 5*s* valence electrons.

CP-09-27

Performance evaluation of a customized bi-modal laser spectroscopy system with conventional methods for the analysis of microplastics

M Vasudeva[1], U K Adarsh[1], Sajan Daniel George[2], Anish Kumar Warrier[3,4] and V K Unnikrishnan[1], [1]Department of Atomic and Molecular Physics, Manipal Academy of Higher Education, Manipal, Karnataka, 576104, India, [2] Centre for Applied Nanosciences (CANs), Department of Atomic and Molecular Physics, Manipal Academy of Higher Education, Manipal, 576104, India, [3] Department of Civil Engineering, Manipal Institute of Technology, Manipal Academy of Higher Education, Manipal, 576104, India, [4]Centre for Climate Studies, Manipal Academy of Higher Education, Manipal, 576104, India, * Email:unnikrishnan.vk@manipal.edu*

Microplastics are one of the most concerning environmental pollutants because of their ubiquity. Their capability to adsorb other environmental pollutants increases the risk even further. Current methods for microplastic characterization for polymer class and surface adsorbed heavy metal detection require the utilization of multiple resources. This work discusses the applicability and advantages of a Laser Induced Breakdown Spectroscopy (LIBS) - Raman spectroscopy system by comparingit's performance with conventional methods such as Attenuated Total Reflectance- Fourier Transform Infrared (ATR-FTIR) spectroscopy, confocal Raman spectroscopy, and Scanning Electron Microscopy- Energy Dispersive X-ray Spectroscopy (SEM-EDS) to analyze microplastics for polymer characterization and heavy metal detection. Raman analysis identified Polyethylene (PE), polypropylene (PP), and polyethylene terephthalate (PET) plastics, which is confirmed by confocal Raman and FTIR study of the same. LIBS study of microplastics detected heavy metals such as Al, Ni, Co, and Zn, along with Ca and Mg trace elements. The cross-examination with EDS validates these trace elements' presence on the microplastics' surface.

CP-09-28

Non-destructive Profiling of the Photosynthetic Pigments of the Black Carrot by Laser Induced Fluorescence Spectroscopy

Shruti Shukla[1], Chhavi Baran[2] and K. N. Uttam[1], [1]Saha's Spectroscopy Laboratory, Department of Physics, University of Allahabad, Prayagraj [2]Centre for Environmental Science, IIDS, University of Allahabad, Prayagraj, Email: shrutishukla718@gmail.com;

kailash.uttam@rediffmail.com

The requirement of high quality agriculture products by consumers and industry demands reliable, cost effective and fast data acquiring technique that has practical applicability for the non-destructive monitoring. For this, potential and applicability of the laser induced fluorescence technique has been examined for the investigation of the ripening process of the widely consumed carrot. The study highlights the applicability of the laser-induced fluorescence spectroscopy for the label free, extraction free, rapid identification and characterisation of pigments present in the biosamples having complex matrix like black carrot. For this, fluorescence spectra of the black carrot have been acquired in the spectral region 400-800 nm by exciting the specimen using 405 nm diode laser. The analysis of the acquired spectra reveals the rich presence of fluorochromes like chlorophyll, carotenoids, and anthocyanin in the black carrot. The spectral signatures obtained in this study can be used for the identification of the various pigments present in the products made by the black carrot.

CP-09-29

Label Free Mapping of the Biochemicals in Black Carrot by Confocal Raman Microspectroscopy

Shrayashi Pandey[1], Aradhana Tripathi[1], Chhavi Baran[2], and K. N. Uttam[1], [1]Saha's Spectroscopy Laboratory, Department of Physics, University of Allahabad, Prayagraj, [2]Centre for Environmental Science, IIDS, University of Allahabad, Prayagraj, Email: pandeyshrayashi66@gmail.com; kailash.uttam@rediffmail.com

Raman scattering based technique coupled with microscope provides information about the chemical structure of biological specimen at the molecular and cellular scale non-destructively without the requirement of chemical extraction. Confocal Raman microspectroscopy presents a new approach to investigate the cellular structure of vegetables and the biochemical contents in them. This study describes potential of the confocal Raman microspectroscopy for the evaluation of biomolecules and their distribution in the various parts of black carrot. The study highlights the applicability of the spectroscopy probes such as confocal micro Raman spectroscopy for the non-destructive, label free, extraction free, rapid identification and characterisation of biochemicals present in the biosamples having complex matrix like black carrot. For this, Raman scattering spectra of the black carrot have been acquired in the spectral region <2000 cm^{-1}. The analyses of the acquired spectra reveals the rich presence of phytochemicals like carotenoids, glucose, fructose, anthocyanin and cellulose in the different layers of the black carrot in varying amount. The spectral signatures obtained in this study can be used for the identification of the various biochemicals present in the products made by the black carrot.

CP-09-30

Complementary Nature of LIBS and Raman Studies as Inferred from the Analysis of Natural Pigments

S.Harikrishnan, C. Santhosh, S.D. George, V.K.Unnikrishnan, Department of Atomic and Molecular Physics, Manipal Academy of Higher Education, Email: surya.hk@manipal.edu

Laser Induced Breakdown Spectroscopy (LIBS), Raman spectroscopy, and Laser-Induced Fluorescence (LIF) spectroscopy are proven to be very efficient spectroscopic techniques find applications in the analysis of pigments. However, these three techniques do not give the same kind of information about the sample and also differ in the kind of materials on which they are applicable. Ideally, for complete information about a sample specimen, all these techniques have to be employed because they compensate for the shortcomings of each other in terms of the nature of information yielded, and the realm of applicability as can be seen from these studies on pigments. This work reports the application of both LIBS and Raman Spectroscopy on selected samples of natural pigments leading to complementary and comprehensive information about the samples.

CP-09-31

Comparison of temperature sensing performance of Dy^{3+} doped $CaMoO_4$ and $SrMoO_4$ phosphors

Vaibhav Chauhan[1], Prashant Dixit[1], Satyam Chaturvedi and Praveen C. Pandey, Department of Physics, Indian Institute of Technology (Banaras Hindu University), Varanasi–221005, (U.P.) India, *Email: pcpandey.app@iitbhu.ac.in (Praveen C Pandey),*

Herein, we examine the effect of A site cation on the temperature sensing property of Dy^{3+} doped $AMoO_4$ (A=Caand Sr)phosphors. The photoluminescence analysis of the two phosphors manifests that the emission andexcitation intensity is maximum for Dy^{3+} doped $CaMoO_4$. The temperature-dependent PL (TDPL) spectra are studied and two thermally-coupled peaks of Dy^{3+}, show contrasting responses with rising temperature. The ratio of emission intensity ofthese two peaks is used to develop a temperature-sensing design. The relative sensitivity for the Dy^{3+} doped$AMoO_4$ (A=Ca and Sr) phosphors was 0.66% K^{-1} and 1.02% K^{-1}, respectively. With good relative sensitivityvalue, the prepared phosphors have potential value in being utilized for optical thermometers.

CP-09-32

Rare-earth Ions Doped UpconversionNano-phosphors: Preparation and Their Newer Applications

K. Kumar, Department of Physics, IIT(ISM), Dhanbad-826004, Email: kkumar@iitism.ac.in

The rare earth doped nanomaterials have also shown some interesting properties despite the atomic transitions of RE ions and thus opened possibilities of newer applications. Triply ionized rare earth ions doped upconverting nanoparticles have been successfully synthesized via chemical preparation routes. For upconversionnano-phosphor, only few efficient upconversion emission phosphors have been produced due to the limited number of sensitizers (Yb^{3+}) and activators like Er^{3+}, Ho^{3+} and Tm^{3+} ions, and thus the application is focused on such rare earth ions doped phosphors. Here temperature sensing and fingerprint detection using the upconversion luminescence of nano-phosphors is discussed.

CP-09-33

Up-conversion luminescence and temperature sensing properties of Mg^{2+} co-doped $YMoO_4$: Er^{3+}/Yb^{3+} nanophosphor

*Shriya Sinha**[1,2] and Kaushal Kumar[1], [1]Optical Materials & Bio-imaging Research Laboratory, Department of Applied Physics, Indian Institute of Technology (Indian School of Mines) Dhanbad-826004, India, [2]Department of Physics, Govt. P.G. College, Jhabua, Madhya Pradesh – 457661, India, *Email: shriya.sinha6@gmail.com*

In this work, Mg^{2+} ion enhanced up-conversion emission of $YMoO_4$ Er^{3+}/Yb^{3+} nanophosphor was prepared via a hydrothermal method. The co-doping of Mg^{2+} ions into $YMoO_4$:Er^{3+}/Yb^{3+} has shown significant enhancement in the green (530 nm and 552 nm) and red (656 nm) up-conversion emission bands upon laser excitation at 980 nm. The optimized materials were further investigated to study the temperature sensing behavior using the fluorescence intensity ratio (FIR) technique from the two thermally coupled energy levels ($^2H_{11/2}$ and $^4S_{3/2}$) of Er^{3+} ions. The obtained results indicate the use of Mg^{2+} co-doped $YMoO_4$:Er^{3+}/Yb^{3+} phosphor in temperature sensing application.

Category - 10
Lasers in Chemistry, Biology and Medicine

CP-10-01

Raman spectroscopic study for monitoring spoilage of milk

Anita Dalal[1,2], Amrita Srivastava[1,2], Jyoti Kumawat[1], H. Krishna[1] and S. K. Majumder[1,2]*
[1]Laser Biomedical Applications Division, Raja Ramanna Centre for Advanced Technology, Indore-452013 [2]Homi Bhabha National Institute (HBNI), Training School Complex, Anushakti nagar, Mumbai-400 094 [*]Email: shkm@rrcat.gov.in

We report here the results of an exploratory study carried out to monitor time dependent spoilage of milk using Raman spectroscopic technique. Milk sample was kept in an incubator at constant temperature of 27 °C and after every 4 hours, 3.5 ml sample was drawn into a cuvette to perform the Raman measurement and pH measurements were also carried out simultaneously. Over the period of 32 hours of experimentation, the pH of the milk was found to change from 6.5 to 4.2, indicating lactic acid and acetic acid formation. An increase in the 868 cm^{-1} Raman band was observed because of the fermentation by products of lactose, this also corroborates with the results obtained from the pH measurements. Also, Raman bands that can be assigned to lipids and proteins at 1260, 1300 and 1440 cm^{-1} were found to decrease with the increase in the duration of the incubation of milk samples. Thus, results of the study show that Raman spectroscopy has potential for the detection of milk spoilage in real time.

CP-10-02

Raman spectroscopy based monitoring of storage related rancidity in mustard oil

A. Srivastava[1,2], A. Dalal[1,2], R. Shrivastava[1,2], J. Kumawat[1], H. Krishna[1] and S. K. Majumder[1,2][1]Raja Ramanna Centre for Advanced Technology, Indore 452013, India [2]Homi Bhabha National Institute, Mumbai 400094, India, Email:amrita@rrcat.gov.in

The results of a feasibility study on Raman spectroscopy-based detection of physiochemical changes in mustard oil over a period of one year when kept in three different containers viz., steel, glass and plastic are presented. Home-built Raman spectroscopy set up with excitation at 532 nm was used to measure Raman spectra of mustard oil from three different samples available in the local market of Indore. The study shows that the beta carotene present in the oil decreases with time which is attributed to the formation of oxidation products in the oil during storage. It has also been observed that the oil gets more rancid when kept in a plastic rather than in a steel or a glass container.

CP-10-03

Surface Enhanced Raman Scattering Detection of Se (IV) Ions in the Aqueous Medium by Ninhydrin-Coated Silver Nanoparticles

Sweta Sharma[a b], Aparna Tiwari[b], Aarti Jaiswal[c], and K. N. Uttam[d] [a]Department of Environmental Sciences, Dr. Harisingh Gour Vishwavidyalya, Sagar [b]Saha's Spectroscopy Laboratory, Department of Physics, University of Allahabad, Prayagraj [c]Centre for Material Science, IIDS, University of Allahabad, Prayagraj Email: swetasharma3989@gmail.com

The present study exploits the potential of ninhydrin coated silver nanoparticles (N-AgNPs) synthesized by chemical reduction method for the selective and sensitive detection of Se (IV) ions using surface enhanced Raman scattering. For this, the N-AgNPs have been synthesized by chemical reduction method and used as prepared. The characterization revealed that the nanoparticles were of 10-20 nm size range and coated by ninhydrin molecules. The synthesized nanoparticles were used to detect the Raman signals of the Se (IV) ions in the aqueous media excited by 785 nm laser. The water samples spiked by Se(IV) ions upon the addition of N-AgNPs leads to the development of characteristic peaks at 200, 448, 697 and 777 cm^{-1} whose intensity increases dramatically with increasing concentration of Se (IV) from 3 mM to 90 mM in the medium. The Se(IV) ions leads to the aggregation of the nanoparticles thereby creating hotspots which results in the development of unique spectral profile with enhanced signals.

CP-10-04

Band-target entropy minimization (BTEM) for spectral unmixing of Raman spectra measured from a layered turbid media

Khan Mohammad Khan[1], Hemant Krishna[1] and Shovan Kumar Majumder[1,2] [1]Laser Biomedical Applications Division, Raja Ramanna Centre for Advanced Technology, Indore 452013 [2]Homi Bhabha National Institute, Mumbai 400094 Email: khanmdkhan@rrcat.gov.in*

Depth-sensitive Raman spectroscopy has drawn substantial attention in recent years as a promising novel tool for disintegrating molecular makeup of different layers of a layered turbid medium. However, one limitation noted is that the Raman spectrum measured from a particular depth does not have all its Raman characteristics belonging to that layer. Computational approaches are required to get the pure Raman spectrum from the set of the measured Raman spectra. We report, development and use of a Band-Target Entropy Minimization (BTEM) code for obtaining pure Raman spectra of polystyrene and Teflon from a set of Raman spectra measured from a two-layered non-biological phantom using confocal Raman spectroscopy (CRS). It was found that all the relevant Raman characteristics observed in the deconvoluted spectra have a very good match ($R^2 = 0.98$) with those found in the reference Raman spectra of the authentic polystyrene and Teflon constituting the layers of the phantom. The reasonable matching of the estimated ratios of intensities of the prominent Raman peaks of polystyrene at 995 and 1598 cm^{-1} (i.e. I_{995}/I_{1598})

and of Teflon at 730 and 1375 cm^{-1} (i.e. I_{730}/I_{1375}) with those found in their reference Raman spectra further supported the findings.

CP-10-05

Design and Development of Autofluorescence Tools for Early detection of Tissue Abnormalities

Ajeetkumar Patil, Department of Atomic and Molecular Physics, Manipal Academy of Higher Education(MAHE), Manipal, India, Email : ajeetkumar.p@manipal.edu

Biophotonics tools offer noninvasive and easily applicable tools for the detection of alternations in structural and biochemical compositions of tissues and cells, which may indicate the presence of disease. The present work discusses about developing reliable, sensitive and objective biophotonics tools for various biomedical applications. Our methods have the added advantage of being label-free, objective because of the fact that diagnostic evaluation is by statistical methods, eliminating errors from lack of experience, fatigue factor, and subjectivity in the decision making.

CP-10-06

Biochemical Investigation of the Verbena Flower by Laser Raman Spectroscopy

Rahul Uttam[1], Aishwary Awasthi[2] and AS Achalkumar[3], [1, 3]Department of Chemistry, IIT, Gawahati, [2]Department of Physics, University of Allahabad, Prayagraj Email: ruttam95@gmail.com

In the present work, the applicability of confocal micro-Raman spectroscopy has been examined for the investigation of biochemical present in the different variety of verbena flower, non-destructively, noninvasively, ecofriendly, extraction free, simultaneous detection of multi-compounds in a rapid manner. For this, the Raman spectra of the five different variety of verbena flowers have been acquired in the spectral region <2000 cm^{-1}. The analysis of the acquired spectra depicts the occurrence of the flavonoids, carbohydrates, polysaccharides, aliphatic, carotenoids, phenols and anthocyanins with varying amount in different variety flower. The study shows that the verbena flowers are the rich source of bioactive compounds that are useful for the health sectors and Raman spectroscopy can be used for the shorting and grading of the flowers.

CP-10-07

Investigation on LaF_3 based nanophosphor for Bioimaging Application

Pratik Deshmukh[a, b], Bhumika Sharma[a],S Chakraborty[a], K Sahu[a, b] , S. Satapathy[a, b*], S. K. Majumder[a, b] [a] Functional Bio-Materials Lab., Laser Biomedical Application Division, Raja Ramanna Centre for Advanced Technology, Indore, India - 452013 [b]Homi Bhabha National Institute, Anushaktinagar, Mumbai,Maharashtra, India - 400 094,.*

*Email: ppdeshmukh@rrcat.gov.in; srinu73@rrcat.gov.in

In-vivo fluorescence imaging contrast agent relies on its ability to absorb within the biological window (900–1200 nm), reducing autofluorescence and enhancing tissue penetration. The potential of upconversion nanoparticles is that it can be used to absorb in above mentioned optical range and emits in visible which is required for imaging of biological samples. Hence, human serum albumin-coated Er^{3+},Yb^{3+}-doped LaF_3 nanohybrids (around 20-30 nm in diameter) of spherical morphology were synthesized. The spectroscopic analysis revealed distinct emission peaks in the visible spectrum (e.g., at ~540 and 660 nm), attributed to specific transitions in Er^{3+} under 976 nm excitation, facilitated through Yb^{3+} absorption. Their suitability for cellular imaging was evaluated by testing its toxicity on HeLa cells and its dispersibility in Dulbecco's Modified Eagle Medium (DMEM). These findings collectively highlight the biocompatibility and potential of these nanoparticles as contrast agents in various biomedical imaging applications. The in-vitro imaging of nanohybrid loaded HeLa cells were carried out using Confocal microscope.

CP-10-08

Photoluminescence studies on*Azadirachta indica (AI)* leafextract coated ZnO-*AI* nanocore-shell particles for antibacterial applications

Bhumika Sharma[1],Pratik Deshmukh,[1] Sourabrata Chakraborty,[1] Khageswar Sahu,[1,2] Srinibas Satapathy*[1, 2] and Shovan Kumar Majumder [1, 2 1]Functional Biomaterials Lab, Laser Biomedical Applications Division, Raja Ramanna Centre for Advanced Technology, Indore 452013, Madhya Pradesh, India [2]Homi Bhabha National Institute, Training School Complex, Anushakti Nagar, Mumbai, Maharashtra, India. *Email: sbhumika@rrcat.gov.in, srinu73@rrcat.gov.in*

The increasing challenge of microbial resistance to conventional antibiotics necessitates urgent exploration of novel and effective antibacterial agents. An innovative approach involves combining plant extract with nanoparticles which may lead to novel ways of treating infections. This study focuses on fabrication of Zinc Oxide nanoparticles(ZnO NPs)/*Azadirachta indica (AI)*core-shell structure and its potential applicability as an antibacterial agent. ZnO NPs were synthesized by precipitation method and subsequently coated with *AI* leaf extract to produce ZnO-*AI* nanocore-shell structures. The structural and morphological characterization includes x-ray diffraction and field emission scanning electron microscopy, respectively.Photoluminescence spectroscopy was carried outto investigate the formation of ZnO-*AI* nanocore-shell structures. Antibacterial efficacy against Methicillin-Resistant *Staphylococcus aureus* (MRSA) was evaluated through a zone of inhibition assay. The results showed a ZnO-*AI* nanocore-shell concentration-dependent increase in the diameter of the inhibition zone, which confirmsits superior antibacterial properties.

CP-10-09

Investigations on effect of red-light exposure on adipose derived mesenchymal stem cells

Mahima Rastogi[1,2], Sourabrata Chakraborty[1],Khageswar Sahu[1,2*]and Shovan Kumar Majumder[1,2], [1]Laser Biomedical Applications Division, Raja Ramanna Centre for Advanced Technology, Indore 452013, [2] Homi Bhabha National Institute (HBNI), Training School Complex, Anushakti Nagar, Mumbai-400 094. [*]Email: mahima@rrcat.gov.in, khageswar@rrcat.gov.in*

Photobiomodulation (PBM) is an emerging treatment modality based on the application of light to promote tissue repair and stimulate cells. Stem cell priming with visible light is gradually gaining importance. However, the exact mechanism behind light mediated activation of stem cells is not clearly understood. In this study, we report the effect of red light exposure on cell proliferation, cytoskeleton remodeling and migration potential of human adipose derived mesenchymal stem cells. Stems cells were exposed to different red light fluence,~3/6/9/15 J/cm^2 followed by tetrazolium reduction assay, confocal microscopic evaluation of actin stained cells and scratch wound assay. Stem cells irradiated with ~15 J/cm^{2}showed increased cell proliferation in comparison to other irradiated and un-irradiated groups. However, we did not observe significance difference among the remaining light exposed groups.Confocal microscopic analysis suggestshighest densification of actin in cells exposed to red light fluence of ~15 J/cm^2, as compared to all other light irradiated groups. The percent scratch wound closure, with respect to initial time point, in un-irradiated control, ~3,6,9 and 15 J/cm^2 red light exposure groups were ~ 45,60,73, 75,and 90 %, respectively. Taken together, these results indicate a potential role of PBM in modulating cytoskeleton of stem cells. The details of this work will be presented.

CP-10-10

Investigation on the effect of antimicrobial photodynamic therapy combined with probiotics on methicilin resistant *Staphylococcus aureus*

Sai Sarbani Mund[1,2], Sourabrata Chakraborty[1], Khageswar Sahu[1,2], and Shovan Kumar Majumder[1,2*] [1]Laser Biomedical Applications Division, Raja Ramanna Centre for Advanced Technology, Indore-452013 [2]Homi Bhabha National Institute (HBNI), Training School Complex, Anushakti Nagar, Mumbai-400094 [*]Email: khageswar@rrcat.gov.in, shkm@rrcat.gov.in*

In view of the rapid emergence of multidrug resistant microbes worldwide, antimicrobial photodynamic therapy (aPDT) and Probiotics hold considerable promise as alternate therapeutic modalities. However, single treatment of either Probiotics or aPDT may suffer from obstacles in effective management of biofilm-associated infections. In this study, the antimicrobial activity of Methylene blue (MB) mediated antimicrobial photodynamic therapy (aPDT) combined with cell-free supernatants (CFS) derived from *Lactobacillus*

acidophilus (LA) on methicilin resistant *Staphylococcus aureus* (MRSA) was investigated. For investigating the combined action aPDT and Probiotics, MB treated MRSA suspension were exposed to different red light (~660 nm) fluence followed by incubation with 20/40 % probiotic cell free supernatant (CFS) for 2 h. Colony forming unit assay and flow cytometric analysis were performed for monitoring loss of cell survival and membrane integrity, respectively. The results show that percent survival loss obtained in aPDT alone, CFS alone and aPDT + CFS groups are ~90 %, ~95 % and ~99.99%, respectively. Flow cytometry data also show that compared to aPDT or CFS alone, combined treatments elicit significantly higher membrane damage in MRSA. Taken together these results indicate the additive action of the combined treatment modality on MRSA. The details of these results will be presented

CP-10-11

Assessing the influence of buffer on protein topology by Light Emitting Diode-induced autofluorescence

B Shaik, CM Darshan, R Jackson, C Subhash, K Ameera, B Shimul, KK Mahato[*] Department of Biophysics, Manipal School of Life Sciences, Manipal Academy of Higher Education, Karnataka, Manipal 576104, India. [*]Email: mahato.kk@manipal.edu, kkmahato@gmail.com

Current study reports the effect of different buffers on the structural alterations of Fibrinogen and Human Serum Albumin (HSA), using Light Emitting Diode (LED)-induced autofluorescence (LED-IAF). In order to record the autofluorescence spectra of the proteins in different buffer conditions, 285 nm LED was used and the structural variations induced were further confirmed using ThT assay.

CP-10-12

Comparison of Indocyanine Green Fluorescence Guided verses Fluorescein Sodium based Sentinel Lymph Node Biopsy in the Patients with Breast Cancer

D. Qaiser[*], P. Ranjan, A. Srivastava Department of Surgical Disciplines AIIMS New Delhi-110029. [*]Email : qaiser.d@gmail.com

Assessment of lymph node in the breast cancer patients is of prime significance for staging and treatment plan. All enlarge lymphnodes are not metastatic. Sentinel lymph node biopsy is recommended for negative axilla patients. But there is no standard guideline available for patients having enlarge axillary lymphnode. **Aim:** To identify the metastatic lymph node using dual tracer. **Methodology:** The present study is a randomized controlled trial and was conducted at AIIMS New Delhi on 20 operable breast cancer patients after written consent. The patients are divided in two groups A & B. In Group A, Patients were enrolled for Indocyanine green dye and in group B patients were enroll for fluorescein dye. Results:

Identification rate for metastasis in case of group A is 100% where as in case of group B it is found to be 80%. **Conclusion:** Based on the interim results of this randomized controlled study, the single dye technique using Indocyanine green seems to be non-inferior to the Fluorescein. This would be of particular importance for use in developing countries with limited nuclear medicine facilities. . Besides time saving and non-toxic, this technique predicts the metastatic status of axillary lymph node during surgery, aiding appropriate surgical intervention.

CP-10-13

Pulsed Laser Deposition of Zirconia Thin film on Titanium Bio-alloy to Improve Hemocompatibility: An Effect of Substrate Temperature

Prabha S[1], Sunita Kedia[1,2], J. Padma Nilaya[1,2] [1]Laser & Plasma Technology Division, Bhabha Atomic Research Centre, Mumbai, 400085, India [2]Homi Bhabha National Institute, Anushaktinagar, Mumbai - 400094, India [*]Email:prabhas@barc.gov.in*

Titanium alloy-Ti6Al4V has been recognized as the best suitable biomaterial for dental, orthopedic and load-bearing applications owing to its prominent mechanical strength, biocompatibility, high elastic modulus, low density, nontoxicity, and higher corrosion resistance. Functional coating is an effective technique to improve *in-vitro* and *in-vivo* activities of these biomaterials. We present here the experimental results of the effect of pulsed laser deposition (PLD) of zirconia (ZrO_2) film on Ti6Al4V biomaterial at elevated substrate temperatures ranging from Room temperature (RT) to 800°C on its morphology, structuraland hemocompatibility. The hemocompatibility test was evaluated on the basis of human whole blood adsorption and distribution of red blood cells (RBC) on the samples. The results were revealed that an improvement of film quality with increased substrate temperature. We have observed improved hemocompatibility with 4.5 times increased RBC counts in case of samples coated at 800°C substrate temperature as compared to the pristine. This shows that PLD coating at high substrate temperature may be a promising approach to prevent several post implantation issues.

CP-10-14

Generation of Periodic Cone Structures on Bio-alloy by Picosecond Laser Irradiation: Topography and Structural Analysis

Prabha S[1], Sunita Kedia[1,2], and J. Padma Nilaya[1,2] [1]Laser & Plasma Technology Division, Bhabha Atomic Research Centre, Mumbai, 400085, India [2]Homi Bhabha National Institute, Anushaktinagar, Mumbai - 400094, India [*]Email: prabhas@barc.gov.in*

Titanium is an extensively studied and used biomaterial for implant applications. Notably, Ti6Al4V is one of the titanium alloys widely used for dental and orthopedic applications due to its outstanding properties such as biocompatibility, high strength and corrosion resistance. However, it has low bioactivity that can be improved by surface modification.

In particular, surface texturing enhances their *in-vitro* as well as *in vivo* performances. Laser surface texturing (LST) is now being widely used by researchers as it is highly efficient, environment-friendly, and accurate with excellent controllability. Microstructures obtained by LST have more effective surface properties with enhanced biological activity. It also induces cell growth through increased possibility of intercellular signaling.The present work, the experiment was carried out at fixed laser power at different scanning speeds (800, 400, 200 and 100 µm/sec) for the formation of various sizes of cone structures over the surface of Ti6Al4V substrate. The morphology results were showed that as more pulse overlapping with lower scanning speed increased length and base width of the cone microstructure. The wettability results of LST samples confirm their higher surface energy and hydrophilic nature. These properties point to the possibility of greater applicability of LST biomaterial substrates for implant application.

CP-10-15

Spectroscopic Insights into Arsenic Detoxification Mechanisms: A Focus on QYMF-ArsD Protein

Upendra Nayek, Suresh K, Sajan Daniel George, Abdul Ajees Abdul Salam Department of Atomic and Molecular Physics, Manipal Academy of Higher Education, Manipal, Karnataka 576 104, India. *Email: abdul.ajees@manipal.edu;*

Arsenic, a hazardous metalloid, has been extensively researched for its impact on human health.The ars operon of *E. coli* plasmid R773 is well-known, consisting of vital genes *arsD* and *arsA*. ArsA acts as an ATPase, while ArsD plays a crucial role as an arsenic metallochaperone for ArsA. ArsD, with its 120 amino acids, facilitates the transfer of As(III) to ArsA, enhancing ArsA's affinity for As(III). Notably, R773-ArsD contains six cysteine residues, with cys12-cys-13-cys18 forming a binding site with a tri-sulfate coordination for As(III).In a relatively less-explored context, the *Alkaliphilus metalliredigens* QYMF features an *ars* operon with QYMF-ArsD as a distinct component comprising 99 amino acids and three conserved cysteine residues. This study aimed to comprehensively examine the arsenic binding mechanisms of QYMF-ArsD. Native and cysteine mutant QYMF-ArsD proteins were cloned, expressed, and purified for detailed investigation. The metallochaperone function of these purified proteins was studied using Raman spectroscopy.The spectroscopic analyses revealed noticeable differences in QYMF-ArsD's response to As(III) and As(V). Particularly, the presence of As(III) led to significant spectral changes that differed from its behavior in the presence of As(V). This intriguing observation underscores QYMF-ArsD's strong affinity for As(III) binding and its comparatively weaker inclination for As(V) binding. The intricate coordination of cysteine residues and the clear preference for As(III) binding provide insights into the mechanisms governing QYMF-ArsD's behavior.This study not only advances our understanding of arsenic interactions but also highlights the effectiveness of multifaceted spectroscopic analyses in unraveling complex biomolecular interactions.

CP-10-16

A simulation study to investigate the effect of variation of blood-suspending medium on the photoacoustic signal

Subhadip Paul[1], Hari Shankar Patel[2], Ratan K Saha[1] [1]Department of Applied Sciences, Indian Institute of Information Technology Allahabad, Prayagraj, 211015,India [2]Laser Biomedical Applications Division, Raja Ramanna Centre for Advanced Technology, Indore, 452013, India, Email: rss2021008@iiita.ac.in, harish@rrcat.gov.in, ratank.saha@iiita.ac.in

The study of blood has been a subject of great interest for decades in understanding human physiology. The optical properties [absorption coefficient (μ_a), scattering coefficient (μ_s), and anisotropy coefficient (g)] of blood play key role in generation and determining the strengths of photoacoustic (PA) waves. Red blood cells (RBCs) are the dominating PA sources in blood and the magnitudes of these optical parameters depend on the medium in which RBCs are suspended. Two types of media [phosphate buffer saline (PBS) and blood plasma (PLS)] have been investigated hereinfor excitation wavelengths involving 480, 650, and 1050 nm and for five different hematocrit levels, Hct=10- 45%. The distinguishability of the PA response lines for PBS and PLS media is much more prominent ($\approx$17% at Hct=45%) at 650 nm than those of 480 and 1050 nm. The reason might be the variation of g factor ($\approx$0.8%) between two types of samples at 650 nm, whereas g almost remains the same at other wavelengths. Our study might be helpful in understanding the effect of the blood-suspending medium on PA signal properties at multiple optical wavelengths.

CP-10-17

Observation of patterns in laser light coupled dye-doped soap film

Sheetal Lalji Yadav[1], Rodney Bernard[2], Kiran Kolwankar[1], and Aditya K Dharmadhikari[2],[1]Department of Physics,Ramniranjan Jhunjhunwala College, [2]Department of Nuclear and Atomic Physics, Tata Institute of Fundamental Research, Mumbai. 400005, India, Email: sheetalyadav1@gmail.com

We report on the coupling of laser light into a planar dye-doped soap thin film. The thickness of soap film is not constant and is a function of both location and time. The soap film shows different light colour when illuminated with white light as a function of time. Eventually before rupture we observe a broad black region. The evolution of the soap film is osberved for three different conditions, liquid soap in deionized water, tap water and deionized water added with glycerine.The laser light of wavelength 532 nm is focused (using a 25 x 0.45 NA microscope objective) inside an optical fiber. The light from the fiber is then coupled into the thin soap film. The observed patterns show intense light channels that break into smaller channels as the light propagates.

CP-10-18

Confocal Micro Raman Spectroscopy Characterization of Pollen Grains of *Hibiscus* Flower

Chhavi Baran[1], Renu Singh[2], Shristi Sharma[2] and K.N.Uttam[2] [1]Chhavi Baran, Centre of Environmental Science, IIDS, University of Allahabad, Prayagraj [2]Saha's Spectroscopy Laboratory, Department of Physics, University of Allahabad, Prayagraj Email: rs2780@rediffmail.com; kailash.uttam@rediffmail.com

Hibiscus plant is often used in the traditional medicine being rich in phytochemicals like polyphenols especially anthocyanins, polysaccharides and organic acids thus having enormous prospective in modern therapeutic uses. Analysis of pollen grains yields valuable information on biology, ecology, forensics, climate change, insect migration, food sources and aeroallergens. Therefore, it is important to explore biochemical present in the different colour flower pollen grains. Raman spectroscopy offer chemical characterization of pollen via identifiable spectral features without any sample pretreatment. Therefore this study explores the utility of nondestructive Raman spectroscopy technique for the composition of biochemicals and monitoring bioprocess in the pollen grains of hibiscus flowers. The Raman spectra of the different colour *Hibiscus* flower have been acquired in the spectral region <2000 cm^{-1} by exciting 785 nm diode laser. The analysis of the procured spectra reveals the presence of proteins, carbohydrates, carotenoids and sporopollenins of varying concentrations have been identified with varying amount in the different colour flowers. The findings shows that the confocal micro Raman spectroscopy techniques as a nondestructive, noninvasive, cost-effective, eco-friendly, rapid, sensitive, extraction, and chemical free economical technique for the assessment of biochemicals present in the pollen grains.

CP-10-19

Development of a fluorescence imaging system capable of hyperspectral and multi-wavelength time-lapse imaging for tissue analysis

Siddharth Pal[1,2], Hemant Krishna[2] and Shovan K. Majumder[1,2] [1]Homi Bhabha National Institute, Mumbai, [2]Raja Ramanna Centre for Advanced Technology, Indore, Email: palsiddarth2000@gmail.com

A liquid crystal tunable filter (LCTF) based dual-mode fluorescence imaging system was developed. The system is equipped with a graphical user interface (GUI) for automated acquisition of full sequence of hyperspectral images (spectral scanning mode) and multi-wavelength time-lapse images (temporal scanning mode) from the biological tissue. The GUI provides synchronized control of the electronically tunable band-pass filter (i.e., LCTF) and the CCD camera for acquisition of the spectral images for both the scanning modes. To enhance the usability of the system for tissue analysis, the GUI is integrated with mathematical and statistical tools to provide fluorescence spectral profile and photobleaching rate at pixel level. The availability of photobleaching characteristics, in addition to fluorescence profiles, at every pixel on the tissue surface can help obtain a

comprehensive snapshot of the spatial extent of disease. The system is validated by recording the images from pathologically certified tissue blocks to highlight the differences between biochemical/ morphological make-up. The details of these results will be presented.

CP-10-20

Photo-induced calcium influx under various irradiation conditions through channelrhodopsin-2 in mice pancreatic ß cells

Nidhi Maharwal[1, 2], Rashmi Shrivastava[1,2] and Shovan K Majumder[1, 2*, 1] Laser Biomedical Applications Division, Raja Ramanna Centre for Advanced Technology, Indore -452013, [2] Homi Bhabha National Institute, Anushakti Nagar, Mumbai - 400094 [*]Email: rshrivastava@rrcat.gov.in, shkm@ rrcat.gov.in*

Calcium is a significant intracellular secondary messenger, regulating numerous signaling pathways. One of its important roles is in insulin secretion from pancreatic ß cells. Here we have modified pancreatic ß cells to express light gated cation channel rhodopsin (ChR2) from *Chlamydomonas reinhardtii*. The photo induced calcium influx in modified pancreatic β cells was investigated under different irradiation conditions. It was observed that increasing power density resulted in increased ca influx. And intermittent irradiation was found to result in increased Ca^{2+} influx with respect to the continuous irradiation for long periods of 2 and 5s. Maximum influx was observed for 1s continuous irradiation under all studied power densities.

CP-10-21

Preliminary Studies on SERS by DNA Origami based Assembly of Gold Nanoparticles

P. Dangi[1.2], R. Shrivastava[1.2], C. Mukherjee[2.3], A. Srivastava[1.2], and S. K. Majumder[1.2 1] Laser Biomedical Application Division, Raja Ramanna Centre for Advanced Technology, Indore-452013 [2]Homi Bhabha National Institute (HBNI), Anushakti nagar, Mumbai-400094 [3]High Energy Lasers and Optics Section, Raja Ramanna Centre for Advanced Technology, Indore-452013 Email: *rshrivastava@rrcat.gov.in*

Specific patterning of nanoparticles for various photonic applications, mostly surface enhanced Raman spectroscopy (SERS) is increasingly gaining attention for the development of novel ways to achieve efficient signal enhancement. Recently there is interest in using DNA origami structures for patterning of nanoparticles. The precisely engineered DNA origami has potential to serve as a template for arranging nanoparticles in specific configuration generating hot spots and thereby enhancing the Raman signals of molecules attached to or near the nanostructured surface. In this work, we demonstrate arrangement of gold nanoparticles on designed and synthesized rectangular DNA origami templates to achieve Raman signal enhancement of Rhodamine 6G (R6G). The results showed that the characteristic peaks of R6G at1300cm^{-1} and 1502cm^{-1} are significantly enhanced. The enhancement factor achieved was 1.7. The details of these results will be presented.

Category - 11
Laser based Instrumentation

CP-11-01

A multi-point distributed FBGs Interrogation System fortemperature measurement

Vinay Kumar Dubey, P. Saxena, Sandeep Talwar[1],Inderjeet Singh, Avinash Singh,Jitendra Kumar[2] Om Prakash[2], Rajesh Arya,S.K. Dixit[3] and S.V. Nakhe[4] LTD, [1]LCID, [2]FSOSS, [3]LG, [4] RRCAT, Indore (M.P.) 452013, Email: vkd@rrcat.gov.in

In recent time, Fiber Braggs Gratings (FBGs) based sensing is getting popularity over electrical counterparts because of their unique properties such as absolute measurement, electrically passiveness, light weight, radiation hardened and ideal for distributed sensing etc. Physical parameters like temperature or strain are measured in term of shift in wavelength. Quantifying wavelength shift with pico-meter resolution in distributed sensing is quite challenging task and also un-economic. A prototype FBG interrogator consist of super luminescent diode (SLD) based broad-band source (BBS), electrically tunable Fabry-Perot (FP) filter, sensitive photo-diode detector and ARM controller-baseddata acquisition system is developed. Tuning coefficient of filter is ~ 5.7 pm/mV. Wavelength interrogation is experimentally demonstrated using convolution of filter pass band and reflected spectra of multipoint FBG on test bench with nine-point FBGs distributed sensor by using adjustable temperature setup.

CP-11-02

Thin glass plates based white-light ronchigrams for measurement of optical aberrations and distances with micron accuracy for tiling of optical surfaces;

A. K. Sharma, High Energy Laser and Optics Section, RRCAT, Indore, India; Email:aksharma@rrcat.gov.in;

In this paper, I present white light ronchigrams generated using single/ multiple thin glass plates to act as shadow generator for estimation of linear and angular movements required for coherent tiling of optical assembalies, in particular, with micron level accuracies in a simple non-interferometric optical setup. Both incoherent visible coloured/ white light from light emitting diodes and coherent light from He-Ne laser has been used to create shadow owing to thin glass plates kept in different planes in on- and off-axis optical geometries for isolated enhanced accuracies for various movements in a single lens imaging system. Results are also compared with low coherence scanning interferometry.

CP-11-03

Theoretical Analysis of the Message Quality in a Multimode diode Laser based Secure Optical Communication System

*Neethu. K[†] and S. Sivaprakasam[*] Department of Physics, Pondicherry University, Pondicherry – 605014 *Email: siva@pondiuni.ac.in, †neethu@pondiuni.ac.in*

High-quality message recovery is the key to secure optical communication, and it is validated from time to time. Optical communication using multimode semiconductor lasers as transmitter and receiver system is investigated. Two types of coupling of modes were considered: one is global coupling, where the output of transmitter modes is coupled to the corresponding receiver modes, and the second is cross-modal coupling, in which we introduced a detuning equivalent to the frequency spacing of modes. The effect of the transmission coefficient on the quality of the message transmitted is being studied. A good quality message is recovered in the first case, whereas in the second coupling scheme exhibits a neutral behavior in message recovery quality.

CP-11-04

Development of FBG based multi-point sensor system for temperature profile monitoring of Pinger magnet ceramic chambers of Indus-2,

*J. Kumar[*1], M. K. Saxena[1], K.V. A. N. P. S. Kumar[2], B. K. Sindal[2], V. K. Srivastava[1], S. Kumar[1], R. Mahakud[1], D. P. Yadav[2], O. Prakash[1,5], S. K. Dixit[3,5], S. V. Nakhe[4], [1]Fiber Sensors and Optical Spectroscopy Section, [3]Ultra High Vacuum Technology Section, [3]Laser Group, [4]Material Science and Advanced Technology Group, Raja Ramanna Centre for Advanced Technology, Indore, [5]Homi Bhabha National Institute, Mumbai, [*]Email: jkmadaan@rrcat.gov.in*

This paper presents the development and deployment of multi-point fiber Bragg Grating sensor for temperature profile measurement of alumina ceramic vacuum chamber of Pinger magnet of synchrotron radiation source Indus-2. For this purpose, 14 FBGs at different Bragg wavelength were inscribed on a single fiber by second harmonic of copper vapour laser (CVL). This multi-point FBG sensor was installed to measure the temperature distribution along the alumina ceramic vacuum chamber wall of Pinger magnet. It was observed that the temperature of wall of ceramic chamber varied from 20 ^{o}C to 40 ^{o}C during the operation of Indus-2. This will be useful for early detection of electron beam mis-steering events followed by online temperature monitoring and optimization of electron beam alignment for reliable operation of Indus-2.

CP-11-05

Development of a novel laser-based technique for sag measurement of coolant channels of pressurized heavy water reactor during pre-service inspection.

Y. Pavan Kumar[1], Sanjiv K. Tiwari[1], Rishipal[1], Sarthak Gupta[1], Sarvendra Singh[1], Inderjeet Singh[1], G. Muralidharan[1], Rajiv Jain[1], Piyush Saxena[1], Viraj P. Bhanage[1], Rajesh*

Arya[1], D. N. Sanyal[2], N. S. Benerji[1], [1]Raja Ramanna Center for Advanced Technology, Indore, [2]Nuclear Power Corporation of India Ltd, Mumbai. Email: ypk@rrcat.gov.in

Pressure tubes (PTs) sag over time due to the weight of the fuel bundles, coolant and self-weight. Over sagging of PTs may hinder the free movement of fuel bundles. Hence, the sagging condition and sag profile of PT is required to be monitored periodically. We have developed a novel laser-based technique for sag measurement of coolant channels during pre-service inspection. The proposed technique is based on the height profiling method in which the PT is flooded with an expanded visible laser beam and an optically opaque probe with a small through hole at its center scans the entire length of the PT. The height variation of PT along its length varies the height of the output laser beam emerging from the probe and using software the laser spot height variations are converted to sag profile of PT. Sag profile measurement of PT mockup channel at KAPP 3&4 are presented.

CP-11-06

Role of Ge doping concentration in fiber core on the thermal behavior of type-I fiber Bragg gratings

V. K. Srivastava[1], J. Kumar[1], R. Mahakud[1], S. Kumar[1,2], P. K. Saini[1], G. Yadav[1], O. Prakash[1,2] [1]Fibre Grating Lab, Fibre Sensors and Optical Spectroscopy Section, Raja Ramanna Centre for Advanced Technology, Indore, [2]Homi Bhabha National Institute, Mumbai, *Email: jkmadaan@rrcat.gov.in*

In this paper the studies on thermal behaviour of type-I fiber Bragg grating for different Ge doping concentration of fiber core is carried out. The Ge concentration varied from 3 % for telecommunication fiber to 18 % for high photosensitive fiber. The FBG writing was carried out by high repetition rate (5.5 kHz) 255 nm UV beam generated from the second harmonic conversion of copper vapour laser (CVL). Growth of refractive index modulation during FBG fabrication in these fibers scales up with doping concentration. The thermal stability of the FBG fabricated in low Ge doping concentration was higher.

CP-11-07

Analysis and Fabrication of -phase-shifted long period fiber grating,

R. Mahakud, S. Kumar, J. Kumar, G. Yadav, O. Prakash, FSOSS, RRCAT, Indore, E.mail : rkmahakud@rrcat.gov.in

In this paper, transmission spectra of -phase phase-shifted long period fiber gratings were analysed theoretically. The results obtained from numerical analysis were verified experimentally by in-house writing of gratings in photosensitive fibers by point-by-point method.

CP-11-08

Fiber Bragg Grating Sensors for Healthcare Monitoring

Santosh JotiramJagatap, Vidyalankar Institute of Technology, Mumbai Email:

santosh.jagtap@vit.edu.in Dr. Ashok Jetawat, Pacific University of Higher Education, Udaipur, Rajashtan Email: drashokjain61@gmail.com Dr. Saurabh Mehta,Vidyalankar Institute of Technology,Mumbai, Email: saurabh.mehta@vit.edu.in

Emerging digital technologies are creating potential for healthcare systems around the world to enhance the quality of healthcare services. Although there has been significant progress in sensing mechanisms used for monitoring of healthcare parameters, more research innovation, dissemination, and technologies are needed to explore new opportunities and move towards healthcare 5.0 standard. Conventional electronic sensors have limitations due to their compactness, measurement accuracy and immunity to Electromagnetic Interference. The optical fiber sensors can provide better sensing solution to meet future healthcare standards.

CP-11-09

Development of Fiber Optic Distributed Vibration Sensor based on Phase-OTDR

Amit Sur, N R Singnurkar, Bhaskar Sharma, Varsha Kale, Pravin Mahajan and K D Joshi Applied Physics Division, Bhabha Atomic Research Center, Mumbai-400085, Email* : amitsur@barc.gov.in*

In present study, a fiber optic based fully distributed vibration sensor is demonstrated using phase sensitive optical time domain reflectrometry (OTDR). Heterodyne technique is used and interference fringe is formed by combining Rayleigh Back Scattering (RBS) light with local unshifted light. Both amplitude and phase is extracted from interference fringe based on I/Q demodulation.The vibration location is identified from amplitude data using moving differential and moving averaging algorithm. Further, phase of the demodulated signal is used for quantifying the vibration signal. The proposed algorithm is experimentally demonstrated using 5.06 km long single mode fiber (SMF) with varried spatial resolution from 10 m to 30 m. At a distance of 5.01 km a 5 m long section of fiber is wrapped on a 2 mm thick Al plate and a resistive strain gage is attached at the center of the plate. Al plate is tapped with hammer for creating disturbance and corresponding strain gage signal is used for synchronising and triggering the oscilloscope. The recorded fringe signal is analysed and vibration location is successfully identified.

CP-11-10

High precision local surface slope measurement using dual beam based low coherence interferometer

P. Sharma[1], M. Chaturvedi[1], K. K. Malakar[2], B. C. Pant[1], Y. Verma[1,2], S. Raja S.[1], [1]Advanced Electro-Optics Systems Section, RRCAT, Indore, [2] Homi Bhabha National Institute, Anushaktinagar, Mumbai, Email: pri786@gmail.com

Technologically advanced light sources such as synchrotron radiation sources and free electron lasers require optics with surface slopes of nano-radian level precision.Therefore, metrological systems that can provide surface slopes measurements with nano-radian

(nrad) level precision are required. In this paper we describe a dual beam based low coherence interferometer-based approach to measure the local surface slope of the sample with better than 100nrad resolution for a spatial separation of 3 mm. For proof of principle, the technique has been demonstrated in a test case where the mirror was tilted in small angular steps and corresponding optical path difference and slope values were calculated.

CP-11-11

Design and experimental demonstration of mode switching in few-mode fiber using all-fiber cantilever beam deflection configuration

I. Sharma[1], P. Roy Chaudhuri[1], [1]Department of Physics, Indian Institute of Technology Kharagpur, Kharagpur 721302, India, Email : soni1995sharma@gmail.com

We experimentally demonstrate the switching between different linearly polarized modes in a few-mode-fiber using an all-fiber cantilever beam deflection configuration. We performed the experiment with an optimized composition of cobalt-modified bismuth ferrite coated ($BiFe_{0.9}Co_{0.1}O_3$) on the selected length of fiber tip as a transducer. A theoretical platform is finally modelled to estimate the launching conditions corresponding to the excited mode.

CP-11-12

Detection of Ethanol in Ethanol Blended Petrol using high Sensitivity Tilted Fiber Bragg Grating Sensor

P. K. Saini[a,b,], G. S. Purbia[a], J. Kumar[a], O. Prakash[a,b], and S. V. Nakhe[c] [a]Fibre Sensors and Optical Spectroscopy Section, Raja Ramanna Centre for Advanced Technology, Indore 452013 [b]Homi Bhabha National Institute, Anushakti Nagar, Mumbai 400094 [c]Raja Ramanna Centre for Advanced Technology, Indore 452013 [*]Email: pankaj@rrcat.gov.in*

This paper presents the tilted fiber Bragg grating (TFBG) sensor for ethanol concentration measurement in ethanol blended petrol (EBP). Use of Bio-ethanol blended petrol has become essential worldwide due to concern towards environment and unsustainable use of petrol. TheTFBG sensor principle relies on the measurements of shift in cut-off mode spectral position to quantify the ethanol concentration. TFBG Cut-off mode being the highest order bound cladding mode have maximum evanescent field penetrationin the surrounding medium beyond cladding boundary and consequently offers largest sensitivity. The ethanol measurements are done in the wide concentration range of 0 – 100 % v/v. The minimum ethanol concentration of 0.1 % v/v in EBP is detected with the present sensor. The TFBG sensor shows excellent linearity with regression coefficient R^2 = 0.99949throughout the ethanol concentration measurement range. The observed sensitivity of the TFBG sensor is 251.52 ± 1.4 pm/% v/v of ethanol and the resolution is ~0.1 % v/v ethanol in EBP.

CP-11-13

Fabrication of cascaded turn around point long period fiber grating

S. Kumar[1,2], R. Mahakud[1], J. Kumar[1], V. K. Srivastava[1], O. Prakash[1,2], [1]Fiber Grating Lab, Fiber Sensors and Optical Spectroscopy Section, RRCAT, Indore, [2]Homi Bhabha National Institute, Anushaktinagar, Mumbai, Email: sudhir@rrcat.gov.in

In this work, cascaded turn around point long-period gratings (CTAP-LPG) were fabricatedin Ge-B co-doped fiber. The efficient fast writing was carried out by point by point method using frequency converted copper laser beam (CVL-UV). Cascading of two identical LPGs operating near turn around point resulted in multiple narrow transmission peaks in the band width of a turnaround point long-period gratings (TAP-LPG). The fabricated CTAP-LPG may be utilised in the development of high sensitivity refractive index (RI) and temperature sensor.

CP-11-14

Integration of All-Optical MOEMS Optical Coherence Tomography on a Chip

Lokendra Singh Chouhan, Ashish Singh Bais and Joseph Thomas Andrews[†] Applied Photonics Laboratory, Department of Applied Physics and Optoelectronics, Shri G. S. Institute of Technology and Science, 23 Park Road Indore, MP 452003 India. *Also at St. Paul HSS, Indore, MP 452001 India, Email: jtandrews@sgsits.ac.in*

Spectral domain optical coherence tomography works primarily on the dispersion and chirping of a broadband light source. We designed and fabricated a spectral delay line by combining a multimode interference coupler and a chirp Bragg grating. Using industry standard S1813 polymer, we integrated the optical components such as 3dB directional coupler, circulator, and spectral delay line generator. The simulation of all-optical devices is carried out with industry standard COMSOL Multiphysics. The masks are designed using open-source software. The photolitho process is completed the home made designed UV laser photolitho setup from Holmac. Low cost and sensitive devices of size 1cm 2cm are fabricated.

CP-11-15

Investigation on the Temperature-Sensing Capability of NiTiCu-Coated Optical Fiber for Cryogenic Environment

Navneet Chouhan[1], Nandini Patra[2], I. A. Palani[2] and Vipul Singh[1*] [1]Molecular and Nanoelectronics Research Group (MNRG), Department of Electrical Engineering, IIT Indore, [2]Opto-Mechatronics Lab, Department of Mechanical Engineering, Indian Institute of Technology Indore, India, Email : phd2201102019@iiti.ac.in*

In this work we have investigated the performance of the SMA-coated Single-Mode Optical Fiber for testing the cryogenic temperatures.The impact of SMA starins have been

studied on the light intensity under low temperatures.It has been observed that the coated fiber shows increased sensitivity towards low temperatures. We have obtained ~ 6.15 mV/°C sensitivity within tempratures ranging from 0 to -153 °C. The proposed sensor has the potential to monitor temperatures in the cryogenic range with good sensitivity without getting much degraded.

CP-11-16

Design and Development of Dichroic Beam Splitter for Common Apertures Laser Instruments

Anil Kumar, A. S. Upadhyay,SumanAwasthi and L M pant, Instruments Research & Development Establishment (IRDE), Dehradun, Email: asu.irde@gov.in

In the present course of work, we have developed a dichroic beam splitter for separating 1064nm Nd:YAG laser and 1571nm eye-safe laser for a common aperture laser instrument. This developed beam splitter includes ARC at 1064nm on one side of a fused silica glass plate and dichroic coating to reflect 1571nm and transmit 1064nm on the second surface of the sample. Dichroic coating was fabricated with 19 layers HfO2 and SiO2 stacks giving ~97% reflection at 1571nm while transmission archived at 1064nm is ~96%. The beam splitter have environmental stability as per MIL-C-48497.

Category - 12
Electronics, Instrumentation, Machine Learning & AI for Lasers

CP-12-01

Development of Microcontroller based Tool Controller Unit for In-Situ Laser Cutting of Recirculation Loop at TAPS-1 Reactor

Dhruvdeep Narwat, B. N Upadhyaya, P. Saxena, R. Arya, Laser Technology Division, RRCAT, Indore, Email : dnarwat@rrcat.gov.in

In this paper, work on development of a microcontroller-based tool controller unit for laser-based cutting system for removal of segments of large diameter and high thickness recirculation piping loop along with bevelling is presented. The tool controller developed, controls the motion precisely as required for cutting & bevelling and also facilitates adjustment, through a touch panel based user-friendly interface, of tool speed, direction, number of cutting rounds and tool overlap degree to accomplish the desired application. The tool controller has been successfully deployed for cutting of recirculation piping loop with thickness of about 30mm at TAPS-1 reactor.

CP-12-02

Laser Intensity Controller for Cold Atom Interferometry Experiments

Sasikumar K. K., Sajeevkumar A., Hriday Dath, Radhika V.N., Rekha.AR, Radhakrishna Pillai C., ISRO Inertial Systems Unit, Trivandrum, Email: sasikumarkk2000@yahoo.com

In atom interferometry experiments, the intensity of laser beams should be kept constant during the experiment. A laser intensity control circuit is required to monitor the intensity variations of different beams independently, throughout the experiment and correct it in real time. A portion of laser beam is captured to identify the fluctuations and a proportional- integral (PI) based control circuit was designed to correct the intensity fluctuations as well as to meet the response requirements. An intensity locking circuit was designed and realised for linearization and compensation of the system along with control loop, to reduce the intensity fluctuations to be within 0.1V with a response of <10 micro s. Initial testing carried out and obtained satisfactory performance.

CP-12-03

Development of SCADA software for IRFEL operation from integrated operator console

Ayukt Kumar Pathak, Shradha Tiwari, H R Bundel, Praveen P Deshpande, Viraj P Bhanage, Laser Control and Instrumentation Division, Raja Ramanna Centre for Advanced Technology, Indore Email: ayukt@rrcat.gov.in

RRCAT has developed an Infrared Free Electron Laser (IRFEL) with a wavelength ranging from 12.5 to 50 μm. The IRFEL was operated with large numbers of parameters in engineering mode with individual PC for each sub-system. The IRFEL users put forward requirement for integrated control of IRFEL with operator mode and minimal control. Integrated GUI is aimed to provide convenient operation of IRFEL for single operator. For this purpose, a network of industrial embedded controllers (IEC) is established and development of software is carried out as per standard SCADA framework and network. This paper explains functionalities of this SCADA system of IRFEL at RRCAT. The overall update rate of SCADA is 1 Hz and it manages more than 500 data points.

CP-12-04

Development of software package for auto-focussing and processing of materials using femtosecond laser based micro-structuring setup

H.R. Bundel, R. S. Verma, S. Tiwari, S.Kushwaha, P. P. Deshpande, R. Kaul, V. P. Bhanage, Raja Ramanna Centre for Advanced Technology, Indore *Email: shradha@rrcat.gov.in*

Ultrafast pulse laser based micro-structuring of material is ubiquitous due to its precision, speed and cost effectiveness in the field of research and industry for surface/volume processing of materials. For material processing like surface texturing, the process requires laser beam focussing on the sample, thereafter sample movement in XY plane in the region of interest with a desired pitch and set laser parameters. A software package capable of laser auto-focussing, sample alignment and micro-structuring for femtosecond laser micro-structuring setup has been developed. The auto focussing of laser spot is achieved by acquiring the laser spot image on sample and applying the developed focussing algorithm. The XY stage control software module allows micro-structuring in raster scanning mode in rectangular/ circular region of interest. This software package offers better repeatability, better accuracy in laser focusing compare to user level focal adjustment by viewing the laser spot using camera and saves times and effort in the entire material structuring process.

CP-12-05

Prototype Supervisory Control System for Green Ophthalmic Laser Coagulator

Shradha Tiwari, Lalita Jain, Amarjeet Singh, M.A.Ansari, P.P. Deshpande, V. P. Bhanage, Raja Ramanna Centre for Advanced Technology. Email : shradha@rrcat.gov.in

A compact intracavity frequency doubled diode pumped Nd:YVO4/KTP based green laser (DPSS green laser) generating ~2W of continuous (CW) power has been developed by LTD, RRCAT. In order to operate this green laser for ophthalmic applications, a control system was developed and integrated with the green laser. The control system was

designed to overcome the limitation of power supply control and make it suitable for ophthalimic applications. It controls the shape of current pulses applied to laser, along with safety interlock features and user friendly GUI software. The paper discusses key features of the control system for above green ophthalmic laser coagulator.

CP-12-06

Economical Pulsed Laser Diode-based Pumping Source for Non-invasive Photoacoustic Screening Applications

S. Khan, M. Kumar, Y. Sahu, A. Verma,R. Patidar, M.S. Ansari, and S. Vasudevan Department of Electrical Engineering, Indian Institute of Technology Indore 453552, India LPSD, Raja Ramanna Centre for Advanced Technology (RRCAT), Indore, 452013 India, Email: svasudevan@iiti.ac.in.*

Proper light-generation techniques are essential for biomedical photoacoustic diagnostic systems, and the laser is preferable to the LED/diodes as a light source due to its high energy and high coherence length to provide deeper tissue analysis. Nd:YAG crystals are used in the experiments as they have high gain, low threshold, and various oscillation wavelengths, of which 1064 nm has the highest gain. These conventional lasers are bulky, complex, and very expensive. This paper proposes a portable pulsed laser diode-based customized power supply for Nd:YAG pulsed laser pumping. The developed power supply unit provides advantages in cost, mobility, and flexibility in modifying the laser parameter to achieve different laser frequencies, energy, and pulse width. The developed unit successfully delivered 30 A peak current to pump laser and achieved 12 mJ laser energy that is more than sufficient for photoacoustic applications.

CP-12-07

Development of Laser Beam Position Finder for India Security Press, Nashik.

Dharmendra Kumar, M.O. Ittoop, Manoj Kumar, Bhupendra Singh, Deepak Tamboli and Rakesh Kaul, Material Engineering Section, Laser Materials Processing Division, Raja Ramanna Centre for Advanced Technology, Indore, M.P., India – 452013. Email:dharmendrak@rrcat.gov.in

This paper presents the design, implementation, and performance evaluation of a Laser Beam Position Finder (LBPF). The LBPF system consists of a quadrant thermal detector head interfaced to an Arduino UNO based development board with a dedicated graphical user interface display. The system is developed for India Security Press (ISP), Nashik for accurate and real-time measurement of the position of laser beam of their laser in a two-dimensional plane. The integration of a quadrant thermal detector allows for precise detection of the laser beam's location through the analysis of thermal differentials on the detector surface. The Arduino microcontroller board along with 8-channel 24bit ADC card facilitates data processing, interpretation, and user interface for laser aligning applications.

The firmware program running in the Arduino board reads the temperature values from four detector elements and calculates the beam position. The position of the beam is displayed on the 10-inch graphical user interface (GUI)display.

CP-12-08

Deciphering the dielectric behaviour of SiO_2 decorated ZrO_2 core shell nanocomposites

S Cathrin Lims[1] and M. Jose[1] [1]Department of Physics, Sacred Heart College (Autonomous), Tirupattur-635601, Tamilnadu, India [*]Email: jose@shctpt.edu, Alternate mail:mjosh1231@gmail.com*

ZrO_2@SiO_2 core shell nanocomposites (CSNs) were synthesized using a co precipitation cum modified Stober method and systematically characterized through various physical characterization techniques, including XRD, TEM and dielectric measurements. XRD analysis confirmed the presence of monoclinic crystalline ZrO_2 and amorphous SiO_2 phases in the CSNs. TEM results visualized highly crystalline ZrO_2 NPs (50 nm) fully encapsulated by amorphous SiO2 with a thickness of 24 nm, confirming the formation of core-shell structure. The dielectric constant (e_r) and dielectric loss (tand) were shown to be substantially rely on frequency and temperature. Impedance analyses indicate a non-Debye type of relaxation behavior.

CP-12-09

Comprehensive noise profiling in an iCCD detector using photon transfer curve

Anandhu Mohan[a], Anannya Banerjee[b], and Arnab Sarkar[ab] [a]Homi Bhabha National Institute, Anushakti Nagar, Mumbai 400 094, India [b]Fuel Chemistry Division, Bhabha Atomic Research Centre, Mumbai 400 085, India Email:arnab@barc.gov.in, asarkar@ymail.com*

Laser ablated molecular isotopic spectrometry (LAMIS) stands as a rapid and adaptable optical spectroscopy method used across diverse fields due to its simplicity in instrumentation and potential for remote real-time analysis. Despite its utility, the sample matrix dependency and scarcity of enriched isotopic standard poses as a significant obstacle. To address this, calibration-free methodologies have emerged, avoiding the need for standard samples by employing mathematical simulation and correlation of spectra. However, various noises such as read noise, photon-shot noise, and laser shot-to-shot fluctuation impacts the correlation between simulated and experimentally recorded spectra. Utilizing the photon transfer curve (PTC) for noise profiling, this study specifically focuses on identifying and incorporating different noises from aspectrograph with iCCD detector into simulations. The experimentally obtained PTC revealed distinct regions associated with specific noise sources, notably read noise, photon-shot noise, and

fixed pattern noise (FPN). While the study provides these noise components, further characterization of additional noises, including Fano noise, system noise, and dark current, is required to comprehensively profile the various noise sources for improved simulation accuracy and precision in LAMIS.

CP-12-10

Development of 3 phase powered 6kW PFC rectifier based on single switch DCM boost converter;

*Sajith Kumar T R, Dipen M. Vachhani, R.Varma, P. Pandey, R. Porwal, K. K. Pant, A. Sharma, P. Saxena, R.Arya, Laser Technology Division, RRCAT, Indore. *Email: sajith@rrcat.gov.in*

The paper presents development and implementation of a 6 kW Discontinuous Conduction Mode (DCM) single switch boost-basedpower factor corrected (PFC) rectifier fed by 380 V- 450 V 30 - 50 Hz ac mains andfor end use in a CW diode laser power supply. The output dc voltage is regulated at 800V by a low bandwidth single feedback loop and robust safety measures have been followed. The main advantages achieved are a) Simple topology requiring only one active switch b) DCM operation ensures that the input current waveform nearly follows the input voltage without requirement of current sensor or current control loop. Hence a single 1st order loop suffices to regulate the output voltage c) Owing to zero current turn-on of power MOSFET in DCM mode, its turn-on switching losses as well as reverse recovery losses of boost diodes are nearly eliminated.The measured input power factor at full load is 0.98 and input current THD of <16% at rated output power.

CP-12-11

Enhancement of energy deposition in high repetition rate Copper Vapor laser

Anil S. Nayak, Rajasree Vijayan, Dheeraj K Singh, Suvendu Mandal, B. Gangwane, V S Rawat, S Kundu Advanced Tunable Laser Applications Division, Bhabha Atomic Research Centre, Email: anilsn@barc.gov.in.*

Copper Vapor Laser (CVL) is a high repetition rate, high power pulsed laser source generating Green (510 nm) and yellow (578 nm) wavelength in the electromagnetic spectrum. The CVL is excited by pulsed electric discharge where the high voltage pulses are in the range of a pulse repetition rate of 9 kHz. This paper is intended to report the technique to enhance the electrical power deposition into the CVL load there by resulting in the higher energy per pulse of the optical output power. This upgradation is attained by increasing the energy storage capacitance in the primary circuit of the pulse transformer.The electrical parameters of the upgraded pulse power supply compared with the earlier system. The optical power enhancement of the single CVL system is presented in this paper. The long term electrical energy deposition and consequently the optical power output stability of the CVL is discussed.

CP-12-12

Design and Simulation of a Feedback Control System for Pulsed Nd:YAG Laser Power Supply

Piyush Kumar, Vijay Bhawsar, Jagriti Khanwalkar, P. Saxena, R. Arya, Laser Technology Division, RRCAT, Indore, Email: piyushkr@rrcat.gov.in

Laser-based material processing with a Nd:YAG laser system necessitates precisely tailored current pulses for the flash lamp. The precise regulation of current pulse parameters requires the utilization of a power supply controller. This paper presents work on design and simulation of a controller for a pulsed current power supply for pulsed Nd:YAG laser. The controller has been designed to meet the required time domain specifications, regulate the amplitude of the output current pulse within tolerance limit and would be used to drive the buck convertor-based switching power supply which provides regulated rectangular or complex shaped current pulses to drive flash lamp.The simulation result demonstrates that the designed control system successfully regulates the lamp current within the tolerance limit of 3%, ensuring that it settles to the expected value after exhibiting the desired transient response i.e.,rise time, peak time, overshoot and settling time of the control loop is 0.2 ms, 0.3 ms, 8.26% and 2 ms respectively in response to step changes reference voltage.

CP-12-13

Shack Hartmann based Wave Front Sensor

M. J. Joshi, N. O. Kawade, and A. S. Rawat, Laser Application Section, Laser and Plasma Technology Division, BARC,Mumbai, Email : mandarj@barc.gov.in*

A wavefront sensor is a device for measuring the aberrations of an optical wavefront. Shack-Hartmann wavefront sensor(SHWFS) is a simple, compact, robust, and relatively vibration insensitive wavefront. It makes passive measurements of wavefront of the incident light and is wavelength-independent. The paper describes Shack Hartmann wavefront sensor being developed at BARC, Mumbai. The software developed computes the Zernike coefficients and reconstructs the wavefront of unknown beam. The image analysis involves following three steps: determination of the spot positions, calculation of wavefront slopes, and the wavefront reconstruction. The software has been tested using multiple simulated images. The algorithm was tested for Gaussian lenslet spots and overall Gaussian beam intensity variation. The error is slope calculation is <0.02 % .

CP-12-14

Analysis and modification in flashlamptrigger circuit for Nd: glass laser power supply

Deepak Naphade, Abrat Verma, Bhupinder Singh, Anand Pagare, M.S. Ansari, Laser Power Supplies Division, Raja Ramanna Centre for Advanced Technology, Indore *Email: naphaded@rrcat.gov.in*

MOPA based high energy solid state laser systems consists of flashlamp pumped Nd: glass laser amplifier stages for high energy pulsed laser generation[1].Linear shaped Flashlampsof arc lengths ranging from from 280 mm to 900 mm are used which are usually xenon or krypton filled. They are driven by pulsed power supplies that deliver electrical pulsesofrequired energy and pulse width for producing high energy broadband pulsed light emission. Type of the fill gas, currentand pulse width decide spectral contentof the light emitted from flash lamp. A typical flashlamp power supply consists of Capacitor Charging Power Supply (CCPS), flashlamptrigger circuit and Pulse Forming Network (PFN).Power supply topologies that produce constant current output are used for charging of capacitor banks in PFN[3],while forflashlamp triggering, series triggering and external triggering methods are commonly employed. The paper discusses the techniques adopted to improve the reliability of trigger circuit by reducing stresses on critical components thereby ensuring longer life.

CP-12-15

Effect of Niobium Doping on the Dielectric Properties of Sol-Gel Synthesized $CaCu_3Ti_4O_{12}$ Ceramics

M Ehthishamul Haque[a], M. Jose[a] [a] Department of Physics, Sacred Heart College (Autonomous), Tirupattur635601, India. *Email: jose@shctpt.edu, mjosh1231@gmail.com*

In this work, Nb doped $CaCu_3Ti_4O_{12}$ (CCTO) ceramics is prepared via sol gel process sintered for 6hrs at 1000° C and a giant dielectric constant with a very low dielectric loss is reported. The powder XRD analysis revealed the cubic perovskite structure and XPS analysis revealed the oxidation states of the constituent elements. The SEM micrographs shows the grain size of 2.65±0.10µm for pure and 2.40±0.19µm for Nb doped CCTO. The Nb doped CCTO exhibited remarkably high dielectric constant (?$_r$) of 1.26×10^5 with low dielectric loss (tand) of 3.7 in comparison with pure CCTO ceramics which demonstrated relatively low ?$_r$ of 2.39×10^4 and moderately high tand of 9.1 at 10 Hz and 673K. The Nyquistplots established deviation from Debye type relaxation with a negative temperature coefficient of resistance type behaviour.

Category - 13

Machine Learning and AI in Laser Applications

CP-13-01

Erroneous Signal Detection in Raman Optical Fiber Based Distributed Fire Detector System Using Support Vector Machine

A. K. Sahoo[1, 3], M. K. Saxena[1, 3, 6], R. K. Sharma[1], J. Kishore[1], S. Kumar[1], C. K. Suman[1], D. Pachori[4], M. Khare[5], O. Prakash[1, 3], S. V. Nakhe[2], [1]Fiber Sensors & Optical Spectroscopy Section, [2]MSATG, Raja Ramanna Centre for Advanced Technology, Indore, [3]Homi Bhabha National Institute, Mumbai, [4]IIIT, Nagpur, [5]SGSITS, Indore [6]Email: manojsaxena@rrcat.gov.in

This paper presents a study on detection of erroneous anti-Stokes (AS) signal in Raman optical fiber distributed fire sensor (ROFDFS) system that may produce misleading/false indication. The desired functioning of the ROFDFS system necessitates the optimal operation of the light source and detector along with the precise alignments of the optical components. Any deviation from proper operating conditions will produce erroneous AS signal. The paper initially outlines the conditions that could generate erroneous AS signal followed by a discussion on the application of various machine learning algorithms on features of AS signal to identify such situations. The results demonstrate an accuracy of 96% in detection of misleading/false alarms by employing signal processing and machine learning techniques on the received Raman back scattered AS signals.

THESES

TH-01

Study of parity- time symmetry in mutually coupled semiconductor diode lasers

Prachi (Ph.D. Scholar)
Department of Physics, Pondicherry University
prachiphy16phd@gmail.com

It is well-known that the non-Hermitian Hamiltonians exhibit real spectrum if the Hamiltonian is Parity – Time (PT) symmetric [1,2]. This opens up new window for studies on physical systems governed by non-Hermitian Hamiltonians in various disciplines of physics. An optical system is proved to be one exciting area for the study of PT symmetric systems [3-7] with non-Hermitian Hamiltonians. Study of PT symmetry has obtained relatively faster momentum due to its possible applications in optical lattices, stable single mode operation of lasers, micro ring lasers, phonon laser, optical solitons and in semiconductor diode lasers [8]. Here the semiconductor diode lasers are one of most wanted candidates for the study of PT symmetry due to its potential in wider applicability. Studies of PT symmetry in diode lasers typically assume a scheme in which a pair of semiconductor lasers are coupled face to face. Theoretical investigations on semiconductor lasers uses the normalized Lang-Kobayashi rate equations, for which a transformation Hamiltonian is constructed. Specific evolutionary properties of eigen values of these Hamiltonians would qualify if the system is being operated at PT symmetric regime or at broken PT – symmetric regime. Earlier research works [8] had investigated the evolution of both real and imaginary eigen values in a system with zero-time delay between the two lasers being optically coupled. Parametric studies could identify the existence of exceptional points, broken and unbroken PT symmetric regimes [9].

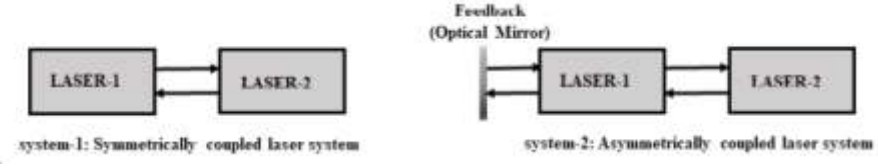

Figure-1: Schematic diagram of coupled laser system either symmetrically(system-1) or asymmetrically(system-2)

In my thesis work, we consider two different configurations for our investigations as shown in Figure- 1. One is the symmetrically coupled diode laser which consists of two semiconductor diode lasers coupled face-to-face with a non-zero, finite time delay between them being called here as system-1 and other is System – 2, where one of the diode lasers considered in System-1, is subjected to optical feedback obtained from an external cavity mirror with a finite external cavity delay time. In the first part of the work, both the systems are theoretically investigated, using normalized Lang–Kobayashi rate equations for the complex electric field and for the

carrier densities. Where these two lasers are identical except that their emission frequencies are not equal and thus effecting a small frequency detuning between them whenever needed. If the lasers are operated near threshold, the effect of excess carrier densities is negligible and thus two of the rate equations pertaining to the carrier densities become irrelevant and thus we are left with two rate equations for the respective electric field amplitudes. These rate equations contain terms with time delay(s). The time delay (τ_1) between the lasers, and the external cavity time delay (τ_2) are considered to be small but not negligible and thus it is possible to expand the electric field terms containing time delay, neglecting the higher order term in expansion.

The resultant two rate equations for the electric field amplitudes can be expressed in a matrix form and thus a transformation matrix is being constructed. This transformation matrix (M) is equivalent to the Hamiltonian operator. Expressions for eigen values of these Hamiltonians are obtained keeping non-zero-time delay and specific properties of both the real and imaginary eigen values are studied for their dependence on primarily the time delay parameter(s), and on other operating parameters including frequency detuning. As the time delay between the lasers is varied, we are able to identify specific regimes in which the systems exhibit PT symmetry as well broken PT – symmetry (figure-2). The periodicity of these occurrences is an important outcome of our studies as it has a direct utility is designing devices. We carried out parametric studies on the occurrence of PT symmetry and broken PT symmetry on parameters such as, coupling strength, feedback strength and external cavity time delay. As example, one outcome of these parametric studies can be seen in figure-3 also.

In the next part of the work, we carried out numerical investigations of these systems, especially System-2, using standard Lang – Kobayashi rate equations. The equivalent condition for the existence of PT symmetry would depend upon the evolution of the laser phases (figure-4). If the first order differentials of the laser phases are identical between two lasers, then they are said to satisfy the primary condition for PT symmetry. The external cavity feedback strength is optimized such that the lasers do not exhibit chaos, but are stable and self-pulsating. Parametric studies are carried out on the existence of PT symmetry and its transition to broken PT symmetry by varying system parameters such as, frequency detuning between the lasers, coupling strength, feedback strength and external cavity time delay. We are able to provide a qualitative comparison between the theoretical studies and that of numerical studies. An important outcome of this study is the synchronization properties between the lasers and its direct correspondence to the existence of PT symmetry.

The novelty of our work lies in the fact that we have investigated the PT symmetry properties and its dependence on the time delay between the lasers for both symmetric and an asymmetric system which is more realistic then zero delay systems.

The thesis consists of an overview of preserving the PT-symmetry characteristics in semiconductor diode laser systems through one peer-review article and few conference papers. The present thesis consists of six chapters and a brief outline of each chapter is given below.

Chapter-1 provides a general introduction to the concept of PT-Symmetry and its applicability in the field of optics, essentially for Non-Hermitian Hamiltonian systems that can exhibit real spectra under some conditions. The requisite conditions for the existence of PT-Symmetry and its transition to broken PT symmetry are presented in this chapter. Objective of

the thesis and its organization are outlined in this chapter.

Chapter 2 describes two different schemes along with the complete theoretical model being employed for this study (figure-1). The details of necessary analytical and numerical methods are presented in this chapter. Lang – Kobayashi rate equation model and its normalized version are presented in detail with proper explanations to the term involved.

In Chapter 3, we investigate PT symmetry properties of System-1, i.e., symmetrically coupled diode laser system. Here, the coupling is such that the electric field of one laser is coupled to the electric field of the other laser with a non-zero time delay (τ). The rate equations are simplified to reduce the nonlinearity and degree of complexity, as the excess carrier densities are considered smaller at near the threshold condition [3,4]. It is interesting and worth noting that if time delay is set to zero ($\tau = 0$), our eigen value expression reduces to a simple form and is in concurrence with earlier studies [3]. As an outcome of this study, we find the existence of PT-Symmetry and a transition to broken PT- Symmetry which occur at regular intervals of time delay between the lasers, shown in figure-2. At a particular delay time of occurrence of PT symmetry, any alteration to other parameters such as frequency detuning or coupling strength would result in its transition to broken PT symmetry and this can be seen in figure-3. A systematic study has been carried out to identify the effect of the parameters on the PT symmetry. Thus, we can say from figure-2 and figure-3, that PT transition occurs at exceptional points and also otherwise but with a recurring character. Where, P or Q are exceptional points as well as PT-symmetry point, A or C are PT-symmetry point only and other points as B or D is PT-broken points. Figure-3 here represents the stable PT-symmetric regimes at a particular fixed PT-symmetric point as point A or C with respective to variable coupling coefficient and detuning, justify that the point A or C is stable PT-symmetry points.

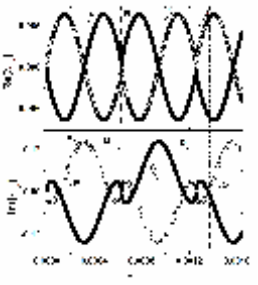

Figure-2: *Eigen values as a function of delay time () at a constant coupling coefficient (= 0.1) and at constant frequency detuning (ω = 0.1). The top panel has the real part of eigen values and bottom panels has the imaginary components of eigen values. Closed circles (open circles) represent first (second) eigen values.*

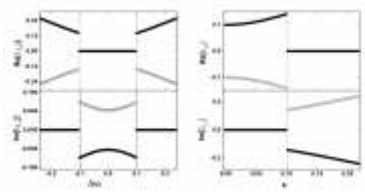

Figure-3. *Eigen values are shown as a function of (a) detuning at constant coupling coefficient and (b) coupling coefficient at constant detuning, for time delay corresponding to vertical lines P (or Q) of figure-1. (non-exceptional, PT symmetry transition point).*

In **Chapter 4**, we have investigated the System-2, which is an asymmetrically coupled diode laser system. We have carried out similar investigations as in chapter-3, while keeping the time-delayed external cavity feedback. As a result, we found that, asymmetry of the system has a

systematic role in existence of PT symmetry or in its transition to broken PT symmetry and external cavity feedback rate (asymmetry factor) induces a bistable character in the real eigen values if it is strong enough. It's our findings that, for a relatively weak asymmetry factor, the external cavity time delay has little or no influence on the occurrence of PT symmetry. There exists complementary correlation between the eigen values, this is a requirement and is confirmed in our studies. For a constant asymmetry factors, the mutual coupling coefficient between the lasers does play a significant role in the occurrence of PT symmetry or its breaking. In other words, we can say that the asymmetry of the system provides us an additional tool to control the occurrence of PT symmetry and /or its breaking.

Chapter 5 includes the numerical investigations of asymmetrically coupled semiconductor diode lasers where the numerical calculations have been carried out by solving the suitably adopted Lang – Kobayashi Rate equations for the asymmetrically coupled system of diode lasers. The condition for identifying PT symmetry regime has been obtained in terms of rate of change of phase evolutions. Additional requisite conditions on the laser field amplitudes have been identified. Correspondence between numerical identification of PT symmetry regime with analytical conditions have been established here. We have found that the frequency detuning between the lasers is an important factor influencing the existence of PT symmetric regime. The external cavity feedback, also the asymmetric factor, plays a crucial role in rendering a transition from PT- symmetry to broken regime. Synchronization between field amplitudes have been studied along with the phase synchronization properties. Figure-4 shows the temporal evolution of electric field amplitude and phase as well, and gives visualization of correlation in field and phase too. A detailed investigation is done in this chapter.

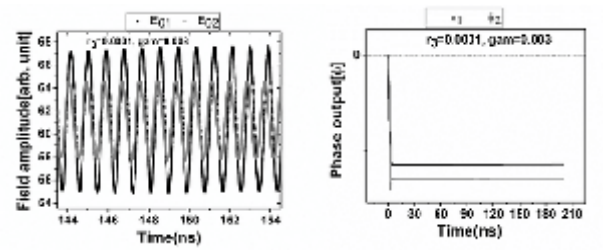

Figure-4. *(a) and (b) represents temporal evolutions of the laser field amplitudes and phases for laser-1 and laser-2 respectively.*

In **Chapter 6**, we briefly summarize the overall work done and its understanding obtained from the findings of this thesis work on PT-symmetric studies and also presents possible future scope of this field of research.

References:

1. C. M. Bender, S. Boettcher, Real spectra in non-hermitian Hamiltonians having PT symmetry, *Phys. Rev. Lett.*, 80 (1997) 5243–5246.
2. M. Bertolotti, PT symmetry in quantum and classical physics, *Contemp. Phys.*, 60 (2019) 196–197.
3. C. E. Rüter, K. G. Makris, R. El-Ganainy, D. N. Christodoulides, M. Segev, D. Kip, Observation of parity–time symmetry in optics, *Nat. Phys*., 63 (2010) 192–195.
4. M. A. Miri, A. Alu, Exceptional points in optics and photonics, *Science*, 363 (2019) 7709.
5. Y. Kominis, k. d. Choquette, A. Bountis, V. Kovanis, Exceptional points in two dissimilar coupled diode lasers, *Applied Phys. lett.* 113 (2018) 081103.
6. Y. Kominis, V. Kovanis, T. Bountis, Spectral signetues of Exceptional Points and Bifucations in the Fundamental Photonic Dimer, *Phys. Rev. A.*, 96 (2017) 053837.
7. Zyablovsky, A.P. Vinogradov, A. A. Pukhov, A. V. Dorofeenko, A. A. Lisyansky, PT-symmetry in optics, *Physics-Uspekhi, Reviews of Topical Problems*, 57 (2014) 1063–1082.
8. Wilkey, J. Suelzer, Y. Joglekar and G. Vemuri, Parity–time symmetry in bidirectionally coupled semiconductor lasers. MDPI -*Photonics*, 6, (2019) art. No. 122; J. S. Suelzer, Y. N. Joglekar, G. Vemuri, Parity-time symmetry breaking in optically coupled semiconductor lasers. *Proc. of SPIE,* 9920, M1-M8, 2017, doi: 10.1117/12.2239487.
9. Y. Choi, C. Hahn, J. W. Yoon, S. H. Song, Observation of an anti-PT-symmetric exceptional point and energy-diference conserving dynamics in electrical circuit esonators, *Nat. Comm*. 9 (2018) art. No. 2182.
10. Prachi, S.V.M. Satyanarayana, S. Sivaprakasam, PT-Symmetry in mutually coupled semiconductor lasers with a non-zero time delay, *Physics Letters A* 452 (2022) 128449.

TH-02

Studies on multimode interference and pulse shaping in fiber lasers

Pradeep Kumar Gupta[1,2]

[1]*Laser Technology Division, Raja Ramanna Centre for Advanced Technology, Indore*

[2]*Homi Bhabha National Institute, Training School Complex, Anushakti Nagar, Mumbai*

Email: pradeepg@rrcat.gov.in

The fiber lasers are receiving increased attention not only for scientific, medical and industrial applications but also a lot of academic interest due to inherent nonlinear dynamics present in the laser oscillators. Particularly, passively mode locked fiber lasers provide a versatile platform to study numerous nonlinear phenomenon affecting the patterns of pulse formation as well as their pulse shapes. Since the pulse dynamics is very intricately dependent on intra-cavity dispersion, nonlinearity and dissipative processes acting in the resonator, generation of laser pulses with desirable shapes and reasonably good stability becomes quite challenging. Based on net dispersion in the fiber resonator and pulse formation dynamics, several operating regimes in the mode locked fiber lasers have been identified viz. soliton[1], dispersion-managed soliton[2], similariton[3] and dissipative soliton[4] mode locking. Among these, dissipative solitons generated in all-normal dispersion (ANDi) configuration have attracted significant research interest due to their energy scaling capability and all-fiber configurability. Pulse shaping mechanism of dissipative solitons is based on strong spectral filtering, which trims the temporal wings of the pulses. Spectral filtering and transmission profile of saturable absorbers have strong role on dissipative soliton pulse shaping and various pulse shapes and associated spectral dynamics have been studied theoretically and experimentally. In this thesis work, fiber optic component based spectral filters and saturable absorbers have been explored to study pulse shaping dynamics in fiber lasers.

A simple way to construct a band pass filter (BPF) in all-fiber format with tunable peak transmission wavelength is to splice single mode fibers (SMF) on either ends of a segment of a multimode fiber (MMF). The light coupled from SMF to MMF will excite several higher order modes in the MMF which interfere to create self-images of the input SMF end along the length of the MMF. This is called multimode interference (MMI) in optical fiber[5]. If the second SMF is spliced at the location of one of the self-images, the entire structure acts like a BPF. The transmission wavelength and the transmission bandwidth of such MMI filter can be tuned by applying stress and changing the length of the MMF respectively. One of the objectives of this thesis was to use MMI based devices to investigate its influence on pulse shaping dynamics in Q-switched and mode locked fiber lasers. Our studies using MMI based spectral filter in actively Q-switched Yb-doped fiber laser have shown that it not only reduces the Q-switched pulse duration, but also leads to wavelength tunable Q-switching operation. The Q-switched pulse duration was reduced from 110 to 88ns after introducing MMI filter in the cavity. Wavelength tunable Q-switching operation was achieved from 1022 to 1038 nm by tuning the peak transmission wavelength through MMI filter[6]. For wider wavelength tunability, MMI filter was

replaced with commercially available fiber integrated acousto-optic tunable filter (AOTF) which resulted into more than 70 nm wavelength tunability (1008.6 to 1080.3 nm). Also, presence of AOTF lead to spectral narrowing from 9.6 to 1.1 nm and associated pulse shortening from 110 to 65 ns. For further pulse duration shortening, the duty cycle of acousto-optic modulator was reduced which lead to generation of sub-cavity round trip time duration pulses[7] (10 ns).

In 2013, it was proposed that MMI can be used as saturable absorber based on Kerr induced nonlinear effects[8]. Soon after, experimental study was reported on passively Q-switched fiber laser using MMI based saturable absorber[9]. Later, efforts were made to use MMI based saturable absorbers for mode locking in fiber lasers. For the construction of MMI based saturable absorber, different geometries of MMF were explored viz. step index MMF, graded index MMF, no-core fiber or even their hybrid combinations to design mode locked fiber lasers. Previous studies have shown that due to very small self-imaging length of graded index MMF, it becomes very difficult to control the length of MMF with the fiber cleaver, however a combination of graded index and step-index MMF relaxes this requirement to some extent[10]. These limitations motivated us to explore nonlinear MMI based saturable absorbers consisting only of step-index MMF for designing mode locked fiber lasers. For the first time, we demonstrated mode locking in Yb-doped ANDi oscillator by using nonlinear MMI in step-index optical fiber as shown in figure 1(a). The MMI was observed in step index single mode-multimode-single mode (SMS) fiber structure. The intensity and wavelength dependent transmission of SMS structure was analyzed (figure 1(b)) to understand the saturable absorber properties of nonlinear MMI in step-index fiber which shows that presence of a narrow band wavelength tunable spectral filter is necessary for nonlinear MMI based saturable absorber. A fiber integrated AOTF was incorporated in the laser resonator for wavelength tunability and to provide pulse shaping mechanism of dissipative solitons as required in ANDi laser. Mode locking in single pulse operation was realized at a very low pump power of 56.3 mW where 180 ps duration pulses are generated at 9 MHz repetition rate as shown in figure 1(c). The corresponding optcal spectrum and radio frequency measurement traces are shown in figure 1(d) and (e) respectively. The SNR of RF trace is ~50dB indicating reasonably stable mode locking[11]. At higher pump power, laser operated in multi-pulse regime.

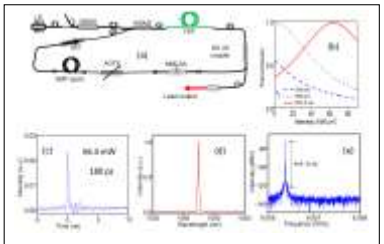

Fig 1: *(a) Mode locked fiber oscillator based on MMI based saturable absorber, (b) Calculated intensity transmission of MMI structure at different operating wavelength , (c) mode locked pulse and (d) opti cal spectrum of pulses at 56.3mW pump power. (d) Radio frequency tr ace of train of mode locked pulses.*

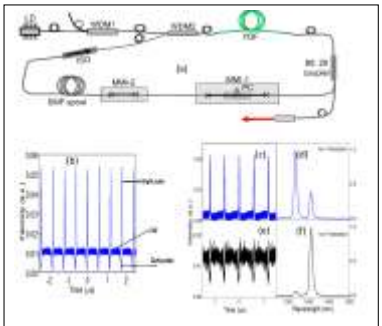

Fig 2: *(a) Mode locked fiber oscillator consisting of two MMI structures, (b) Train of dark -bright pulses at 200mw pump power and (c,d,e,f) Polarization resolved bright and dark pulses and optical spectrum.*

In the next experiment, we used two MMI structures in Yb-doped fiber laser as shown in figure 2(a). This combination of two MMI structures acted as a saturable absorber leading to

mode locking in the resonator. By adjusting the polarization controller attached to one of MMI structure, stable dark-bright pulses[12] are observed at fundamental repetition rate of 1.67MHz as shown in figure 2(b). The duration of dark and bright pulses was measured to be 54 and 20.5 ns respectively at 146 mW pump power. The intensity of bright pulses and darkness of dark pulses increases with increase in pump power. Bright and dark pulses are resolved by placing a polarizing component confirming their polarization domain wall nature as shown in figure 2 (c-f). Dark pulses have attracted considerable attention not only due to the rich nonlinear dynamics involved in the generation of such pulses in optical fiber but also due to their potential applications in various fields particularly in optical communication and signal processing as dark pulses are less sensitive to the background noise, suffer less broadening during propagation and are less influenced by stimulated Raman scattering in comparison to the conventional bright pulses[13].

The NOLM and NPR based artificial saturable absorbers, whose transmission is sinusoidal, have been used more frequently in reported mode locked fiber lasers[14]. The combined transmission of NOLM-NPR pair may yield some unusual transmission characteristics that may be useful for temporal shaping of mode locked pulses in ultra-long fiber resonators. Motivated by this, we analyzed the power and spectral transmission of NOLM-NPR based saturable absorber in figure-8 shaped fiber resonator. The power transmission characteristics have shown that the NOLM-NPR transmission becomes non-sinusoidal for some specific settings of polarization states inside the resonator. Based on numerical calculations, we designed an Yb-doped fiber resonator (length 445 m) mode locked by combined effect of NOLM-NPR based saturable absorber as shown in figure 3(a). The resonator generated burst of pulses, long duration flat-top pulses and short duration high peak power pulses as usual at different biasing of polarization controllers placed inside the cavity. However, at some specific settings of polarization controllers, laser generated long duration (11 ns) flat-top pulses and short duration (300 ps) narrow pulses simultaneously (figure 3 (b)) which can be merged together to mimic the shape of a chair as shown in figure 3(c). Such kind of chair-like pulses directly from mode locked resonator were demonstrated for the first time by us. It was found that the chair-like pulses are suitable for energy scaling. In all-fiber amplifier, energy of chair-like pulses was scaled to ~70 mJ level with negligible contribution from amplified spontaneous emission or stimulated Raman scattering[15].

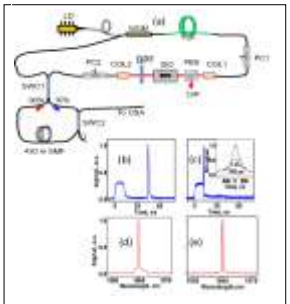

Fig 3: *(a) Figure-8 shaped mode locked fiber oscillator using NOLM-NPR. (b,d) flat-top & narrow pulse and their spectrum, (c, e) Chair -like pulse and corresponding optical spectrum*

The numerically simulated spectral transmission of NOLM-NPR shows that cavity birefringence based spectral filtering introduced by polarization controllers may be useful for tailoring of mode locked pulses in ultra-long figure-8 resonators. The spectral response is single peaked and multi-peaked depending on the applied stress induced birefringence by polarization controllers. Furthermore, the spectral transmission

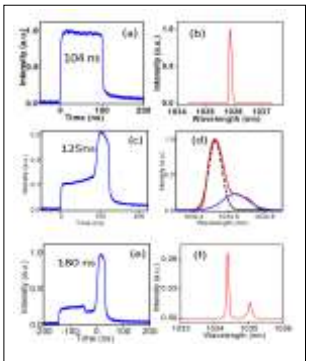

Fig 4*: Temporal and spectral profile of (a, b) flat-top, (c, d) step-like and (e, f) J-shaped pulses*

profile changes dynamically even at fixed setting of polarization controllers by varying intra-cavity power. To verify these simulation based observations, another Yb-doped fiber resonator consisting of NOLM-NPR based saturable absorber was designed in figure-8 shape configuration similar to figure 3(a). The NOLM loop length was kept ~1 km and total resonator length was ~1.02 km. In contrast to previous experimental set-up used for generation of chair-like pulses, the band pass filter was removed from the cavity to understand the influence of NOLM-NPR spectral transmission. The laser generated flat-top, step-like and J-shaped pulses at different cavity birefringence controlled by polarization controllers as shown in figure 4. Also, shape of pulses transformed from J-shape to step-like and from step-like to flat top on decreasing the pump power even at fixed cavity birefringence. Experimentally, a strong correlation between spectral and temporal profile of the generated pulse shapes is established where it has been observed that asymmetric spectral filtering is responsible for generation of J-shaped and step-like pulses[16].

Generation of ultrashort laser pulses of femtosecond duration in mode locked fiber lasers poses a problem due to inherent fiber nonlinearity. In general, the mode locked fiber laser pulses are associated with side lobes when compressed to femtosecond duration[17]. We investigated an all-fiber, ANDi Yb-doped fiber laser (figure 5(a) mode locked by NPR based saturable absorber under different pump power regimes. Particularly at 500 mW pump power, the oscillator generated highly chirped 5 ps duration pulses which are compressed to 146 fs duration with clean temporal profile without any side lobes (figure 5b: optical spectrum and 5c: AC trace). This may be due to reduced accumulated nonlinear chirp in the output pulses at this particular biasing of NPR based saturable absorber and pump power. The signal to noise ratio of train of mode locked pulses was 85 dB, indicating stable mode locking operation. The generalized nonlinear Schrödinger equation has been solved numerically to understand pulse formation dynamics in passively mode locked Yb-doped fiber oscillator which qualitatively support the experimental results. Also, a method for calculation of de-convolution factor has been investigated based on zero phase Fourier transform of optical spectrum that is useful for estimation of pulse duration from autocorrelation trace of pulses which have not a well-defined shape like Gaussian or secant hyperbolic pulses. In a chirped pulse Yb-amplifier, the signal power is scaled to 10 W level and the amplified pulse is compressed to 355 fs duration[18]. The optical spectrum of amplified mode locked pulses is shown in figure 5 (d) and AC trace of compressed amplifiued pulses is shown in figure 5(e) respectively.

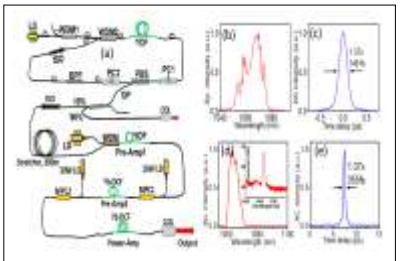

Fig 5: (a) Schematic of all-fiber mode locked oscillator-amplifier set-up, (b, c) Optical spectrum and AC trace of mode locked pulse at 500mW pump power. (d, e) Optical spectrum and AC trace of compressed amplified mode locked pulse at 10W average power.

In conclusion, in this thesis work, efforts are made to understand the pulse shaping dynamics in fiber lasers using MMI and other fiber optic components based spectral filters and saturable absorbers through theoretical modeling, numerical simulations and experimentations. The results reported in the thesis will not only help to understand pulse shaping in Q-switched fiber lasers and enrich the database of pulse profiles generated in ANDi lasers but also provide relevant background for future research in this direction. The whole thesis work constitutes eight chapters. The thesis related works have been published in several peer reviewed journals.

Acknowledgement: I am grateful to my thesis supervisor, Prof. Pranab K. Mukhopadhyay for his valuable guidance throughout the course of this doctoral studies, and Prof. Satya Ram Mishra, Chairman of the Doctoral Committee for his encouragement and useful suggestions at several stages of the doctoral work.

References:

1 L. F. Mollenauer, R. H. Stolen and J. P. Gordon, *Phys. Rev. Lett.* **45**, 1095-98 (1980).
2 H. A. Haus, K. Tamura, L. E. Nelson and E. P. Eppen, *IEEE J. Quantum. Electron.* **31**, 591-98 (1995).
3 F. O. Ilday, J. R. Buckley, W. G. Clark and F.W. Wise, *Phys. Rev. Lett.* **92**, 213902 (2004).
4 A. Chong, J. Buckley, W. Renninger and F. Wise, *Opt. Express* **14**, 10095-100 (2006).
5 Q. Wang, G. Farrell and W. Yan, *J. Light. Technol.* **26**, 512-519 (2008).
6 P. K. Gupta *el al*, *National Laser Symposium-28*, VIT Chennai, Jan. 08-11, 2020.
7 P.K. Gupta *et al*, *Laser Physics* **30**, 095105 (2020).
8 E. Nazemosadat and A. Mafi, *J. Opt. Soc. Am. B* **30**, 1357-67 (2013).
9 S. Fu et al, *Opt. Express* **23**, 17255-62 (2015).
10 S. Thulasi and S. Sivabalan, *Appl. Opt.* **59**, 7357-63 (2020).
11 P. K. Gupta *et al*, *Applied optics* **60**, 3888-94 (2021).
12 P. K. Gupta *et al*, *Laser Physics* **33**, 045105 (2023).
13 S. A. Gredeskul and Y. S. Kivshar, *Phys. Rev. A* **41**, 3994-4008 (1990).
14 H. Chen, S. P. Chen, Z. F. Jiang and J. Hou, *Opt. Lett.* **41**, 4210-13 (2016).
15 P. K. Gupta *et al*, *Applied Optics* **55**, 9961-67 (2016).
16 P. K. Gupta *et al*, *Laser Physics* **30**, 065105 (2020).
17 Y. Han et al, *Prog. Quantum. Electron.* **71**, 100264 (2020).
18 P. K. Gupta *et al*, *Applied Optics* **58**, 5533-39 (2019).

TH-03

Studies on Al_2O_3/TiO_2 nanolaminates for energy storage applications

Partha Sarathi Padhi[1,2,*]

[1]Laser Materials Processing Division, RRCAT, Indore

[2]Homi Bhabha National Institute, Training School Complex, Anushakti Nagar, Mumbai

*E-mail: partha.rrcat@gmail.com

Introduction: Electrical energy storage plays a vital role in day-to-day life because of our dependence on numerous mobile electronic devices. Currently, there is worldwide interest in developing high-density energy storage devices like super-capacitors, which are capable of storing and delivering charges relatively faster as compared to normal capacitors and batteries. The miniaturization of electronic devices and the growing demand for these rechargeable storage capacitors have triggered the need for high dielectric constant (k) and low loss (*tan* δ) materials. Due to continuous downscaling, conventional ceramics, as well as high-k binary metal oxide thin films, suffer from serious degradation of dielectric properties and large leakage current (J_{leak}) issues, which restrict their practical applications in metal-insulator-metal capacitor (MIMCAP) based energy storage devices. [1] Hence, there is an ever-growing demand for developing new dielectric materials in thin film form using a simple fabrication process with reduced cost, having a k value greater than several hundred along with low *tan* δ and J_{leak}values. In the last decade, several binary oxide nano-laminates (NLs) have been investigated to address this issue.[2]However, the interface-controlled Maxwell-Wagner (M-W) relaxation-driven high-k values (~1000) observed in $Al_2O_3/TiO_2/Al_2O_3$ NLs (ATA NLs) have recently opened up a channel for exploring new generation energy storage applications. [3-5]

Although ATA NL-based MIMCAPs look promising, there exist a number of challenges, including the fabrication of ATA NLs with distinct interfaces and sufficient sublayer conductivity contrast to realize appreciable M-W relaxation, which need to be addressed before their commercial application in energy storage capacitors. Most of the previous reports lack an explicit discussion regarding the influence of carrier dynamics on the dielectric and transport properties of ATA NLs, which is most likely to contribute to device failure.[3-5] The correlation between structural and dielectric properties as well as the impact of elemental interdiffusion and interface-generated defect states on the dielectric properties of these NLs have not yet been addressed. In addition, a clear understanding of the microscopic provenance of the M-W relaxation mechanism in these NLs is scarce in the literature. Although the atomic layer deposition (ALD) technique is preferred for NL fabrication, the tailorable sublayer conductivity contrast facility by controlling the reactive oxygen ambient, the scope of sequential ablation of target materials, and the controllable laser pulse parameters make the pulsed laser deposition (PLD) technique suitable to fabricate device grade NLs. [6,7] However, owing to the high energy tail of ablated species and the highly coupled PLD growth parameters, it is challenging to grow NL structures with long-range thickness uniformity and distinct interfaces. As a result, only a

few reports exist on PLD ATA NLs. [5,8]To address these issues and to bridge the gap in the literature, this thesis primarily focuses on the successful in-house fabrication of device-grade ATA NLs and a systematic study to tailor and improve the M-W relaxation-assisted various dielectric performance parameters, which are inevitable for energy storage applications. [9-13] To ease the particular points of discussion and for clarity, the NLs with targeted t_s of (say) ~ 1, and 0.8 nm will be referred to as 1A-1T, and 0.8A-0.8T, respectively, in the rest of the document. The experimental findings of this thesis work are structured into four major parts, and the results are presented below.

(1) Pulsed laser deposition of device grade ATA NLs and its dielectric characterization: Since the interface morphology and the sublayer conductivity contrast of ATA NLs are crucial parameters in deciding the device performance, the effect of deposition temperature (T_d) and laser fluence on the interfacial and dielectric properties of a set of ATA NLs was thoroughly investigated to ensure the smooth interface morphology of ATA NLs, even in the subnanometric regime. Finally, a set of ATA NLs, with t_s decreasing from 2 to 0.5 nm and total stack thickness of ~ 60 nm, were fabricated using the optimized PLD deposition parameters, i.e., T_d of 300 ? C, laser fluence of ~ 0.5 j/cm^2 (close to the ablation threshold), oxygen pressure of ~ 0.01 mbar, substrate to target separation of ~ 4.5 cm, and a repetition rate of 5 Hz. The well-defined layer structures in the cross-sectional TEM image of representative 2A-2T NL and 0.8A-0.8T NL in Fig. 1(a) and (b), respectively, validate the formation of artificial periodic structures with long-range thickness uniformity and physically distinct interfaces. There was no crystalline phase detected in the selected area electron diffraction (SAED) patterns of these NLs, (insets of Fig. 1(a) and (b)), which confirmed the amorphous nature of the NLs.(c)

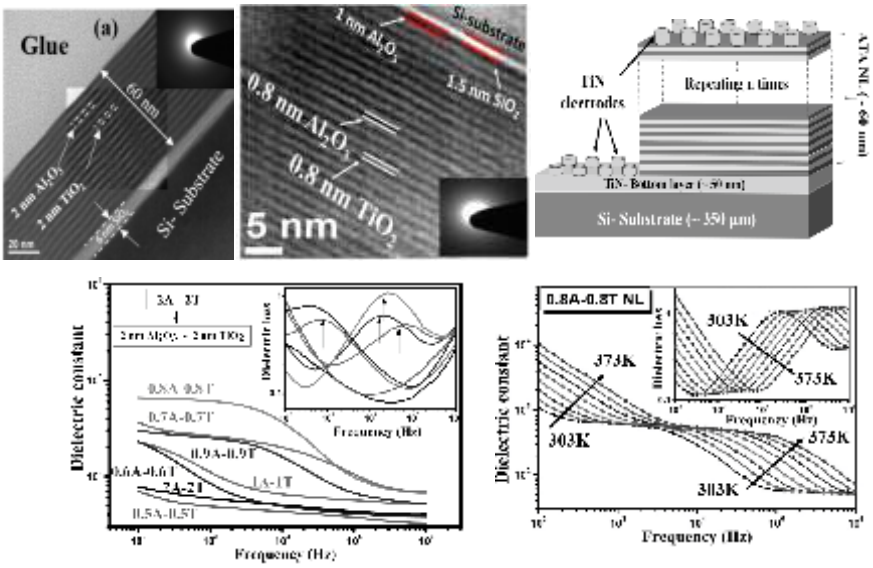

Figure 1. *Cross-sectional TEM image of representative (a) 2A-2T NL and (b) 0.8A-0.8T NL with distinct layer structure. Selected area electron diffraction (SAED) patterns are shown in*

insets, (c) Schematic of crossectional view of TiN/ATA-NL/TiN device structure, (d) frequency dispersed dielectric constant and (inset) dielectric loss curves for ATA NLs with t_s varying between 2 and 0.5 nm, (e) Frequency dispersed ε_r and (inset) tanδ spectra for0.8A-0.8T NL measured in a temperature range from 303K to 373K and at a regular interval of 10K.

To investigate the role of interface density on the dielectric properties of the as-grown ATA NLs, MIMCAPs were fabricated by sandwiching the as-grown NLs between top-bottom RF magnetron sputtered TiN electrodes (Fig. 1(c)). From the frequency dispersed relative permittivity (ε_r) and *tan d* spectra of TiN/ATA-NL/TiN based MIMCAPs (Fig. 1(d)), a monotonic increment in ε_r values from ~ 60 to 670 and a decrement in *tan d* values from ~ 0.9 to 0.16 were observed by reducing t_s from ~ 2 to 0.8 nm, owing to an enhanced M-W interfacial polarization effect. [9] Whereas a further reduction in t_s below 0.8 nm led to the deterioration of the dielectric performances, owing to an enhanced interface intermixing of sublayer constituents,as revealed by X-ray reflectivity (XRR) and TEM measurements.[9] Furthermore, the linear increase in *tan d* towards the low-frequency side was assigned to the gradual enhancement of the DC conductivity across the NL structure owing to the gradual thinning of the Al_2O_3 barrier layers. [9] Additionally, the M-W relaxation peaks (marked as arrows in the *tan d* vs *f* plot) were found to shift towards the higher frequency side with decreasingt_s, which indicated an increasing conductivity of TiO_2 sublayers owing to an increase in the concentration of interface defect states, specifically oxygen vacancies (Ovs) and reduced TiO_2 ions (Ti^{3+}).The ε_r values of ~ 670 obtained for 0.8A-0.8T NL correspond to a capacitance density of about ~ 97 fFμ m^{-2} and an equivalent oxide thickness (EOT) of 0.28 nm. The high-frequency shift of the relaxation peak positions of a representative 0.8A-0.8T NL with an increase in temperature from ~303 to 373 K, (insetof Fig. 1(e)), indicates a thermally activated nature of the M-W relaxation process. From the Arrhenius fitting, the activation energies for interfacial carrier relaxation were found to be ~ 0.395 eV, which closely matches with the donor energy level (trap level) introduced by oxygen vacancy (OV) defect states in TiO_2 thin films,[9]and was further confirmed by valence band-resonant photoelectron spectroscopy (VB-RPES) measurements across the Ti 2p-3d transition (~ 458.4 eV) of 0.8A-0.8T NL using a tunable synchrotron source, (Fig. 2(c)). The temperature-dependent AC conductivity measurements confirmed defect-mediated small polaron hopping transport in active layers and quantum mechanical tunneling in barrier layers of ATA NLs, which were further complemented using VB-RPES and current-voltage measurements. [13]

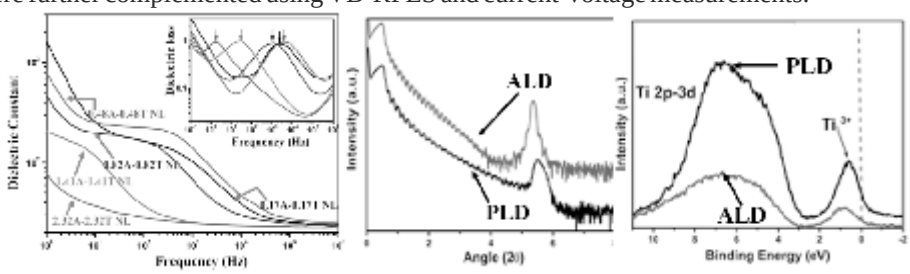

Figure 2. *(a) Frequency dispersed dielectric constant (inset) dielectric loss of ATA NLs with sublayer thicknesses varying between 2.31 and 0.17 nm. (a) XRR (b) RPES profiles for ALD and PLD 0.8A/0.8T NL.*

(2) Dielectric spectroscopy of device grade ATA NLs grown by atomic layer deposition technique: A Beneq made TFS 200 thermal ALD system was optimized for fabricating the device grade ATA NLs with distinct interfaces using $TiCl_4$ and Al $(CH_3)_3$ as Ti and Al precursor, whereas H_2O as source of oxygen. At the optimized process temperature of ~ 200 ± 2 °Cand purging time of ~ 4s, the growth rate of Al_2O_3 and TiO_2 was found to be ~ 1.76 and 0.44 Å/cycle, respectively.[10-12] A set of ATA NLs, with targeted stack thickness of ~ 60 nm, were deposited by decreasing t_s from 2.3 to 0.17 nm, wherein the XRR measurements confirmed the distinctive layered structure down to t_s= 0.35 nm. From the frequency dispersed relative permittivity (ε_r) and *tan* δ spectra of Au/ATA-NL/Au based MIMCAPs, (fig. 2 (a)), a monotonic increment and decrement in ε_r and *tan* δ values from ~ 23 to 217 and ~ 0.8 to 0.06 were observed with t_s decreasing from ~ 2.4 to 0.5 nm, respectively, owing to an enhanced M-W interfacial polarization. Further reduction in t_s down to ~ 0.17 nm deteriorated the dielectric performance due to enhanced interface intermixing. The increasing OV induced charge carrier concentration with the decrease in t_s values down to 0.5 nm was assigned responsible for such improved dielectric properties of ATA NLs and it was verified using RPES measurements. Although, the 0.5A-0.5T NL displayed the highest capacitance density and low *tan* δ of ~ 31 fF/μm^2 and ~ 0.06 at 10 Hz, the J_{leak} of ~ 8.5×10^{-4} A/cm^2 at 1V and EOT of ~ 1.12 nm, the overall performance is inferior as compared to PLD grown optimized 0.8A-0.8T NL. (b)

(3) A qualitative comparison between ALD and PLD-grown ATA NLs: Toinvestigate the origin of superior k values in PLD grown ATA NLs and also to qualitatively compare the interfacial and chemical properties of PLD and ALD grown ATA NLs, the XRR and resonant photoelectron spectroscopy measurements, across Ti 2p-3d transition edge of PLD and ALD grown 0.8A/0.8T NL sample were carried out. The less intense and broad Bragg peak inPLD NL (fig. 2 (b)), specifies comparatively higher interface interdiffusionas compared ALD NL, which indicated the possibility of higher Al interdiffusion into the TiO_2sublayers from both the neighboring Al_2O_3 sublayers of PLD grown NL, owing to smaller cation size of Al as compared

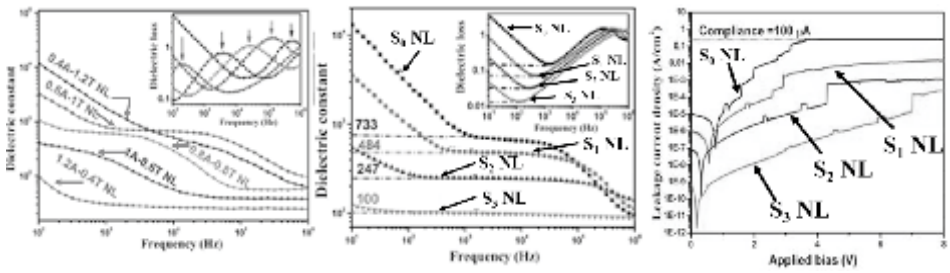

Figure 3.*The measured frequency dispersed* ε_r*and (inset) tan* δ*profiles for (a) ATA NLs with ts varying between 1.2 to 0.4 nm. (b)0.6A/1T/0.6A NL withcapping layer thickness varying between 1 to 5 nm, (c) The* J_{leak} *vs applied bias characteristics curve for 0.6A/1T/0.6A NL with capping layer thickness varying between 1 to 5 nm, where as the inset shows the cumulative probability of the electrical breakdown field of these NL structures.*

to Ti.[9,10] This Al interdiffusion is sufficient enough to completely reduce the TiO_2 sublayer, resulting an enhanced Ti^{3+} and OVs related charge carrier concentration in TiO_2 sublayers, which generate an intense in-gap state in VB-RPES spectra (fig. 2(c))and is actually enhancing the sublayer conductivity contrast assisted high-k values (~ 670) in PLD grown NL.Although PLD is not a large area deposition technique, the tunability in sublayer conductivity contrast in oxide-based NLs through controlling the OV defect concentration, makes it highly suitable for research and development purposes. Combining these results from the above studies, it can be safely concluded that, the results from PLD ATA NL seem to be favorably comparable with the works reported in literature counterparts, [3-5] however there is still a scope of improvement in dielectric and electrical properties to meet the current technological requirements.

(4) Improvement in dielectric and electrical properties of PLD ATA NLs: The interface confined carrier relaxation mechanism was further engineered by precisely controlling the t_s in a given bilayer.The 0.6A/1T NL (S_0 NL) has demonstrated a high dielectric constant of ~ 770 up to ~2 x 10^5 Hz cut-off frequency, although with a relatively higher *tan* δvalues owing to thinner Al_2O_3 sublayers(fig. 3(a)).By introducing Al_2O_3barrier layer of thickness of 1, 3 and 5 nm, across the S_0 NL/electrode interfaces, termed as S_1, S_2, andS_3 NL, respectively, the leakage paths were substantially reduced, resulting in significant improvement in dielectric loss (reduced from 0.1 to 0.01), leakage current density (reduced from ~1.1×10^{-5} to 2.1×10^{-9} A/cm^2 at 1V applied bias), and breakdown field (increase from 0.26 to 1.01 MV/cm), albeit with an adverse effect on the dielectric constant (fig.3(b) and (c)). The optimized ATA NL with ~ 3 nm Al_2O_3 interfacial barrier layer has demonstrated a high-k value ~250 (up to 0.5 MHz) resulting in a high capacitance density of ~ 36.4 fF/μm^2, a low EOT of ~ 0.8 nm, along with a low *tan* δ (~ 0.1) and reduced J_{leak} of ~ 3.1×10^{-7} A/cm^2 at 1 V. Furthermore, by replacing TiN by a high work function metal electrode i.e. Pt, better voltage and temperature stability of capacitance density with improved cut-off frequency and low J_{leak} and *tan* δ were achieved. For Pt/ATA-NL/Pt MIMCAPs, a high capacitance density of ~ 37.50 fF/μm^2, small quadratic voltage coefficient of capacitance α of - 121 ppm/V^2 and linear coefficient β of - 116 ppm/V, together with a temperature coefficient of 80 ppm/ °C, very low J_{leak} of ~ 6.08×10^{-8} A/cm^2 at 1 V were achieved.

These values are very close to reaching all the requirements set by international technology road-map of semiconductors (ITRS-2023) for MIMCAPs. This study not only reports novel approaches to improve the overall dielectric performance of NL-based capacitors for high density storage applications but also establishes correlation between their structural, interfacial, and dielectric properties using state-of-the-art characterization techniques. The combination of the promising electrical properties and the desirable process integration renders this PLD ATA NL as a promising candidate for next generation energy storage applications.

References

1. J. Robertson, *J. Vac. Sci. Technol., B: Microelectron. Nanometer Struct. Process., Meas., Phenom.***18(3),**1785-1791 (2000).
2. J. Azadmanjiri, C. C. Berndt, J. Wang, A. Kapoor, V. K. Srivastava, & C. Wen, *J. Mater. Chem. A,***2(11),** 3695–3708 (2014).
3. W. Li, Z. Chen, R. N. Premnath, B. Kabius, O. Auciello, *J. Appl. Phys.* **110**, 024106 (2011).
4. A. Kahouli, O. Lebedev, M. B. Elbahri, B. Mercey, W. Prellier, S. Riedel, M. Czernohorsky, F. Lallemand, C. Bunel, and U. Lu¨ ders., *ACS Appl. Mater. Interfaces*, **7(46),** 25679–25684 (2015).
5. P. Walke, R. Bouregba, A. Lefevre, G. Parat, F. Lallemand, F. Voiron, B. Mercey, and U. Lüders, J. *Appl. Phys.*,**115(9)**, (2014).
6. L. Liu, Z. Mei, A. Tang, A. Azarov, A. Kuznetsov, Q.- K. Xue, X. Du, *Phys. Rev. B*, 93, 235305(2016).
7. E. L. Papadopoulou, M. Varda, K. Kouroupis-Agalou, M. Androulidaki, E. Chikoidze, P. Galtier, G. Huyberechts, E. Aperathitis, *Thin Solid Films*, **516**, 8141- 8145 (2008).
8. M. Ben Elbahri, A. Kahouli, B. Mercey, O. Lebedev, W. Donner, and U. Lüders, *J. Phys. D. Appl. Phys.*, **51(6),** (2018).
9. P.S. Padhi, S.K. Rai, H. Srivastava, R.S. Ajimsha, A.K. Srivastava, and P. Misra, *ACS Appl. Mater. Interfaces*,**14(10),** 12873-12882 (2022).
10. P. S. Padhi, R. S. Ajimsha, S. K. Rai, U. K. Goutam, A. Bose, S. Bhartiya, and P. Misra, *Nanoscale***, 15,** 8337-8355 (2023).
11. P. S. Padhi, R. S. Ajimsha, S.K. Rai, A. Bose, and P. Misra,*J Mater Sci: Mater Electron*, **34**, 1160 (2023).
12. P.S. Padhi, R.S. Ajimsha, S.K. Rai, S. Bhartiya, A. Bose, B. Das, M.K. Tiwari, and P. Misra, *Journal of Vacuum Science & Technology A*, **41(6)**, (2023).
13. P. S. Padhi, R.S. Ajimsha, S.K. Rai, Kritika Vijay, H. Srivastava, Soma Banik, A.K. Srivastava and P. Misra, Coexistence of small-polaron hopping and tunneling in Maxwell-Wagner relaxation dominated Al_2O_3/TiO_2 sub-nanometric laminates. (Under review in *PRB*).

TH-04

The Origin of Optical Nonlinearity in Anatase TiO_2

Sruthil Lal SB

Department of Physics, Pondicherry University, R. V. Nagar, Kalapet, Puducherry 605014

Introduction

The search for materials that can generate and process optical signals on compact chips at a speed exceeding today's electronic device is an ongoing endeavour.Developments in this direction has been phenomenal thanks to silicon lithography techniques. In the present architectures, the speed-up was made possible by the exponential miniaturization of electronic circuit elements. Electronic integrated circuits or interconnects clocking up to 100 GHz are widely currently operational [1]. As lithography reaches the atomic scale, emergent quantum mechanical effects present practical limitations for implementing logic gates on silicon. In addition, the delay and loss of signals at the electrical interconnects will become prominent as the size shrinks [2]. To meet the rising bandwidth demand, new paradigms for computing architectures are being sought for.

Electronic switching circuits could potentially be replaced by its optical counterparts (i.e., optical switching). All-optical switches operating at high pulse-repetition rates are the basis for developing optical parallel data processing. High switching speeds, however, have to be coupled with low switching energy and ultrafast recovery times, and these requirements could be met by materials with enhanced non-resonant optical nonlinearities. One of the important implementations of all-optical signal processing or switching in photonic integrated circuits is based on the refractive index variation of nonlinear materials induced by a control light, known as the optical Kerr effect. In the optical Kerr effect, the refractive index n of nonlinear material's change in proportion to the incident light intensity where is the linear refractive index, is the nonlinear refractive index, and l is the intensity of the control light. The Kerr-effect could originate due to the refraction either by photo-excited virtual carriers or real conduction band electrons. The former is a typical scenario when the incident photon energy is lower than the material's band gap [3]. Due to the ultrashort lifetime, the virtual carriers respond as fast as the field itself, and they return to the ground state as the electric field is removed. However, when the field strength increases, electrons begin to excite to the conduction band via multiphoton absorption. It leads to an intensity-dependent absorption coefficient (a). Multiphoton absorption generated free carriers in turn causes free carrier absorption (FCA) and free carrier-induced index change (FCI), modifying the refractive index.In contrast to the bound electrons, the long-life time of multi-photon ionized carriers will ultimately become detrimental by slowing down the speed of the photonic devices. The challenge in nonlinear optics is therefore to find a material that has both a large Kerr nonlinear coefficient and a small multiphoton absorption coefficient. Material's switching efficiency is often expressed in terms of a figure of merit (FOM), defined as the ratio of Kerr coefficient n_2 to the two-photon absorption (TPA) coefficient a_2.

Silicon is one of the primary platforms for optical integrated circuits owing to its high compatibility with CMOS framework. Ready availability of silicon-based foundries makes it easier to combine new optical functionalities with electronics on a single silicon chip with a lower cost. However, because of its small electronic bandgap (1.12 eV), its performance is limited due to free-carriers effects arising due to two-photon absorption (TPA) in the telecommunication wavelength (1550 nm) and linear absorption in the interconnect band (800-900 nm) [4].Silicon nitride (Si_3N_4)and tantalum pentoxide (Ta_2O_5), silicon-rich nitride waveguides have been proposed as potential alternatives, which are currently at various stages of development and implementation. Materials for all-optical switching requires to have a high figure of merit in the low wavelength (800-900 nm) inter-connect region, which desirably operate also at telecommunication wavelengths.

Titanium dioxide (TiO_2), commonly used as a saturable absorber in passively Q-switched fibre lasers [5], appears as a promising candidate for photonic integrated circuits. TiO_2 can be formed at low temperatures (<400 ?C) and offers advantages over silicon nitride ($Si_3N_{4)}$ with its higher refractive index (2.4 vs. 2.0) and more than three times stronger Kerr non-linearity [6,7].It has a large TPA-free bandgap (>3.1 eV) at 1550 nm, and a broad transparency window from visible to mid-infrared wavelengths. The nonlinear optical response of anatase TiO_2 has a typical recovery period of approximately 1.5 ps [8]. The n2 of bulk and thin-film of TiO_2 in the range $8^{-3}\times10^{-14}$ cm^2/W [6, 9], which is greater than that of silica fibre (2.48×10^{-16} cm^2/W [10]). Moreover, the two-photon absorption of TiO_2 at 800 nm is minimal, making it ideal for waveguides operating near 800 nm [6]. TiO_2 waveguides have been fabricated, exhibiting linear losses around 5 dB/cm at telecommunication wavelengths (4 dB/cm [7], 5 dB/cm [11], 5.8 dB/cm [6, 9], 4 dB/cm [12], and TiO_2 photonic devices including directional couplers (DCs) [9], and micro ring resonators (MRRs) [6] have also been demonstrated. TiO_2fulfils the requirements on compactness, low loss, high nonlinearity, and capabilities for mass production for dense integration of photonic integrated circuits.

The central objective of this dissertation is to understand the origin of optical nonlinearities in TiO_2 (anatase) thin films under different laser illumination conditions and its dependence on the material's parameters like bandgap. We aim to understand the origin of ultrafast nonlinear optical response of anatase TiO_2 by combining femto-second laser experiments and state-of-the-art first-principle simulations. Here, we measure the nonlinear refraction and absorption coefficients TiO_2 thin films using femtosecond z-scan experiment [13]. Ab-initio simulations based on the time- dependent density functional theory (TDDFT) [14] is used to model the electron dynamics under ultrashort pulses. Unlike the empirical methods like nonlinear pulse propagation equations to derive nonlinear optical coefficients, first-principle simulations relies on the microscopic electron dynamics by time-dependent Schrodinger equation without any assumptions of the underlying mechanism.

Thin film sputtering and its characterization

TiO_2 thin films were grown on 1 mm thick quartz substrates using RF magnetron sputtering. A base pressure of 4×10^{-6} mbar, working pressure of 1×10^{-2} mbar and 100-Watt RF power were used to deposit TiO_2 thin films for the 1-hour duration. Films were then annealed at 600°C to allow phase formation. The XRD spectrum of the thin films is shown in Fig. 1(a). It

predominantly contains the poly-crystalline anatase phase. The observed crystalline peaks agree with the pattern(reference CODE: 96-1526932) from the crystallographic Open Database (COD). By analysing the peaks corresponding to (101) and (004) at 2θ angles 25.4° and 38.3° we estimate the lattice constants a = 3.759Å and c = 9.438 Å (c/a = 2.511). This is off by less than 1% compared to the matched COD data and within 5% compared to other literature. Ab-initio structural relaxation of the anatase TiO_2 using DFT yields lattice parameters a = 3.805 Å and c = 9.781 Å (c/a = 2.57). these values are within 4% of that measured using XRD (δa = 1.22% and δc = 3.7%), The films are of 50 nm thick as obtained from the X-ray reflectivity (XRR) data by fitting using Parratt formalism [15] and shown in Fig. 1(b). The surface morphology of the TiO_2 thin films were investigated by atomic force microscopy (AFM). The AFM images of selected 2×2 square micrometres area of the as-deposited (AD)and 600°C annealed films are shown in Fig. 1(c). All the films display a smooth surface with rms roughness ranging from 1.54 to 3.00 nm. In particular, annealed film forms grains defined by crystalline domains compared to rather uniform distribution of particles in the AD film. The low RMS roughness values imply a formation of the smoother and more homogeneous surface. We have used the poly- crystalline anatase thin film for all further measurements, including nonlinear optical characterization.

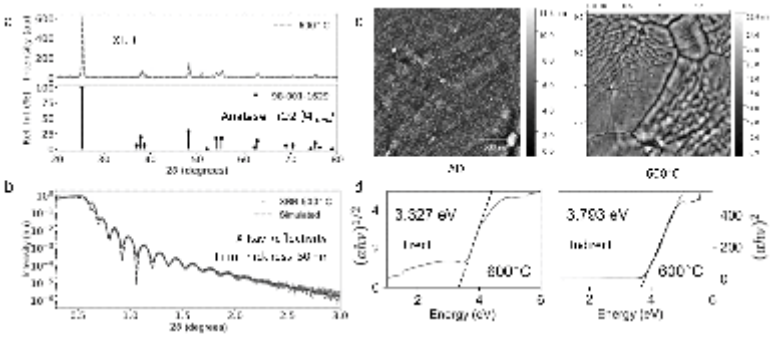

Figure 1: Characterization of sputter deposited TiO2 thin films: (a) XRD spectra of the 600°C annealed thin films and the corresponding matched pattern from the crystallographic open database (b). X-Ray Reflectivity (XRR) of the thin thin film and fitting using Parratt formalism to determine the thickness (c) surface morphology of the as-deposited(AD) and 600°C annealed films using AFM (d) Tau plot derived from the UV -Visible absorption to determine indirect and direct band gaps.

The fundamental and optical gap (direct gap) of TiO_2 film is determined from the optical absorption spectra by the Tauc analysis. The Tauc plots for 600°C thin films are shown in Fig. 1(d). We calculate indirect and direct gaps of 3.327 and 3.793 eV, respectively. The indirect and direct band gaps obtained using density functional theory (DFT) is 2.11 and 2.15 eV respectively, which is underestimated compared to accepted experimental values and our measurements in the present work. The underestimation of bandgap is a result of the well-know "band-gap problem" of DFT when PBE exchange-correlation functionals are used to represent electron-electron interactions [16].

The nonlinear absorption and refraction of TiO_2 have been measured using open and closed-aperture z-scan [11] experiments, respectively. The experiments are carried using 520

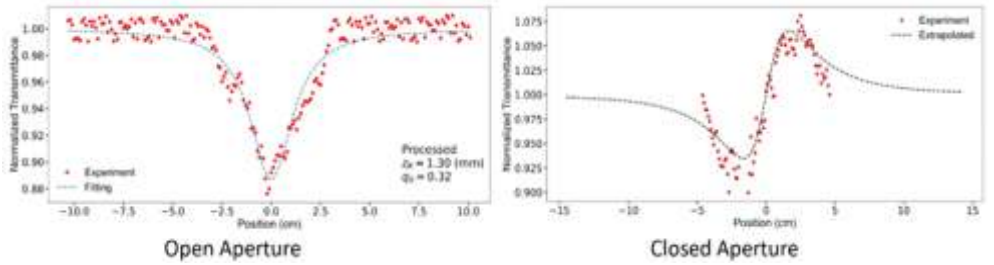

Figure 2: The Open aperture and closed-aperture z-scan transmittance spectra of anatase TiO_2 for 520 nmNonlinear absorption and refraction of TiO_2: Z-scan

nm (2.388 eV), 80 fs pulses and 1.35×10^{11} W/cm^2 peak intensity. Since the synthesized film has a direct gap of 3.793 eV, the measured nonlinearities are non-resonant. The open and closed-aperture transmittance is given in Fig. 2.We observed significant changes (10-15%) in the transmittance under open and closed aperture conditions with peak intensities as small as ~10^{11} W/cm^2. We estimate nonlinear absorption coefficient B= 8.28×10^{-7}cm/W at 520 nm from open aperture spectra. The closed aperture spectrum is characterized by a positive value for the nonlinear refractive index arising due to the self-focussing. From the closed-aperture spectra we extract the nonlinear refractive index $n_2 = 3.65\times10^{-12}$cm^2/W TiO_2 thin films.

Ab-initio modelling of Intense light-matter interaction and ultrafast dynamics

The fundamental microscopic mechanism governing the strong-field light-matter interactions in TiO_2 is investigated using ab-initio simulations based on the time-dependent density functional theory (TDDFT). The electronic motion under a given potential is described by the evolution of single-particle orbitals (Kohn- Sham orbitals) given by the time-dependent Kohn-Sham equation (TDKS). TDKS can be viewed as an alternative formulation of time-dependent quantum mechanics. Still, in contrast to the standard approach that relies on wave functions and the many-body Schrödinger equation, its primary variable is the one-body electron density. From the density obtained by TDKS, we obtain the time-dependent polarizability *p(t)* essentially contains all information of the system interacting with the external

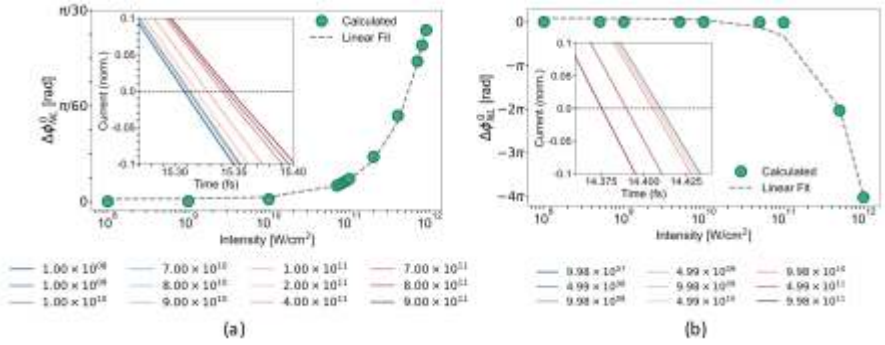

Figure 3. The intensity dependence of maximum accumulated phase shift $\Delta\phi^{\Omega}_{2\omega}$ of the photo-induced current at 800 nm (a) and 400 nm (b). Due to the resonant excitation at 400 nm the $\Delta\phi^{\Omega}_{2\omega}$ at 400 nm is larger and negative compared to that at 800 nm.

field. We apply TDDFT to describe the nonlinear weak-field and non-perturbative electron dynamics of TiO_2 induced by intense ultrashort laser pulses.

In the following, the microscopic electron dynamics leading to n_2 measured from z-scan is discussed. Note that the experiments are performed at 520 nm (2.388 eV), which is a non-resonant excitation for the thin film with a direct gap of 3.793 eV. In the simulations, due to the bandgap underestimation, the dynamics is shown at 400 nm (3.10 eV) to represent a typical resonant excitation (linear) regime and 800 nm (1.55 eV) to represent a typical non-resonant bound electronic (perturbative) nonlinearity. Note that beyond the threshold intensity, two-photon absorption at 800 nm can create free carriers.

The motion of the electrons in response to the electric field of the pulse induces electric currents in the material. For weak electric fields, typically in the beginning of the laser pulse, the photo-induced current is in phase. As the electric field of the given pulse increases in magnitude, the induced current starts accumulating a phase shift. The maximum phase shift () occurs at the zero-crossing of the pulse, whose intensity dependence is shown in Fig. 3 (a) and (b). The phase shift is computed from the time delay of the current by comparing it to that at an intensity of 1x10 W/cm2 (reference). Fig. 3 (a) depicts the phase variation at 800 nm, which is far-off resonant and (b) represents the phase variation at a resonant case of 400 nm (Optical gap = 2.15 eV). The increase in phase shift observed can be related to the optical Kerr effect. For 800 nm pulses the phase shift increases in linear proportion with intensity such that with $m = 1.06\times10^{-13}$ cm^2/W for 800 nm, where k=2 / and l = 3.79 A is the propagation length, the nonlinear refractive index $n_2 = 3.54\times10^{-11}$ cm^2/W can be extracted. This is an order of magnitude larger than the $n_2 = 3.65\times10^{-12}$ cm^2/W measured for off-resonant 520 nm. Interestingly, the n_2 calculated for the 400 nm pulses is -2.16×10^{-9} cm^2/W, which is larger than that obtained for 800 nm pulses and is negative too.

The sign reversal of n2 from positive to negative when the probe wavelength changes from 800 nm and 400 nm, respectively, signifies fundamentally distinct mechanism at play.To understand further, we look at the energy transfer dynamics at these wavelengths shown in Fig. 4(a). Non-resonant excitation at 800 nm with weak pulses creates bound electrons. The interaction with bound electrons produces the characteristic energy oscillations synchronously with the pulse's electric field, as shown for 1×10^{-10} W/ cm^2 laser pulses. Under these conditions, for the lack of any real excitations, the absorbed energy is released to the laser pulse when the

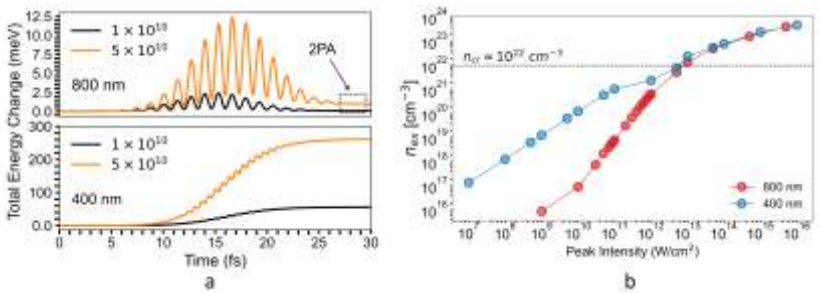

Figure 4. (a) Energy transfer dynamics of the interaction of TiO_2 and 30 fs pulse of 800 nm and 400 nm wavelengths. At 800 nm, excitation with weak pulses creates bound electrons causing energy to change synchronously with the electric field. Two-photon absorption will create free electrons at higher intensities. The energy at 400 nm is due to resonant excitation. (b). The variation of excited electron density with incident intensity. n_{cr} represents the critical carrier density.

pulse leaves the material. On the contrary, the resonant single-photon absorption at 400 nm creates free carriers in the conduction band, further refracting the incoming pulse. Here, the energy of the system grows in linear proportion to the incident intensity as shown for the typical cases of two peak intensities in Fig. 4 (a). It is to be noted that, at higher peak intensities [eg. for 1×10^{-10} W/ cm^2 in Fig. 4(a)] two-photon absorption (2PA) at 800 nm will also contribute to free carriers.However, it remains very low at all intensities considered here, for determining n_2.

The (irreversible) excited electron density for the interaction at 800 nm and 400 nm at different intensities is shown in Fig. 4 (b). The resonant excitation at 400 nm creates a greater number of free carriers than that at 800 nm photons. Even for weak intensities in the range 10^9-10^{11} W/cm^2, the free carrier density at 400 nm is about three orders larger than 2PA-generated carrier density at 800 nm. Though the excited electron density at 800 nm grows faster than 400 nm as the intensity increases due to contribution from 2PA generated carriers, it remains lower than the carrier density at 400 nm. This is attributed to the large magnitude of n_2 at 400 nm compared to 800 nm. We find that the nonlinear refraction at 400 nm is primarily due to excited free carriers, while that at 800 nm is predominantly due to bound electrons in the perturbative regime. This explains the change of sign of n_2 as the bound carriers lead to a positive n_2 for 800 nm while free carriers give rise to a negative value of n_2 for 400 nm as observed in experiments as well as in simulations.

Conclusion

We systematically analyzed the nonlinear optical properties of anatase TiO_2 by combining femtosecond z-scan experiments and state-of-the art ab-initio calculations. The z-scan yields the nonlinear refractive index of anatase $n_2 = 3.65\times10^{-12}$ cm^2/W at non-resonant 520 nm. TDDFT simulations at resonant (400 nm)and non-resonant (800 nm) wavelengths gives an n_2 in reasonable agreement with the experiments. Simulations also reveal that bound nonlinear refraction is mainly due to bound electrons and free electrons at 800 and 400 nm respectively. The difference between the experimental and computed values of n_2 be attributed to many factors, including frequency and duration of the laser pulses. The neglect of ionic movement in the TDDFT formalism and bandgap underestimation by the GGA functional used in the study are also potential sources for discrepancy. Within these limitations of the study, we observe that the non-resonant, perturbative interactions at 800 nm and the accompanying nonlinear phase shift observed in TiO_2 well below the damage threshold hold promises incorporating TiO_2 in optical switches. The present study could guide the further exploration of laser parameters and structural and defect engineering of TiO_2 with tailored properties for specific applications, potentially leading to improved performance in nonlinear photonics devices.

References

1. Zhu, D., Yu, H., Patel, D., Doussiere, P., Mahalingam, H., Lin, W., &Akulova, Y. (2022). Integrated Silicon Photonics Transmitters for 100 Gb/s, 400 Gb/s, 800 Gb/s and beyond. Optica Publishing Group, NeTu1D.3.
2. Markov, I. L. (2014). Limits on fundamental limits to computation. Nature, 512, 147–154.
3. Yafet, Y., &Yablonovitch, E. (1991). Virtual photoconductivity due to intense optical

radiation transmitted through a semiconductor. Phys. Rev. B, 43(15), 12480–12489.

4. Leuthold, J., Koos, C., &Freude, W. (2010). Nonlinear silicon photonics. Nat. Photonics, 4, 535–544.
5. MohdRusdi, M. F., Latiff, A. A., Paul, M. C., Das, S., Dhar, A., Ahmad, H., & Harun, S. W. (2017). Titanium Dioxide (TiO_2) film as a new saturable absorber for generating mode-locked Thulium-Holmium doped all-fiber laser. Opt. Laser Technol., 89, 16–20.
6. Evans, C. C., Bradley, J. D. B., Martí-Panameño, E. A., & Mazur, E. (2012). Mixed two- and three-photon absorption in bulk rutile (TiO_2) around 800 nm. Opt. Express, 20(3), 3118–3128.
7. Bradley, J. D. B., Evans, C. C., Choy, J. T., Reshef, O., Deotare, P. B., Parsy, F., ...Mazur, E. (2012). Submicrometer-wide amorphous and polycrystalline anatase TiO_2 waveguides for microphotonic devices. Opt. Express, 20(21), 23821–23831.
8. Elim, H. I., Ji, W., Yuwono, A. H., Xue, J. M., & Wang, J. (2003). Ultrafast optical nonlinearity in poly(methylmethacrylate)-TiO_2 nanocomposites. Appl. Phys. Lett., 82(16), 2691–2693.
9. Castillo-Matadamas, H. A., Lima-García, R. M., & Quintero-Torres, R. (2010). Ultrafast nonlinear optical properties of TiO_2 nanoclusters at 850 nm. Journal of Modern Optics, 57(12), 1100-1106.
10. Milam, D. (1998). Review and assessment of measured values of the nonlinear refractive-index coefficient of fused silica. Appl. Opt., 37(3), 546–550.
11. Häyrinen, M., Roussey, M., Gandhi, V., Stenberg, P., Säynätjoki, A., Karvonen, L., ...Honkanen, S. (2014). Low-Loss Titanium Dioxide Strip Waveguides Fabricated by Atomic Layer Deposition. J. Lightwave Technol., 32(2), 208–212.
12. Qiu, F., Spring, A. M., & Yokoyama, S. (2015). Athermal and High-Q Hybrid TiO2–Si3N4 Ring Resonator via an Etching-Free Fabrication Technique. ACS Photonics, 2(3), 405–409.
13. Van Stryland EW, Hagan DJ. "Measuring nonlinear refraction and its dispersion" In Self-focusing: Past and Present: Fundamentals and Prospects 2009 Jan 1 (pp. 573-591). New York, NY: Springer New York.
14. E. Runge and E. K. Gross, "Density-functional theory for time-dependent systems", *Physical Review Letters* 52, 997 (1984).
15. Parratt, L. G. (1954). Surface Studies of Solids by Total Reflection of X-Rays. Phys. Rev., 95(2), 359–369.
16. Kohn, W., & Sham, L. J. (1965). Self-Consistent Equations Including Exchange and Correlation Effects. Phys. Rev., 140(4A), A1133–A1138.

TH-05

6Study of high voltage discharge and optimisation of electrical parameters in copper vapour laser

Dheeraj Kumar Singh[*1, 2]

[1]Homi Bhabha National Institute, Anushaktinagar, Mumbai, India

[2]Beam Technology Development Group, Bhabha Atomic Research Centre,Mumbai, India

*Email: dheeraj@barc.gov.in

Introduction

The CVL is a widely used efficient laser known for its high power. It is used in several applications such as laser isotope separation, material processing, high-speed photography, and communication [1,2]. The CVL has come a long way since its invention by Walter, with improvements in performance and technology [2-4]. However, research has shown that the average power scaling of CVLs is limited by the residual electron density between high-voltagedischarge pulses [4]. A different type of CVL called the Kinetically Enhanced CVL (KE-CVL) has emerged which reduces the residual electron density by using trace gas additives such as HCl and H_2 leading to improved optical performance and the ability to operate at high pulse repetition rates [4,5]. However, these lasersrequire storage of toxic and corrosive gas which can be hazardous if leaked.Additionally, there was a gap in the study related to the impact of electrode geometry on the CVL performance such as optical output power, discharge stability, efficiency, impedance, EMI etc. Jitter requirements are stringent in some applications of CVL and the parameters contributing to jitter are not well quantified in the literature. Finally, in the elemental CVL, the optical power drops during laser operation due to an impedance mismatch with its power supply, which must be investigated and checked. In this work, the above scientific and technological problems of the CVL are studied in detail and some innovative solutions are implemented. The results obtained are described below.

Improvement in the laser performance by electrode geometry

The current pulse in CVL appears before the breakdown of voltage in the laser discharge tube, as depicted in Fig. 1. This current, which begins approximately 50-70 nano-seconds prior to the voltage breakdown, was referred to as "phantom current" by Hogan (indicated as "x" in Fig. 1) [6]. The magnitude of this current can be up to 70% of the peak breakdown current and is due to free electrons generated in the previous excitation pulse that failed to recombine during the inter-pulse period.

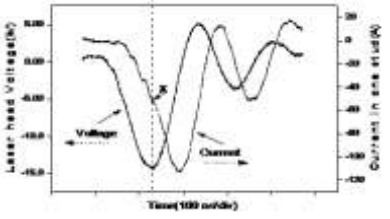

Fig. 1. Phantom current observed from voltage and current waveform (Stable discharge)

In KE-CVL, the phantom current is reduced by eliminating pre-pulse electrons using complex and hazardous chemical means. This necessitates finding other means of reducing the phantom current in the elemental CVL. This research presents an effective and simple approach to reduce the phantom current in the CVL by changing the electrode pins configuration. Additionally, this approach offered better discharge stability which is crucial in the application having stringent jitter requirements in CVL [7].

Following high-voltage excitation in the laser, free electrons generated during the process recombine with ions after the excitation pulse. The rate of recombination is directly proportional to the density of charged ions and electron density, while inversely proportional to electron temperature and ion charge [8]. To maximize the rate of recombination during the afterglow, the best approach is to reduce the electron temperature [4].

The metallic pins in the electrodes play a crucial role in facilitating the discharge in the long discharge tube in CVLs. The sharp points of these pins increase the electric field in their vicinity, creating a localized region of enhanced electric fields. This phenomenon, known as field enhancement, is not dependent on the applied voltage or external field but instead is influenced by the geometrical configurations of the pins, such as the height, tip radius, and distance between them [9-10]. The increase in electric fields can result in higher phantom current, or residual electron density, due to an increase in electron temperature.

In this research, a correlation has been established between phantom current and the electrode pin configuration. These findings suggest that by utilizing appropriate electrode configuration, it is possible to reduce the phantom current in CVLs and improve its performance.This has been experimentally validated by conducting experiments with three different electrode configurations: 36 pins, 8 pins, and 0 pin (without discharge pins). During each experiment, both the high-voltage and low-voltage electrodes had the same pin configuration. The discharge pin holder of the electrodes had an inner diameter of 39mm and an outer diameter of 53mm, with a pitch circle diameter of 46mm. The discharge pins were made from tungsten rods, with a diameter of 3mm, a length of 18mm, and a sharp edge (tip) diameter of approximately 0.01mm.

The electric field enhancement continues to grow with the addition of more pins until the distance between the pins equals their height. Beyond this, increasing the number of pins decreases the distance between them, which increases the shielding factor and decreases the overall electric field enhancement [9]. This led to the selection of 8 pins, where the separation between the pins is nearly equal to their height, beyond which the shielding factor will rise. To demonstrate the impact of maximum shielding, 36 pins were chosen, beyond which increasing the pins was not mechanically feasible. The flat electrode or the electrode with no pins was selected to observe the effect without field enhancement.

The comparison of three different pin configurations showed that the 8-pin configuration, which has the highest electric field enhancement and phantom current, resulted in lower output power (27.7 W) in a plane-plane mirror oscillator configuration of the CVL. The best performance was seen with the zero-pin configuration, which produced an average optical output power of 36.6 W, while the 36-pin configuration produced 35.4 W of optical power.The experimental observation has been compared with the KE-CVL [5] in which various amounts of gas additives (HCL or HBr etc.) were added to the discharge tube to reduce pre-discharge electron density (phantom current). The reported waveforms obtained for KE-CVL is compared

with the corresponding voltage, current and optical pulse obtained from elemental CVL with different electrode pin configuration. It was found in both approaches that by reducing the phantom current voltage hold off is considerably higher, the onset of the optical pulse happens earlier with respect to the peak of the current pulse, and the opticalpulse width becomes wider.

The decline in electric field enhancement not only increases optical power but also lessens thermal instability in the CVL by preventing discharge constriction. In a glow-discharge plasma, the cathode region faces a high electric field and thermal loading [11]. A higher field enhances local charge generation, reducing cathode fall width at a constant pressure. Narrower cathode fall results in a highly localized electric field at the same voltage, causing high current density and discharge constriction, increasing thermal load and initiating instability.Localized heating raises the gas temperature and lowers density, enhancing ionization and electron density. Even a small temperature fluctuation of 10% to 20% can trigger instability [12].So, a 0-pin electrode configuration, without localized field enhancement, improves optical performance and discharge stability.

Jitter reduction in solid-state pulse power supply of CVL

Previously thyratron-based pulse power supply was employed to excite CVL. However, due to the limited operational lifespan of thyratron and advancements in semiconductor technologies,IGBT-based pulse power supplies are now used. In IGBT-based pulse power supplies, a magnetic pulse compression (MPC) circuit is used to reduce the voltage pulse rise time at the output, which can lead to increased jitter [14,15]. This jitter makes it challenging to achieve temporal synchronization of the various lasers required in a Master Oscillator Power Amplifier (MOPA) configuration [2]. Jitter also impacts the extraction of output power from the amplifier unit and its stability in the MOPA configuration of CVL. Since multiple parameters contribute to output jitter in pulse power supply simultaneously, it is difficult to determine experimentally the individual contribution of each parameter. Typically, the total jitter is measured experimentally, and to the best of our knowledge, no method or model exists for quantifying the jitter due to individual parameters in the pulse power supply of CVL.

A simulation model was developed to assess and quantify the parameters that contribute to jitter in the pulse power supply. The study showed that variations in load impedance are the dominant contributor to jitter. This variation in load impedance results in fluctuations in residual voltage on the resonant charging capacitor, which subsequently impacts the peak capacitor voltage in the next cycle. The study was used to demonstrate that modifying the electrical circuit to reduce the impact of dynamic loads can reduce the output current jitter of the pulse power supply from ~ 47ns to ~ 18ns. The same model was used to study the dynamics of MPC stages.

Study of discharge plasma impedance of CVL and improvement in laser performance

The electrical discharge of a CVL can be analyzed as an RLC circuit in the immediate aftermath of the breakdown. The discharge plasma forms the resistance-inductance (R-L) part and the capacitance is provided by the peaking capacitor of the pulse generation unit (PGU) [16-18]. The peaking capacitor is mounted close to the laser head and hence the stray inductance can be neglected. Invoking the concept of time domain analysis in step response of a series RLC circuit, the discharge plasma parameterswere calculated. Fig. 2. shows the voltage waveform across the laser head and the red plot shows the step input.It was found that the laser head

inductance (0.47 μH) remains almost constant and only the laser resistance value varies. From the theory of the underdamped RLC circuit and the experimentally obtained voltage waveform, laser resistance is calculated for different operating conditions of the CVL such as different operating voltage, different electrode geometry, different laser pressure etc. and the explanation is provided for the variation in laser resistance. It was found that 0 0-pin electrode offers the highest resistance (16 ?) and improved impedance matching as compared to 8-pins and 36-pin electrode geometry (8 Pins – 12 ? , 36 pins - 13 ?).

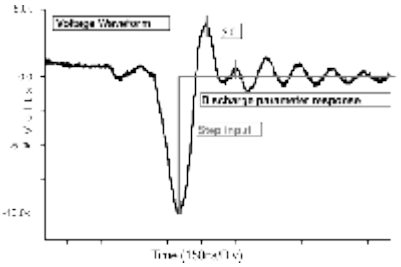

Fig 2. The voltage pulse across the laser head

In this thesis, a new method for controlling the discharge plasma impedance by trigger modulation was proposed and implemented. The rate at which charge carriers recombine can be increased by extending the recombination time through controlled interruptions in the high-voltagedischarge pulse. The timer card is modified to miss trigger pulses for a short duration (5ms), providing more time for the charge carrier to recombine. The modified timer card and trigger pulse missing are shown in Fig.3 and Fig. 4. The green pulse (top waveform) in Fig. 4 shows the modulating signal and the yellow signal (bottom waveform) shows the modified trigger waveform that is applied to the switch. For the duration during which no trigger is present, there will be the absence of high voltage across the laser discharge tube. The absence of high-voltage discharge for a short time reduces the electron temperature and leads to an increase in the recombination rate. By missing 0.1% of the discharge pulse, the drop in the laser optical power is reduced by 10% at the end of 6 hours of CVL operation due to improved impedance matching.

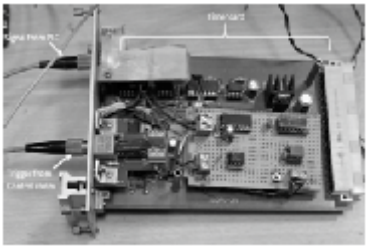

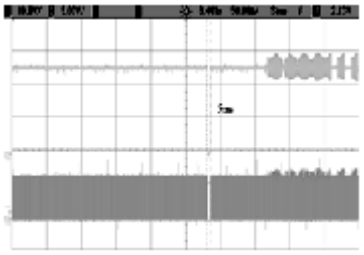

Fig. 3. Modified timer card Fig. 4. The missed trigger pulse output of the modified timer card.

This study reveals a correlation between laser parameters and conducted noise. Electrically excited CVLs with high power and repetition rates are found to be significant sources of both radiated and conducted electromagnetic interference (EMI). To generate copper vapor and achieve population inversion, the CVL requires a high-voltage pulse and high current pulse of

very sharp rise time in the range of a few hundred ns. The high voltage and current, combined with the discharge in the laser tube, create substantial EMI that can affect the performance of nearby electronic devices. Reported literature on electromagnetic compatibility from CVLs has only examined the level of conducted and radiated emissions from the CVL, without exploring the relationship between conducted noise and CVL parameters. Thisstudy provides a comprehensive investigation of the conducted electromagnetic interference (EMI) resulting from the CVL system, as well as its impact on the laser performance. It is demonstrated that the conducted noise is related to the laser impedance and is directly proportional to the magnitude of load mismatch. To mitigate this issue, a straightforward and effective technique is presented to reduce the conducted noise from the CVL. Additionally, the correlation between the laser electrode pin configurations and the conducted noise is also presented in detail.

It is found that the conducted noise increases with an increase in the impedance mismatch between the laser head and pulse power supply. The energy from this mismatch is radiated and coupled with the wire, propagating conductively. Moreover, due to the presence of a high-voltage discharge, there is a dominant common mode noise in the system. To mitigate this, a simple approach is proposed whereby the impedance mismatch is reduced by increasing the laser resistance through the removal of electrode pins. The 0-pin electrode configuration results in higher laser resistance and brings the system closer to a critically damped condition, thereby reducing the radiated noise from the CVL. Transitioning from an 8-pin to a 0-pin electrode configuration, with a corresponding increase in laser resistance from approximately 12? to around 16? , resulted in a 2 dBμV decrease in conducted noise at the output of the DC supply.

Conclusions

This research links CVL's phantom current to electrode geometry, aiming to boost laser performance. By altering electrode pin configurations, phantom current is reduced, enhancing output power, beam profile, and pulse duration. In the past, only chemicals reduced the phantom current in KE-CVL lasers, and this research compares the results with KE-CVL. It shows a 71% to 57% phantom current drop when changing from an 8-pin to a 0-pin configuration. In the plane-plane resonator, optical power increased from 27.7 W to 36.6 W, and the pulse duration extended from 35 ns to 75 ns switching from 8 pins to 0 pins.Electrode geometry's impact on discharge stability and performance is rarely studied. The thesis finds that the eight-pin electrode, with high electric field enhancement, can initiate thermal instability at higher laser pressure compared to 0 and 36-pin configurations. The research also examines radiated and conducted EMI in high-power, high-repetition-rate electrically excited CVL, showing that impedance mismatch causes EMI via load reflection. Changing the electrode pin configuration from 8 pins to 0 pins reduced the conducted EMI by 2 dBμV.The thesis presents a new method for calculating laser discharge electrical parameters, emphasizing the benefits of the 0-pin electrode configuration.It also covers the jitter in CVL's pulsed power supply, demonstrating how to reduce the jitter from 47 ns to 18 ns by dissipating residual voltage on the capacitor before the next charging pulse.

Bibliography

1. BateninV. M., BuchanovV. V., et.al; High-brightness Metal Vapour Lasers, CRC Press, (**2017**).
2. Little C. E.; Metal Vapor Laser, Wiley Publication, (**1999**).
3. Walter W., Solimene N., PiltchM., Gould G.; 6C3 - Efficient pulsed gas discharge lasers, IEEE Journal of Quantum Electronics, **2**, Issue 9, 474 - 479 (**1966**).
4. Withford Michael J., Brown Daniel J. W., Mildren R. P., et al, Advances in copper laser technology: Kinetic enhancement; progress in quantum electronics **28,** 165-196 (**2004**).
5. Jones D. R., Halliwell S. N., Little C. E.; Influence of remanent electron density on the performance of copper Hybrid lasers, Opt. Comm. **111,** 394-402, (**1994**).
6. Hogan G. P., Webb C.E.; Pre-ionization and discharge breakdown in the copper vapour laser: the phantom current, Opt. Comm. **117,** 570-579 (**1995**).
7. Chang J. J., Arnold P. A., Warner B. E.; Improvement of high-current large-volume discharge with profiled hollow-cathode electrodes, IEEE Transactions on Plasma Science, **25**, 2, 392 - 399 (**1997**).
8. Zhukov V. V., Latush E. L., MikhalevskiiV. S., Sem M. F.;Recombination lasers utilizing vapors of chemical elements. I. Principles of achieving simulated emission under recombination conditions; Sov. J. Quantum Electron., **7,** 704. (**1977**).
9. Biswas D., Rudra R.; Shielding effects in random large area field emitters, the field enhancement factor distribution, and current calculation; Physics of Plasma,**25**, 083105, (**2018**).
10. Harris J. R., Jensen K. L., et al; Shielding in ungated field emitter arrays, Applied physics letters **106**, 201603 (**2015**).
11. RaizerY. P.; Gas Discharge Physics, Germany, Springer-Verlag, (**1991**).
12. Francis G.; The Glow discharge at low pressure, Springer, (**1956**).
13. Ghodke D. V. and Muralikrishnan K.; All solid-state pulsed power supply for copper vapor laser, RRCAT Newsletter, **22**, Issue-1,26-32. (**2009**).
14. Kumar D. D. P., GantayetL. M., et al;Analysis of temporal jitter in a copper vapor laser system, Rev. Sci. Instrum. **83**, 025105 (**2012**).
15. Mishra R. K., Raju D. V.S.,Nakhe S. V.; A novel and robust circuit for jitter reduction in copper vapor laser system, Rev. Sci. Instrum. **86**,116107 (**2015**).
16. Biswal R., Agrawal P. K., Mishra G. K., et al; Analysis of pulsed discharge characteristics of solid-state switch (IGBT) based 16 kHz repetition rate, 100w average power copper–HBr lasers, Journal of Russian Laser Research, **33** , 319-335,(**2012**).
17. AstadjovD. M., VuchkovN. K., SabotinovN. V.; Parametric study of the CuBr laser with hydrogen additives, IEEE J. Quantum Electron., **24**, pp. 1927-1935, (**1988**).
18. BlauhP.; Analysis of the Impedance of a Co, axial Large-B ore Copper-Vapor Laser, IEEE Journal of Quantum Electronics, **30**, Issue: 3, 763-769, (**1994**).

TH-06

Studies on quantum interference effects in atomic ensemble

Rita Behera Sahoo
Advanced tunable laser application division
Bhabha Atomic Research Centre, Mumbai
Email: rita.behera@gmail.com

Quantum interference is a coherent phenomenon where the interaction of multiple light field with an atomic ensemble through common level(s) leads to observation that defy the classical expectations. Specifically, quantum interference and the formation of superposition of states due to the coherent interaction of the atomic system with light fields can be combined for the realization of ultra-narrow resonances. For a simplistic three level system, the dipole allowed transitions are judiciously coupled by the light field that inherently makes the transition between the uncoupled state dipole forbidden. The width of these resonances is not limited by the rapid spontaneous emission between the coupled states but determined by the long-lived lifetime between the uncoupled states. The resultant ultra-narrow resonance is the basis for the operation of quantum devices like atomic clock and magnetometer. The atomic susceptibility exhibits resonant enhancement due to quantum interference at multi-photon Raman resonances. It changes the absorptive and optical activity properties of atoms over a very narrow frequency span of the light field. This provides a platform to study many aspects of non-linear physics while working with very low light field. The physical process provides the foundation for slow and super-luminal light propagation, addressing higher order susceptibility while working at low light intensity, lasing without population inversion, quantum information processing and other fundamental studies. Thus, it is a rich field encompassing both applications to advance technologies as well as study on fundamental physics and is the motivation behind the thesis.

The light field gets maximally absorbed as the single photon resonance condition is established during its interaction with an atomic ensemble. The process is associated with anomalous dispersion at the resonance frequency and normal dispersion for off-resonant light field. It poses difficulty in accessing the subtle physical processes associated with anomalous dispersion as the light field gets significantly attenuated at atomic resonance. These conventional effects can be designed and controlled by two-photon processes. The light field can show enhanced absorption or transmission by suitably configuring the associated field. Further, the fascinating area of anomalous dispersion can be realized without significant absorption of the light field.

In addition, the phase relationship between the participating light fields plays a crucial role in determining the outcome of the processes involving quantum interference. Thus, phase locked laser systems are appropriate for such investigation. The simultaneous interaction of the two phase-coherent photon leads to the formation of superposition of bare atomic states. The resultant states originate from the constructive and destructive quantum interference. The state generated due to destructive interference is not coupled to the excited state and is termed as dark

state. Consequently, the light field shows enhanced transmission. Similarly, the state due to constructive interference is resonantly coupled to the excited and is termed as bright state. However, the population in the bright state gets progressively transferred to the dark state whereas, the reverse path is not allowed. The bright state becomes empty as all the population gets confined in the dark state. Since the atomic population gets coherently trapped in the dark state, the process is also known as coherent population trapping (CPT). The spectral width of the enhanced transmission signal due to CPT is not limited by the natural linewidth rather it depends upon the lifetime of the superposition of states. Since the transition between the dark and bright state is dipole forbidden, the resonance width is very narrow. The resultant ultra-narrow width of the resonance plays the central role in the operation of atomic clock and magnetometer.

The study of the fundamental processes involving quantum interference provides the basic motivation to focused our research on three-axis atomic magnetometry as an application of quantum interference effect. The critical requirement for the compact operation of the magnetometer is achieved by the single elliptically polarized beam and by in-situ frequency stabilization. Here, the component of elliptically polarized light couples the degenerate Zeeman levels. This provides the competing path for realization of quantum interference. Therefore, the envisaged magnetometry geometry can be an ideal system for space application where restricted overall size and weight of the device is a primary requirement. The methodology for characterization of the three-axis magnetometer using Lissajous plot has been established. The sensitivity of the magnetometer along three orthogonal directions are measured. Bloch equation based theoretical model has been developed with appropriate modifications for providing a description of the associated physical processes. The realistic experimental conditions are incorporated in the model by using suitable assumptions. The validity of the assumptions is discussed. Our calculations are found to be consistent with our experimental observations.

We have also investigated the fundamental aspect of quantum interference in an atomic ensemble near zero magnetic field by using a multi-frequency light field. The frequency components of the light field are phase coherent with each other and are equally spaced in the frequency domain. We report the splitting of the magnetic resonance for atomic ensemble where spin preservation is maintained without increasing the associated homogeneous width of the transition. It is also found that the splitting can be observed only for a specific class of atomic transition coupled with linearly polarized light. Such kind of split profile of the magnetic resonance is not observed for pure circularly polarized light as it does not provide a competing pathway for establishing the quantum interference. Similarly, we study the enhancement of steady state atomic polarization as the separation between the frequency components approaches Larmor's frequency. It gives an apparent splitting of the magnetic resonance. Interestingly, the coupling scheme and physical processes for individual split components are not same. Their different response to single photon detuning as well as to orthogonal magnetic field is established. In order to probe the associated mechanism, we have developed a theoretical model for the interaction of a frequency modulated light field with the atomic system by following density matrix formalism. The model can calculate the steady-state solution using Lindblad master equation and incorporating various experimental parameters.

Further, in order to get a microscopic and a clear picture of the associated mechanism behind the interaction of frequency comb with an atomic ensemble, we have developed a model termed trichromatic field model. The complex interaction of large number of frequency components of a frequency comb simultaneously with an atomic sample is simplified by

truncating it to only three frequencies only. The three frequency components have a definite phase relationship among themselves owing to different laser detuning. The model simulates the interaction of a tri-chromatic field with a simple four level atomic model. The essential attributes of the split profile are consistently calculated using the tri-chromatic model. Moreover, the influence of phase relationship between the trichromatic field can be studied that plays the central role for the disappearance of the odd split components at single photon resonance. These observation opens a window for sub-Doppler single photon spectroscopy. It also provides a platform to investigate the change in optical activity of the atomic medium. The quantum interference leads to enhancement in the optical activity over a narrow frequency span. The measurement of change in optical activity for interaction of multiple light field with an atomic system is investigated. Similar to the absorptive response, the optical activity also shows resonance structure as the frequency separation between the light fields approaches (sub) harmonics of the Larmor's frequency. The optical activity can originate from a variety of processes like resonant circular birefringence, off-resonant circular birefringence, resonant circular dichroism, off-resonant circular dichroism etc. The trichromatic field model is used to calculate these responses as a function of the Larmor's frequency. The distinct spectral profile of these processes for different ellipticity of the light field is investigated. The overall experimental observation is impacted by all these processes and it is challenging to separate effect of each of these processes individually. However, the spectral profile associated with these processes are distinct and their relative contribution can be controlled by changing the ellipticity of the light field. The spectral profile under different experimental conditions are compared with the calculated profiles to get the knowledge of the associated processes. The investigation provides a path to incorporate Zeeman coherence in frequency comb spectroscopy.

In chapter-1, we introduce various types of magnetometer. This includes brief description of the operation principle of Fluxgate, proton precession, Super-conducting Quantum interference devices (SQUIDs) based magnetometer. The pros and cons associated with these magnetometers are discussed. The Quantum interference-based atomic magnetometer is another technique that relies on coherent interaction of the light field with the atom. It operates near room temperature and can be made very compact in size. The other advantages include high sensitivity and in-situ field calibration with respect to atomic constant. It has promising prospect for a variety of applications.

In chapter-2, a brief theoretical background on the quantum interference effect is introduced. The atomic structure of the element of interest and its interaction with external electric / magnetic field is discussed. The interaction of atoms with light field is formulated using a semi-classical approach. The importance of dipole approximation and rotating wave approximation in the evolution of the states is explained. The density-matrix-based calculation procedure involving interaction of two-level and three-level atomic system with the light field is described. The contrasting spectral profile for absorption and polarization rotation is discussed and is shown in Fig.1.

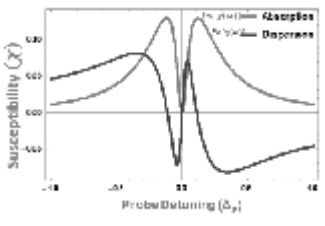

Fig.1Three level susceptibility as a function of two-photon detuning.

In chapter-3, we describe the operation of the three-axis atomic magnetometer based on Hanle-kind of resonance. A detailed explanation of the utilized experimental set-up(Fig.2), methods for realizing zero magnetic field, calibration of magnetic coils, methods for in-situ laser frequency stabilization of the magnetometer is discussed.

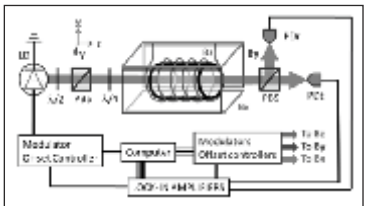

Fig. 2Experimental set-up

The single beam operation for the realization of three axis magnetic field is carried out by signals as shown in Fig.3.The use of single elliptically polarized resonant light performs the dual job of polarizing and monitoring the atomic spin simultaneously. A theoretical model is developed using Bloch equation to describe the working of magnetometer. The validity of the two assumptions i.e. rotation of equilibrium spin polarization with respect to laser beam and equivalence of the oscillating magnetic field as a DC magnetic field is explained. The other studies include realization of large dynamic range, measurement of sensitivity and crosstalk between three orthogonal directions using Lissajous figures.

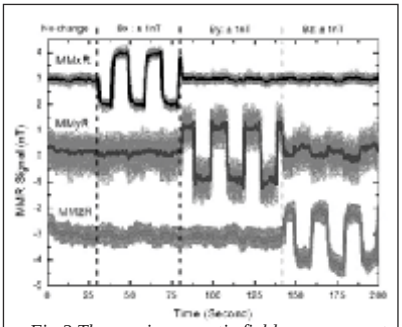

Fig.3 Three axis magnetic field measurement by MMxR, MMyR and MMzR signals

In chapter-4, we studied the interaction of frequency modulated light field with an atomic sample near zero magnetic field. The development of a steady-state atomic polarization at the (sub) harmonics of the Larmor's frequency is observed by using Magnetometric Method(MM). The MM method measures the steady state atomic polarization in contrast to the earlier reported procedure that extract the oscillating atomic polarization. The appearance of the magnetic resonances at the (sub) harmonics of the Larmor's frequency as shown in Fig.4 and its parametric dependence is studied in detail. A theoretical framework based on density matrix for addressing the interaction of the frequency modulated light with atomic ensemble is discussed. The various experimental observations like spectral profile of magnetic resonances for different Rubidium transitions, observation of apparent splitting of the magnetic resonance, dependence of the split magnetic resonance on laser polarization, dependence of split profile on laser modulation parameters, laser detuning dependence of the split profile, apparent intermittent magnetic resonance at higher modulation amplitude, dependency of the split profile on transverse magnetic field are presented. The calculated spectral profiles are consistent with our experimental observations.

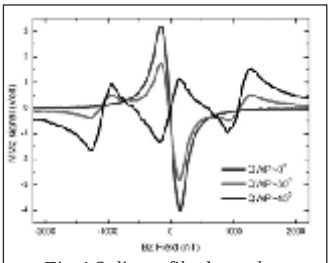

Fig.4 Split profile dependency with laser polarization

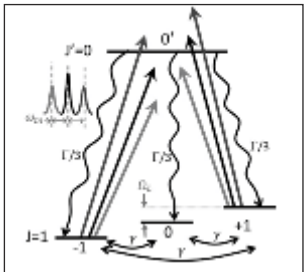

Fig.5 A simplified trichromatic field to represent the complex interaction of NBFC with the atomic ensemble

In chapter-5, a different approach (compared to chapter-4) is established to study the interaction of frequency modulated light with an atomic ensemble. The resemblance between the frequency modulated light and a narrow band frequency comb (NBFC) is discussed. The role of individual teeth component of NBFC for the enhancement of optical activity at multi-photon resonance is explained. The steady state atomic polarization assisted by quantum interference and the interplay of optical pumping is discussed. It is facilitated by developing a theoretical model using Lindblad master equation where the NBFC is approximated to a trichromatic field. The simplified trichromatic model (as shown by Fig.5) provides a microscopic picture of underlying mechanism. The model successfully explained the detuning dependency of the magnetic resonances by changing the relative phases of the trichromatic field. Further, it also successfully explains the dependence of atomic absorption, nonlinear magneto optic rotation on various experimental parameters. The model is used to calculate the dichroism, birefringence for different detuning of the light field. It provides clues in exploring the underlying physical processes that is responsible for changes in the spectral profile of the optical activity for different experimental parameters. It is found that the observed spectral profile of the reflected light (through the polarization analyzer) is governed by various physical processes like bi-refringence, dichroism, quantum interference assisted enhanced transmission, and Zeeman-state population redistribution.

In chapter-6, we summarize the work carried out in this thesis. The experimental development for study of quantum interference is described as a part of future scope of the work. The cold atom will provide an interesting platform to extend the research work carried out in this thesis. The preliminary development in this direction is presented. The future work will be quantum information processing using ultracold atoms confined in an array of optical tweezer. A brief description on the proposal is be presented. A bibliography of referred article is included at the end of the thesis.

TH-07

Generation and Characterization of Spatially Controlled Structured Light with Exotic Propagation Properties

Vasu Dev
Department of Physics, Indian Institute of Technology Ropar,
Rupnagar, Punjab 140001, India.

Light possesses various spatial and temporal degrees of freedom, such as amplitude, phase, polarization, time, and frequency. Controlling these aspects for generating light with complex field distributions possessing exotic propagation properties, has renewed its interest in numerous applications both in fundamental science as well in applied fields[1]. Due to this there has been growing interest in synthesizing such complex light field distributions, also called as structured light. Typically, the output from a laser consists of a Gaussian distribution, which exhibits physical limitations for various applications. However, with continuous advancements, it has become possible to control the distribution of light in different degrees of freedom[2]. In this thesis, our aim has been to develop simple, cost-effective, and efficient outer-cavity and intra-cavity methods for the generation and characterization of novel spatially structured light with customised intensity and phase distributions as well as possessing exotic propagation properties. In addition to these, our emphasis has also been to improve the quality, resolution, resilience against perturbations, and spectral range of spatially controlled structured light.

Chapter 1 is an introduction to the thesis, where we begin with the role of structured light in the modern world by mentioning its applications in fundamental and applied fields where conventional Gaussian beams pose physical limitations. We have discussed various types of spatially structured light along with their propagation properties, obtained by tailoring light in its various spatial degrees of freedom[1,2,3]. Further, we have discussed the generation of spatially structured light based on various outer-cavity and intra-cavity methods[3]. We have also described the analytical and numerical methods for modelling the laser cavities as well as the propagation and quantification of spatially structured light. We have also provided a brief overview of spatial light modulators including the mechanism for modulating light in the amplitude and phase degrees of freedom.

In **Chapter 2**, we have presented an outer-cavity method for tailoring the light inamplitude degree of freedom to generate high-quality uniform-intensity beams with customized shapes, using diffractive optical elements (DOEs). The phase of DOEs is obtained by an iterative method (modified Gerchberg-Saxton algorithm) that involvesspatial Fourier filtering (Fig. 1)[4]. The obtained DOEs consist of a simple design (smooth phase distribution), which makes them easier to fabricate. An input laser beam with Gaussianintensity distribution illuminates the DOE, and after propagating a certain distance (working distance) transforms into the desired uniform-intensity output beams with customized shapes such as square, annular, rectangular, hollow square, and plus spatial shapes. The quality of the output beams is quantified by calculating root

mean square error (RMSE)with respect to the ideal beams. We have performed a detailed robustness analysis on the quality of shaped output beams against various types of imperfections in an input beam, such as misalignment with respect to DOE, presence of speckle noise, asymmetry, presence of higher order transverse modes, and mismatch of beam sizes. We have found that the shaped output beams with reasonably good quality are obtained over a broad range of imperfections. However, in the case of speckle noise, the quality of shaped output beams can be further improved by an additional external spatial Fourier filter of suitable transmission function. Furthermore, to investigate spectral properties of method, we have designed a DOE for a particular wavelength and illuminated it with an input beam over a broad range of wavelengths. We have found that the quality of shaped output beams remains excellent over a broad spectral range. However, the working distance decreases with an increase in the wavelength[4].

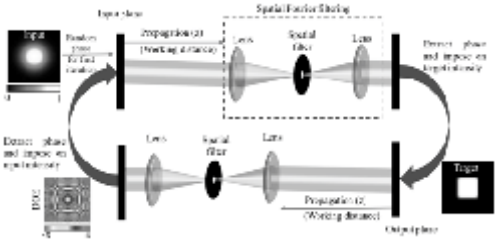

Figure 1. Modified Gerchberg-Saxton algorithm to obtain phase distribution of DOE.

In **Chapter 3**, we have presented tailoring of light in the amplitude and phase degreesof freedom for generating special type of structured light (called aberration laser beams(ALBs)) containing multiple bright lobes and possessing unique propagation features, suchas autofocusing and self-healing in both free space as well as in turbulent media[5].The ALBs are generated, based on an outer-cavity method, using a DOE whose phase distribution consists of radial and periodic angular dependence. We have presented a detailed mathematical formulation for describing the propagation of ALBs in turbulent media by solving Huygen-Fresnel integral using stationary phase method. We have found that the presence of turbulence leads to distortions in the spatial intensity distribution of ALBs, as well as causes beam wandering. The effect of turbulence on the propagation of ALBs is quantified by calculating overlap integral with respect to ALB in free space.The ALBs possess good autofocusing properties both in free space as well as in turbulent media, where on-axis peak intensity becomes maximum with tight focusing. In particular, the autofocusing properties of ALBs remain invariant, irrespective of turbulence strength.The autofocusing distance can be controlled from any small to large values, by controlling the ALB parameters. Further, we have also investigated the spectral dependence of autofocusing of ALBs in a turbulent medium and found that autofocusing distance doesnot depend on the turbulence, however, it decreases with an increase in wavelength. Furthermore, we have performed a detailed investigation of self-healing of ALBs bothin free space as well as in turbulent media of different turbulence strengths. We havefound that, both in free space and turbulent media, the truncated ALB self-heals by redistributing the intensity within the beam. The ALBs self-heal reasonably well evenor a large amount of truncation (60%). The maximum self-healing always occurs atautofocusing distance, which remains invariant irrespective of the

amount of truncation and strength of turbulence. A good agreement between theory, simulations, and experimental results is obtained[5].

In **Chapter 4**, we have presented the generation of asymmetric aberration laser beams(aALBs) with controlled intensity distribution, based on an outer-cavity method employing a DOE with phase asymmetry[6]. We have introduced the phase asymmetry inDOE by shifting coordinates in a complex plane, which provides additional controlover spatial intensity distribution of beam. We have derived the mathematical formulations for general aALBs as well as the special cases of it. We have shown that in anideal ALB containing equal intensity bright lobes (Fig. 2(a)), by introducing asymmetry most of the intensity can be transferred to any one of the single lobe, and generates a high-energydensity (Figs. 2(b)-2(d)). Further, we have explored the mechanism of asymmetric control of intensity inaALBs, and found that the asymmetry parameters control the position of indeterminate phase point of the trigonometric phase term in a ALB, which creates a controlled asymmetric intensity distribution in the near-field plane. As a result of propagation, it provides a controlled transfer of intensity within a ALB. In general, for a given parameter *m* ofaALB, the precise spatial location of high-energy density lobe can be controlled bythe precise variation in the asymmetry parameters(*w*, β), and we have determined empirical relations for them. We have found that for the specific values of β and *m*, the intensityin the high-energy-density lobe can be enhanced by several times the intensity in other lobes (Figs. 2(b)-2(d)). Where amount of intensity in a particular lobe is calculated by the method of diffraction efficiency which is the ratio of intensity in a lobe to the total intensity of the beam. Further, we have investigated the propagation of aALBs, and found that similarto ALBs, the aALBs possess good autofocusing properties, which are not affected by the asymmetry. The autofocusing distance in a ALBs can be varied from small to large values by changing the beam parameters. We have found a good agreement between the experimental results and numerical simulations[6].

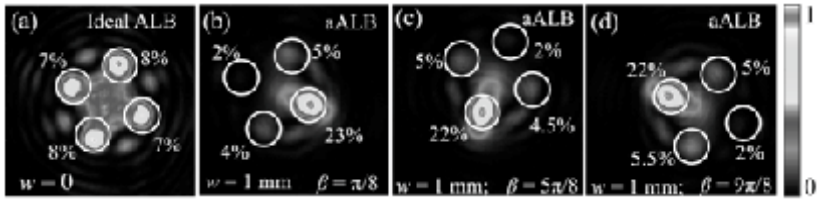

Figure 2 Experimental results. Intensity distributions of (a) ideal ALB and (b)-(c) asymmetric ALBs for different values of β. *White circles mark the location of each lobe along with its diffraction efficiency.*

In **Chapter 5**, we have presented the generation of high-energy densities by suppression of higher-order sidelobes in the far-field of phase-locked lasers. We have generated an array of lasers in various 1D and 2D array geometries in a degenerate cavity and phase-locked them in the in-phase [out-of-phase] configuration with the far-fieldcoupling using Gaussian apodizer [binary circular aperture][7]. Owing to the non-uniformamplitude and definite geometry, the far-

field of phase-locked lasers consists of higher-order sidelobes. These sidelobes contain a significant amount of energy, which limits theuse of an output beam for high-power applications. Our method relies on modifying thecombined field (near-field and far-field) distribution of phase-locked lasers to obtain uniform amplitude and phase distributions in a near-field plane, which enables the formation of a high-power density lobe (zeroth-order) in the far-field. We have demonstrated ourmethod for phase-locked lasers in various array geometries, such as square, triangular, Kagome, random, and 1D ring. The results are quantified by calculating the diffraction efficiency of the zeroth-order lobe. It is found that for long-range in-phase locked laser arrays, the diffraction efficiency of the zeroth-order lobe can be improved by several factors(3 - 4). The improved diffraction efficiencies are found to be in a range of 90% - 95%(for 2D arrays) and 75% (for 1D ring array). Further, we have analyzed the robustness ofour method against various factors, such as the range of phase-locking, system size, andpresence of topological defects in a 1D ring array. We have also investigated our methodfor out-of-phase locked lasers in a square array, where the zeroth-order has no intensity. We have obtained a high-energy-density zeroth-order lobe with a high diffraction efficiency of 81%[7].

In **Chapter 6**, we have presented a novel and efficient intra-cavity method for thegeneration of high-power discrete optical vortices with precisely controlled topologicalcharges (l) by phase-locking one-dimensional (1D) ring array of lasers in a degeneratecavity that involves spatial Fourier filtering[8]. Owing to the special geometry of a degenerate cavity, it enables an efficient formation of a 1D ring array of lasers, where eachlaser consists of a nearly fundamental Gaussian distribution, and is independent from eachother. Initially, the lasers consist of random phase distribution and are equally probable.To force them into a desired phase-locked state of optical vortex configuration, we employa special Fourier filter (amplitude mask) at the Fourier plane inside the cavity (Fig. 3(a)). The spatial Fourier filtering mechanism helps to eliminate the undesired phase distributionsby introducing additional losses to them, thereby, enabling the lasers to find a correct phasedistribution in the form of a desired discrete optical vortex (Fig. 3). We have performed a detailed investigation on the propagation, such as divergence and self-healing, of discrete opticalvortices, and compared them with the conventional continuous optical vortices. We have found that for a given system size (number of lasers) and fixed distance between the neighboring lasers, the size of a discrete optical vortex and its divergence does not dependon the topological charge, which is found to be different than the conventional continuous optical vortices (Laguerre-Gaussian/Bessel-Gaussian beams). Further, we have performed a detailed investigation of self-healing by partially truncating a discrete optical vortex inthe waist plane ($z = 0$) and propagated plane ($z > 0$). To quantify the self-healing,we have calculated an overlap integral to analyze the similarities between the self-healedand ideal discrete optical vortices. The results show that partially truncated discrete optical vortex can self-heal reasonably well. Moreover, we have found that the self-healingdistance increases with the value of topological charge of discrete optical vortex. The self-healing distance is also found to be dependent on the amount of blocking, particularly, itincreases with an increase in the amount of blocking. We have obtained a good agreementbetween the analytical and numerical results[8].

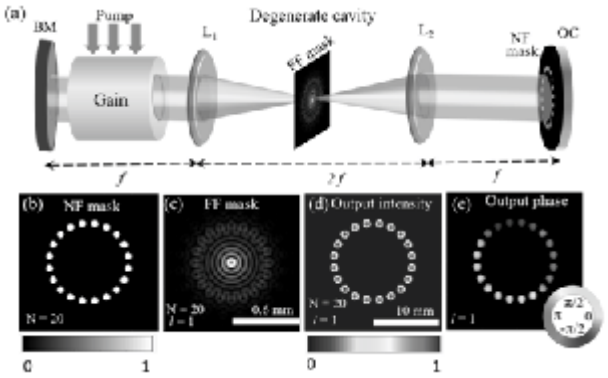

Figure 3 (a) Schematic of the degenerate cavity. Transmission functions of (b) near-field mask and (c) far-field mask. (d)-(e) Intensity and phase distributions of generated discrete vortex with N = 20 and l = 1.

In **Chapter 7**, we present a novel and efficient method for accurate determinationof magnitude and sign of topological charge (l) of an unknown discrete optical vortex,which is formed by an array of lasers in a 1D ring geometry[9]. We have presented asimple analytical formulation of working principle of our method. It relies on measuringthe interference pattern of a discrete optical vortex, which is obtained by interfering asingle selected laser with itself and with all the other lasers in a 1D ring array, usinga Mach-Zhender interferometer (Figs. 4(a)-4(c)). The interference pattern is quantified by analyzing thefringe visibility at each laser in a 1D ring array. The discrete laser arrays with $l = 0$ and$l \neq 0$ have different phase distributions, thus produce interference patterns with shiftedinterference fringes. The averaging of these phase-shifted interference patterns gives riseto a variation in the fringe visibility as a function of laser number in the discrete optical vortex, thus enablingthe identification of l(Figs.4(c)-4(f)). The magnitude of l of a discrete optical vortexis found to be proportional to the number of dips observed in the fringe visibility curve (Fig. 4(g)).Further, for an accurate determination of sign of an unknown discrete optical vortex ($l \neq 0$),we have averaged the interference pattern of it with the interference pattern of known$l$ = +1. The number of dips in the fringe visibility curve increases by one for a positive value of l and increases by one for a negative value of l. We have also investigated the robustness of our method against the presence of phase disorder that may occur due to the presence of aberrations in a system. It is found that the phase disorder does not affectan accurate measurement of the topological charge of an unknown discrete optical vortex. We have demonstrated our method for discrete optical vortices with topological charges from small to large values and accurately determined their magnitude and sign. We have provided a theoretical description along with numerical and experimental results, and found an excellent agreement between them, indicating that our method is accurate and highly efficient[9].

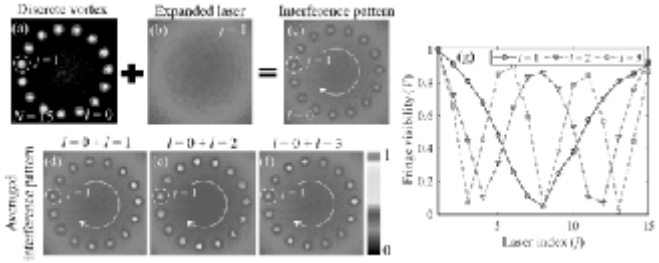

Figure 4 Experimental results for determining TC of DOV of system size N = 15 and l=1-3.

At the end, the conclusive chapter (**Chapter 8**) contains a summary of the resultsdiscussed in the aforementioned main chapters of the thesis. We also consider somefuture directions that might aid in gaining a deeper understanding of structured light andits propagation properties.

[1] F. M. Dickey and S. C. Holswade, Laser Beam Shaping – Theory and Techniques (Marcel Dekker, 2000).
[2] A. Forbes, M de Oliveira, M.R. Dennis, *Nat. Photon.***15**, 253 (2021).
[3] A. Forbes, *Laser Photonics Rev.***13**, 1900140 (2019).
[4] Vasu Dev, Andra N. K. Reddy, and Vishwa Pal, *Opt. Commun.***475**, 126226 (2020).
[5] Vasu Dev, et al., *Phys. Rev. Appl.* **16**, 014061(2021).
[6] Sachleen Singh, Vasu Dev, and Vishwa Pal, *J. Opt.* **24** 125601, (2022).
[7] Vasu Dev, Andra N. K. Reddy, and Vishwa Pal, *J. Opt. Soc. Am. B***39**, 2254 (2022).
[8] Vasu Dev, and Vishwa Pal, *J. Opt. Soc. Am. B***38**, 3683 (2021).
[9] Vasu Dev and Vishwa Pal, *Phys. Rev. Appl.***20**, 034071 (2023).

TH-08

Development and characterization of widely tunable solid-state laser

Siba Prasad Sahoo

SUMMARY

The focus of this thesis was the development and experimental study of a widely tunable, gain-switched Cr:forsterite solid-state laser. It can provide a complementary tunable source to the dye lasers for a variety of applications. The dye lasers have a limited tuning range which is a few tens of nanometres and are associated with difficulties like flow fluctuation, and photo-degradation, along with health and fire hazards. On the other hand, the vibronic solid-state lasers are widely tunable over a few hundred nanometres along with advantages like simple and reliable operation, better wavelength stability, and are not associated with any fire or health hazards. From a wide range of tunable solid-state crystals, the Cr-doped forsterite crystal was considered the gain medium for the development and study of the widely tunable solid-state laser due to its suitable spectral and temporal characteristics. The second harmonic of the Cr:forsterite laser will cover the missing wavelength gap between the fundamental and the second harmonic wavelength of the Ti:sapphire laser.

A detailed characterization of the Cr:forsterite crystal was carried out which includes its spectroscopic as well as lasing properties. The spectroscopic characterization includes measurement of the absorption spectrum, emission spectrum, and saturable absorption properties of the crystal. The broadband lasing characteristics of the Cr:forsterite crystal was carried out by establishing different laser resonator cavities in which the input-output energy characteristics and spectral properties of the laser are studied. The broadband lasing performance of different laser resonator cavities like concave-concave, concave-plane, and plane-plane were compared in terms of their slope efficiency and threshold pump pulse energy.Six different output couplers of discrete reflectivity values were characterized and their performances were evaluated. It was observed that with an increase in the output coupler reflectivity, the lasing threshold decreases continuously whereas the laser slope efficiency increases, attains optimum values, and then decreases. The highest slope efficiency of 14.1 was obtained for the concave-plane laser resonator where the output coupler has a reflectivity of 85%. The spectral characteristics of the broadband Cr:forsterite laser for these six output couplers were compared. The peak lasing wavelength and the lasing linewidth were measured to be 1232.6 nm and 22.3 nm respectively for 85% output coupler reflectivity where the laser efficiency was maximum.

A novel polarization-based laser resonator cavity was designed and developed which can provide continuous tuning and optimization of different laser and cavity parameters preserving the cavity alignment. The polarization-based resonator cavity consists of an intracavity PBS and retardation plate inside a confocal resonator cavity in which rotation of the retardation plate provides continuous tuning of the output coupler reflectivity without imposing any

misalignment to the cavity.Two different retardation plates (an achromatic QWP for 690-1200 nm and a zero-order HWP at 852 nm) were used as an output coupler in this resonator cavity. The output coupler reflectivity values of these retardation plates as a function of their angle at the lasing peak wavelength were determined using Jones matrix formalism.From the experimental results, it was concluded any of these retardation plates can be used as an output coupler once their reflectivity values are calibrated using the Jones matrix. This exercise was to test the compatibility of the polarization-based cavity for further incorporation of wavelength-tuning elements. This resonator cavity was characterized by measuring various laser parameters like the cavity output energy, the intracavity energy, cavity buildup time, laser pulse width, and the threshold pump energy as a function of the output coupler reflectivity. The round trip resonator losses and small signal gain coefficient of the laser system were determined using Findlay-Clay analysis. This resonator cavity allows accurate determination of the optimum and threshold output coupler reflectivity at different pump pulse energies. The cavity output energy was calculated as a function of output coupler reflectivity at different input pump energies and compared with the experimental results.This polarization-based resonator cavity provides in situ control of the delay of the laser beam without major changes in the laser pulse width which suggest its possible use in different spectroscopic experiments where the delay of multiple laser beams needs to be synchronized. This resonator cavity acts like a laser with a variable output coupler for optimizing the laser output at different input pump pulse energies.

An innovative temporal separated pumping (TSP) configuration was developed for the enhancement of laser efficiency of the low or moderately-doped gain-switched solid-state lasers to overcome the depletion of the ground-state population. This pumping configuration helps in the enhancement of the laser output by increasing the repumping of the ground state population as well as decreasing the excited state absorption at higher pump pulse energies. In this configuration, the crystal was pumped by two temporally separated pump pulses (pump and control pulse) of distributed energies instead of a single pump pulse of higher energy. The crystal was pumped by the pump pulse of low energy followed by a control pulse of higher energy. The control pulse was applied just before the initiation of the laser pulse. The ground state population accumulated by the pump pulse during the buildup time of the laser pulse was repumped to the ULL by the control pulse in the TSP configuration and increases the laser output energy. This configuration also reduces the ESA effect and helps in the enhancement of the laser output at higher pump pulse energies. The TSP configuration is experimentally studied for the gain-switched Cr:forsterite laser using a polarization-based resonator cavity. The output energy of Cr:forsterite laser in the TSPconfiguration is increased by a factor of two as compared to the SP configuration of the same pump pulse energy. The optimum value of delay between the pump and control pump pulse is found to be the buildup time for the maximum laser output energy.The polarization-based cavity has an inherent advantage of continuously varying buildup time without misalignment of the laser cavity, which is suitable for the TSP configuration to match the buildup time for a fixed delay between the pump and the control pulse. This resonator cavity eliminates the requirement of variable delay at different pump pulse energies through delicate optical alignment. Further, it was experimentally verified that at different pump pulse energies with a fixed delay, the maximum output energy is obtained when the buildup time closely matches the delay value. We have developed a rate-equation-based model including the ESA effect to validate the experimental results and the associated mechanism. It was found that the

ESA strongly deteriorated the efficiency of the laser at higher pump pulse energies in comparison to the lower pump pulse energies. The theoretical results of both the SP and TSP configurations are compared with the experimental results which show good agreement. This technique suggests that instead of a single pump beam of higher pulse energy, two temporally separated pump beams of distributed energy are more suitable for the optimum performance of the laser system. This pumping method will reduce the probability of damage to the crystal due to temporally separated pump beams and hence will allow pumping of the crystal at higher pulse energies compared to the conventional pumping configuration. It will also help in reducing the adverse thermal effects in the laser crystal at higher pump pulse energies due to lower thermal load. The TSP configuration can be a useful solution where the ESA effect plays a dominant role and adversely affect the laser output energy.

The developed polarization-based laser resonator cavity acts as an instrumental technique for this TSP pumping configuration where the cavity buildup time can be matched to a fixed delay between the pump pulses. This resonator cavity eliminates the requirement of variable delay at different pump pulse energies through delicate optical alignment in the TSP configuration.

A Rate-equation-based numerical model was developed to study the temporal dynamics of the gain-switched sloid-state laser. This model incorporates the effect of the excited-state absorption (ESA) both at the pump and the laser wavelength. The evolution of the Cr:forsterite laser pulse inside the resonator cavity and the ULL population (N_2) was numerically obtained by solving the rate-equations of the cavity photon density and population density. The temporal variation of the upper-level population and the cavity photon density shows spiking behaviour as a consequence of the relaxation oscillation. The effect of various pump beam parameters like the pump pulse energy and the pump pulse widthon the output pulse profile was studied in detail. The variation of the output pulse profile, pulse width of the principal pulse, and cavity buildup time were studied as a function of the above parameters. The number of spikes in the output pulse profile, the pulse width of the principal pulse, and the cavity buildup time decrease with an increase in the pump pulse energy. In the case of pump pulse width, the number of spikes in the output pulse, cavity buildup time, and the pulse width of the principal pulse increases with an increase in the pump pulse width. The output pulse profile of the Nd:YAG pumped Cr:forsterite laser was experimentally measured by setting up a concave-concave resonator cavity in which spiking behaviour was obtained. The spiking behaviour in the output pulse profile at different pump pulse energies was found consistent with the computed results. The cavity buildup time and pulse width of the principal pulse were experimentally measured as a function of the pump pulse energy which is closely matching with the simulated results.

The tunable, narrowband Cr:forsterite laser was developed and characterized by using different frequency-selective elements and their combinations. Initially, a Littrow grating-based laser cavity was developed using a 600 lines/mm grating as the frequency-selective element. A wide tuning range of 164 nm (1160 nm to 1324 nm) was obtained with a peak wavelength at 1244 nm and a conversion efficiency of 8.2%. The lasing threshold of 0.9 mJ and a slope efficiency of 9.3% was measured for this Littrow grating-based cavity. The Littrow grating-based cavity was modified to obtain a constant path output beam during the tuning of the laser. In the Littrow grating-based cavity a laser linewidth of 1.48 nm was obtained. The laser linewidth was further reduced using FP etalons inside the Littrow grating cavity. Three different

narrowband configurations named grating and E1 etalon-based cavity, grating and two etalon-based cavity, and a concave-concave cavity with two etalons were studied from which laser linewidth of 68 pm, 42 pm, and 14 pm respectively were obtained. This work was further extended for visible wavelength generation through SHG of the Cr:forsterite laser using a BBO non-linear crystal. In the SHG, a wide tuning range of 82 nm (580 to 662 nm) was obtained with the Littrow grating-based cavity having a peak wavelength of 622 nm with a SH conversion efficiency of 9%. In this Littrow grating-based cavity, a laser linewidth of 0.83 nm was obtained. The SHG of the three narrowband cavities was also studied and characterized. The lasing wavelength and the laser linewidth of these SH narrowband lasers were simultaneously measured using the wavelength meter as well as an FP etalon-based measuring system. A laser linewidth of 3.8 pm was obtained from the SH of the grating and E1 based which gives multimode laser oscillation. The SH of the grating and two etalon-based cavity as well as the concave-concave cavity with two etalons gives the SLM lasing with linewidths of 650 fm and 250 fm respectively. The SLM behaviour was confirmed from the wavelength meter (WS-7L) as well as from the fringes of the FP etalon-based system with a 7.5 GHz FSR etalon. The stability of the SLM laser, its temporal behaviour, and the spatial beam properties were also studied. The wavelength and linewidth stability of the SH SLM Cr:forsterite laser around the mean value was measured to be ±100 fm and ±200 fm respectively for a time duration of 40 minutes without any active feedback. The temporal pulse width of the SH SLM Cr:forsterite laser was measured which gives an FWHM pulse width of 9.7 ns and a rise time of 5.5 ns. The spatial beam profile of the SLM laser gives a good (> 90%) Gaussian beam quality in both transverse directions.

Although the thesis work focuses on the development of widely tunable Cr:forsterite laser, some of the techniques and theoretical models developed can also be applied to other systems. The developed polarization-based laser resonator cavity can be used with any other laser system for continuous tuning of different laser parameters and their optimization. The TSP configuration can be applied to other gain-switched lasers having a low-density gain medium for enhancement of laser efficiency. The developed rate-equation-based models to study the temporal spiking behaviour and the TSP configuration areapplicable to the other gain-switched solid-state lasers.

In future, it is planned to extend this current research work for the development of a portable tabletop-type laser system with enhanced efficiency and to use it for spectroscopic applications.The future laser system will implement the TSP configuration with polarization-based laser resonator cavityfor narrowband generation and power enhancement of Cr:forsterite laser in a single crystal using both longitudinal and transverse pumping.

TH-09

Novel, Hybrid Plasmonic Materials Aided with Machine Learning for SERS-Based Trace Detection of Multiple Explosives

Reshma Beeram
Advanced Centre of Research in High Energy Materials (ACRHEM),
DRDO Industry Academia – Centre of Excellence (DIA-CoE)
School of Physics,University of Hyderabad, Hyderabad 500046, Telangana, India.
e-mail: reshmabeeram@gmail.com

ABSTRACT

SERSis a powerful evolving tool for trace detection of explosives and biomolecules. Despite all its advantages, there are many challenges associated with SERS standing in the way of translating the benefits to real world [1]. SERS signals are known to have poor spatial reproducibility owing to inhomogeneous distribution of hotspots, random adsorption of molecules on the metal structure, coupling of the molecule with the substrate etc. [2]. Periodic and predictable structures like those produced by e-beam lithography and laser ablation that are ligand free (pure) are promising in this regard [3]. The SERS substrates as they involve noble metals like Ag, Au and Pt are known to be expensive and are often not reusable and durable as they are prone to rapid oxidation. The cost of the substrates can be brought down drastically if instead a semiconductor material like Si is used as the base material with deposition of Ag/Au by different methods [4]. The combination of Ag and Au is also known to prevent rapid oxidation of the substrates thus increasing their durability [5]. Often on field it is advantageous to have a flexible substrate that would enable swabbing the surface. A flexible substrate is defined as something that is easy to bend and fold [6].

SERS is also known to have inherent signal fluctuations because of very factors that are known to enhance the SERS signal. The hotspots that lead to signal enhancement through electromagnetic effects are localized to small areas causing point to point signal variations in SERS [7]. These hotspots are also known to evolve under the presence of laser light causing signal 'blinking' in SERS [1]. The vibrational spectrum in SERS is also different from Raman with significant peak shifts and enhancement/quenching of certain modes depending on the adsorption, orientation of the molecule with respect to the metalnanostructure (NS). In many applications, it is also useful to quantify the trace analyte that is being studied using SERS. However, the signal intensity and quantity of analyte is non-linear and is complex for the signal blinking effects in SERS. Going beyond the detection limit of fabricated plasmonic substrates to achieve ultra-trace sensitivity involves changing the experimental parameters like choosing the right wavelength. Resonant excitation in the case of SERS is known to enhance the SERS signal further by at least 10^6 times [8]. With a combination of ultrafast lasers, novel methods for low-cost synthesis of durable and flexible SERS substrates and ML techniques, this thesis attempts to address these.

This thesis work explored and addressed several tenacious challenges in the SERS measurements for trace analyte detection. Through different plasmonic nanostructures that were fabricated via both ultrafast laser ablation and simple chemical methods we achieved reproducible, low-cost, flexible and durable SERS substrates. Our findings have not only addressed the research objectives but have also provided valuable insights to envision SERS for real field applications making a potential impact for explosives and other hazardous materials detection. Furthermore, this thesis work has identified several avenues for future research and development. The future scope of this work encompasses extension of the current application of machine learning (ML) techniques and also prospects to extend the SERS studies for biology applications. The conclusions drawn from this research lay the foundation for further advancements and investigations. It is our hope that this work will serve as a catalyst for future research endeavours and inspire future researchers to refine the results and applications.

In the last decade the SERS technique has seen a tremendous increase in applications addressing tenacious causes like homeland security, forensics, environmental safety, and disease detection including the recent covid-19 pandemic [9]—[10]. However, translating the benefits from research to the field has been a challenge limiting the performance only to lab scale. The challenges on the way of field, especially for achieving real world applications of SERS can be summarized as below[1].

Reproducibility: SERS is known to have poor spatial reproducibility caused by signal fluctuations from point to point owing to the localization of hotspots. This manifests more prominently during trace detection when the molecules on the plasmonic surface are sparse. Higher enhancement factor, as is the case for trace detection, often comes at the cost of reproducibility. Ripple like nanostructures formed during laser ablation on metals were found to highly reproducible substrates with a reproducibility of nearly 10% RSD for SERS spectra collected in 100 m^2area with nearly 5000 spectra [11].

Durability and cost: Most often than not, gold and silver NSs are used as SERS substrates as they have desirable optical properties for enhanced field in the visible region. However, these samples are expensive and often prone to rapid oxidation (especially silver-based substrates). Having a semiconductor substrate as a template for gold and silver NPs would bring down the cost of the substrate. Wafer scale, highly anisotropic Au nanoparticles decorated on Ag nanodendrites were developed which were low cost, versatile and sensitive substrates [12]. Laser ablated MoS_2 in combination with plasmonics Si nanowires has resulted in nearly ~2-fold enhancement in addition to the enhancement from plasmonic materials and has significantly increased the durability of the substrate to more than 200 days [13].

Signal fluctuations: Signal fluctuations are inherent to SERS through the same mechanism of signal enhancement. Electromagnetic and chemical enhancement are known to cause signal fluctuations through various mechanisms deviating from the normal Raman signal. This makes SERS hugely reliable on an expert thus limiting the measurements to be carried out outside the lab atmosphere. Using a signal to noise ration approach, a deep learning model called Neural Network Aided SERS (NNAS) has been developed to bridge the gap between laboratory and field performance devoid of any expert achieving an accuracy greater than 96% for the case of trace explosives [14].

Quantification: Though SERS has a potential for quantitative trace detection, accurate

quantification is limited for very reasons of signal fluctuations and reproducibility. The intensity and the quantity are not directly correlated. Machine learning algorithms that are known to capture complex patterns were used in the thesis work in order to address this challenge. Nonlinear ML models, PCA and SVR have been used in sequence to quantify the analyte molecule under study. Using a portable Raman spectrometer, two analyte molecules, PA and CV were detected with sensitivity of 5 M and 100 nM, respectively. Significant data of nearly 900 spectra has been collected for both the analytes with nearly 100 per concentration to full sample the substrate surface. The time required to run the program was less than 10s and this is the fastest algorithm so far used for quantification in SERS [15].

Ultra-trace detection: Making the best of the SERS substrates to achieve ultra-trace detection goes beyond fabrication of plasmonic substrates. Choosing the right wavelength close to the resonant excitation would enable

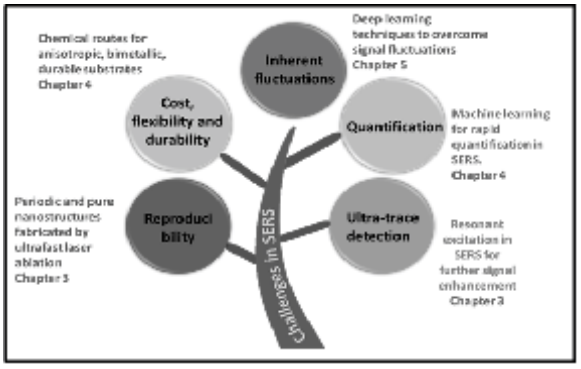

Figure 1:Schematic of different challenges in SERS and different chapters presented in the thesis addressing the challenges.

achieving lower detection limits through SERRS. Using femtosecond laser structured Ag-Au nanostructures, ultra-trace detection of R6G, CV, PA and cysteine, respectively has been achieved with sensitivity of 10 fM, 100 fM, 100 nM, and 100 nM using resonant excitation through SERRS [11].

Flexible substrates for easy sampling: Ease of sample collection is a key feature for field applications. Flexible substrates are not only low cost but would enable sample collection through swabbing as on when needed unlike rigid substrates. For the first time, using a simple method of coating with Si oil, low-cost alternative for modifying the wettability of the Si oil has been proposed. Through a simple technique of wet etching in the presence of electric field, porous Si has been fabricated and was further decorated with Ag through etching in the presence of HF and $AgNO_3$ [16].

This thesis successfully attempted to address these challenges with different projects that have been taken up as shown in figure 1. Different plasmonic materials that were fabricated, molecules detected, and the highlights are summarized in table 1.

In addition, in this thesis I have illustrated a novel and graphic way to represent the

performance of any SERS substrate. There are five important metrics to evaluate a SERS substrate, namely a) Cost, b) Durability, c) Reproducibility, d) Enhancement Factor and, e) Sensitivity. Our visualization is a summary of this parameters which communicates complex information in one image.These representations can also be used as a guide to improve the performance of a particular substrate based on the short comings. They also provide a powerful tool to analyse, compare and estimate room for improvement for different SERS substrates.

Table 1: Summary of the SERS substrates and the molecules studied in the thesis work.

S. No.	SERS Substrate	Molecules	Lowest detected	Highlights
1	fs laser structured Cu	Tetryl, AN, MB	100 mM, 50 mM and 5 mM	Low cost, reproducible (5 %)
2	fs laser structured Ag	Tetryl, RDX, Cytosine	50 nM, 1 mM, 100 nM	Highly reproducible with RSD of 6%.
3	Chemically synthesised AuNPs@AgNDs	CV, adenine, cytosine, penicillin G, kanamycin, ampicillin, AN, and Thiram	1 nM, 100 nM, 10 nM, 10 nM, 100 nM, 10 nM, 100 nM, 10 nM	Low cost, durable substrates. Substrates were used to develop NNAS model to overcome signal fluctuations in SERS
4	Hybrid MoS_2 layered plasmonic Si NSs	Malachite Green, Melamine, Naphthalene, L - Cysteine, tetryl and E.coli	0.5 nM, 100 nM, 300nM, 100 nM, 50 nM	Highly durable and low -cost substrates that could be even used for live organism sensing
5	Flexible porous Si substrate	MB, PA, AN, and Thiram	....	Free standing, flexible and low - cost substrate.
6	Hydrophobic plasmonic filter paper	Picric Acid and Crystal Violet	5 mM and 100 nM	Novel substrate, fabricated for the first time and used for rapid quantification using ML techniques.
7	fs laser structured web-like Si coated with Au	Methylene Blue	1 mM	Formation of web -like NSs is studied and the mechanism is understood.
8	fs laser structured Ag-Au	Rhodamine 6G, crystal violet, picric acid, and cysteine	10 fM, 100 fM, 100 nM, and 100 nM	SERRS has been used for ultra - trace detection. The relationship between enhancement and reproducibility is studied.

Key words: SERS, Trace detection, Explosives, Machine Learning, Biomolecules.

REFERENCES

1) A.I. Pérez-Jiménez, D. Lyu, Z. Lu, G. Liu, B. Ren, *Chem. Sci.* 11, 4563 (2020).
2) D.P. Dos Santos, M.L.A. Temperini, A.G. Brolo, *Acc. Chem. Res.* 52, 456 (2019).
3) S.V. Rao, G.K. Podagatlapalli, S. Hamad, J. Nanosci. Nanotechnol. 14, 1364 (2014).
4) V.S. Vendamani, S.V.S. Nageswara Rao, S. Venugopal Rao, D. Kanjilal, A.P. Pathak, J.

Appl. Phys. 123, 014301 (2018).

5) R. Beeram, V.R. Soma, Opt. Mater. 137, 113615 (2023).
6) V.S. Vendamani, R. Beeram, S.V.S. Nageswara Rao, A.P. Pathak, V.R. Soma, Opt. Express. 29,30045 (2021).
7) E.C. Le Ru, M. Meyer, E. Blackie, P.G. Etchegoin, J. Raman Spectrosc. 39, 1127(2008).
8) E.C.L. Ru, Pablo Etchegoin, Elsevier (2008).
9) B. Sharma, R.R. Frontiera, A.I. Henry, E. Ringe, R.P. Van Duyne, Mater. Today. 15, 16(2012).
10) F. Saviñon-Flores, E. Méndez, M. López-Castaños, A. Carabarin-Lima, K.A. López-Castaños, M.A. González-Fuentes, A. Méndez-Albores, Biosensors. 11, 66 (2021).
11) R. Beeram, V.R. Soma, Opt. Mater. 137, 113615(2023).
12) M. Lee, K. Oh, H.K. Choi, S.G. Lee, H.J. Youn, H.L. Lee, D.H. Jeong, ACS Sensors. 3, 151(2018).
13) N. V. Godoy, D. García-Lojo, F.A. Sigoli, J. Pérez-Juste, I. Pastoriza-Santos, I.O. Mazali, Sensors Actuators, B Chem. 320, 128412 (2020).
14) Beeram Reshma, V. S. Vendamani, and Venugopal Rao Soma. Spectrochimica Acta Part A: Molecular and Biomolecular Spectroscopy 289, 122218 (2023).
15) R. Beeram, D. Banerjee, L.M. Narlagiri, V.R. Soma, Anal. Methods. 14, 1788 (2022).
16) V.S. Vendamani, R. Beeram, M.M. Neethish, S.V.S.N. Rao, S.V. Rao, iScience. 25, 104849(2022).

TH-10

Assessment of Breast Tumor Progression by Photoacoustic Spectroscopy

Jackson Rodrigues
Department of Biophysics, Manipal School of Life Sciences,
Manipal Academy of Higher Education, Manipal, India - 576104

Summary

Breast cancer is a dreaded disease affecting women most in cancer-related deaths over other cancers. However, early detection of the disease can help increase the survival rates. The existing breast cancer detection tools do not support early disease diagnosis. Therefore, there is a great need to develop early diagnosis tools, such as photoacoustic spectroscopy, which is a sensitive, simple, and robust technique for detecting sensitive biochemical changes. In the current study, to assess the breast tumor progression, we have designed and developed an aseptic chamber and a PA probe to assess the breast tumor progression in breast tumor xenografts *ex vivo*/*in vivo*/PDX. The in-house designed and developed aseptic chamber was optimized. Initially, microbial analysis and animal survival analysis validated the aseptic chamber's efficiency in providing optimum environment for animal survival during the experiment. The chamber did not show any microbial load during the experiment, and there was 100% survival of animals.

The PA probe was designed and developed to record *ex vivo* and *in vivo* tumor signals. This was initially tested for its detection ability and limit of detection. The PA probe developed also showed its ability to differentiate the structural change in HSA protein when treated with solutions of different pH. The PCA analysis of the PA spectra obtained from HSA treated with varying pH buffer solutions demonstrated distinct clustering and explained the variance of more than 95% with PC1 and PC2.

Further, the potential of the PA probe to characterize different tissue types using the heart, kidney, liver, lungs, and spleen from athymic nude mice was assessed. The PA spectra from the organs were pre-processed, wavelet transformed, and subjected to the mRMR algorithm to select the features from the spectra. The top 10 features were selected as input to the machine learning algorithm. In this study, we used multiclass SVM with RBF kernel and trained the model using 60% of the training data set. We used the remaining 40% of the data to test the trained model and obtained good organ classification based on their photoacoustic spectra with an overall accuracy of 99% for the model. This study demonstrated the potential of photoacoustic probes in detecting different tissue types under study.

Further, a breast tumor xenograft was established in athymic nude mice by subcutaneous injection of the MCF-7 cell line and assessed the tumor progression by photoacoustic spectroscopy combined with machine learning tools. The advancement of breast tumors in nude mice was validated by tumor volume kinetics and histopathology and corresponding image analysis by TissueQuant software compared to controls. The *ex vivo* tumors in progressive

conditions belonging to time-points, day 5th, 10th, 15th, & 20th, were excited with 281 nm pulsed laser light and recorded the corresponding photoacoustic spectra in the time domain. The spectra were then pre-processed and subjected to wavelet packet transformation for feature extraction and selection using MATLAB software. In this study, the top 10 features from all the time-point groups under study were selected based on their prediction ranking values using the mRMR algorithm. The chosen features of all the time-point groups were then subjected to multi-class Support Vector Machine (SVM) algorithms for learning and classifying into respective time-point groups under study. The analysis demonstrated accuracy values of 99.5%, with SVM-Radial Basis Function (SVM-RBF). The serum metabolomic levels during tumor progression complemented photoacoustic patterns of tumor progression, depicting breast cancer pathophysiology. The current study reports the assessment of tumor progression in athymic nude mice by Photoacoustic spectroscopy-based machine-learning tools. The progressive tumors were classified using multi-class Support Vector Machine (SVM) algorithms with 99.5% accuracy.

The in-house designed and developed aseptic chamber integrated PA probe is now standardized and demonstrates good ex vivo breast tumor progression classification. Further, the same device was used to assess the breast tumor progression *in vivo*. In the *in vivo* study, an aseptic chamber integrated photoacoustic (PA) probe is designed and developed to monitor MCF-7 cell line-derived breast tumor progression *in vivo*, established in nude mice. The aseptic chamber-integrated PA probe serves the dual purpose of transporting tumor-bearing animals to the laboratory from the animal house and performing PA experiments in the same chamber, maintaining sterility. The *in vivo* study induced the breast tumor in nude mice by MCF7 cell injection and recorded corresponding PA spectra at different time points of tumor progression *in vivo*. The recorded photoacoustic spectra were subsequently pre-processed, wavelet transformed, and subjected to filter-based feature selection. The selected top-20 features, by minimum redundancy maximum relevance (mRMR) algorithm, were then used to build an input feature matrix for machine learning (ML) based classification of the data. The model's performance demonstrated specificity, sensitivity, and accuracy of 94.5%, specificity of 100%, and sensitivity of 95%, 85%, 90%, and 72% for days 5th, 10th, 15th, & 20th, respectively. These results suggest the potential of PA signal-based classification of breast tumor progression, which is simple and sensitive. The PA signal contained information on the biochemical changes associated with disease progression, providing a clear hint for early disease diagnosis through molecular/functional imaging.

We further extrapolated our study on patient-derived breast tumor since they reiterated the diverse nature of breast tumors, recapitulating their behavior and histological features and reflecting the metastatic properties of the parental breast tumor. For this purpose, the PDX model in athymic nude mice was established using a triple negative *ex vivo* tissue from a breast cancer patient. The breast tumor xenograft developed from the patient's *ex vivo* breast cancer tissue in athymic nude mice was observed for tumor progression. The established patient derived tumor xenograft was *in vivo*passaged into fresh animals for tumor kinetics study. The histological findings revealed that the tumor tissue obtained from the patient sample and the established PDX model had the same property, depicting the reproducibility of the patient tumors in the animal xenograft model.Hence, photoacoustic spectral measurements carried out subsequent tumor progression assessment.

A differential photoacoustic spectral pattern was observed for different experimental groups under study. Each group's mean pre-processed photoacoustic spectra after WPT demonstrated varied amplitude along the time axis. The wavelet transformed spectra were subsequently subjected to the mRMR algorithm, and the top 10 features necessary for the discrimination of all the spectra belonging to different groups based on their prediction ranking values were obtained by the analysis. These top 10 features from all the time-point groups were fed to the machine learning algorithm as an input feature matrix for classification. A multi-class SVM learning model (RBF) was trained using 60% of the feature matrix data belonging to each group under study and 40% used for testing of the model, and the accuracy of the trained model was 99.3%.

The current study reports an in-house design and development of an aseptic chamber integrated with a PA probe (device) for the *in vivo* assessment of breast tumor progression. Initially, the device was tested using standard chemical proteins, followed by organ characterization for its standardization. After the successful standardization of the device, it was used to assess MCF-7 cell line derived breast tumor progression ex vivo and in patient-derived xenograft models in athymic nude mice. The in-house designed and developed *in vivo* device successfully demonstrated the assessment of tumor progression non-invasively with an accuracy of 94.5%. This demonstrated the potential of PA-based assessment for breast tumor progression *in vivo*, suggesting its translation in a clinical setting.

RESEARCH OUTCOMES:

Publications (*Original articlesrelated to thesis*)

1. **Rodrigues J**, Ashwini A, Raghushaker CR, Chandra S, Joshi MB, Prasad K, Rai S, Nayak GS, Ray S, and Mahato KK*. "Exploring photoacoustic spectroscopy-based machine learning together with metabolomics to assess breast tumor progression in a xenograft model *ex vivo*." ***Laboratory Investigation***, 101(7), (2021): 952-965**.(Q1, IF-5.6)**
2. **Rodrigues J**, Ashwini A, Chandra S, Nayak GS, Ray S, Satyamoorthy K, and Mahato KK*. "Detecting Breast Tumor by Photoacoustic Spectroscopy Integrated Machine Learning: A Comparison of Statistical and Algorithm Based Features."***Frontiers in Optics***, Optica Publishing Group, 2021. pp. JW7A-10.-***Scopus indexed***
3. **Rodrigues J**, Akhil KA, and Mahato KK*. "Discriminatory potential of photoacoustic spectroscopic fingerprints integrated with machine learning to distinguish between different organs: *ex vivo*." ***Frontiers in Optics***, *Optica Publishing Group*, 2022, pp. FTh3B-5.-***Scopus indexed***
4. **Rodrigues J**, Ashwini A, Chandra S, Mulla NJ, Nayak GS, Rai S, Ray S, and Mahato KK*. "Machine learning enabled photoacoustic spectroscopy for noninvasive assessment of breast tumor progression *in vivo."****ACS Sensors*** (Under review -after revision) **(Q1, IF-9.61)**

TH-11

Investigation of ultrafast carrier dynamics on emerging optoelectronic materials

Sayan Prodhan
Department of Physics
Indian Institute of Technology Kharagpur
Kharagpur, West Bengal-721302, India

1. Introduction

Following the discovery of laser [1], the last five decades have been the era of intense research and achievements in the topic of ultrafast carrier dynamics of semiconductors. The most important material for today's electronic and optoelectronic application is semiconductors. Researches on the basic ultrafast phenomena of semiconductors are the main pillar behind the success of optoelectronic devices. In the pursuit of understanding various ultrafast dynamical behaviors, the realm of excitation of semiconductor to non-equilibrium state and its subsequent relaxation to the ground state has to be carefully explored. In the context of continuous reduction of optoelectronic device size, spatial dimension as well as the timescales at which fundamental phenomena are taking place has been important. Development of ultrafast lasers, capable of producing tens of femtosecond pulses, has significantly improved the temporal resolution of time-resolved pump-probe spectroscopy. The fundamental of pump-probe technique is the use of ultrafast pump pulse creating non-equilibrium state in the material that is getting recorded by time-delayed optical probe pulse. Optical spectroscopy using ultrafast pump-probe technique has done wonders as it can give us the information about carrier generation, thermalization, cooling, relaxation, and recombination as well as investigate electronic and vibrational properties of semiconductor materials. This basic information's are invaluable in the context of choosing and optimizing semiconductor materials for specific opto-electronic applications.

The core of opto-electronic materials is their ability to efficiently absorb light in broadband region encompassing ultra-violet, visible and near-infrared (near-IR) region. Unlike traditional electrical materials, these materials possess additional properties such as strong light matter interactions, nonlinear optical effects, and quantum mechanical phenomena. These unique properties create the possibility for developing novel devices with enhanced functionality, sensitivity, and efficiency. The evolving opto-electronics field is continuously in the quest for novel materials with enhanced properties and capabilities. Based on the working principle, world of emerging opto-electronic material generally can be divided in three groups- (i) energy conversion, (ii) sensors, and (iii) logical circuit material. Light energy conversion into electrical energy is based on the photovoltaic effect. Photovoltaic devices, such as solar cells, can directly convert solar energy into electricity. In the dominant market of silicon based solar cell, organic-inorganic mixed halide perovskite (MHP) based solar cell (PSC) seems to be the most promising

candidate to dethrone silicon from the market due to its dramatic rise in the photo-conversion efficiency (PCE) from 3.8 % to 25.8 % in just one decade [2].This has been possible due to its favorable properties toward solar cell application. Although the performance of PSC has been phenomenal, the quest to find new ways for the increment of its PCE is not over yet. Surface modification through nano-crystal (NC) has been an effective route to increase the efficiency of PSC. For sensingor photo-detection application,two-dimensional (2D) materials have been widely used due to their diverse advantages device fabrication, manipulation, ultra broad band absorption band with suitable carrier dynamics. Elemental 2D group-VI material, selenium (Se), exhibits intriguing properties that makes it a promising candidate for opto-electronic applications. Despite of their remarkable successes and high prospect, the basic understanding of ultrafast carrier dynamics associated with their optoelectronic application are still at large. This motivates the ground work of the thesis to understand the fundamental properties of the NC modified MHP and 2D Se such as carrier dynamics related to their optoelectronic application.

5. Content of the thesis

This thesis is consists of seven chapters. Content of each chapter is briefly discussed next highlighting the major contribution as follows:

5.1 Chapter 1: Introduction

Chapter 1 gives a brief introduction to emerging optoelectronic materials and ultrafast pump-probe technique. This chapter also shows the importance of ultrafast carrier dynamics of optoelectronic materials.

5.2 Chapter 2: Emerging optoelectronic material

This chapter introduces to specifically two emerging optoelectronic materials- perovskite and 2D Se. It discusses the basic structural, electronic and optical properties of bulk perovskite and 2D Se.

5.3 Chapter 3: Experimental Techniques and Data Analysis for Ultrafast Carrier Dynamics

This chapter discuss in details about the main linear and nonlinear spectroscopic techniques, basic theory, operating principles and relevant data analysis used in this thesis for explaining the ultrafast carrier dynamics. The linear spectroscopy techniques used are steady state absorption spectroscopy and photoluminescence spectroscopy indescribes details. The details about regenerative amplifier laser at 808 nm, 50 fs, 1 kHz repetition rate with 3 mJ energy per pulse source (Libra-He, Coherent) and optical parametric amplifier are also discussed. The important non-linear spectroscopy technique, transient absorption spectroscopy, is used to investigate the excited state carrier dynamics as shown in Figure .1. These spectroscopic techniques probe the information of electronic transition in the material after photo-excitation. Data analysis methods used for investigating the ultrafast carrier dynamics are described and adopted throughout this thesis.

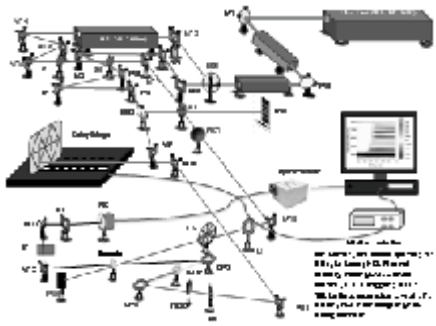

Figure 1: Schematic of transient absorption spectroscopy set-up.

5.4 Chapter 4: Suppressed recombination induced longer carrier diffusion length in CZTS nano-crystal embedded perovskite

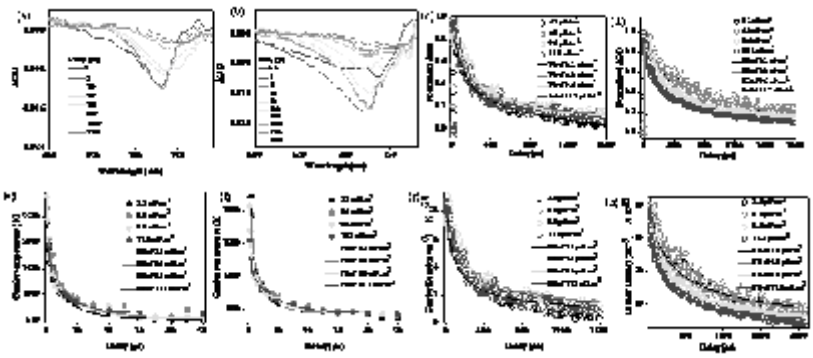

Figure 2: Transient absorption spectra of (a) unmodified and (b) CZTS NC modified $MAPbI_{3-x}Cl_x$ at 470 nm (2.64 eV) pump excitation for various time delays.Pump fluence-dependent fs-transient bleach decay kinetics with corresponding tri-exponential decay fits for (c) unmodified and (d) CZTS NC-modified $MAPbI_{3-x}Cl_x$ perovskite films at their respective bleaching wavelengths (735 nm and 730 nm).Bi-exponentially fitted carrier temperature decay dynamics of both (e) unmodified and (f) CZTS NC modified $MAPbI_{3-x}Cl_x$ perovskite films. Pump fluence-dependent fs-transient carrier density decay kinetics sequentially fitted with the rate equation for (g) unmodified and (h) CZTS NC modified $MAPbI_{3-x}Cl_x$ perovskite films

This chapter explores the complete charge carrier dynamics in unmodified (S1) and CZTS NC modified $MAPbI_{3-x}Cl_x$ mixed halide perovskite (S2) following the ultrafast optical excitation. Steady state absorption spectra fitted with Elliot's formula shows excitonic interaction is very weak and thus optical properties of both perovskites are dominated by free carriers. We have used 470 nm (2.64 eV) pump and a broadband probe (600- 790 nm) in our transient absorption experiment. They show a broadband bleaching from 600 to 775 nm having peak around 735 nm

and 730 nm for S1 and S2 at 10 ps pump-probe delay respectively (Figure-1(a,b).We observed higher bleaching amplitude for S2 signifying higher pump-excited carrier density at bleaching wavelength due to the CZTS NC modification. So the modification by CZTS NC results in blue-shifted higher bleaching peak revealing increase in the band gap and higher absorption. Two distinct direct band transitions are observed from the transient absorption measurement (shown in Figure. 2. a as PB1 and PB2) and have not been observed earlier in MHP to the best of the author's knowledge. The decay kinetic of bleaching signal relatedto electronic transition in S1 and S2 is sequentially fitted with three exponential function- as shown in Figure.2 (c, d). The result shows nearly unaltered hot carrier cooling dynamics after the modification whereas trap state assisted and auger recombination decay constant has increased from 115 ps to 289 ps and 984 ps to 2180 ps respectively after the CZTS NC modification. Hot carrier cooling is also investigated by fitting carrier temperature decay dynamics with bi-exponential decay function (Figure-2 (e,f)). It shows unchanged carrier cooling decay dynamics after the modification. To further confirm the modification in recombination dynamics, the generated carrier density (n) decay is modeled with recombination rate model considering trap (monomolecular, k_1), radiative (bimolecular, k_2) and Auger (tri-molecular, k_3) recombination pathwaysas shown in Figure.2. (g,h).Nearly one order decrease in recombination rate constants for (a) trap state (b) band-to-band () and (c) Auger recombination () for bulk perovskite after surface modification are observed. We have also calculated carrier diffusion length using the values of rate constants. The result shows increase in the diffusion length from 0.3 µmto 1 µm. Passivation and charge transfer facilitated by CZTS NC play a significant role to reduce the recombination rate with longer diffusion length, which signifies bright prospects in optoelectronic device application

5.5 Chapter 5: Tailoring hot carrier cooling and recombination dynamics of mixed-halide-perovskite by incorporating Au@CZTS core-shell nanocrystal

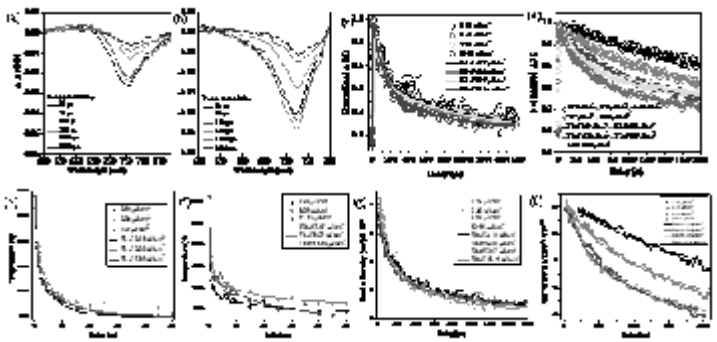

Figure-3: Transient absorption spectra of (a) unmodified and (b) Au@CZTS core-shell NC modified $MAPbI_{3-x}Cl_x$ at 470 nm (2.64 eV) pump excitation for various time delays.Pump fluence-dependent fs-transient bleach decay kinetics with corresponding tri-exponential decay fits for (c) unmodified and (d) Au@CZTS core-shell NC modified $MAPbI_{3-x}Cl_x$ perovskite films at their respective bleaching wavelengths (735 nm and 730 nm).Bi-exponentially fitted carrier temperature decay dynamics of both (e) unmodified and (f) Au@CZTS core-shell NC modified

$MAPbI_{3-x}Cl_x$ perovskite films. Pump fluence-dependent fs-transient carrier density decay kinetics sequentially fitted with the rate equation for (g) unmodified and (h) Au@CZTS core-shell NC modified $MAPbI_{3-x}Cl_x$ perovskite films

Organic-inorganic halide perovskite has emerged as the front-runner of absorber materials for highly efficient solar cells in the recent years. Incorporation of metallic (Au, Ag) nano-particles (NP) within the perovskite contributes towards effective tuning of their opto-electronic properties via enhancing the channels of solar energy transfer and promotion of carrier transport. Placing dielectric shell over metal nanoparticle further enhances the carrier mobility and reduces the carrier recombination in semiconductor material. Here, in this chapter, we have extensively investigated the effect of Au@CZTS core-shell nanocrystal (NC) on hot carrier cooling dynamics and excited carrier recombination dynamics in bulk $MAPbI_{3-X}Cl_X$ perovskite using femtosecond transient absorption spectroscopy with temporal and spectral resolution of 120 fs and 0.8 nm respectively.We use pump excitation of wavelength 470 nm (2.64 eV) at varying fluence of 3.19-19.14 $\mu J/cm^2$ corresponding to carrier density of .. and . for unmodified and modified perovskite respectively.The TA spectrum (Figure-3(a)) for unmodified bulk $MAPbI_{3-x}Cl_x$ perovskite contain a negative band from 700 nm to 790 nm which is attributed to ground state bleaching (GSB) peaking around 754 nm (1.64eV) occurring at 10 ps time delay. The TA spectrum of Au@CZTS core-shell NCs modified $MAPbI_{3-x}Cl_x$ perovskite (Figure-3(b)) shows a broad negative signal from 630-770 nm with bleaching peak around 734 nm (1.69eV). The bleaching peak has increased and blue-shifted due to the modification. The decay kinetic of bleaching signal related to electronic transition in both samples are sequentially fitted with three exponential function- as shown in Figure-3 (c, d). Result shows increase average carrier cooling time after the modification. The trap state and auger recombination decay constant increased after the modification. Hot carrier cooling dynamics is investigated by fitting carrier temperature dynamics with bi-exponential decay function. The decay dynamics of excited carrier density is also fitted with recombination rate model considering trap (monomolecular, k_1), radiative (bimolecular, k_2) and Auger (tri-molecular, k_3) recombination pathways as shown in Figure.3. (g,h).Hot carrier (HC) cooling dynamics indicates the formation of longitudinal optical (LO) phonon within first 0.6ps and a delayed conversion of LO phonon to longitudinal acoustic (LA) phonon from 8 ps to 15.87 ps due to incorporation of Au@CZTS core-shell nanocrystal (NC) in bulk perovskite. Delayed conversion of LO-LA phonon confirms the presence of enhanced "hot phonon bottleneck" effect in modified bulk perovskite. Further, the investigation of carrier recombination dynamics shows that at a fixed pump fluence of 3.19 $\mu J/cm^2$, - the rate constants decrease nearly one order of magnitude for (i) Auger recombination (from $1.2x10^{-32}$ cm^6s^{-1} to $1.7x10^{-34}$ cm^6s^{-1}), (ii) band to band recombination (from 8×10^{-14} cm^3s^{-1} to 8×10^{-15} cm^3s^{-1}) and (iii) trap state recombination (from $5.5x10^8$ s^{-1} to $5x10^7s^{-1}$) after the modification of bulk perovskite by Au@CZTS core-shell nanocrystal (NC).. We have also calculated carrier diffusion length using the values of rate constants. The result shows increase in the diffusion length from 0.3 µm to 1.3 µm. Our study reveals the presence of enhanced hot phonon bottleneck effect and reduced recombination rate constants in Au@CZTS core-shell NC modified perovskite that paves the way for the development of highly efficient perovskite based solar cell.

5.6 Chapter 6: Comprehensive Excited State Carrier Dynamics of 2D Selenium: One-photon and Multi-photon Absorption Regimes

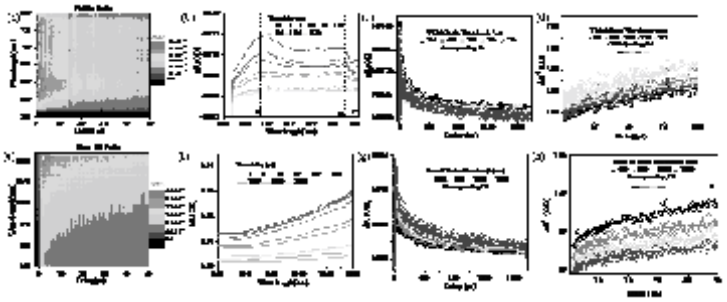

Figure 4: (a) Contour plot and (b) corresponding TR spectrum at different time delay (ps) for 2D Se at visible probe wavelengths. The dotted lines are showing excited absorption peak. (c) The fs-transient bleach decay kinetics with corresponding tri-exponential decay fits and (d) temporal variation of ΔR^{-1} at various visible probe wavelengths with their exponential fit (e) Contour plot and (f) corresponding TR spectrum at different time delay (ps) for 2D Se at near-IR probe wavelengths. (g) The fs-transient bleach decay kinetics with corresponding tri-exponential decay fits and (h) temporal variation of ΔR^{-1} at various near-IR probe wavelengths with their exponential fit. All the above measurements is performed at pump excitation of 500 nm with the fluence of 64

This chapter explores the comprehensive excited state carrier dynamics of bilayer, two-dimensional (2D) Selenium (Se) in one-photon and multi-photon absorption regime using transient reflection (TR) spectroscopy. Our analysis shows the sign of TR and TA is same for our study. In TR spectroscopy, we use 500 nm pump and visible (500-800nm) and near IR (850-1100nm) probe. The pump beam diameter and fluence are fixed at 2mm and 64μJ/cm^2 respectively. In visible probe region, the differential reflectivity spectrum (Figure-4(a, b)) shows a broad positive reflectivity change ranging from 520 nm to 800 nm suggesting occurrence of excited state absorption (ESA) with two peaks around 585nm (A) and 777nm (B). We also observe a narrow bleaching like feature peaking around 790 nm (C) overlapped with the broad ESA background. We observe broadband ESA in near-IR probe region (900-1100 nm) shown in Figure-4(e, f).The decay dynamics at various visible and near-IR probe wavelengths (Figure-4(c,g)) are fitted with the tri-exponential decay function - where, A is the maximum value of ? A, τ_1 is the rise time constant, τ_i and A_i are decay time constants (for i = 2,3) and their corresponding amplitudes respectively. The obtained rise and decay time constants show whole broad ESA region follows similar decay dynamics. The rise time is correlated with the thermalization and average carrier cooling time. The carrier cooling time at all the concerned visible and near IR probe wavelengths are nearly same (0.4-0.7ps) at 64 μJ/cm^2 pump fluence. The fast and long decay times are nearly 14-20 ps and 270-320 ps respectively in visible region whereas 30-33 ps and 515-550 ps in near-IR region respectively.The carrier lifetimes are in the same order with various mono- and few- layer TMDs who have great photo-detector application.To understand the dominant recombination process we have plotted temporal variation of ΔR^{-1} at various

visible and near IR probe wavelengths (Figure-4(d, h)). It follows exponential variation at all probe wavelengths revealing the dominance of trap state assisted recombination [44].

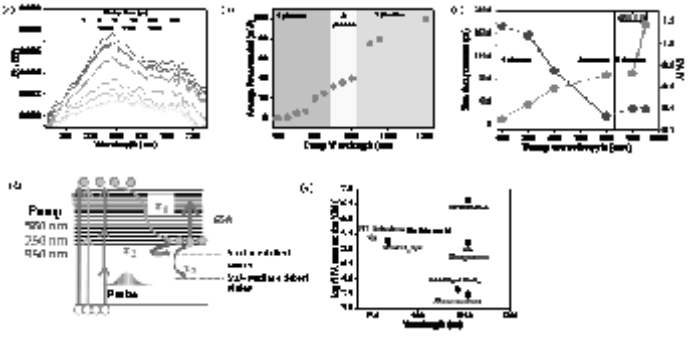

Figure 5: (a) TR spectrum of 2D Se at different time delay (ps) under the excitation of 950 nm pump having fluence of 1272 μJ/cm^2. (b) Variation of average pump power needed for having same ESA amplitude (6 mOD) at various pump photon wavelength with one and multi-photon absorption regime assigned. (c) Variation of slow decay constant () and amplitude ratio (A_2/A_3) of corresponding exponential decay constants with pump photon wavelength. (d) Model diagram to understand single and multi-photon carrier generation and recombination of 2D Se. (e) Comparison of TPA cross section of 2D Se with other 2D materials.

Pump wavelength dependent TR spectroscopy shows presence of multi-photon absorption in 2D Se. Figure-5 (b) shows one and multi-photon absorption regimes of 2D Se. We have calculated the two photon absorption cross section () at 750 nm) and it is compared with other 2D materials. The giant two-photon absorption cross section hints towards the possible application of 2D Se as sub band-gap photo-detector. The carrier recombination process is dominated by surface and sub-surface defect states in one- and multi-photon absorption regime respectively, resulting nearly one order increased carrier lifetime in three-photon-absorption regime (1700 ps) compared to one-photon-absorption regime (103 ps) (Figure-5(c)). We propose a generalized model to explain excited carrier dynamics in different pumping regime (Figure-5(d)).We have also theoretically calculated the responsivity of photo-detector based on 2D Se using our TR results. Our study provides comprehensive insights into the excited state carrier dynamics of bilayer 2D Se and highlights it's potential as a versatile material for various linear and non-linear optoelectronic applications.

5.7 Chapter 7: Conclusion and outlook

This thesis focuses on the ultrafast properties of PSC material and 2D Se which are specifically related to light harvesting and photo-detection application. Chapter 4 and 5 provides a thorough study of carrier recombination dynamics and provides deep insight in ultrafast phenomenon to understand the impact of CZTS and Au@CZTS NC in MHP which shows their great prospect in solar cell application. Apart from this, chapter 6 discusses ultrafast carrier dynamics of 2D Se for the very first time in one- and multi-photon absorption regime. Our result shows excited carrier lifetime in both the regime. It also shows giant two photon absorption cross-section of 2D Se. The high cross-section and carrier lifetime in both the regime highlights its potential as a versatile material for above- and sub-band gap photo-detection application.

TH-12

Numerical Analysis of Modulation and Pulse Generation Characteristics of Transistor Laser

R.Ramya, S.Piramasubramanian and M.Ganesh Madhan

DepartmentofElectronicsEngineering,MadrasInstituteofTechnologyCampus,AnnaUniversity, Chromepet,Chennai, India 600044.

E.mail: ramyaravi80@gmail.com,spirama@annauniv.edu,mganesh@annauniv.edu.

1. Introduction

Transistor Laser (TL), a new optoelectronic device was invented by Feng and Holonyak Jr.,[1] is basically a Heterojunction Bipolar Transistor. The device operates as a transistor as well as a laser. It has one electrical input port, one electrical output port and one optical output port. It provides fast carrier recombination process, a wider modulation bandwidth and high-speed operation. It offers current and voltage-driven operation. For an enhanced cavity, the collector breakdown occurs causing laser quenching[2]. Hence, the operation switches from stimulated to spontaneous emission mode. The phenomenon that the output optical power reduces substantially due to optical absorption is referred as Franz-Keldysh (F-K) effect. It is dependent on electric field across the intrinsic collector to base region and hence on collector to base voltage (V_{CB}).

The electrical output characteristics of TL describing the collector current variation with respect to collector to emitter voltage (I_C -V_{CE}) for various base current exhibits clearly the notable shift to stimulated emission from spontaneous emission. This prominent shift indicates a noticeable transition in the spacing of collector current curves. The uniform spacing to reduced spacing results in the compression of its characteristics. This "signature" behavior of TL reveals the fact that, the current gain (β) reduces due to quantum well recombination of carriers in the base region of TL. Moreover, this phenomenon is accompanied by the reduction in the base carrier lifetime compared to minority carrier base transit time. Further, the increase in the base current manifests the compression of collector current in the output characteristics obviously displays the onset of stimulated recombination process[2].

A slight modification made in the mirror reflectivity enhances cavity which results in a higher collector breakdown phenomenon and a lower threshold current. The occurrence of collector breakdown effect implies more electrons swept towards the collector side leaving less carriers in the base quantum well or active region where recombination process takes place. The collector breakdown effect reduces the possibility of stimulated emission as the number of electrons in the quantum well is less. Hence, there is a quick transition from stimulated emission to spontaneous emission mode and so, the laser quenching takes place under high reverse biased collector-base junction region[3].

Furthermore, TL under Common Emitter (CE) configuration operating in active mode

evidently shows that it can be voltage driven mode, the reverse biased collector voltage (V_{CB}) variation due to Franz Keldysh absorption apart from base current control operation[4]. The experimental works on TL, led by Feng group[5] suggests that the optical and electrical performances can well be leveraged both by voltage modulation and current modulation characteristics. This is done by appropriately changing both the collector-base voltage and base current.

2. Scopeofthethesis

The voltage modulation characteristic of TL enables the output power dependence on reverse bias collector to base voltage and focuses mainly on the improvement of modulation bandwidth and resonance-free modulation response[4]. The feature of TL makes it more suitable candidate for non-linear applications such as switching, and mixing. Moreover, it is a promising optoelectronic device in the field of integrated photonics, as more experimental research is heading towards the development of Transistor Laser based optical digital logic processor. To support the demonstration works led by Feng group[5], requires complete theoretical background knowledge of voltage modulation characteristics of TL. The acquisition of short optical pulse characteristics is mandatorily required for the digital data transmission-based applications. Hence, the TL produces short optical pulses using gain switching technique requires a comprehensive study of short pulse characteristics.

In addition to the digital data transmission, the requirement for the analog transmission applications demands TL to exhibit minimum distortion characteristics and a higher modulation depth[7]. Moreover, TL is a new optoelectronic device which will definitely be the most sought-after photonic device in field of telecommunication-based applications. The demand for the high-speed data transmission via single mode fiber optical link requires TL to be a promising and suitable optoelectronic device that meets out the Gigabit Ethernet speed data transmission at 10 Gbps and 20 Gbps respectively. Hence, this thesis focuses on the numerical analysis of voltage modulation characteristics of TL, intermodulation distortion characteristics of TL, short optical pulse characteristics[9] produced by TL and also on the performance measure of current driven TL[8] based single mode fiber link for Gigabit Ethernet standard.

The work reported in the thesis is organized into eight chapters. Chapter 1 is the introduction of our thesis. The introduction chapter presents with the evolution of semi-conductor based optoelectronic devices. The existing literature works of Transistor Laser is briefly pointed out. In addition to that, the structure, operation, charge distribution profile is presented. Moreover, the features, advantages and applications of TL is been discussed in detail. Also, the current and voltage modulation characteristics of TL is been discussed. In addition to that the objective of the thesis and the summary of all chapters is outlined briefly.Chapter 2 describes the central principle of Photon Assisted Tunnelling (PAT) effect or Franz-Keldysh (F-K) absorption effect[6] by discussing the existing literature works related to F-K effect. The absorption coefficient (F-K) for InGaAs / GaAs based TL is evaluated and reported for various values of reverse-biased collector base voltage. The Franz-Keldysh (F-K) absorption coefficient parameter α is strongly electric field dependent and is found to increase with increasing reverse biased collector to base voltage (V_{CB}). The inference is that, there is an

enhanced photon absorption or output optical loss in the intrinsic V_{CB}region under the strong influence of electric field.

Chapter 3 describes the rate equations that models the TL with F-K absorption effect[4]. The static analysis is performed, by fixing the base current that is well below and above threshold. For the steady state analysis, the rate equation model of voltage-driven based Transistor laser with F-K absorption effect is analyzed by deriving steady solutions of rate equations analytically and the same is verified numerically using Runge-Kutta method.The dynamic response of TL is performed and threshold current for the V_{CB} value of 0 V is found as 33 mA and its values are found to increase for increase in V_{CB} values. The F-K effect in the intrinsic collector to base region causes noticeable optical power loss and a supplementary collector current. For the V_{CB} value of 3 V, a maximum photon loss and the additional collector current are found to be 12 mW and 1.37 mA respectively.

Chapter 4 analyzes the characteristics of small signal and large signal of TL under various reverse biased collector to base voltage values. The resonant frequency and modulation bandwidth (f_{-3dB}) under various biases were evaluated. The analysis of magnitude of intrinsic optical response is carried out as the expression of intrinsic optical response $T_p(\omega)$ models the opto-electronic feedback which is based on the reverse biased collector to base voltage ($_{VCB}$) value indicating F-K absorption effect in the intrinsic collector base junction region. The analysis of intrinsic response indicates the occurrence of 25 dB resonant peak that infers the optoelectronic feedback due to F-K effect. A maximum of 12.5 GHz modulation bandwidth is obtained for the V_{CB} values of 3 V. The magnitude response of TL under various bias currents and V_{CB} values are performed. The modulation bandwidth is found to increase with increasing bias currents and its value decreases with increasing V_{CB} values.

For a reverse biased collector to base voltage (V_{CB}) of 1.6 V, the input base current value is varied from 60 mA to 90 mA and the intrinsic optical responses are evaluated. It is observed that, the AC resonant frequency and the modulation bandwidth are found to increase in the base current. This is due to more injection of minority charge carriers from emitter into the base region which in turn increases the possibility for electron-hole recombination process. This result in the increase of the photon emission from the base active region contributes high modulation bandwidth. Furthermore, the collector bias voltage is varied from 1.2 V to 2.4 V in steps of 0.4 V while the DC bias base current is fixed as 70 mA. The intrinsic optical responses are evaluated. It is observed that, for an increase in the V_{CB}, the AC resonant frequency and the modulation bandwidth are found to decrease for the fixed DC bias input base current. This decrease in the modulation bandwidth is due to the decrease in the photon density as the output optical power is absorbed substantially in the intrinsic collector to base region.

The large signal analysis is performed by applying electrical pulse signal to the base of Transistor Laser.The pulse characteristics i.e., dynamic response of Transistor Laser model incorporating with Franz-Keldysh (F-K) absorption effect is performed by solving the rate equations by Runge-Kutta (R-K) method of 4^{th} order. The electrical signal bias current is kept as 3 mA. A 1 ns electrical pulse signal with magnitude of 79.5 mA is applied to the base.The dynamic response of electron density and output power displays resonance oscillation at the

initial stage and then it is pinned by the steady state output response. The large pulse amplitude decreases with increase in collector bias. The turn-on delay time is also evaluated. There is a substantial reduction in the turn-on delay from 470 ps and 275 ps for an appreciable increase in the injection current at V_{CB} = 3 V that aids in the maximum bandwidth achievement. For the given injection current, the turn-on delay is found to increase for an increase in collector to base voltage (V_{CB}) value

Chapter 5 discusses about the intermodulation distortion characteristics of TL with F-K absorption effect. The distortion characteristics are evaluated at a higher modulation depth. The Third order intermodulation (IMD3) frequency components are evaluated at ($2f_1$- f_2) and at ($2f_2$- f_1) respectively[7]. Those frequencies are found to be 2.15 GHz and 2.45 GHz respectively. For the fundamental frequencies of 2.25 GHz and 2.35 GHz, the fifth order intermodulation (IMD5) frequency components are evaluated at ($3f_1$- $2f_2$) and at ($3f_2$- $2f_1$) respectively. Those frequencies are found to be 2.05 GHz and 2.55 GHz respectively. The third and fifth intermodulation distortion frequency components such as IMD3 and IMD5 are evaluated and analyzed. For a VCB voltage value of 0 V, 1 V, 2 V and 3 V, the magnitude of IMD3 component at 2.15 GHz are obtained as - 10.26 dBc, - 12.37 dBc, - 13.54 dBc and - 15.92 dBc respectively. The magnitudes of IMD5 component at 2.05 GHz are obtained as - 18.89 dBc, - 25.76 dBc, - 28.22 dBc and - 36.05 dBc for the V_{CB} voltage value of 0 V, 1 V, 2 V and 3 V respectively. It is observed that IMD3 (at 2.15 GHz and 2.45 GHz) and IMD5 (at 2.05 GHz and 2.55 GHz) intermodulation distortion product magnitude decreases for an increase in the reverse biased collector bias voltage (V_{CB}). This is due to the increase in the optical absorption effect under high reverse bias condition.

Chapter 6 provides the details about Gain Switching technique for the short pulse generation from the existing literature[9]. Using gain switching technique, the maximum and optimal values of optical pulse peak power and full width at half maximum is obtained at a certain base current pulse. The purpose of generation of the short optical pulse is to open up the possibility to send the pulses at a higher bit rate on par with Gigabit Ethernet standard. The dynamic response of Transistor Laser is evaluated by numerically solving the rate equations using Runge-Kutta method of 4^{th} order. The magnitude of electrical base current pulse is 77 mA and the pulse width is fixed as 100 ps. The DC bias point is kept as 32 mA which is just below the current threshold I_{th} = 33 mA. The V_{CB} values of 0 V, 1 V, 2 V and 3 V respectively are varied and short optical pulse characteristics were evaluated. For the unbiased condition (V_{CB} = 0 V), the full width at half maximum and pulse peak power are determined as 16.83 ps and 111.3 mW respectively. At V_{CB}= 1 V, the pulse peak power is found as 95mW. The pulse peak power is predicted as 75mW for the V_{CB} of 2 V. The optical pulse peak power reduces drastically for an increase in V_{CB}. The full width at half maximum increases noticeably with increasing V_{CB}. For V_{CB} = 3 V, the FWHM and pulse peak power are determined as 21.48 ps and 57.69 mW respectively. A maximum peak power of 156.2 mW and minimum FWHM of 16.08 ps are predicted for the V_{CB} values of 0 V and 3 V respectively. It is observed from the results that the peak power values of the output optical pulse found to decrease with increasing V_{CB}. In contrast, the full width at half maximum parameter values increases with increasing collector

bias voltage (V_{CB}). The obtained results manifest the importance of Franz-Keldysh effect that helps in devising the bias conditions for fixing up the maximum value of output optical pulse peak power and minimum full width at half maximum.

Chapter 7 investigates the digital data transmission performance of TL based fiber optic link operating at the wavelength of 1.3 μm. The transistor laser based single mode fiber optic link is considered. The maximum fiber length is determined at an acceptable BER of 10^{-10} for the Gigabit Ethernet standard such as 10 Gbps and 20 Gbps respectively. The Langevin noise is included in the rate equation model and the performance is predicted[10]. For a BER of 10^{-10}, a maximum fiber length that can be deployed for 10 Gbps and 20 Gbps data rate are predicted as 10 Km and 3 Km respectively. The Langevin noise is included in the rate equationsand the performance of digital data transmission over fiber optic link is predicted by varying current magnitude at 1 Gbps. The digital data performance is also evaluated by varying fiber length at 5 Gbps. Finally, the current-driven based Transistor Laser led digital data transmission performance over fiber optic link is evaluated by varying the data rate between 5 Gbps to 17 Gbps at a fixed fiber length of 1 Km. For the Gigabit Ethernet standard BER of 10^{-10}, a maximum fiber length that can be deployed for 5 Gbps is predicted as 15 Km. Chapter 8 appropriately concludes the predicted results. In addition to that, the further scope of the research work is also pointed out and the same can be considered as an extension work in future.

SelectedReferences

1. N.Holonyak, Jr., and M.Feng, 'The Transistor Laser', IEEE Spectrum, vol. 43, no. 2, pp. 50–55 (2006).
2. A. James, N. Holonyak, Jr, M.Feng, and G.Walter, 'Franz-Keldysh photon-assisted voltage-operated switching of a transistor laser', Photonics Technology Letters, IEEE, vol. 19, no. 9, pp. 680–682 (2007).
3. G.Walter, A. James, N.Holonyak, Jr, M.Feng, andR.Chan, 'Collector breakdown in the heterojunction bipolar transistor laser', Applied Physics Letters, vol. 88, no. 23, article 232105 (2006).
4. C.H. Chang, , S.W. Chang, & C.H. Wu, 'Theory for voltage modulation of transistor lasers using Franz-Keldysh absorption in the presence of optoelectronic feedback', OSA Publishing, Optic Express, vol. 24, 22, pp. 25515-25527 (2016).
5. M. Feng, J. Qiu, C. Y. Wang, and N. Holonyak, Jr., “Intra-cavity photon-assisted tunneling collector-base voltage-mediated electron-hole spontaneous-stimulated recombination transistor laser,” J. Appl. Phys. 119(8), 084502 (2016).
6. K. Tharmalingam, Optical absorption in the presence of a uniform field, Phys. Rev. 130

(6), 2204–2206 (1963).

7. S.V. Vinodhini, S. Piramasubramanian, M. Ganesh Madhan., Analysis of nonlinear distortion and its

   reduction using feedback injection schemes in an 1.3μm transistor laser., Optics Communications, 439
   224–232(2019).

8. M. Shirao, S.Lee, N.Nishiyama and S.Arai, 'Large signal analysis of a Transistor Laser', IEEE Journal of
   Quantum Electron., vol. 47, no. 3, pp. 359-367 (2011).

9. S.Piramasubramanian , M. Ganesh Madhan , A. Sindhuja “Performance analysis of a digitalfiber optic link
   incorporating gain levered laser diode transmitter”, Int J Numerical Model., 2018.

10. M.F.Ahmed, "Influence of transmission bit rate on performance of optical fiberCommunication
    systems with direct modulation of laser diode", J Phys D Appl Phys. 2009; 42:185104(18):185104

PublicationsinJournals

1. R.Ramya, R and S,Piramasubramanian, 'Effect of Franz-Keldysh absorption on short optical pulse generation in Transistor Laser', Optics Communications, vol. 474, article12608 (2020).

2. R.Ramya,R, S.Piramasubramanian, M. Ganesh Madhan, and D. Rebecca, 'Effect of Collector Voltage on the Large and Small Signal Modulation Characteristics of 980 nm Transistor Laser', Defence Science Journal, vol. 70, no. 5, pp. 529-533 (2020).

TH-13

Generation, Modulation and Detection ofPhase Structured Laser Beams for Sensing Application

Pritam P Shetty

Indian Institute of Information Technology, Design and Manufacturing, Kancheepuram, Tamil Nadu

Email: pritamshtty@gmail.com, phy18d005@iiitdm.ac.in

Abstract

Electromagnetic radiation carries energy and momentum. The momentum may involve linear and angular part. Light from laser can carry angular momentum of two types called spin angular momentum associated to polarization and orbital angular momentum associated to spatial distribution.Circularly polarized beam carries spin angular momentum(SAM)and Laguerre-Gaussian (LG) beam carries orbital angular momentum (OAM). In this work, various viable methods for LG beam generation is proposed and demonstrated. The tunability of thermal lens in nanofluid by electrical or optical means allowed for dynamic lenses for beam shaping. Further a new type of common path interferometer called Thermo-optic refraction interferometer (TORI) is proposed. LG beam propagation through milk as medium is studied as a function of its phase structure deterioration. The deterioration in phase structure is quantified and used to measure fat content in milk.

Objectives

The objectives of the research work are as follows:

a) To design and develop an economical method for generating Laguerre-Gaussian(LG) beams with variable topological charges.

b) To understand the properties of Laguerre Gaussian beams and their interaction with different media as a function of their topological charge.

c) To develop a sensing modality using LG beam as illuminating source.

Existing Gaps Which Were Bridged

The research gaps that were bridged in the work:

a) The accessibility to affordable phase and diffractive elements is limited owing to the fabrication complexity and associated materials.

b) Low cost and tunable solution for Hermite Gaussian like beam generation other than spatial light modulator and digital micromirror device.

c) Optically induced thermal lenses in nanofluids can be a potential method for dynamic lens system. The control and tunability of these thermal lenses are not studied well. Further, the electrical modality for thermal lens generation is not well explored for beam shaping.

d) Astigmatic Optical mode converters are useful for beam mode conversion with high

efficiency. But the lenses used in such mode converters are static. A dynamically tunable lens by means of optical and electrical modality can allow switchable mode conversion.

e) A new type of common path interferometry is proposed which is not limited by its usage due to small sample and reference beam separation.

Most Important Contributions

Generation of the Laguerre Gaussian beam using simple optical elements

PET sheets are most commonly found plastic sheets used as overhead projector sheets. These sheets are affordable and available in various thickness. The refractive index of PET transparent sheets is 1.5651. This is also flexible for different azimuthal angles which is important for generating OAM beams. PET sheets allow clean shear cuts with fine edges which is important to have a clean beam profile after transmission. Further, the absorption is minimum in the visible spectrum (450nm to 700nm) which will cause less impact on propagation losses of the beam. PET sheets are cut in square from using scissors and mounted over 3D printed holders as shown in Figure. The screw can be used for adjusting the spiral phase to achieve tunable topological charge of LG beams. The angles were changed upto 10? .

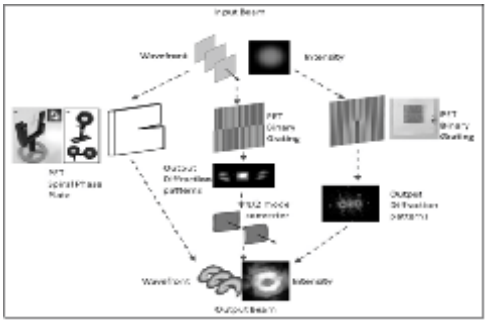

Figure 1: Methods to generate Laguerre Gaussian beam.

Binary amplitude gratings are diffractive optical elements with regions of high and low intensity transmission. The diffraction and the output beam pattern in these gratings can be controlled using the parameters such as pitch, relative fringe shifts, duty cycle of the grating material of grating substrate. This gives better control to generate low topological charges of orbital angular momentum of beams, that include Hermite Gaussian and Laguerre gaussian beams.

A phenomenon to generate Hermite Gaussian structured beams.

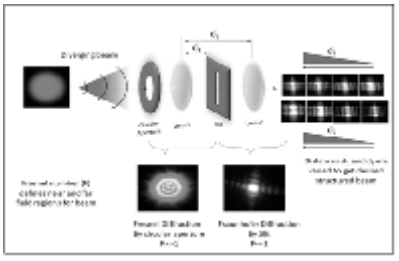

Figure 2: Synergic Fresnel and Fraunhofer diffraction

Diffraction, arising from the wave-like nature of light, manifested at edges. The well-known diffraction phenomena, namely Fresnel and Fraunhofer, have diverse individual applications. However, the combined effects of these two phenomena have not been thoroughly studied and understood, despite their importance in comprehending compound optical instruments. This research investigates and demonstrates the synergistic patterns resulting from the combination of Fresnel and Fraunhofer diffractions. The observed combined diffraction patterns exhibit characteristics similar to Hermite-Gaussian Beam intensity distributions, as validated through both simulations and experimental results. This work contributes to a deeper understanding of complex diffraction in optical instruments and offers a pathway for robust fabrication of micro gratings1.

Imaging and measurement of thermal lens region within nanofluid

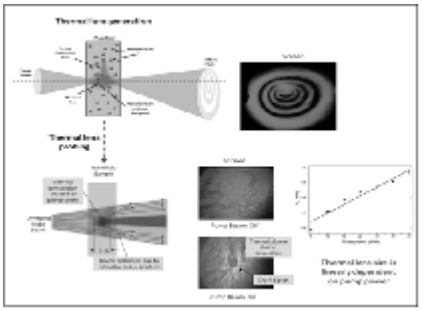

Figure 3: Thermal lens generation in nanofluid and its probing

The remarkable nonlinear optical response exhibited by two-dimensional (2D) nanomaterials such as Molybdenum disulfide (MoS2) has garnered significant attention. In this study, we investigate the formation of thermal lenses in dispersions of MoS2 nanoflakes using a pump-probe configuration with mode mismatch. By observing the intensity patterns of the pump and probe beams, we gain visual insights into the temporal evolution of photothermal lens formation. The influence of MoS2 nanoflake concentration on the thermo-optic properties of the dispersions is explored using thermal lens spectroscopy. Additionally, a novel technique based on thermo-optic refraction is proposed for measuring the size of the thermal lens region. It is observed that the size of the thermal lens region increases with higher pump power. Leveraging the observed thermal lens modulation, we successfully demonstrate a "normally on" all-optical switch that exhibits exceptional modulation of the output beam signal by the pump beam"2.

Near vicinity thermal lens optics with respect to Laguerre Gaussian beams

This study highlights the importance of temporally switchable optical mode conversion in optical communication and computing applications. We have successfully developed an optically switchable mode converter based on thermo-optic refraction. To achieve this, we utilized MoS2 nanofluid as medium, where a thermal microlens is formed by focusing a laser beam (referred to as the pump beam). Above the focal point of the pump beam within the nanofluid, a convective thermal plume is generated, which acts as an astigmatic thermal lens.Through experimentation, it was observed that the thermal lens causes the conversion of Laguerre-Gaussian (LG) beams into Hermite-Gaussian (HG) beams, and vice versa, when they pass through it.

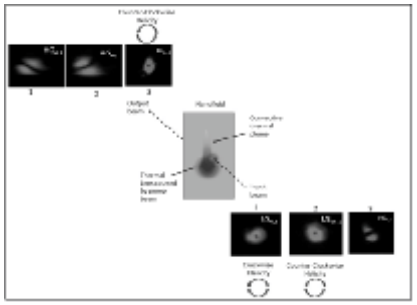

Figure 4: Mode conversion after transmission through thermal lens

Consequently, this mode converter enables the easy determination of the topological charge of the LG beam. A theoretical explanation for this mode transformation by considering the different optical paths experienced by the Fourier components of the LG beam as it propagates through the convective plume is provided3.

An electrically controllable mode converter for topological charge measurement

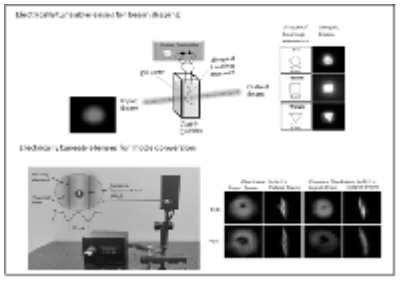

Figure 5: Electrically generated thermal lenses for beam structuring and mode conversion.

Heating elements with distinctive shapes immersed in a fluid have the ability to generate thermal lenses in their vicinity. The strength of these thermal lenses is directly proportional to the current passing through the heating elements. By bending the elements into common shapes such as squares, circles, and triangles, structured beams can be generated. Moreover, when multiple heating elements are arranged in a parallel configuration, a cylindrical lens-like profile is formed within the liquid medium. This profile can be effectively utilized for mode conversion purposes.

A new common path interferometric method called Thermo-optic refraction interferometry and application to milk fat detection.

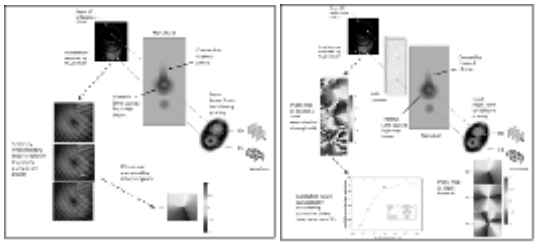

Figure 6: Thermo-optic refraction interferometer (left panel).Milk Fat estimation using Thermo optic refraction interferometer (right panel)

Common path interferometers (CPI) are highly valuable for their compactness and ability to resist vibrations. However, a common challenge in CPI arises from the small separation between the reference and sample beams. This limitation makes it difficult to send a reference beam through a sample, hindering the ability to study the interaction of beams with materials based on their phase structure. This research introduces a promising solution that opens up new possibilities for interferometry. The study proposes and demonstrates a novel approach utilizing thermo-optic refraction to enable both beams to pass through the sample and investigate the phase degradation resulting from their relative interaction within the material medium.

Termed thermo-optic refraction interferometry (TORI), this technique leverages the phenomenon of thermal lensing to superpose a higher order vortex beam with a nonvortex beam. By optically pumping the non-vortex beam, controlled expansion is induced. The interaction between the expanding non-vortex beam and the vortex beam within the sample generates an output interferogram. Analyzing the phase deterioration exhibited in the output interferogram provides insights into the medium-induced phase changes.

To illustrate the effectiveness of TORI, the experiments were conducted using milk samples and measured the root mean square (RMS) azimuthal phase deterioration of the OAM beam. The results showcase the potential of this technique to study phase variations driven by the medium. By overcoming the limitations of traditional CPI setups, this innovative approach broadens the capabilities of interferometric analysis4.

References

1 P.P. Shetty et. al., Opt. Laser Technol. 130(April), 106340 (2020).

2 P.P. Shetty et. al., Opt. Mater. (Amst). 112, 110777 (2021).

3 P.P. Shetty et. al., J. Quant. Spectrosc. Radiat. Transf. 274, 107867 (2021).

4 P.P. Shetty et. al., J. Opt. 25(8), 085601 (2023).

TH-14

Generation and characterization of pair photon source for quantum sensing applications

Sandeep Singh
Physical Research Laboratory, Ahmedabad, Gujarat 380009, India
Indian Institute of Technology-Gandhinagar, Ahmedabad, Gujarat 382424, India
Email:sandeep@prl.res.in

Quantum sensing and metrology is a rapidly growing field due to its outstanding features in measuring physical parameters with great precision and accuracy, outperforming the pre-existing technologies based on the principles of classical physics[1]. In recent years, quantum sensing has enabled the measurement of several key physical quantities, including the measurement of the electrical field[2], magnetic field[3], vacuum[4], temperature[5], and pressure[6] with unprecedented precision and accuracy. Among various quantum sensors as presented in Ref.[7], Hong-Ou-Mandel (HOM) interferometry, since its discovery[8], has found a large number of applications within quantum optics for a variety of advantages, including easy development and implementation, sensitivity only to photon group delay and not to phase shifts[9].

HOM interference, a purely non-classical phenomenon, is observed for two photons that are identical in all degrees of freedom, including spin, frequency, and spatial mode, when simultaneously entering on a lossless, 50:50 beam splitter through different input ports bunch together into one of the output ports. The probability of coincidence detection between the two output ports shows a characteristic low or zero coincidence, known as the HOM interference dip, directly related to the level of indistinguishability or the degree of purity of the photons[10]. As a result, the change in coincidence counts can be treated as a pointer to estimate the indistinguishability parameter between photons properties, forming the basis of the HOM interferometer-based quantum sensors to sense any physical process influencing theindistinguishability between the pair photons. As such, efforts have been made to use the HOM-based quantum sensors to characterize the single photon sources[11], precise measurement of time delays between two paths[8,12,13], characterization of ultrafast processes[14], measurement of frequency shifts[15,16] and the spatial shift[17]. The basic principle of HOM interferometry relies on the generation and manipulation of indistinguishable paired photons. Typically, the pair photonsare generated through a second-order nonlinear optical process called spontaneous parametric down-conversion (SPDC) and are indistinguishable in all degrees-of-freedom incident on a balanced beam splitter, they always bunched together through one of the output ports, resulting in the phenomenon known as the HOM dip. This dip in the interference pattern provides valuable information about the relative optical delay between the photons and allows for measuring various physical quantities, including the group index of dispersive materials. Due to the intrinsic dispersion cancellation,HOM interferometry is utilized to sense the characteristic parameters of a sample material, enabling high-resolution imaging of surface features[17], depth profiling of different layers, and the measurement of group index variations[18].

However, for reliable and fast sensing with high accuracy and resolution, the indistinguishable pair photon source must have high brightness, broad spectral bandwidth, and stability against the external perturbations. Besides the huge potential of the HOM interferometry in quantum sensing domain, there is not a dedicated study addressing the aforementioned issues simultaneously. This lays the foundation for the primary objective of this thesis, which is to generate and characterize SPDC-based pair-photon sources for various quantum sensing applications based on HOM interferometry. We have individually addressed all three challenges present in the earlier configurations of HOM based quantum sensing techniques. Fig.1, shows the flowchart of the approach involved in this thesis to achieve an all-completer solution to overcome the challenges of HOM based quantum sensing.

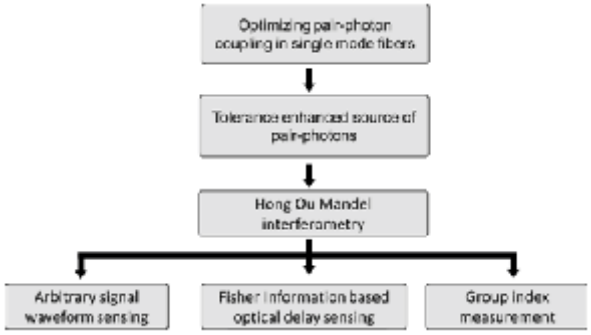

Figure 1: Flow chart of thesis structure

Thesis Structure: This thesis is organized into seven chapters, whereas the first two chapters provide a better perspective on the field, fundamental principles, and theoretical framework to understand non-linear optics, spontaneous parametric down-conversion, pair photon source, and Hong-Ou-Mandel interferometry. Chapters 3-6 are dedicated towards the work done to overcome the challenges of HOM based quantum sensing techniques.

Chapter-3 is dedicated to meet the first objective of improving the pair photon rate and their coupling efficiency into single-mode fibers. We have first studied various parameters affecting the pair photon rate and photon pair coupling efficiency in periodically-poled non-linear (e.g., PPKTP) crystal designed for quasi-phase matching criterion. The motivation behind choosing the PPKTP crystal is its high non-linear gain, but still, there is not much in-depth study on the factors affecting the photon pair coupling efficiency in periodically poled crystals. We have studied how the various parameters of quasi-phase matching conditions, such as crystal temperature, pump beam spot size (ω_p), and the collection beam spot size(ω_c), affect the photon pair coupling efficiency. Using the optimized parameters for generation and detection in a PPKTP crystal of 30mm interaction length, we achieved a maximum coincidence count of 1692.3 ± 8.5 kHz/mW for ω_p = 42 μm and ω_c = 57 μm at a crystal temperature of 29.5°C. We have observed a maximum coupling efficiency of 32.1 ± 0.6 % for the optimum combination of

waist radius of pump, $\omega_p = 84\ \mu m$ and collected photons, $\omega_c = 109\ \mu m$ at a crystal temperature of 26°C. It is observed that both the pump intensity at the crystal center and the divergence of the SPDC photons play a crucial role in the collection of pair photons into single-mode fibers.Both the pump intensity at the center of the crystal and the divergence of the down-converted photons from the crystal center can be controlled by appropriately choosing $\omega_p$and ω_c, respectively.By controlling these parameters, we can optimize the pair photon pair in single photon fibers. While the pair coupling efficiency is majorly controlled by the divergence of the pump and, thus, the divergence of SPDC photons. The rate of generation of photons does not seem to alter the pair coupling efficiency. This conclusion supports the experimental observation that for a fixed collection beam waist, the pump beam waist providing the maximum pair coupling efficiency is different from the providing maximum coincidence counts. Crystal temperature is another parameter that can be utilized to change the radius of the SPDC ring and, thus, the photon density at the fiber coupler. It is observed that a linear decrease in the radius of the SPDC ring provides a quadratic increase in the pair photon rate collected by single-mode fibers and becomes highest near the collinear geometry of SPDC. This study provides a comprehensive solution to choose the pump and collection beam waist to have high spectral brightness of pair photons sources.

After addressing the issue of spectral brightness, in chapter 4, we have addressed the issue related to the stability of the pair photons. The phase-matching parameters of the SPDC process give the freedom to control the various parameters of the paired photons. This versatility derives from the simple manipulation and control of the different characteristics of down-converted photons, such as wavelength, polarization, and spatial geometry, by adjusting the phase-matching parameters of nonlinear interactions, such as temperature, crystal inclination, and pump wavelength. Nonetheless, this adaptable control over the various parameters of down-converted photons renders the SPDC process sensitive to small changes in pump wavelength, crystal temperature, and crystal axial orientation. Such intolerance for fluctuating environmental factors prohibits the deployment of SPDC-based sources in non-ideal environments outside of laboratory settings. To address this issue, we developed a novel system architecture based on a hybrid linear and non-linear solution that increases the source's tolerance without diminishing its spectral brightness. This new configuration involves a hybrid solution that incorporates a lens-axicon pair, commonly available in an optics laboratory, to transform the conventional SPDC annular ring into a new ring. Testing the robustness of this technique with two common non-linear crystals, quasi-phase-matched periodically poled $KTiOPO_4$ and birefringent-phase-matched BiB_3O_6, reveals that this new SPDC ring enhances the tolerance of the conventional SPDC ring to external perturbations in phase-matching parameters without sacrificing the spectral brightness of the source. The spectral brightness of the source is observed to be as high as 22.58 ± 0.15 kHz/mW with a state fidelity of 0.95 ± 0.02 yet requiring a crystal temperature stability of only ±0.8°C, a 5× enhanced tolerance as compared to the conventional high brightness SPDC configurations. It also relaxes crystal tilt stability by more than 3× and the wavelength stability of the pump laser by more than 100 GHz. This new configuration for the generation of pair photons through SPDC is highly useful in quantum sensing experiments of QOCT, and the experiments required field deployment of pair photon source. Such a solution provides a novel approach to deployable high-brightness quantum sources that are environment-resilient, such as in satellite-based quantum optics experiments.

After addressing the issues of spectral brightness and stability, in Chapter 5, we attempted to improve the precision and accuracy of quantum sensing measurements obtained using Hong-Ou-Mandel interferometry. The interference dip has afull width at half maxima (FWHM) proportional to the coherence length of the indistinguishable photons bunching on the beam splitter or inversely proportional to their spectral bandwidth. It is generally accepted that the resolution of any quantum sensing measurement utilizing HOM interference is constrained by the width of the HOM dip.Narrower the FWHM of HOM dip, higher will be resolution obtainedin the measurement, but this demands pair photons having broad spectral bandwidth. Consequently, the spectral bandwidth of interfering pair photons has a significant impact on the resolution of HOM-based sensors. The requirement of indistinguishable photons is generally fulfilled through the parametric down conversion by employing ultrashort pulse lasers so that the broad spectral bandwidth of the pump photons can be translated to the down-converted photons. However, these lasers are highly expensive and bulky in size, limiting their use in space-constrained environments. We address this issue by using a much more economical and small-sized single-frequency, continuous-wave diode laser to generate down-converted photons with broad spectral bandwidth. Using the length of the non-linear crystal as a control parameter, the spectral bandwidth of the down-converted photons is altered. Using a 405 nm, CW laser to pump 1 mm long PPKTP crystal, we have generated paired photons with spectral width as high as 163.42 ± 1.68 nm. The use of photon pairs with such a high spectral bandwidth in a HOM interferometer results in a narrow-width HOM interference dip having an FWHM of 4.01 ± 0.04 μm enabling the real-time sensing of static displacement as low as 60 nm and threshold vibration amplitude as low as ~205 nm with a resolution of ~80 nm at a frequency measurement up to 8 Hz. In addition, we have incorporated the use of Fisher information (FI) and maximum likelihood estimator to measure vibrations with a precision limited by the Cramer Rao bound. We have theoretically modelledand experimentally observed the dependence of FI on the spectral bandwidth of the pair photons and hence on the length of the nonlinear crystal. We observed a 17 × enhancement in the FI value while reducing the crystal length from 30 mm to 1 mm. Such an increase in the peak FI value $(35.06 \pm 1.65) \times 10^{-4} \mu m^{-2}$, which is nearly 24 times higher than the previous study, saturates the Cramér-Rao bound to achieve any arbitrary precision (say ~5 nm) in a lower number of iterations (~ 3300), ~11 times lower than the previous reports. The accessibility of high precision in lower iterations or time establishes the potential of HOM-based sensors for real-time, precision-augmented, in-field quantum sensing.

After successfully addressing the challenges of the HOM based quantum sensing, chapter-6 is dedicated towards the use of precision-enhanced HOM interference technique developed in the previous study, to measure the small optical delays introduced between the interfering indistinguishable photons, which in turn tells us the information of the physical parameter related to the optical delay. One such physical parameter is the group index, which is a characteristic parameter of a dispersive material and a measure of the group velocity of light traveling through it. The group index has a wide range of applications in material characterization, optical coherence tomography, and fiber optics. Specifically, to shape single-mode operation in high-power optical fibers, a precise understanding of the optical properties of the gain medium is required[19]. This necessitates accurate measurements of the group indices of core and cladding of the optical fiber and the difference in their refractive indices.Using the

HOM curve of FWHM width of 4.11 μm resulting from the paired photons generated by a PPKTP crystal of length 1 mm, we have measured the temperature-dependent group index of PPKTP crystal over a temperature range of 3°C, at any arbitrary initial temperature with a resolution of 6.75×10^{-6} per centimetre length of the sample. This resolution is > 400 % better than the previous group index measurement [18]. Such enhancement was possible due to the control of the spectral bandwidth of the paired photons; thus, the width of the HOM curve using the optimized length of the nonlinear crystal to produce paired photons with a high generation rate. Using compensation of group index mediated optical delay by the linear optical delay stage, we observed the possibility of measuring group index with high precision over an unlimited temperate range. The current demonstration opens the possibility of HOM-based quantum sensors for quantum optical coherence tomography with high resolution and measurement range.

In conclusion this thesis builds a pathway for the applications of HOM based quantum using pair photon sources based on spontaneous parametric down conversion. We are currently employing these developed techniques in the domain of quantum optical coherence microscopy to push the standard limits of accuracy and precision in quantum imaging.

References:

[1]. S. Pirandola, B. R. Bardhan, T. Gehring, C. Weedbrook, S. Lloyd, Nature Photonics 2018, 12, 12 724.

[2]. K. Bian, W. Zheng, X. Zeng, et. al. Nature Communications 2021, 12, 1 2457.

[3] M. Tsukamoto, S. Ito, K. Ogawa, Y. Ashida,K. Sasaki, K. Kobayashi, Scientific Reports2022, 12, 1 13942.

[4] J. Hendricks, Z. Ahmed, et al., journal of physics: conference proceedings 2018, 1065, 16 162017.

[5] K. Kakuyanagi, H. Toida, L. V. Abdurakhimov, S. Saito, New Journal of Physics 2023.

[6] L. Shi, Z. Li, M. Chen, Y. Qin, Y. Jiang, L. Wu, Nature Communications 2020, 11, 1 3529.

[7] C. L. Degen, F. Reinhard, P. Cappellaro, Rev. Mod. Phys. 2017, 89 035002.

[8] C. K. Hong, Z. Y. Ou, L. Mandel, Phys. Rev. Lett. 1987, 59 2044.

[9] A. M. Steinberg, P. G. Kwiat, R. Y. Chiao, Phys. Rev. A 1992, 45 6659

[10] K. N. Cassemiro, K. Laiho, C. Silberhorn, NewJournal of Physics 2010, 12, 11 113052

[11] K. N. Cassemiro, K. Laiho, C. Silberhorn, New Journal of Physics 2010, 12, 11 113052.

[12] A. Lyons, G. C. Knee, E. Bolduc, et.al., Faccio, Science ad-vances 2018, 4, 5 eaap9416.

[13] Y. Chen, M. Fink, F. Steinlechner, J. P. Torres, R. Ursin, npj Quantum Information 2019, 5, 1 43.

[14] M. Lipka, M. Parniak, Physical Review Letters 2021, 127, 16 163601.

[15] N. Fabre, S. Felicetti, Phys. Rev. A 2021, 104 022208.

[16] S. Restuccia, M. Toro? s, G. M. Gibson, at.al, Physical Review Letters 2019, 123, 11 110401.

[17] B. Ndagano, H. Defienne, D. Branford, et.al, Nature Photonics 2022, 16, 5 384.

[18] M. Reisner, F. Mazeas, R. Dauliat, et.al, npj Quantum Inf. 8, 58322(2022).

[19] E. Dulkeith, F. Xia, L. Schares, et.al. Opt. express 14, 3853–3863 (2006)

TH-15

Synthesis of Nanomaterials and their Potential Applications

Prof. K. N. Uttam
University of Allahabad

The objectives and findings of each approach are summarized below:

1. **Microwave-assisted synthesis of P-AgNPs**
   - **Objective:** To detect metal ions [Cr (III), Cr (IV), Se (IV), Mn (II), Fe (II), As (V), and Hg (I)] in aqueous solutions using colorimetry and SERS.
   - **Results:** P-AgNPs cause distinct color changes in the presence of different metal ions, enabling visual detection. SERS signal exhibit characteristic peaks facilitating the identification of metal ions in aqueous samples.
2. **Microwave-assisted synthesis of L-AgNPs**
   - **Objective:** To detect Co (II), Cr (III), and Mn (II) ions in aqueous solutions using colorimetry and SERS.
   - **Results:** L-AgNPs induce specific color changes and alter localized surface plasmon resonance (LSPR) bands in response to different metal ions, enabling their identification and quantification.
3. **Synthesis of F-AgNPs using chemical reduction and microwave-assisted method**
   - **Objective:** To detect Al (III), Cr (VI), Mn (II), and As (V) ions in the aqueous medium using colorimetry and SERS.
   - **Results:** F-AgNPs synthesized through different methods show distinct sensitivity and selectivity towards different metal ions, facilitating their detection via colorimetry and SERS.
4. **Synthesis of V-AgNPs**
   - **Objective:** To detect Cr (III) and Mo (VI) ions in aqueous solutions using V-AgNPs.
   - **Results:** V-AgNPs induce color changes in response to various metal ions, enabling their visual detection. Moreover, distinctive Raman spectrum signatures assist in the identification of specific metal ions in the aqueous media.

Nanoparticles are crucial for connecting bulk materials and atomic and molecular structures. They possess strong chemical activity and can be produced using physical, chemical, and biological methods. Physical methods require fewer chemical species and produce larger, more pure particles. Chemical reduction methods stabilize metal nanoparticles using various ligands. They can be spherical, oval, rod, or flower-shaped using microwaves and other methods.

Top-down and bottom-up synthesis techniques are used to produce nanoparticles and

nanomaterials. Bottom-up processes involve molecular changes, while top-down ones involve external influences. Liquid phase processes include liquid/liquid and sedimentation, while chemical reduction, liquid plasma, ultrasonic vibrations, and gamma-ray photoreduction produce various particle morphologies.

The surface and sub-surface structure of a synthesized nanomaterial is examined utilizing microscopic characterization techniques using photons, electrons, ions, or physical cantilever probes. The current thesis work employs Confocal Raman Microscopy, which is also employed for Surface-Enhanced Raman Spectroscopy, as an optical microscopic approach.

Confocal microscopy and the Raman scattering technique have been coupled to provide clear images of the precise plane of focus without any distracting fluorescent light from the backdrops or other parts of the material. Ultraviolet-visible spectroscopy, attenuated total reflection Fourier-transform infrared spectroscopy and confocal micro-Raman spectroscopy measurements, along with X-rays for X-Rays diffraction, are used in spectroscopic characterization procedures to ascertain a material's chemical composition, variation, crystal structure, and photoelectric properties.

Environmental pollution is a growing concern, affecting ecosystem health and functioning. Heavy metals, including chromium, cadmium, lead, arsenic, and mercury, are toxic even at low concentrations. These anthropogenic sources, such as pesticides, fertilizers, pharmaceutical industries, automobiles, and untreated industrial effluents, contribute to the increase in heavy metal ions. These ions cause biomagnifications and bioaccumulation, affecting plant and animal growth. Heavy metals are not biodegradable, posing risks to the ecological system, human health, and the environment. Continuous monitoring is crucial to limit the negative effects of heavy metal contamination on human health.

Monitoring heavy metals is challenging due to their selectivity and concentration. Current methods include flame or graphite furnace atomic absorption spectroscopy, inductively coupled plasma mass or emission spectroscopy, X-ray fluorescence, and spectrophotometric methods. However, these methods are limited by high-cost laboratory equipment, sample collection, transportation, and pre-treatment, leading to high chances of contamination and errors.

Electrochemical techniques, such as potentiostats, voltammetry, impedance measurement, galvanostatic, static, and electro-chemiluminescence, are being developed but lack stability, reproducibility, and environmental friendliness. Therefore, there is a need to explore smaller, portable, and cost-effective devices that can rapidly detect heavy metal presence and have onsite detection capabilities.

The colorimetric method is an emerging alternative to conventional heavy metal ion detection techniques, allowing for rapid, low-cost, and easily detectable colour patterns. Plasmonic nanoparticles, such as gold and silver, offer new avenues for developing colorimetric sensors for heavy metals. These particles have unique surface plasmon resonance properties, resulting in a pronounced absorption profile in visible and near-infrared regions. These properties are influenced by factors like size, shape, coating, dielectric environment, and interaction with surrounding environments and molecules. This phenomenon can be exploited for ultra-sensitive colorimetric sensors for detecting heavy metal ions and molecules.

Plasmonic nanoparticles develop a colour pattern in two distinct manners: surface plasmon coupling and an interparticle distance-dependent process. Surface plasmon coupling and a shift

in the location of the localized surface plasmonic resonance band peak are caused by aggregate formation brought on by interparticle interactions with nanoparticles. Aggregation is influenced by temperature, pH, and external conditions.

Raman spectroscopy is a sensitive analytical technique that provides vibrational information about atom arrangement in molecules without sample preparation stages. It detects chemical bonds, structure, phase, polymorphy, crystallinity, and interactions. However, conventional Raman spectroscopy has a narrow cross-section, making it less sensitive to qualitative and quantitative investigation of trace analytes. Raman spectroscopy is sensitive and focused, providing rich vibrational information about atom arrangement in molecules. Surface plasmon resonance can be combined with Raman spectroscopy to overcome this limitation.

Surface-enhanced Raman scattering signals captured by molecularly functionalized nanoparticles are a promising technique in analytical chemistry. Factors affecting SERS intensity include excitation line, surface structure, coverage, and complex enhancing mechanisms. Silver nanoparticles can amplify analytes' signals by 14 orders of magnitude, surpassing fluorescence spectroscopy. When combined with noble metal nanoparticles, metal ions can be precisely identified using spectroscopic fingerprints and colorimetry.

Heavy metals' environmental load is a major concern, affecting ecosystem growth and causing physiological and metabolic disturbances. Detection methods include spectroscopic, electrochemical, and chromatographic methods. Functionalized metallic nanomaterials, colorimetry, and surface-enhanced Raman scattering sensors can detect harmful metal ions like lead, arsenic, mercury, chromium, nickel, barium, cadmium, cobalt, selenium, vanadium, oils, grease, and pesticides.

Sol-gel, hydrothermal, microwave-assisted, and laser ablation are examples of physical and chemical techniques that can be used to create silver nanoparticles. However, these techniques are constrained by labor, lengthy protocols, and hazardous substances. Chemical reduction techniques provide quick, easy, and economical fixes. Organic compounds like lignin, pectin, ferulic acid, & vanillic acid that can be coated on silver nanoparticles demonstrate potential functionalization capabilities, such as high adsorption and biocompatibility.

The proposed thesis seeks to develop procedures and methods for the synthesis of functionalized nanoparticles from an applications perspective, guided by forces or parameters such as user-friendliness, cost-effectiveness, rapid/fast data generation, robustness, eco-friendliness, environment-friendliness, multimode functionalized or multi-elemental detection capability, point of care, portability, capable of in-situ application, the possibility of paper stick, microfluidic device and selective sensing.

The synthesis of novel pectin functionalized silver nanoparticles (P-AgNPs), lignin capped silver nanoparticles (L-AgNPs), ferulic acid-functionalized silver nanoparticles (F-AgNPs), vanillic acid coated silver nanoparticles (V-AgNPs) and its applications in colorimetric and surface-enhanced Raman scattering detection of metal ions in an aqueous medium, synthesis of sensitive and robust for the detection of cobalt (II), chromium (III), manganese (II), chromium (VI), arsenic (V), aluminium (III), iron (II) and molybdenum (VI) ions in the aqueous medium.

Microwave-assisted P-AgNPs were synthesized for the detection of metal ions [Cr (III), Cr (VI), Se (IV), Mn (II), Fe (II), As (V), and Hg (I)] in aqueous solution using colorimetry and surface-enhanced Raman scattering (SERS). The addition of P-AgNPs causes water samples

carrying Fe (II) and Mn (II) ions to turn black and brown, whereas water samples containing Cr (III) and As (V) ions turn reddish brown. Raman observations of Cr (III), Cr (VI), Se (IV), Mn (II), As (V), and Hg (I) ions mixed with synthesized colloidal P-AgNPs solution were also recorded. The addition of metal ions to the P-AgNPs solution changes the spectrum characteristics of the P-AgNPs peaks. Furthermore, they contribute to the creation of new distinguishing bands. Significant enhancement in these bands was recently detected in the form of SERS signals. These unusual characteristic peaks can be used to detect metal ions in aqueous solutions.

Using microwave-assisted L-AgNPs, Co (II), Cr (III), and Mn (II) were detected in aqueous solution using colorimetry and surface-enhanced Raman scattering (SERS). Water samples containing Mn (II) ion appear black with the presence of L-AgNPs colloidal solution is present. Those that contain Cr (III) ions look reddish brown in contrast. In addition, water samples containing Co (II) ions become translucent and a brownish precipitate appears when L-AgNPs solution is applied. The ultraviolet-visible spectra of Co (II), Cr (III), and Mn (II) spiked water mixed with L-AgNPs colloidal solution demonstrate how these metal ions affect the L-AgNPs localized surface plasmon resonance (LSPR) band, which is caused by metal ion aggregation in the colloidal solution.

Similarly for the detection of Al (III), Cr (VI), Mn (II) and As (V) ions in the aqueous medium using F-AgNPs. These approaches include chemical reduction and microwave assistance. According to the study of colorimetric images, F-AgNPs nanoparticles created using the chemical reduction approach can detect Al (III) ions in an aqueous medium with high sensitivity, whereas nanoparticles created using the microwave reduction method can detect As (V), Mn (II) and Fe (II) ions. Additionally, the Raman spectrum profile of the water samples spiked with Cr (VI) ions is capable of being improved by nanoparticles synthesized by the chemical reduction process, offering unusual vibrational spectral features that can aid in the detection of Cr (VI) ions in aqueous medium. Additionally, F-AgNPs nanoparticles created using a microwave-assisted technique can boost the Raman band intensity in water samples that have been injected with Se (IV), Cr (VI) and Mn (II) ions. By utilizing the phenomenon of aggregation of the distributed silver nanoparticles, F-AgNPs can be detected in aqueous medium by specific and selective interactions with Cr (VI), Cr (III), Mn (II), Al (III) and As (V).

In the V-AgNPs case, except for Cr (III) ions, the solution turns greyish black when synthesized V-AgNPs colloidal solution is added to control and metal ion-laced water samples. The water samples containing Cr (III) ions become transparent when V-AgNPs colloidal solution is added. Additionally, the presence of V-AgNPs in water samples that contain Cr (III) ions and Mo (VI) ions results in distinctive, highly intense Raman spectrum signatures that can be utilized to identify the presence of these metal ions in aqueous solution. When V-AgNPs are added to metal ions, the nanoparticles aggregate, changing colour and producing Raman scattering signals. The size of the synthesized AgNPs ranges from 5 to 15 nm.The obtained results significantly advance our knowledge of the potential of nanoscale materials and their special qualities for the development of affordable miniature devices for the sensitive, selective, affordable, and repeatable determination of metal ions.

TH-16

Development of a Portable LIBS-Raman System for Identification and Classification of Plastics

Adarsh U.K.
Department of Atomic and Molecular Physics
Manipal Academy of Higher Education
Manipal, Karnataka, India-576104
e-mail: adarshuk95@gmail.com

1. Introduction

The accumulation of plastic waste and consequential pollution has been a concern for decades[1,2]. Post-consumer plastic waste leaking into the environment has manifold ways of impacting the ecological balance via habitat destruction and toxicity[1, 3]. Considering the approaches for reducing the number of plastics reaching the environment, recycling has a robust preference[4]. The process of mechanical recyclingis limited due to the lack of a proper plastic waste sorting technique[5] that satisfies the urgency of rapid characterization with maximum accuracy. Hence, developing a methodology to sort Plastic Solid Waste (PSW) into categories underlined by the polymer classes and also governed by the potential toxicity via additives is essential. The application of sorting approaches with a combination of spectroscopic methods is under-discussed in the literature. A combination of LIBS[6] and Raman spectroscopy[7] can provide the elemental-molecular information of the plastic sample, which can predict the class/type of PSWs with a high level of confidence in less analysis time. In addition, the LIBS technique can detect additives from the plastic matrix, so segregation based on the additive content can also be performed. The thesis discusses designing and developing a bimodal LIBS-Raman spectroscopy system to characterize plastics for sorting applications by combining spectroscopy data with different chemometric tools for effective data analysis and prediction of the unknown plastic. Based on the inferences from the literature survey, the design and development of a bimodal LIBS-Raman spectroscopy system for the characterization of plastics is proposed with the following objectives:

1. *Setting up of a portable LIBS-Raman spectroscopic system for analysis of different kinds of plastic samples*
2. *Optimization of the developed system for rapid, reliable, and routine identification of plastics and additives in plastics*
3. *Identification and classification of different plastic classes using combined LIBS-Raman system with multivariate data analysis techniques (such as principal component analysis (PCA), partial least squares discriminate analysis (PLS-DA), etc.)*

2. Methodology

The plastic samples used for the development of the system consisted of pure plastics and post-consumer plastics. Our collaborators from the National Institute of Interdisciplinary

Science and Technology (NIIST), Trivandrum, prepared and provided pure plastics (PC, PE, PP, PMMA, and Nylon 1 1).A graphical representation of the design of the proposed system is shown in Figure 1. The laser source is a frequency-doubled Nd:YAG nanosecond pulsed laser operating with a pulse width of 6 ns, maximum energy of 225 mJ (532 nm), and a repetition rate of 10 Hz. The beam is guided towards an optical prism (fused-silica) of 12.5 mm face dimension using a 532 nm specific dichroic mirror. The prism makes a total internal reflection of the beam towards the focusing lens (lens 1-UV-fused silica) of 60 mm focal length and 50 mm diameter (~f/1.2). The system features a co-axial back-collection geometry where the excitation lens (lens 1) collects the resulting signals (LIBS/Raman) into the optical system.

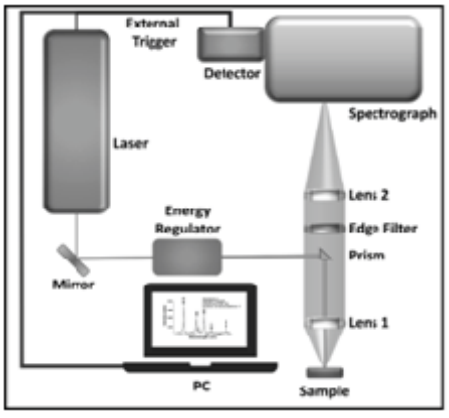

Figure 1: A graphical representation of the proposed bi-modal LIBS-Raman spectroscopy system for plastic characterization and sorting

The collimated signals from lens 1 are passed through a laser line filter to deny the Rayleigh scattered light during Raman measurements. The spectrograph (Czerny-Turner (C-T)) has input aperture of f/4.1, for which an f-matching lens of 200 mm focal length and 50 mm diameter (f/4) lens is chosen for focusing the collected signals into the spectrograph. The spectrograph features three gratings to choose between resolution, throughput, and spectral bandwidth with 600 gr/mm (500 nm blazed), 1200 gr/mm (500 nm blazed), and 2400 gr/mm (300 nm blazed) options. The signal is then focused on the non-gated CCD detector having a pixel size of 26 µm in a 1064 x 256-pixel array. The detector is thermoelectrically cooled down to a minimum temperature of -80^0 C.The detector is connected to the PC for controlling the system and recording signals using the specified software. In addition, the detector receives a trigger pulse through an external trigger mechanism from the laser, where the laser pulse output and detector acquisition are synchronized.Data visualization and evaluation were accomplished using Principal Component Analysis (PCA) via score plot and variance after preprocessing the spectral data through background subtraction and scatter correction. The decomposition of LIBS-Raman spectral data to extract the variables of maximum variance using PCA and PLS (Partial Least Squares), and the initial evaluation of the results was performed utilizing cross-validation on the spectral data. The spectral data decomposition results from PCA and PLS were combined with classifiers such as Logistic Regression (LR), Linear Discriminant Analysis (LDA), Support Vector Machine (SVM), and Partial Least Squares-Discriminant Analysis

(PLS-DA), and the results were compared to construct a prediction model with maximum classification accuracy. The reliability of the models was evaluated utilizing 4-fold cross-validation, and the best-performing model was chosen based on sensitivity and specificity in predictions based on LIBS-Raman spectral data.

3. Results

A photograph of the developed system is shown in Figure 2. The system shown in Figure 2 (a) features the nanosecond laser from Quantel (Q-Smart 450, Quantel, France) and the C-T spectrograph from Andor (Kymera 328i, Andor, Ireland) coupled to CCD (Andor iDus DU420A-BU2). The PC is equipped with Andor SOLIS software for the operation. The optical system consisting of the prism, lens 1, edge filter, and lens 2 is aligned using the cage system, where the individual mounts are interconnected using metallic rods for better robustness. Also, the edge filter is mounted using a filter wheel to be introduced/removed from the optic axis according to the acquisition (Raman/LIBS).

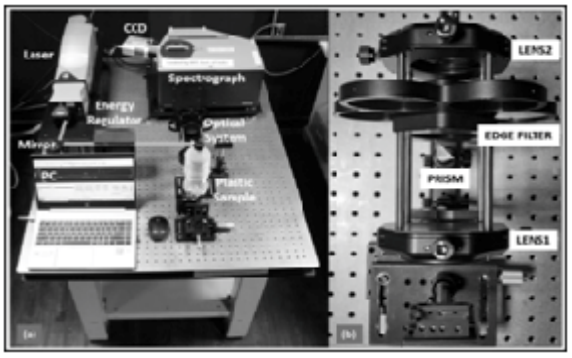

***Figure 2**: (a) A photograph of the developed system (b) optical system*

As per the proposal, the entire optical alignment has been realized on a portable optical table of dimensions 120 cm x 90 cm so that the unit can be easily transported from one place to another.The system's optical alignment is followed by optimizing the system to effectively collect and analyze the LIBS and Raman signals from plastic samples. A summary of optimized parameters for the operation of the proposed system is shown in Table 1.

***Table 1**: An overview of optimized parameters for the operation of the system*

Optimized Parameters		
Parameter	**LIBS**	**Raman Spectroscopy**
Laser Energy	7 mJ	3.5 mJ
Spectrograph Entrance Slit width	--	50 µm
Acquisition Mode	Single-shot	Single-shot
Exposure time	10 ms	10 ms

Optimization of the system for detecting additives from the plastic matrix was carried out by

using known concentrations of heavy metals-lead (Pb) and Cadmium (Cd)-mixed in the PE plastic, and the performance of the system was determined in terms of the relative error in prediction of unknown concentration and the Limit of Detection (LOD). An overview of the system's calibration to detect Pb and Cd in the polyethylene matrix is shown in Table 2.

***Table 2**: An overview of the calibration of the system for the detection of Pb and Cd in the PE matrix*

Parameter	Pb in PE matrix	Cd in PE matrix
Relative error in prediction	12.38 ± 2.06 %	11.83 ± 1.30 %
Limit of Detection	0.032 %w/w	0.020 %w/w

The performance validation of the optimized system was carried out by recording LIBS-Raman spectra of post-consumer plastic samples under seven polymer classes-Polyethylene Terephthalate (PET-Class 1), High-density polyethylene (HDPE-Class 2), Polyvinylchloride (PVC-Class 3), Low-density polyethylene (LDPE-Class 4), Polypropylene (PP-Class 5), Polystyrene (PS-Class 6), and Polymethylmethacrylate (PMMA-Class 7 (Others))[8], followed by the chemometric analysis on the same for constructing a prediction model for correctly identifying the class of an unknown plastic sample. A comparison of LIBS and Raman spectra recorded from seven classes of plastics using the optimized system is shown in Figure 4.

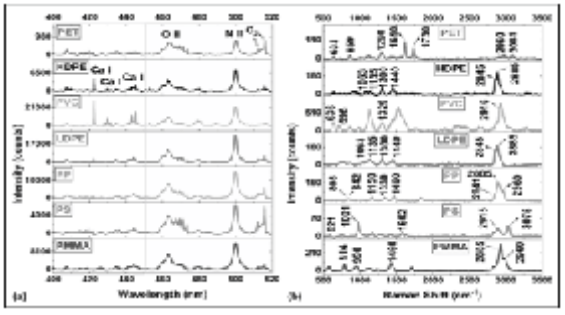

***Figure 4**: A comparison of background corrected (a) LIBS and (b) Raman spectra recorded from seven types of plastics using the optimized system*

For assessing prediction performance, the total data set of 670 spectra is divided into calibration and validation sets in a 70:30 ratio, where 70 % of the total samples are used for calibrating the model, and the remaining 30 % are used for testing the model. A comparison of prediction accuracies based on LIBS spectral data showed the maximum accuracy by PCA-LDA and PLS-DA with 95 % accuracy. To select between the two models and evaluate the classification results' reliability, the 4-fold cross-validation was performed on the models, and the corresponding sensitivity and specificity were compared and are shown in Table 4. A similar comparison for Raman data is shown in Table 5.

***Table 4**: A summary of 4-fold cross-validation on statistical models on LIBS data*

Model	PCA-LR	PCA-LDA	PCA-SVM	PLS-LR	PLS-LDA	PLS-SVM	PLS-DA
Sensitivity (%)	88.85	89.98	89.85	89.37	89.81	88.25	90.28
Specificity (%)	98.04	98.17	98.22	98.14	98.24	97.97	98.29

Based on the results in Table 4, PLS-DA performs the best on LIBS data out of the models constructed with a sensitivity of 90.28% and specificity of 98.29 %.

***Table 5**: A summary of 4-fold cross-validation on statistical models on Raman data*

Model	PCA-LR	PCA-LDA	PCA-SVM	PLS-LR	PLS-LDA	PLS-SVM	PLS-DA
Sensitivity(%)	99.71	99.57	99.85	99.14	99.28	99.28	99.89
Specificity(%)	99.94	99.92	99.97	99.84	99.87	99.87	99.82

On Raman data, all models have a sensitivity and specificity above 99 %, and PLS-DA performs the best in comparison. Thus, the PLS-DA model was selected in combination with LIBS-Raman data for the system's operation.

4. Conclusions

The system design with a single source and single detector configuration in co-axial back collection geometry enabled fast analysis of plastic samples. The system operates in single-shot mode with 10 ms exposure time for LIBS and Raman data acquisition. The optimization of the developed system for detection of additive contents in the plastic matrix using known concentrations of Lead (Pb) and Cadmium (Cd) showed limit of detections down to 0.032 %w/w for Pb and 0.020 %w/w for Cd and the error in prediction of unknown concentrations of these heavy metals in PE matrix below 13.5 %. Integration of data decomposition methods such as PCA and PLS on the LIBS-Raman spectral database constructed by recording the spectral data from seven types of plastics using the optimized system resulted in identifying the spectral features of maximum variance and the incorporation of the variables of maximum variance (PCs and LVs) into classifiers such as LR, LDA, SVM, and PLS-DA shows the applicability of the developed system for predicting the class of the unknown plastic samples. The combination of LIBS and Raman data with the PLS-DA method showed the maximum accuracy in the prediction process, with an accuracy of 95 % for the prediction based on LIBS data and 100 % accuracy for the prediction based on Raman data. The 4-fold cross-validation showed a sensitivity and specificity of 90.28 % and 98.29 %, respectively, for PLS-DA on LIBS data, and for Raman analysis, 99.89 % sensitivity and 99.82 % specificity were obtained. The results imply that the developed LIBS-Raman system, with good analysis speed and classification accuracy, is a potential candidate to be applied in plastic recycling industries. The developed system can fulfill industrial requirements like a high sorting rate (number of samples analyzed per hour) and the least dropouts (number of unidentified samples).

5. References

1. M. MacLeod, P.H. Arp. Hans, M.B. Tekman, and A. Jahnke, The global threat from plastic pollution. Science, 2021. 373(6550): p. 61-65. DOI: 10.1126/science.abg5433
2. A.A. Horton, Plastic pollution: when do we know enough? Journal of Hazardous Materials,

2022. 422: p. 126885. https://doi.org/10.1016/j.jhazmat.2021.126885

3. R.C. Thompson, C.J. Moore, F. S. vom Saal, and S.H. Swan, Plastics, the environment and human health: current consensus and future trends. Philosophical transactions of the royal society B: biological sciences, 2009. 364(1526): p. 2153-2166. https://doi.org/10.1098/rstb.2009.0053
4. J. Hopewell, R. Dvorak, E. Kosior, Plastics recycling: challenges and opportunities, Philos. Trans. R. Soc. Lond. B Biol. Sci. 2009, 364, 2115-2126. https://doi.org/10.1098/rstb.2008.0311.
5. D. Froelich, E. Maris, N. Haoues, L. Chemineau, H. Renard, F. Abraham, and R. Lassartesses, State of the art of plastic sorting and recycling: Feedback to vehicle design. Minerals Engineering, 2007. 20(9): p. 902-912. https://doi.org/10.1016/j.mineng.2007.04.020
6. V.K. Unnikrishnan, K.S. Choudhari, S.D. Kulkarni, R. Nayak, V.B. Kartha, and C.Santhosh, Analytical predictive capabilities of laser induced breakdown spectroscopy (LIBS) with principal component analysis (PCA) for plastic classification. Rsc Advances, 2013. 3(48): p. 25872-25880. 10.1039/C3RA44946G
7. R. Lenz, K. Enders, C.A. Stedmon, D.M.A. Mackenzie, T.G. Nielsen, A critical assessment of visual identification of marine microplastic using Raman spectroscopy for analysis improvement, Mar. Pollut. Bull. 2015 100, 82-91. https://doi.org/10.1016/j.marpolbul.2015.09.026.
8. E.A. Bruno, Automated sorting of plastics for recycling. North Carolina Department of Environment and Natural Resources, 2000.

TH-17

Laser Directed Energy Deposition of Inconel 625 Alloy For Repair & Feature Addition Applications: An Experimental And Numerical Investigation

Jitender Kumar Chaurasia
National Institute of Technology Karnataka, Surathkal
E.mail : jitender.chaurasia@gmail.com; Jitender-177me004@nitk.edu.in

Summary

Engineering components after the prolonged hours of service in harsh environmentsoften go through several defects such as wear, cracks and deformation. These defects alter the actual geometry thereby affect its performance. In general, these parts are changed with new one during the overhauling process. However, replacing a part with a new one is uneconomical, especially if the part has high intrinsic value. For high value engineering parts, repairing the damages surfaces is more cost effective than replacing the entire part with new ones. Welding has been the primary method for repair practices. However, this method has limitations, such as high heat affected zone and inability to repair complex shape cracks. With the advancement in metal Additive Manufacturing (AM), it is anticipated that this technology can be a game changer for repair industries.

To this end, the present thesis is focused to explore the repair capabilities of Laser Directed Energy Deposition (LDED) process which is a class of metal AM process where material is deposited by feeding the stock material (usually metal powder) through a nozzle into the melt pool formed on a substrate by a laser source. The work presented in this thesis starts with the fundamental understanding of LDED process to its applications in the sector of repair and feature addition for Inconel 625 (IN625). First, a laser surface melting study is presented where the focus is to understand how laser material interaction occurs. Effects of the process parameters, such as laser power and scan speed on the melt pool geometry and microstructure were studied. In addition, a Finite Volume Method based numerical model was established to understand the effect of considering fluid dynamics on the predicted melt pool geometry, cooling rates and thermal gradients. For the validation of numerical model, the results of cooling rates and thermal gradients were compared with the microstructure. Next, a single-track study was conducted to identify the process parameter window for sound deposition and to understand effect of process parameters on the deposited track height and width. A finite element based numerical model was established to predict track height and width. Subsequentially, the optimized process parameters were chosen and a total of six thin walls were built to mimic feature addition applications on a IN625 substrate. Effect of process parameters on the thin wall build geometry, surface roughness,microstructure and mechanical properties were investigated. A FE based numerical model was established to understand the variation in melt pool geometry, cooling rates and thermal gradients with the change in process parameters and over the layers. Further, a study was carried out to understand the repair capabilities of LDED process, where the

samples were extracted from a wrought plate of IN625 and were subjected to a fatigue load to mimic a component in service for repairing. Further, deposition was carried out on the surfaces (i.e., Top, Top & bottom, One side and Both sides) of these fatigued tensile sample. The samples were also solution-treated at 1200°C for 90 mins. Microstructure and mechanical properties were evaluated and then compared between the different deposition strategies and sample heat-treatment conditions. Tensile properties were compared for all the three sample conditions viz., wrought alloy, as repaired and solution treated. Results indicate sound deposition with minimal porosity in all the four deposition strategies using the LDED process. IN625 being a choice of material for high temperature applications, it is important to understand the thermal stability of the parts repaired using LDED process. To this end, the repaired samples were also tested for high temperature oxidation. Using the LDED process, an IN625 block was fabricated. The LDED IN625 samples were also subjected to solution treatment. In order to compare the performance of both LDED IN625 and solution treated LDED IN625, test coupons were also extracted from the wrought plate. Oxidation study was carried out for as-built, solution treated and wrought alloy at 800° and 1000°C for up to 100 hours in air.

In the conclusions of this thesis, LDED is found to be a promising technique to repair and add features on existing component with least porosity and high mechanical properties. However, the results of this study do indicate that the selection of an optimum process parameter can be useful to achieve consistent build quality during the thin wall deposition. Also, a suitable post-processing technique such as solution treatment is required for the achieving a homogenized microstructure, consistent mechanical properties and high thermal stability in the repair components.

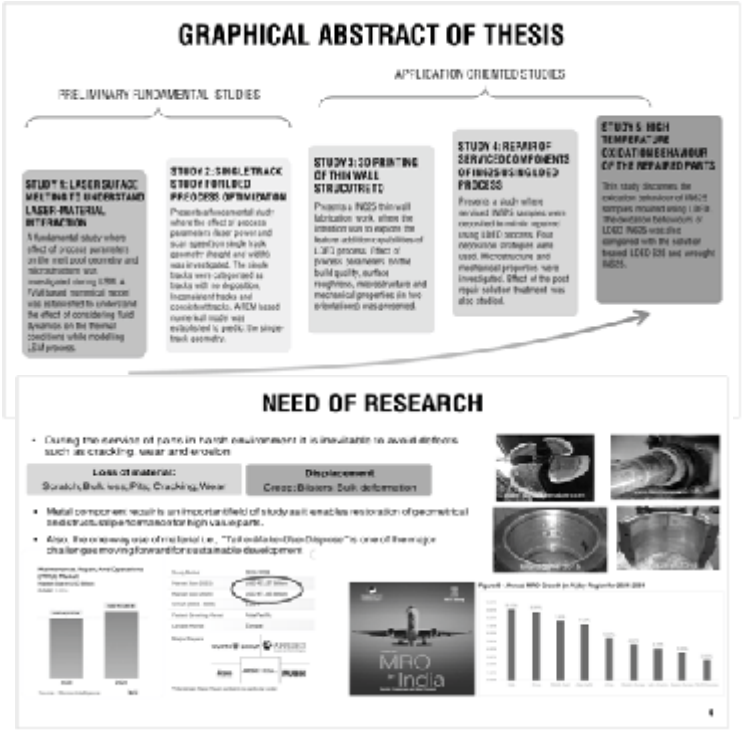

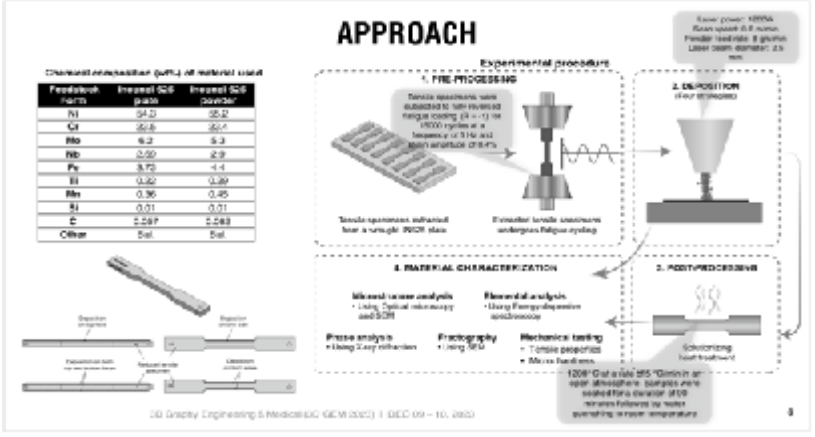

Feedstock form	Inconel 625 plate	Inconel 625 powder
Ni	64.0	58.2
Cr	20.6	20.4
Mo	9.2	9.3
Nb	3.50	3.9
Fe	3.72	4.4
Ti	0.22	0.24
Mn	0.36	0.45
Si	0.01	0.01
C	0.047	0.049
Other	Bal.	Bal.

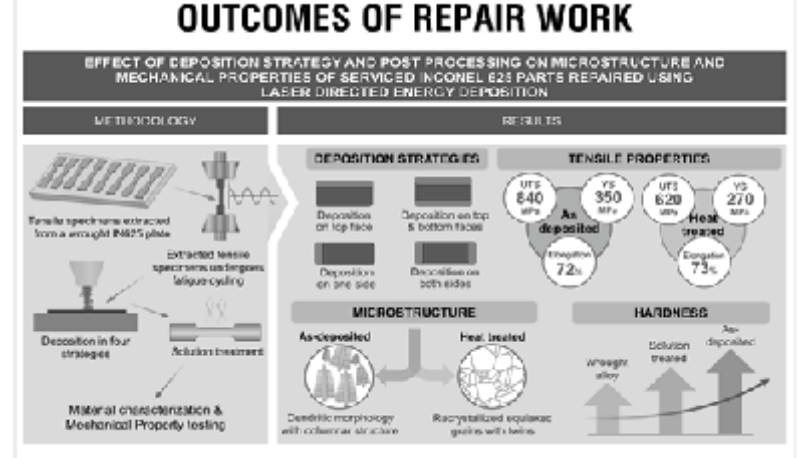

CONCLUSIONS

- **Sound deposition** with minimal porosity in all the four deposition strategies
- **Dendritic morphology with columnar structure** in the case of as-deposited samples
- Microstructure after solution treatment shows complete static recrystallization
- Fractured samples show a ductile mode of failure with clear dimples.
- Yield strength values ranges between **300-350 MPa in as-deposited condition** while **230-270 MPa** in the solution treated condition
- **Deposition strategies have a minimal influence on the YS**
- Significant difference in the YS value can be observed between the as-deposited and solution treated conditions
- **Hardness values of the as-deposited samples were found to be higher by 12%** than that of the solution treated samples

PUBLICATIONS FROM THESIS

- Chaurasia, J. K., Jinoop, A. N., Paul, C. P., Bindra, K. S., Balla, V. and Bontha, S. "Laser Directed Energy Deposition as a Repair Technology for Serviced Inconel 625 Parts: Influence of Deposition Strategy and Heat Treatment on Microstructure and Mechanical Properties", Optics & Laser Technology, 168 (1 January 2024)
- Thanumoorthy, Raja S., Jitender K. Chausasia, V. Anil Kumar, P. I. Pradeep, A. S. S. Balan, B. Rajasekaran, Ankit Sahu, and Srikanth Bontha. 'Effect of Build Orientation on Anisotropy in Tensile Behavior of Laser Powder Bed Fusion Fabricated SS316L'. Journal of Materials Engineering and Performance, 17 July 2023.
- Chaurasia, J. K., Jinoop, A. N., P, P., Paul, C. P., Bindra, K. S., and Bontha, S. (2021). "Study of melt pool geometry and solidification microstructure during laser surface melting of Inconel 625 alloy." Optik., 246

TH-18

Probing Lattice Dynamics in real-space and real-time

Navdeep Rana
Indian Institute of Technology Bombay, Mumbai, India-400076
Email: navdeep@pyh.iitb.ac.in

In my thesis, we aim to probe coherent lattice dynamics in real-space and real-time. In the initial segment of the thesis, we have demonstrated the capability of high-harmonic spectroscopy to probe coherent lattice dynamics in solids. Using this technique, we explored the impact of coherent lattice excitations, specifically the in-plane longitudinal and transverse optical phonon modes, on the electronic response in monolayer graphene. In the later part of the thesis, we delve into imaging the lattice dynamics in both real-space and real-time. For the 4D imagining of coherent lattice dynamics in solids, we have proposed a novel approach, based on the inelastic scattering method. We have illustrated the competence of inelastic scattering techniques, when coupled with theoretical analysis, in offering information comparable to what could be obtained through time-resolved diffraction and imaging measurements within pump-probe configurations.

The strong-field driven nonperturbative light-matter interaction is numerically simulated by solving density matrix-based Semiconductor-Bloch equations. The electronic structure of graphene is computed within a tight-binding approximation. The coherent lattice dynamics in graphene is described classically by making hopping parameters time and atomic coordinate-dependent in tight-binding Hamiltonian.

In Chapter 3, we have illustrated that high-harmonic spectroscopy is able toinvestigate the influence of coherent lattice dynamics on the electronic responsein graphene on the attosecond timescale[2].It has been assumed that a pump pulsecoherently excites either the iLO or iTO phonon mode, which is probed by a linearly polarized laser pulse to generate the high-harmonic spectrum. It has beenfound that the coherent excitation of the in-plane phonon modes results in theappearance of sidebands in the spectrum of the emitted harmonics. The spectralpositions of the sidebands yield the energy of the excited phonon mode. When theiLO phonon mode is excited, the even- (odd-) order sidebands are polarized parallel(perpendicular) to the probe pulse. However, upon excitation of iTO phonon mode,all the sidebands are polarized parallel to the probe pulse. These observations areexplained in terms of a dynamical symmetry analysis within the Floquet framework. Thus, the polarization of the sideband emission offers a sensitive probe ofthe dynamical symmetries associated with the coherently excited phonon modes.We have also explored how HHG is sensitive to various properties of graphene withcoherent phonon and various parameters of the probe laser pulse.

There can be situations when both the phonon modes are coherently excitedwhile maintaining a specific phase difference. In Chapter 4, we have demonstratedthat the phase

difference between these phonon modes can be extracted by analyzing the current associated with the sideband of the main harmonic peak. Circularphonon modes are generated when the phase difference between the phonon modesacquires $90^{?}$, We have shown that high-harmonic spectroscopy characterizes the"chirality" of the circular phonon modes[4]. Consequently, the coherent excitation ofLCP and RCP phonon modes results in distinct modulations in the high-harmonicspectra. It has been observed that the excitation of the circular phonons leadspiezo-optic effect in graphene (Tamaya and Kato, 2021). Therefore, high-harmonicspectroscopy is capable to characterize not only the energy, polarization, and phasedifference but also the "chirality" of the phonon modes.

When a phonon mode is coherently excited in graphene, the six-fold symmetryundergoes a reduction to a two-fold symmetry. This reduction in symmetry pavesthe way for the emergence of symmetry-forbidden harmonics[3]. This change in symmetry is also explored through high-harmonic spectroscopy. Coherently excited in-plane optical phonon mode is probed by the circularly polarized pulse, and thehigher-order harmonic spectrum is generated. It has been observed that the dynamical symmetry reduction, caused by the coherent lattice dynamics in graphene,leads to the generation of forbidden harmonics.

As of now, our discussion has revolved around the probing of lattice dynamicsin real-time. Moving forward, our focus is shifted toward 4D imaging of coherentlattice dynamics in solids. In Chapter 5, we have demonstrated that inelasticscattering methods, with the aid of theoretical analysis, are competent to provide similar information as one could obtain from the time-resolved diffractionand imaging measurements[1]. To illustrate the robustness of the proposed method,our simulated result of lattice dynamics in germanium is in excellent agreementwith the time-resolved diffuse x-ray scattering measurement performed at x-rayfree-electron laser in pump-probe setup. For a given inelastic scattering data inenergy-momentum space, the proposed method is useful to image in-situ latticedynamics under different environmental conditions of temperature, pressure, andmagnetic field. In addition, our approach is suitable to probe first-order states atq ?0 or disorder-activated continuum, and second-order 'squeezed' states in themomentum-time domain.

Our work discussed in Chapters 3 and 4 brings the key advantage of high-harmonic spectroscopy – the combination of sub-femtosecond to tens of femtoseconds temporal resolution – to the problem of probing phonon-driven electronicresponse and its dependence on the dynamical symmetries in solids. This opens anavenue in time-resolved probing of phonon-driven dynamical symmetries in solidswith sub-cycle temporal resolution. Our study can be extended to bilayer graphene,where infrared-active phonon modes can be described in terms of double degenerate in-plane Raman-active phonon modes of monolayer graphene (Gierz et al.,2015; Rodriguez-Vega et al., 2021). The investigation of bilayer graphene wouldprovide further insights into the interplay between lattice dynamics and electronbehavior. In a recent development, it has been demonstrated that incorporatingphonon deformations into the context of HHG enables the probing of mode-specificelectron-phonon coupling and Berry curvature (Hu et al., 2023). This innovativeall-optical high-harmonic spectroscopy offers a promising alternative avenue forcharacterizing electron-phonon coupling, which complements the insights providedby angle-resolved photoemission spectroscopy. On the other hand, work discussedin Chapter 5 will profoundly impact where time-resolved diffraction within thepump-

probe setup is not feasible, for instance, in inelastic neutron scattering. Future investigations can be built upon the mechanisms employed in this thesis andfurther extend the methodology to study diverse solids, including topological materials, under varying conditions.

References:

1. Navdeep Rana, A. P. Roy, Dipanshu Bansal, and Gopal Dixit,*npj Computational Materials***7,** 7 (2021).
2. Navdeep Rana, M. S. Mrudul, Daniil Kartashov, Misha Ivanov, and Gopal Dixit, *Physical Review B***106**, 064303 (2022)
3. Navdeep Rana, and Gopal Dixit,*Physical Review A* **106,**053116 (2022).
4. Navdeep Rana, and Gopal Dixit, In preparation.

List of Exhibitors in the Industrial Exhibition organized by the Indian Laser Association (ILA) during NLS -32

Sl.No.	Name of Exhibitor
1	ATOS Instruments Marketing Services, Bengaluru
2	Suresh Indu Lasers Pvt Ltd, Pune
3	Light Guide Optics Pvt Ltd, Indore
4	Lord's Mark Industries, Mumbai
5	Research India, Bhopal
6	Trokut Solutions Pvt Ltd, Mumbai
7	Yokogawa India Limited, Bengaluru
8	Solutions for Lasers & Photonics Pvt Ltd., Delhi
9	Del Controls, Indore
10	Advanced Photonics, Mumbai
11	Holmarc Opto-Mechatronics Ltd, Kochi
12	AIMIL Ltd., New Delhi
13	Photonics Marketing Company, Mumbai
14	Laser Science Services (I) Pvt. Ltd., Navi Mumbai
15	New Age Instruments & Materials Pvt Ltd, Gurugram
16	Anatech Laser Instruments Pvt Ltd, Mumbai
17	Spectral Instrument System, Gurugram
18	Inde Enterprises, Chandigarh
19	Infrared Optics Pvt. Ltd., Faridabad
20	Photik Scientific Pvt Ltd., Faridabad
21	Specialise Products Private Limited, Navi Mumbai
22	Dynotech Instruments, New Delhi

AUTHOR INDEX

Printing Arts #9826604242